A study of the variation of leukocyte immunoglobulin- like receptors on antigen-presenting cells

Yong, Patrick

Awarding institution:
King's College London

A STUDY OF THE VARIATION OF LEUKOCYTE IMMUNOGLOBULIN-LIKE RECEPTORS ON ANTIGEN-PRESENTING CELLS

By

Patrick Foh Khing Yong

Department of Haematological Medicine
Division of Cancer Studies
King's College London

Thesis submitted in part fulfilment of the degree of Doctor of Philosophy
2013

Abstract

Leukocyte immunoglobulin-like receptors are a family of inhibitory and activating receptors found on a wide variety of immune cells, and are thought to play a significant role in determining immune responses. Their known ligands are HLA Class I molecules; HLA-G is the prototypic ligand which has high affinity for two inhibitory members of the family and mediates its immunosuppressive functions through them.

The hypothesis of this study is that polymorphisms in the non-coding regions are likely to influence both the expression and response of the LILRs to various stimuli. Published data supports this view in that polymorphisms in the LILRs are associated with various immunologically mediated diseases. In addition, these molecules represent a potential target for therapeutic manipulation and attempts to develop a therapy using this route were undertaken.

Expression levels of various LILR molecules on APCs at baseline and after stimulation have shown significant variation between subjects. Genomic variation in the promoter regions of LILRB2 was established by sequencing. The relationship between LILRB2 SNPs and cell expression levels was tested both directly and in a luciferase assay, but no significant associations were found. Engagement of LILRB2 by monoclonal antibodies was shown to affect TLR-induced cytokine secretion, but no relationship was found between LILRB2 expression levels and the effect on cytokine secretion.

A synthetic construct (the “G-body”) utilising the LILR-HLA-G interaction has been developed for testing as a potential therapeutic molecule. This construct comprises two functional domains – an anti-HLA class I domain and an HLA-G domain. This construct would be expected to modulate allogeneic responses by localisation of an immunosuppressive signal (HLA-G) to the allogeneic HLA molecule; and (ii) potentially masking the allogeneic HLA class I molecule. Testing has shown that the construct suppresses lymphocyte proliferation with enhancement of this effect dependent on the presence of allogeneic HLA class I.

Table of Contents

Abstract 2
List of figures 10
List of tables 12
List of abbreviations 13
Preface 17
Chapter 1: Introduction 18
Leukocyte immunoglobulin-like receptors (LILRs) 18
Nomenclature 18
Genetics 19
Expression 19
Structure, ligands and binding interactions with ligands 19
Signalling 27
Orthologues and homologues 28
PIR genetics, expression and protein structure 29
Expression in neuronal tissue 31
PIR Ligands 31
PIR Signalling 32
Functional effects 34
Murine LILRB4 38
LILRs and influence on immune responses/functional effects 39
Antigen presenting cells 39
Human leukocyte antigen G (HLA-G) 42
HLA-G and LILRs 45
Potential therapeutic implications 45
Hypothesis 46
Aims and Objectives 48
Figures 49
Tables 50
Chapter 2: Materials and methods 58
Cell Lines 58
Generation of stable K562 transfectants with LILRB1, LILRB2 and pcDNA3.1(+) 59
Purification of monoclonal antibody from hybridoma supernatant 60
Isolation and manipulation of primary cells 61
PBMC separation 61

Purification of $CD14^+$ monocytes 61
Generation of MoDCs 61
General molecular biology techniques 62
Transformation of competent E. Coli 62
DNA Minipreps 63
DNA Midipreps/Maxipreps 63
DNA gel extraction 64
Purification of PCR products 64
Restriction enzyme digestion 65
DNA ligation 65
RNA extraction 65
Reverse transcription 66
DNA sequencing 66
PCR amplification 66
DNA Agarose electrophoresis 67
Development of assays to measure variance in LILRs 67
Measurement of LILR levels on DCs and other immune cells 67
Effect of cytokine stimulation on LILR expression 70
Sequencing of polymorphisms in the LILRB2 promoter region 70
DNA extraction 70
PCR to amplify the LILRB2 promoter region 71
Sequencing of the amplified PCR fragment 72
Analysis of LILRB2 polymorphisms 73
Real time PCR to quantify LILRB2 mRNA levels 73
Cell types used and experimental conditions 73
RNA extraction and genomic DNA removal 74
Conversion of RNA to cDNA 74
Real time PCR reaction 74
Luciferase assay 75
Cloning of LILRB2 region upstream of start codon into promoterless luciferase vector for sequencing 76
Sequencing of cloned 1000 bp LILRB2 region upstream of start codon 77
Gene synthesis of LILRB2 promoter region for use in luciferase assay 78
Transfection of THP-1 cells with luciferase plasmids 78
Measurement of luciferase activity 79
Functional assays with anti-LILRB2 antibodies 79

Stimulation with TLR ligands ... 79
ELISA for cytokine secretion ... 80
Development and testing of the G-Body ... 81
Generation of recombinant G-body and control materials ... 81
Hybridoma sequencing ... 81
DNA synthesis ... 82
Generation of plasmids for transfection ... 82
Transient transfection of cell lines ... 83
Generation of chemically conjugated G-body ... 83
Conjugation of streptavidin to BB7.2 ... 83
Measurement of endotoxin levels ... 84
Endotoxin purification of biotinylated HLA-G ... 84
Protein measurement ... 84
Conjugation of biotinylated HLA-G monomers to streptavidin-conjugated BB7.2 ... 85
Generation of controls for chemically conjugated G-body ... 85
Testing of constructs ... 85
Immunoprecipitation ... 85
SDS-PAGE ... 86
Western blotting ... 86
HLA-G ELISA ... 87
Flow cytometry ... 87
Functional testing of G-Body ... 88
Lymphocytes proliferation experiments ... 88
Mixed lymphocyte reactions ... 89
Cytokine measurements ... 89
Statistical analysis ... 90
Generation of control materials ... 91
Cloning of green fluorescent protein (GFP) into pcDNA3.1 for use as transfection control ... 91
Cloning of full-length HLA-G, soluble HLA-G, β2-microglobulin into pcDNA3.1 for use as experimental controls ... 93
Cloning of LILRB1 and LILRB2 for use in ligand binding experiments ... 94
Chapter 3: Characterisation of expression levels of LILR molecules in healthy individuals ... 98
Background ... 98
Optimisation of whole blood LILR expression assay ... 99

Determination of antibody concentrations to be used 99
Determination of assay characteristics 100
Optimisation of whole blood stimulation assay to measure LILRs 100
LILR expression levels in 26 healthy individuals at baseline and after stimulation with cytokines 102
Differential LILR cell surface patterns on monocytes and DCs at baseline 102
Incubation of whole blood ex vivo alters LILR expression on monocytes and DCs . 103
LILRs are upregulated on monocytes and DCs by inflammatory cytokines 103
LILRs are downregulated on monocytes and DCs by stimulation with TGF-β..... 104
Discussion 104
Tables 109
Figures 112
Chapter 4: Genomic variation in the LILRB2 promoter and its effect on protein expression 128
Background 128
Sequencing of the putative LILRB2 promoter region 131
PCR amplification of 2306 bp region containing the LILRB2 promoter 131
Sequencing of amplified PCR product and identification of SNPs contained in the amplified PCR region 131
Relationship between SNPs identified and LILRB2 protein expression levels 132
Demonstration of the transcriptional regulation of LILRB2 133
Dual luciferase reporter assay to determine if LILRB2 promoter SNPs affect protein expression levels 134
Cloning of the 1000 bp region upstream of the ATG start codon to determine individual LILRB2 promoter region haplotypes 135
Sequencing of cloned promoter regions and identification of the LILRB2 promoter haplotype 135
Gene synthesis of a region from -533 to +74 from the putative transcription initiation site for LILRB2 and cloning into pGL4.10/luc2 vector 136
Effect of LILRB2 promoter SNPs on luciferase expression 136
Discussion 137
Tables 143
Figures 148
Chapter 5: Development of a therapeutic product utilising the LILR molecules .. 183
Background 183
Design of the recombinant G-body 187
Recombinant G-Body version 1 (ORIGBv1) 187

Recombinant B11 G-body (B11GBv1) 189
Sequencing of B11 plasmid 189
Synthesis of B11 insert to replace BB7.2 fragment 190
Cloning of the B11 insert into ORIGBv1 190
Binding characteristics of B11GBv1 191
Original G-Body version 2 (ORIGBv2) and B11 G-Body version 2 (B11GBv2) 191
PCR cloning of ORIGBv2 and B11GBv2 192
Binding characteristics of ORIGBv2 and B11GBv2 193
Measurement of recombinant G-body concentrations 194
Design of the chemically conjugated GBody 195
Binding characteristics of cGBOD 195
Discussion 197
Tables 201
Figures 203
Chapter 6: Functional assays to determine the effect of ligation of LILRB2 on cellular responses 224
Background 224
Effect of anti-LILRB2 antibodies on LPS and ssRNA induced cytokine secretion 234
Optimisation of the concentration of antibody and stimulus for use in the assay 235
Results of anti-LILRB2 antibodies on TLR ligand-induced cytokine secretion in 5 individuals 236
Relationship to LILRB2 expression levels 237
Effect of the chemically conjugated G-body in functional studies 238
Effect of the chemically conjugated G-body on lymphocyte proliferation assays 238
Effect of the chemically conjugated G-body in lymphocytes stimulated with anti-CD3/CD28 beads 239
Effect of the chemically conjugated G-body in lymphocytes stimulated with SEB 239
Effect of the chemically conjugated G-body in lymphocytes stimulated with anti-CD3 mAbs 240
Effect of the chemically conjugated G-body on allo-proliferation reactions 241
Effect of anti-LILRB2 antibodies on lymphocyte proliferation assays 241
Discussion 242
Cytokine suppression by anti-LILRB2 antibodies 242
Effect of the G-body on lymphocyte proliferation 244
Summary 247
Figures 249

Chapter 7: Discussion 266
Experimental results 268
Future work 273
Conclusions 275
References 277
Appendices 311
Appendix 1: International Union of Pure and Applied Chemistry (IUPAC) code for nucleic acids 311

List of figures

Figure 1.1 49
Figure 2.1 69
Figure 2.2 92
Figure 2.3a 96
Figure 2.3b 97
Figure 2.3b 97
Figure 3.1a 112
Figure 3.1b 113
Figure 3.2 114
Figure 3.3 115
Figure 3.4 116
Figure 3.5 118
Figure 3.6 119
Figure 3.7 120
Figure 3.8 121
Figure 3.9 122
Figure 3.10 123
Figure 3.11 124
Figure 3.12 125
Figure 3.13 126
Figure 3.14 127
Figure 4.1 148
Figure 4.2 150
Figure 4.3 152
Figure 4.4 164
Figure 4.5a 174
Figure 4.5b 175
Figure 4.6 176
Figure 4.7 177
Figure 4.8 181
Figure 5.1 203
Figure 5.2 204

Figure 5.3 205
Figure 5.4 206
Figure 5.5 207
Figure 5.6 209
Figure 5.7a 210
Figure 5.7b 211
Figure 5.8 212
Figure 5.9 213
Figure 5.10a 214
Figure 5.10b 215
Figure 5.10c 216
Figure 5.10d 217
Figure 5.11a 218
Figure 5.11b 219
Figure 5.12a 220
Figure 5.12b 221
Figure 5.12c 222
Figure 5.12d 223
Figure 6.1 249
Figure 6.2 250
Figure 6.3 251
Figures 6.4a 256
Figures 6.4b 257
Figure 6.5 258
Figure 6.6 260
Figure 6.7 262
Figure 6.8 263
Figure 6.9 264
Figure 6.10 265

List of tables

Table 1.1..... 50
Table 1.2..... 54
Table 3.1..... 109
Table 3.2..... 110
Table 3.3..... 111
Table 4.1..... 143
Table 4.2..... 145
Table 4.3..... 147
Table 5.1..... 201
Table 5.2..... 202

List of abbreviations

AIDS	Acquired immunodeficiency syndrome
ANOVA	Analysis of variance
APC	Allophycocyanin
APC	Antigen-presenting cell
ATCC	American Type Culture Collection
BMDC	Bone marrow derived dendritic cell
BSA	Bovine serum albumin
CD	Cluster of differentiation
cDNA	Complementary DNA
CMV	Cytomegalovirus
CV	Coefficient of variation
DC	Dendritic cell
DMEM	Dulbecco's modified essential medium
DNA	Deoxyribonucleic acid
dNTP	Deoxyribonucleotide triphosphate
ECD	Electron coupled dye, also known as PE-Texas Red
EDTA	Ethylenediaminetetraacetic acid
ELISA	Enzyme linked immunosorbent assay
EMEM	Eagle's minimal essential medium
FCS	Foetal calf serum
FHC	Free heavy chain
FITC	Fluorescein isothiocyanate
FRET	Fluorescence resonance energy transfer
GAPDH	Glyceraldehyde-3-phosphate dehydrogenase

gDNA	Genomic DNA
GFP	Green fluorescent protein
GM-CSF	Granulocyte macrophage colony-stimulating factor
GVHD	Graft versus host disease
HBSS	Hank's balanced salt solution
HCl	Hydrochloric acid
HIV	Human immunodeficiency virus
HLA	Human leukocyte antigen
HPA	Health Protection Agency
HRP	Horseradish peroxidase
Ig	Immunoglobulin
IL	Interleukin
ILT	Immunoglobulin-like transcript
IMC	Isotype matched control
ITAM	Immunoreceptor tyrosine-based activating motif
ITIM	Immunoreceptor tyrosine-based inhibitory motif
KIR	Killer immunoglobulin-like receptor
LAL	Limulus amebocyte lysate
LB	Lysogeny broth
LILR	Leukocyte immunoglobulin-like receptor
LPS	Lipopolysaccharide
LRC	Leukocyte receptor complex
mAb	Monoclonal antibody
MAG	Myelin associated glycoprotein
MDC	Myeloid dendritic cell

MEF	Molecule of equivalent fluorochrome
MFI	Median, or mean fluorescence intensity
MHC	Major histocompatibility complex
MIR	Myeloid inhibitory receptor
MLR	Mixed lymphocyte reaction
MMC	Mitomycin-C
MoDC	Monocyte-derived dendritic cell
mRNA	Messenger RNA
NCBI	National Center for Biotechnology Information
NK	Natural killer
NMR	Nuclear magnetic resonance
OVA	Ovalbumin
PBMC	Peripheral blood mononuclear cell
PBS	Phosphate buffered saline
PC7	Phycoerythrin-Cy7
PCR	Polymerase chain reaction
PDC	Plasmacytoid dendritic cell
PE	Phycoerythrin
PGE2	Prostaglandin E2
PIR	Paired immunoglobulin receptor
PVDF	Polyvinylidene fluoride
RA	Rheumatoid arthritis
RBL	Rat basophil leukaemia
RNA	Ribonucleic acid
RPMI	Roswell Park Memorial Institute

ScFv	Single chain variable fragment
SCID	Severe combined immunodeficiency
SEB	Staphylococcal enterotoxin B
SNP	Single nucleotide polymorphism
ssRNA	Single stranded RNA
TBS	Tris buffered saline
TBS-T	Tris buffered saline-Tween
TGF-β	Transforming growth factor beta
TLR	Toll-like receptor
TNF	Tumour necrosis factor
TNP	Trinitrophenol
UTR	Untranslated region
β2m	Beta-2 microglobulin

Preface

The primary subject of the research presented in this thesis is the group of molecules known as the leukocyte-immunoglobulin like receptors, or LILRs. Despite being first described in the late 1990s, there is still relatively little understanding of these molecules, and it is hoped that the data presented in this thesis goes some way towards addressing that.

This document is divided into an introduction summarizing the current state of knowledge in the field, a chapter on the materials and methods used for the research, four results chapters describing the main findings in this project and an overall discussion of the project. The page numbers for the main chapter headings are listed in the table of contents at the beginning of the document. The list of page numbers of figures and tables, as well as a list of abbreviations used immediately follows this. The list of references and appendices are at the end of the document.

Briefly, the four main areas investigated are (i) the characterisation of the expression of LILRs on healthy individuals, (ii) exploration of how genomic variation affects this expression (with respect to one specific member, as proof of principle), (iii) the development of a synthetic molecule to utilize the LILRs therapeutically and (iv) testing the effect of LILR ligation in various functional experiments. Each chapter contains the tables and figures associated with that chapter and are placed at the end of the chapter (apart from chapter 2 where they are in the text). Each results chapter also contains a discussion relating to the experiments described within.

Chapter 1: Introduction

Leukocyte immunoglobulin-like receptors (LILRs)

The leukocyte immunoglobulin-like receptors (LILRs, also known as immunoglobulin-like transcripts, ILTs; leukocyte Ig-like receptors, LIRs; myeloid inhibitory receptors, MIRs and CD85) are a family of receptors expressed on a wide variety of immune cells. They are thought to play a significant role in both innate and adaptive immunity and can broadly be divided into activating and inhibitory receptors based on the presence of either immunoreceptor tyrosine-based activating motifs (ITAMs) or immunoreceptor tyrosine-based inhibitory motifs (ITIMs) in the cytoplasmic tail. Their role can be seen as analogous to the TLRs which are innate immune receptors which recognise microbial patterns, whereas the LILRs are innate immune receptors which recognise self molecules. (1)

Nomenclature

Due to the simultaneous discovery of many of these receptors, they have been ascribed various names with ILTs and LIRs being the most commonly used ones. For standardisation, these molecules are now referred to as LILRs with LILRA being those with short cytoplasmic tails thought to have activating properties and LILRB being those with ITIMs in their cytoplasmic tail.

Genetics

The LILRs are encoded on chromosome 19q13.4 in a region known as the leukocyte receptor complex (LRC), which also encodes the killer immunoglobulin-like receptors (KIRs) expressed on NK and cytotoxic T cells. They are thought to have arisen due to large-scale inverted duplication with further loss/gain of genes. (2;3) In total, there are 13 members belonging to this family of genes, with 6 activating LILRs, 5 inhibitory LILRs and 2 pseudogenes. The LILR molecules are considerably less polymorphic than the neighbouring KIR molecules with little variation in their sequence.

Expression

LILRs are predominantly expressed in cells of the myeloid lineage; and some of the members of the family are found on plasmacytoid dendritic cells as well as lymphocytes (Table 1).

Structure, ligands and binding interactions with ligands

The LILR molecules share a similar structure with two or four extracellular immunoglobulin-like domains, a transmembrane region and a cytoplasmic tail. (Figure 1.1) LILRA molecules have a short cytoplasmic tail with no signalling domains but indeed possess a charged arginine residue to allow interaction with adaptor proteins for downstream signalling. LILRB molecules, on the other hand,

possess a cytoplasmic tail containing two to four immunoreceptor tyrosine-based inhibitory motifs (ITIMs), with sequences NxYxxV, VxYxx(L/V) or SxYxxV.

In addition to the membrane-bound LILR molecules, some members of the LILR family can also be expressed both in a membrane-bound form or as a soluble molecule, or only as a soluble molecule (i.e. LILRA3 and LILRB2).

The ligands for the LILRs have only been established for some members of the family and generally, have been shown to be HLA class I molecules. (Table 1.1) It has been suggested that LILRs can be divided into two groups based on the amino acid sequence similarity in the regions thought to bind to HLA. (4) Members of group 1 have high sequence similarity and are predicted to bind to Class I HLA molecules – members of this group include LILRB1, LILRB2, LILRA1, LILRA2 and LILRA3. All of these have been shown to bind HLA Class I molecules apart from LILRA2. (5) Group 2 molecules (LILRB3, LILRB4, LILRB5, LILRA4, LILRA5 and LILRA6), on the other hand, had poor conservation of the same residues and are thought to bind a different group of ligands, most likely not MHC Class I molecules. (4)

UL18, which is a human CMV protein that resembles HLA I has been shown to bind to LILRB1 in immunoprecipitation experiments and is thought to be one of the mechanisms by which the virus subverts the host immune response. In addition, LILRB2 has been shown to bind to CD1d, a member of a family of non-polymorphic MHC I like proteins that have a role in presentation of lipid antigens.(6) The functional implications of this remained to be established as CD1d

is primarily expressed on APCs, which also express LILRB2. It is not certain whether LILRB2 acts in a self-regulatory capacity to regulate CD1d antigen presentation or whether it is LILRB2 expression on other cells that are responsible for the inhibitory effect, in view of the fact that LILRB2 interacts with classical HLA I molecules in a *trans* manner.

In addition to viral particles, some of the LILR molecules have also been shown to bind to intact bacteria. LILRB1 and LILRB3 have been shown to bind *S. aureus* and LILRB1 binds *E. coli*, although neither of these receptors bound *H. pylori* unlike PIR-B. (7) In these experiments, NIH3T3 cells were infected with retrovirus expressing LILR (and PIR) cDNA; and incubated with fluorescently labelled live or heat-killed bacteria prior to analysis using flow cytometry or immunofluorescence microscopy. The differences in binding patterns to different bacteria suggests that these molecule may play an important role in the innate immune response against these organisms. Further functional work undertaken by the same group investigating the effects of PIR (the LILR orthologues) binding to bacteria is discussed below.

HLA-G, a non-classical HLA class I molecule is the prototypic MHC ligand for the LILRs and has high affinity for LILRB1 and LILRB2. It is discussed further below. In addition to HLA-G, LILRB1 has also been shown to bind to non-classical HLA molecules HLA-E and HLA-F, and LILRB2 to HLA-F. (8-10)

The structural interaction between HLA-G and LILRB1 and HLA-A2 and LILRB2 has been explored in detail using co-crystal structures and by nuclear magnetic

resonance. (4;11;12) LILRB1 and B2 use the two membrane distal Ig-like domains (D1 and D2) to interact with their ligands. The contact sites on the MHC molecule lie in the α3 domain and β2m; with the D1 domain interacting with the α3 domain and the D1-D2 hinge interacting with β2m. However, LILRB1 preferentially binds β2m compared to LILRB2 which preferentially binds the α3 domain, as demonstrated by its ability to bind β2m free MHC molecules. (11) As the α3 domain and β2m are the most conserved parts of the MHC molecule, this explains the wide spectrum of MHC I and MHC I-like molecules that can interact with the LILRs. In view of this, it has also been suggested that one of the functions the MHC molecules might be the generation of self-tolerance through binding of the LILRs and might play a role as important as antigen presentation to T cells. (13)

Further data has demonstrated that four different Class I HLA alleles showed different binding affinities to LILRB1 and LILRB2. (14) Using surface plasmon resonance, Shiroishi *et al* analysed the interaction of soluble LILRB1 and LILRB2 with HLA-A*1101 (with peptide AIFQSSMTK), HLA-B*3501 (with peptide IPLTEEAEL), HLA-Cw*0401 (with peptide QYDDAVYKL) and HLA-G1 (with peptide RIIPRHLQL). (14) This showed that LILRB1 and LILRB2 bound with a >20-fold difference in affinities (K_d of 2 – 45 μM) to the various HLA I molecules. LILRB1 bound with a 2 to 3 times greater affinity compared to LILRB2 for the same HLA molecule; with both LILRB1 and LILRB2 showing 3 to 4 times greater affinity for HLA-G compared to conventional class I HLA molecules. In this study, LILRB1 and LILRB2 were also shown to compete with CD8 for binding to HLA I, suggesting that LILRB1 might modulate $CD8^+$ T cell activation by blocking CD8 interaction, in addition to its function through its ITIM motifs.

The crystal structure of the D1 domain of LILRA3 has also been researched and its binding to HLA-A2 and HLA-G1 shown in surface plasmon resonance studies. (15) Crystallography showed that LILRA3 contained the essential fold necessary for HLA class I binding, one or two amino acid changes in the binding region of LILRA3 reduced binding affinity compared to LILRB1 and LILRB2; and that there was a unique self interaction between Lys42 and Glu68 in the LILRA3 D1, which was thought to contribute to the lower LILRA3 binding to classical HLA class I molecules.

Although previously thought that LILR interactions with their HLA ligands were relatively static, due to their interaction with the non-polymorphic parts of the molecule, more recent data has emerged to indicate that this might not be the case and that HLA structure could affect binding affinity. In part, previous binding studies had focused on the interaction of LILR molecules with the regions of the HLA molecule most proximal to the cell membrane. Variability in LILR binding affinity for different HLA alleles was demonstrated in data published by Jones *et al*, who undertook a study to more comprehensively evaluate the binding of LILR receptors to >90 HLA class I alleles. (5) They tested the binding by using a panel of >90 HLA class I single antigen beads, manufactured by One Lambda. (16) LILR-Fc fusion proteins were generated for LILRB1, LILRB2, LILRB3, LILRA1 and LILRA3 by cloning the extracellular portion of the LILR molecules into a vector containing the human IgG_1 Fc domain. The fusion proteins were then used in assays to determine binding to HLA present on the beads, in β2m associated and β2m free forms.

They found that allelic variation in the HLA I molecules influenced the binding affinity of all the LILR molecules investigated. LILRB1 had lower affinity for HLA-A alleles with Ala^{193} and Val^{194}, which corresponded to a known binding site for LILRB1. (4) However, the presence of the Val^{194} variation in the absence of other polymorphisms did not influence the binding affinity in other HLA molecules (i.e. several HLA-B alleles, B*35, B*51, B*58 and most HLA-C alleles). LILRB2 showed more variable binding to HLA molecules, with strongest affinity for HLA-A alleles and weakest affinity for certain HLA-B molecules, particularly B*2705 and B5701. The investigators found that a cysteine residue at position 1 and/or aspartate residue at position 9 in HLA-C molecules correlated with stronger LILRB2 binding. These positions are known to influence peptide loading within the peptide binding groove. However, similar correlations were not found for HLA-A and HLA-B alleles, nor did variations in these positions influence LILRB1 binding. LILRA1 and LILRA3 were shown to have similar binding patterns suggesting that they recognised similar binding sites.

Some of the LILR molecules have also been shown to interact with β2m-free forms of several HLA molecules. LILRB2 (but not LILRB1) and LILRA1 have been shown to bind HLA-B27 free heavy chain in flow cytometry experiments. (17;18) Crystallography and NMR binding studies has shown that LILRB2 can bind to β2m-free HLA-G, mainly through interactions with the hydrophobic site of the HLA-G α3 domain. (11) In their larger study, Jones *et al* confirmed that LILRA1, LILRA3 and LILRB2 (but not LILRB1) all bound to a wide variety of Class I HLA free heavy chains. (5) In addition, LILRA1 and LILRA3 were shown to have

increased affinity following removal of β2m, unlike LILRB2 which showed reduced binding. LILRB2 showed a preference for binding to the FHC of HLA-A whereas LILRA1 and LILRA3 showed a more marked preference for binding to HLA-C FHC. (5)

Crystal structure studies initially showed LILR interaction with the non-polymorphic regions of the HLA molecules, although subsequent work has also demonstrated that LILR binding to polymorphisms within the peptide groove affect overall affinity. The studies done to date also indicate that the different LILR molecules recognise different parts of the HLA structure.

It has been hypothesized that the differences in LILR binding affinity to different HLA alleles may alter the overall balance between activating and inhibitory signals, predisposing to disease. In the study by Jones *et al*, they suggest that the weaker binding of LILRB2 to HLA-B*2705 might be relevant in autoimmune diseases associated with HLA-B27 (e.g. ankylosing spondylitis). (5) On the other hand, this weaker affinity with HLA-B*2705 (and B*5701) may be beneficial in infectious conditions – both these alleles are associated with delayed onset of AIDS in HIV infection. (19) HLA-B*3503 (which showed strong binding to LILRB2) has conversely been associated with greater inhibition, reduced DC responsiveness and more rapid onset in AIDS. (20)

There is also data indicating that HLA-B27 homodimers and FHCs have stronger binding affinity for LILRB2 than classical class I HLA molecules; and that the membrane-distal D1 and D2 regions are critical for binding to B27 homodimers.

(21) This was not specifically described in the study by Jones et al. Relating this to the development of ankylosing spondylitis (AS), the authors suggested that as LILRB2 could inhibit osteoclast activity, (22) the increased strength of HLA-B27 homodimer binding might result in inhibition of osteoclast activity resulting in new bone formation, that is seen in AS. In addition, HLA-B27 homodimers and FHCs could also interfere with immune tolerance by *cis* recruitment of LILRB2 on dendritic cells, preventing its interaction with HLA-G, which has been shown to induce a tolerogenic phenotype. (23;24)

In view of the possible similarities in LILRA1 and LILRA3 binding sites, it has been suggested that LILRA3 (which is predicted to encode a soluble protein) may act as a competitive inhibitor of LILRA1 and reduce its activating function. (5) A similar phenomenon has been demonstrated for a soluble form of LILRB1. (25) In support of this hypothesis, LILRA3 deficiency has been described and is associated with the development of multiple sclerosis and Sjogren's syndrome. (26-28)

The binding of the so-called Group 2 LILR members is less clear. LILRA4 has been shown to bind to bone marrow stromal cell antigen 2 (BST2). (29) Engagement of LILRA4 on PDCs by its cognate ligand has been shown to result in strong inhibition of production of interferon and proinflammatory cytokines. Studies of the crystal structure of LILRB4, however, have suggested that it is both conformationally and electrostatically unsuitable for binding to MHC class I, although its cognate ligand remains to be identified. (30)

LILRB2 has been shown to interact *in cis* with MHC class I on human basophilic leukaemia cell line, KU812 which expressed LILRB2, LILRRB3 and class I HLA molecules. (31) Masuda *et al* used confocal microscopy and FRET to confirm that LILRB2 was co-localised with HLA-A, B and C on KU812 cells unlike LILRB3. Although not confirmed in human cells, experiments in murine mast cells suggest that the *in cis* interaction increases the threshold for activation signalling. (31) The inhibitory NK cell receptor Ly49A has been shown to bind *in cis* to H-2D^{d} as well, (32) although conversely, it prevents binding of Ly49A to its target cells and reduces the activation threshold instead. (32;33)

Signalling

The activating LILRA molecules possess short ITAM motifs that do not have docking sites for downstream signalling molecules. Instead, they possess single basic arginine residues which allow interaction with FcεRIγ. (34) So far, this is the only adaptor protein known to interact with LILRs, although it is possible that other adaptor proteins may share an interaction as well. Clustering of the activating receptors on the cell surface is thought to result in phosphorylation of a tyrosine residue within the ITAM sequence on FcεRIγ allowing recruitment of protein tyrosine kinase with Src2 homology (SH2), which then leads to intracellular signalling through Ca^{2+} mobilisation. (35)

However, not all the so-called "activating" receptors have activating functions. LILRA2 activation can result in inhibition of GM-CSF induced DC differentiation, antigen presentation and response to TLR stimulation in a leprosy model. (36)

LILRA4 engagement has been shown to downregulate TLR stimulation of type I interferons and other cytokines by plasmacytoid DCs. (37)

The inhibitory LILRB receptors possess long cytoplasmic tails that contain 2 to 4 ITIM motifs that can recruit the protein tyrosine phosphatase SHP-1 to modulate downstream signalling. (38-40) LILRB1 has also been shown to bind C-terminal Src kinase (Csk), which phosphorylates Src kinases at the C-terminal tyrosine residue, and is thought to regulate its function. (41) In an experimental model with transfected rat basophilic leukaemia cells (RBL), LILRB2 and LILRB3 have been shown to inhibit serotonin release following FcεRI engagement. (40) There is also data to suggest that the inhibitory LILRs may modulate signalling through FcγRI, FcγRII, HLA-DR and the B cell receptor. (39;40;42-44) The interaction of LILRB1 and LILRB2 with HLA Class I molecules may also modulate the secretion of cytokines and chemokines by CD40 stimulated monocytes. (43)

Orthologues and homologues

Homologous genes (or homologues) are two genes that are related by a common ancestral DNA sequence. If this is a result of a speciation event resulting in two different species, then the homologous genes are referred to as orthologues (compared to paralogues, which are homologous genes arising due to gene duplication). The paired immunoglobulin receptors (PIRs) in mice have been identified as LILR orthologues. The PIRs were originally identified as being homologous to FcαRI, the human Fc receptor for IgA. (45) However, these molecules were shown to not have any interaction with IgA and subsequently,

based on similarity in expression, structure and genome location were thought to be orthologues for the LILRs. (45-47) In addition, a further homologue, LILRB4 (previously known as gp49B1) in mice has also been found. (48;49)

Orthologues for the LILRs have also been described in other species. Rat PIR-A and PIR-B which share similar structural sequences to the mice homologues have been described. (50) Similar genes in chickens (CHIR-A and CHIR-B), (51-53) chimpanzees, (54) gray seals (55) and cows (56) have also been identified.

PIR genetics, expression and protein structure

The PIR molecule are encoded at the proximal end of mouse chromosome 7, which is syntenic to the LRC on human chromosome 19q13.3-13.4. (46;47) PIR-A is encoded by at least 6 *Pira* genes and PIR-B (also known as LIR-3 and gp91) is encoded by *Lilrb3* (also known as *Pirb*). (57)

PIR-A and PIR-B are present on cells of the myeloid lineage (including mast cells, dendritic cells, macrophages, granulocytes and osteoclasts) and B cells (which express PIR-B but not PIR-A), but not on thymocytes, T cells or NK cells. (22;45;46;58) PIR-B has also been shown to be expressed transiently on early prethymic progenitors of T cells, NK cells and DCs although its exact role in this developmental stage remains unknown. (59) They are typically expressed in a pair-wise fashion. (58) However, frequently there is greater cell surface expression of PIR-B compared to PIR-A. (31;58;60) Cell surface expression of PIR-B varies depending on the state of activation and differentiation of myeloid or B cells;

mature naïve B cells express PIR-B exclusively, and their levels are highest on marginal zone B cells. (58;60;61) Experiments looking at the expression of PIR-A and PIR-B on either *Lilrb3* -/- or *Fcrg* -/- mice have shown dominant expression of PIR-B (compared to PIR-A) on splenic macrophages, splenic DCs and bone-marrow derived cultured mast cells; with only PIR-B expression on splenic B cells. (60;62) Expression levels of PIR-A and PIR-B were also consistent with deletion of the other paired receptor, suggesting that the surface expression of the two molecules is fairly consistent for a given cell type in resting conditions, with PIR-B likely to have a dominant inhibitory effect through continuous interaction with the MHC. (63)

PIR-A and PIR-B have very similar extracellular structures with 92% identity in their ectodomains. Both PIR-A and PIR-B are type I transmembrane glycoproteins with six extracellular immunoglobulin-like domains. PIR-B possesses a hydrophobic transmembrane region and four intracellular ITIM or ITIM-like sequences.(45;46) In contrast, PIR-A possesses a different pre-transmembrane, transmembrane regions and cytoplasmic sequences with ITAM motifs. (46) The transmembrane region in PIR-A has a positively charged arginine residue which allows association with homodimeric FcγR. This interaction with FcγR is necessary for expression of PIR-A on the cell surface and delivery of an activating signal. (58;64;65)

Comparison of the extracellular sequences of PIR from several strains of mice (129/Sv, B10.A and BALB/c) show a high degree of sequence similarity, although multiple amino acid polymorphisms have been noted, similar to the LILR

molecules. (39;46) However, it has not yet been determined if these polymorphisms affect the binding affinity of the PIR molecule.

Although PIR-B is thought to be related to LILRB1 and LILRB2, it only has about 50% amino acid homology and has six Ig-like domains, unlike the 4 present in LILRB. (46;63) Similarly PIR-A also has six Ig-like domains unlike the four found in the orthologous LILRA2.

Expression in neuronal tissue

In addition to their role in the immune system, PIR-B has also been found to be broadly expressed in neuronal tissue. (66;67) Further work by Atwal *et al* has also shown that the PIR-B (and human LILRB2) can bind the myelin inhibitor neurite outgrowth inhibitor protein (Nogo66). (67) In addition, PIR-B also bound other myelin inhibitors, myelin-associated glycoprotein (MAG or Siglec-4) and oligodendrocyte myelin glycoprotein (OMgp). From these experiments, it was postulated that PIR-B (and possibly LILRB2, although there is little data on this) also functions as a necessary receptor for neurite inhibition and plays a role in neuronal regeneration.

PIR Ligands

PIR-B (and most likely PIR-A) bind to murine H-2 (MHC I) molecules although the exact interaction with the MHC remains to be determined. In surface plasmon resonance experiments, PIR-B has been shown to bind monomeric H-2 molecules at

affinities of K_d= 1.9 to 5.6 x 10^{-7}M. (68) These values are similar to the binding affinities between IgG and its low-affinity receptors, FcγRIIB and FcγRIII. (69) Recombinant PIR-B has also been shown to bind to murine β2m, (68) which suggests that the interaction is likely to be the same as that of the LILRB molecules, i.e. involving the constant α3 domain of the MHC and β2m. (14) In addition, the PIR molecules have also been shown to bind to human HLA-G. (68;70)

In addition to MHC, the PIR molecules can also bind non-self ligands. Similar to pattern recognition receptors (e.g. TLRs, scavenger receptors and lectins), PIR-B can bind *S. aureus*, *E. coli* and *H. pylori*. (7) However, PIR-B was not able to bind *B. subtilis*, *L. monocytogenes* or *P. aeruginosa*. (7) In contrast, only one isoform of PIR-A, PIR-A1 was shown to bind to bacteria. The differential recognition of different bacterial species suggests that the PIR molecules do play a role in innate immune responses.

PIR Signalling

In a rat mast cell line (RBL-2H3) transfected with PIR-A, engagement of the receptor with antibodies results in calcium mobilisation and degranulation. (71) Activation signalling via PIR-A in this model was mediated through associated molecules including FcγR and the FcεRIβ chain; the residues Arg626 and Glu643 are critical for PIR-A activating function and association with the FcR molecules. (64) In experiments with the ligand for PIRs, binding of H-2 tetramers induced phosphotyrosylation of FcRγ in peritoneal macrophages. (68) This phosphotyrosylation was further increased in mice that were PIR-B deficient,

suggesting that PIR-A could deliver an intracellular activation signal via FcRγ after engagement with its ligand, and that this signal was continuously blocked by interaction with PIR-B expressed on the same cell. (68)

PIR-B exerts its inhibitory signalling effect by recruitment of the SH2-containing tyrosine phosphatases, SHP-1 and/or SHP-2 to the phosphorylated ITIM motifs. (72-74) Although *in vitro* experiments have shown binding of peptides in third and fourth ITIM to SHP-1, SHP-2 and SHIP-1, (47) inhibition experiments show loss of PIR-B function in SHP-1 and SHP-2 double negative DT40 chicken B cells, but not loss of function in SHIP-deficient cells. (75) This implied that PIR-B can negatively regulate B-cells through non-redundant functions in SHP-1 and SHP-2 but not SHIP. (75) It has also been noted that PIR-B is constitutively phosphorylated in macrophages and B cells regardless of the activation status of the cell, and that PIR-B in splenocytes was constitutively associated with SHP-1 and Lyn. (76) This suggests that PIR-B inhibition does not require co-ligation with the B-cell receptor by a shared ligand.

PIR-B has been shown to bind to MHC I *in cis* in fluorescence energy transfer (FRET) experiments done on mast cells. (31) Cis interactions have also been demonstrated on osteoclast precursor cells, B cells and DCs. (22;77) Mast cell stimulation by LPS or IgE cross-linking were shown to be suppressed by *in cis* binding of PIR to MHC I. (31) In addition, osteoclast development is regulated by the PIR-B *cis* interaction with MHC I on the surface of osteoclast precursor cells. (22) PIR-B has been shown to bind *in trans* to MHC I in the immunological synapse. (77)

Functional effects

The availability of PIR-B knockout mice has enabled better understanding of the functional effects of these molecules. In *in vitro* experiments, B cells, neutrophils and macrophages with a Pirb knockout have been shown to be hyper-responsive. Pirb -/- splenic B cells have increased proliferation when stimulated with anti-BCR antibodies, and this effect becomes more marked with the addition of blocking antibodies against FcγRIIB. (60) This was taken to indicate that the inhibitory effect of these molecules was additive, possibly because PIR-B recruited SHP-1 and FcγRIIB recruited SHIP. Pirb -/- B cells were also shown to have increased phosphorylation of proteins, suggesting that there was constitutive activation. (60) In keeping with this, Pirb-/- mice also had a greater increase in IgM when vaccinated with T-independent antigens (trinitrophenol-Ficoll and trinitrophenol-LPS). (60)

PIR-B is thought to be important in the regulation of neutrophil and macrophage integrin signalling. Pirb-/- neutrophils have been shown to have an increased respiratory burst, secondary granule release and hyperadhesive phenotype after engagement with integrin. (78) In addition, bone marrow derived macrophages form Pirb-/- mice also demonstrated a hyperadhesive phenotype and more rapid spreading after cross-linking with β2 integrins. (78)

In terms of antibody responses, Pirb-/- mice demonstrate an increased response to vaccination with TNP-keyhole limpet haemocyanin or ovalbumin with alum as an

adjuvant. (60) There was both an elevated IL-4 and reduced IFN-γ cytokine response and increased production of IgG1 and IgE. The reason for this difference was thought to be due to the immature phenotype of DCs generated in Pirb-/- mice. Bone marrow derived DCs from the knockout mice showed an immature phenotype when assessed for surface MHC II, CD80 and CD86 expression, and had reduced production of IL-12 on antigen loading. Tyrosine phosphorylation of PIR-B was altered on exposure to GM-CSF and these profiles were different in Pirb-/- cells - suggesting that the H-2 interaction with PIR-B could be significant for DC maturation and control of humoral responses. (60)

However, Pirb-/- DCs have been shown to generate greater activation in $CD8^+$ T cells (77) despite their immature phenotype and inability to fully activate $CD4^+$ T cells. (60)The reason for this phenomenon is thought to be due to PIR-B on DCs competing with CD8αα on T cells for interaction with MHC I on DCs (as demonstrated by surface plasmon resonance). (77) Hence, the absence of PIR-B results in greater activation of $CD8^+$ T cells, and this has been shown to also result in greater rejection of skin grafts and tumours *in vivo*. (77) However, it is not certain whether PIR-B is more likely to interact *in cis* with the MHC on DCs or *in trans* with the MHC on T cells in the immunological synapse.

In view of the interaction between human HLA-G and PIR-B, work has been done to determine the effects of this interaction, particularly as HLA-G is likely to play a significant role in feto-maternal tolerance by inhibiting NK cells. BMDC from HLA-G transgenic mice have poor maturation, with increased phosphorylation of PIR-B. Similarly, HLA-G tetramers have been shown to inhibit in vitro maturation

of murine BMDC. (70) Whether a similar phenomenon occurs in the mouse system with murine MHC Class Ib molecules (e.g. Qa-1) remains to be determined.

Pirb-/- knockout mice have also been used to investigate the consequences on immune tolerance in a GVHD model. (68) Pirb-/- or wild type mice were irradiated and received allogeneic splenocytes intravenously. The Pirb-/- mice developed accelerated, lethal GVHD due to increased activation of recipient DCs, with upregulation of PIR-A, increased production of IFN-γ and proliferation of donor cytotoxic T cells.

In a rat model of cardiac transplantation, Liu *et al* demonstrated the importance of $CD8^+$ T suppressor cells for tolerance. (79) These $CD8^+$ T suppressor cells induced upregulation of PIR-B in dendritic cells and heart endothelial cells, resulting in tolerance similar to the induction of LILRB2 and LILRB4 in human dendritic and endothelial cells by human CD8+ FOXP3+ T suppressor cells. Furthermore, when heart allografts with PIR-B positive endothelial cells were transplanted into a second allo-recipient, there was no rejection.

It has been shown in eosinophils that PIR-B potentially has dual functionality and can perform both an activating and inhibitory role depending on the circumstances and signals resulting in activation. (80) Pirb was shown to be upregulated in an eosinophil dependent manner in the lungs of allergen-challenged and IL13-overexpressing mice. Eosinophils had high levels of PIR-B expression and Pirb-/- knockout mice had increased eosinophils in the gastrointestinal tract. Eotaxin dependent eosinophil chemotactic responses were negatively regulated by PIR-B;

however, leukotriene B4 (LTB4) stimulation in Pirb-/- eosinophils resulted in decreased chemotactic responses. (80) Furthermore, it was shown that LTB4, but not eotaxin stimulation, resulted in PIR-B recruitment of multiple activating kinases; and that Pirb-/- eosinophils activated by eotaxin had increased ERK1/2 phosphorylation whereas LTB4 stimulation resulted in reduced ERK1/2 phosphorylation.

PIR-B has been shown to play a role in responses to bacteria, and this has been demonstrated in responses to *Staphylococcus aureus* and *Salmonella enterica*. (7;81) Pirb-/- knockout mice have greater susceptibility to Salmonella infection in part due to failure of Pirb-/- macrophages to control intracellular replication of the organism, thought to be due to imbalance in the signals generated by PIR-A and PIR-B in the response to bacteria. (81) Interference with PIR-B binding to *S. aureus* (either by blocking monoclonal antibodies or gene deletion) resulted in increased TLR-mediated inflammation in response to bacteria, although the significance of this finding is unclear. (7) Bone marrow derived macrophages produced higher levels of IL-6 and TNF-α with suppression of IL-10 in response to stimulation with *S. aureus* with either Pirb-/- knockout or blockade with monoclonal antibody. (7) Interference with PIR-B function did not make any difference to TLR responses on exposure to LPS or PAM_3CSK_4. There was a similar enhancement of IL-6 production on exposure of Pirb-/- macrophages to *H. pylori* but not *P. aeruginosa*, again providing evidence that PIR-B discriminates between different bacteria. (7)

PIR-B regulation is also relevant in the TLR9 system in B-1 cells. (61) PIR-B exerts its effects at the level of Btk; PIR-B phosphorylation is enhanced by activation of

Lyn (76) via the TLR9 pathway and this results in increased recruitment of SHP-1 to the phosphorylated ITIMs of PIR-B resulting in Btk dephosphorylation, (82) which in turn attenuates the phosphorylation level of NF-κB p65RelA. (83;84) It has been suggested that this has potential implications in autoimmunity as B-1 cells are the main producers of rheumatoid factors and other autoantibodies; (85) and manipulating the PIR-B inhibitory system for therapeutic benefit while maintaining adequate TLR9 sensing of microbes would be an important consideration. (86)

Murine LILRB4

Murine LILRB4 is expressed on mast cells, neutrophils and macrophages and possesses two Ig-like domains as well as two intracellular ITIM motifs , similar to the PIR/other LILR molecules. (48;49;87) Its natural ligand has been identified as the integrin αvβ3. (88) It has been shown to inhibit *in vitro* activation of mast cells via IgE by recruitment of SHP1 to the cell membrane. (89) *Lilrb4-/-* knockout mice are more prone to severe IgE mediated mast cell dependent anaphylactic reactions compared to wild type mice (90) and also mast cell-dependent inflammation due to stem cell factor (SCF) interaction with Kit. (91) This indicates that LILRB4 can block inflammation both caused by Fc receptors signalling through ITIMs but also signalling through a receptor tyrosine kinase.

Additionally, LILRB has been shown to play a role in modulating neutrophilic inflammation as well. *Lilrb4 -/-* mice demonstrate greater inflammatory responses in LPS and autoantibody induced neutrophilic inflammation. (92;93) Wild type

mice have a rapid upregulation of LILRB4 in response to LPS, suggesting that this may represent a regulatory response to prevent excessive inflammation. (92)

Lilrb4 -/- mice are also more prone to develop eosinophilic pulmonary inflammation following inhaled sensitisation to ovalbumin and LPS, and ovalbumin airway challenge. (94) These mice had increased levels of ovalbumin-specific IgE and Th2 cytokines from ovalbumin restimulated cells from lymph nodes. Following sensitisation or challenge, LILRB4 was upregulated on MHC II^{high} $CD86^{high}$ OVA-bearing DCs in lymph nodes draining the lung. Conversely, in *Lilrb4-/-* mice, there were more mature DCs and IL4-producing lymphocytes in the draining lymph nodes. Adoptive transfer of OVA-pulsed *Lilrb4-/-* bone marrow derived DCs into *Lilrb4+/+* mice resulted in increased allergic lung inflammation, compared to bone marrow derived DCs from *Lilrb4+/+* mice. Taken together, these data suggest that upregulation of LILRB4 occurred in the maturation and migration of pulmonary DCs to the lymph nodes; and that LILRB4 ameliorated the ability of these DCs to generate pathological Th2 inflammation. (94)

LILRs and influence on immune responses/functional effects

Antigen presenting cells

Dendritic cells are potent antigen presenting cells (APCs) which are capable of initiating primary immune responses and determining the subsequent outcome of the immune response. (95;96) DCs originate from haematopoietic stem cells in the

bone marrow and can broadly be divided into two major differentiation pathways depending on the expression of CD11c. (95) $CD11c^+$ DC population includes blood myeloid DCs, Langerhans cells and interstitial DCs. The $CD11c^-$ DC population are referred to as plasmacytoid DCs, and express CD123 (IL3Rα).

The LILRs vary in their expression on various types of APCs. LILRA2, LILRB1, B2, B3 and B4 are found on myeloid DCs whereas LILRA4 appears to be restricted to PDCs. (37) It is also not known at present how engagement of multiple different LILRs on the cell would affect subsequent downstream events. However, there has been recent work exploring the contribution of some of these molecules towards DC function.

The cell surface expression of LILRB1 (and to a far lesser extent, LILRB2 and LILRB4) has been shown to increase or be present during the differentiation process of monocytes into DCs *in vitro*. (97-99) Engagement of LILRB1 by monoclonal antibodies or the CMV protein, UL18 during the process results in failure of DC maturation and inability to stimulate primary and memory T cell responses. The CD80-CTLA4 costimulatory pathway was thought to play a role in this mechanism as blockade reversed the effect of LILRB2 engagement. (99) The cytokine profile and migratory capacity of the DCs were also affected. (97-99)

LILRB2 and LILRB4 have also been shown to play a role in the context of tolerogenic DCs generated by exposure to alloantigen specific $CD8^+$ $CD28^-$ T suppressor (Ts) cells. (100;101) These DCs express high levels of LILRB2 and LILRB4 and show a phenotype with reduced levels of the costimulatory molecules

CD80 and CD86, as well as impaired ability to activate T cells. (100;101) In addition, these DCs are capable of anergizing allospecific $CD4^+$ $CD45RO^+$ $CD25^+$ T cells converting them into regulatory T cells which can then further propagate the suppression cascade. LILRB2 and LILRB4 may produce their effects through different mechanisms; LILRB2 binding to its ligand results in failure of costimulatory molecule and MHC molecule upregulation (24;100) whereas LILRB4 may provide its signal through its T cell ligand as there is data to suggest that soluble forms of the receptor are capable of providing inhibitory stimuli. (102;103)

In addition to the inhibitory LILRB family members, some of the so-called "activating" LILRAs also have inhibitory effects on DCs as described above. LILRA2 has been shown to inhibit MoDC differentiation, antigen presentation and response to TLR stimulation (36) whereas LILRA4 engagement results in reduction of type I interferon secretion by PDCs. (37)

Although engagement of some of the LILRs has been shown to affect cytokine production, conversely cytokines can influence LILR expression; IL10 and interferon-α have been shown to upregulate LILRB1, LILRB2 and LILRB4 to generate tolerogenic DCs. (23;104-107)

The differential recognition of HLA molecules by LILR may represent part of the explanation how these molecules regulate and fine tune immune responses. For example, enhanced HLA FHC recognition by LILRA1 and LILRA3 may be relevant in an inflammatory context. Increased FHC expression is found with lymphocyte and APC activation; (108-113) HLA-C is prone to formation of FHC

due to its stability in the absence of β2m and this form is specifically upregulated on macrophages during differentiation. (114-117) Furthermore, class I HLA molecules clustering on activated T cells is influenced by increased FHC levels; (113;118;119) and this clustering can potentially enhance receptor recognition and downstream activity. (120)

Human leukocyte antigen G (HLA-G)

HLA-G is one of the non-classical HLA Class I molecules and shares a structure similar to the rest of them, with 3 α domains associated with β2m, although it has markedly less polymorphism. It was first discovered in the context of expression on cytotrophoblast cells, acting as a ligand for inhibitory receptors present on uterine NK cells, and thought to play a role in feto-maternal tolerance. (121) It differs from other MHC class I molecules by its lower degree of polymorphism, restricted tissue distribution, expression as 7 different isoforms due to alternative mRNA splice variants and its contribution as an immunosuppressive molecule. (122)

HLA-G only has 14 different protein variants encoded by 44 alleles; many of which are silent mutations. (123) However, polymorphism in the noncoding regions has been shown to alter HLA-G expression with functional effects. (124) The 3' UTR region which plays an important role in regulation of HLA-G expression has been shown to have 2 main polymorphic sites: a 14bp insertion associated with lower, but more stable mRNA production and a +3142 SNP, which is thought to act as a target for microRNA. (123) HLA-G polymorphisms have been shown to be

associated with rejection in heart transplants, inflammatory bowel disease, recurrent spontaneous abortion, pemphigus vulgaris and sarcoid. (123;125-128)

HLA-G transcription can be found in most cells and tissues in healthy individuals, although translation is restricted to specific sites including trophoblast, thymus, cornea, nail matrix, pancreas and erythroid and endothelial precursors. (129) Neo-expression of HLA-G has been seen following organ transplantation, or in malignancy, viral infections and autoimmune disease. (129)

HLA-G can be expressed as 7 different isoforms as a result of alternative splicing of the primary mRNA transcript. (129) Four of these isoforms (G1 to G4) are membrane-bound and three (G5 to G7) are soluble. In addition, the membrane-bound forms of HLA-G can be shed through proteolysis. HLA-G1 and G5 have a structure similar to the classical HLA molecules with 3 globular α domains that associate with β2m. The remaining isoforms lack one or more of the globular domains (although all contain the α1 domain) and should not associate with β2m or peptide. HLA-G (similar to HLA-B27) is also known to form homodimers (and potentially homotrimers) through disulphide bond formation between 2 unique cysteine residues at position 42 and 147. (130-132) HLA-G dimerisation has been shown to increase binding affinity to LILRB1 and LILRB2 potentially by generating an oblique orientation exposing these binding sites. (130) In addition, HLA-G dimers have also been shown to have more potent immunosuppressive effects. (132;133)

The principal ligands for HLA-G are LILRB1, LILRB2 and KIR2DL4.(39;40;134) In addition, HLA-G binding to CD8 has also been demonstrated. (135) LILRB1 is expressed on all monocytes/dendritic cells, B cells, some T cells and some NK cells (39) whereas LILRB2 is only expressed on monocytes/DCs. (40) KIR2DL4 is expressed on $CD56^{bright}$ NK cells, which constitute the majority of uterine NK cells but only a minority of peripheral cells. (136-138) Through these receptors, HLA-G can effectively interact with a broad array of immune cells.

The main physiological function of HLA-G is thought to be facilitation of maternal tolerance of the foetus. HLA-G has been shown to protect cytotrophoblast cells from maternal NK cells through interaction with inhibitory receptors on the NK cells. (121) In addition, HLA-G secretion by embryos appears to be necessary for implantation and pregnancy in *in vitro* fertilisation. (139;140) Given the broad expression of HLA-G ligands, its role in pathological scenarios, particularly in transplantation and oncology has also been investigated. HLA-G has been studied in the context of heart, kidney, liver, combined liver-kidney transplants and as would be expected, higher expression of HLA-G in the graft or in plasma was associated with better allograft acceptance. (141-147) Conversely, in malignancy, HLA-G expression would be expected to result in tumour tolerance and poorer outcomes. To date, HLA-G expression has been shown to protect tumour lesions from cytolysis (148-150), to be associated with malignant ascites in ovarian and breast carcinomas (151), to be upregulated in malignant melanoma (152), and to signify poorer outcomes and immunodeficiency in chronic lymphocytic leukaemia (153); and shortened survival time in colorectal cancer. (154)

HLA-G and LILRs

β2m associated HLA-G is a high affinity ligand for LILRB1 and LILRB2, which is enhanced by dimerisation through disulphide bonds. (14) In view of this, it would be expected that situations where expression of HLA-G occurs would result in dominant immunosuppressive effects. In addition, HLA-G free heavy chains can bind to LILRB2 (but not LILRB1) and exert immunosuppressive effects as well. (155) It has also been shown that expression of HLA-G can upregulate LILRB1, LILRB2 and LILRB4 expression; (156) and that IL10 upregulates both LILRB molecules and HLA-G. (104;106;157;158)

Potential therapeutic implications

The widespread distribution of the LILRs on multiple immune cells suggests that they are likely to play a role in many disease processes. Although data is beginning to accumulate, several studies have demonstrated the association and influence of LILRs in transplantation, autoimmune disease, infection and tumour evasion (summarised in Table 1.2).

Consequently, the development of therapeutic manipulation utilising the inhibitory LILRs for immunosuppressive effects, for example through its natural ligands, including HLA-G or by artificial constructs such as monoclonal antibodies could be beneficial in various scenarios including transplantation, autoimmune and inflammatory disease. Conversely, engagement of the activating LILRs could be

used in various scenarios where enhancement of the immune system would be beneficial, for example, malignancy and infectious diseases.

This represents an exciting area for development in that there is much that remains to be discovered about this family of molecules, with potentially significant benefits and uses in many clinical scenarios.

Hypothesis

The main hypothesis of the project is that genetic polymorphisms (both coding and non-coding) in the LILR molecules are likely to affect their expression levels and the function of immune cells. At present, there is some although very limited data to indicate that polymorphisms in the LILRs (similar to other immune system genes) can influence individual susceptibility to rheumatological disease and no work on the role of polymorphisms in the context of antigen presenting cells, particularly monocytes and dendritic cells which play important roles in determining the nature of immune responses.

Consequently, it is hoped that a greater understanding of the basic science will enable development of therapeutic modalities. To this end the other part of the project has also focused on the development of a therapeutic molecule, the "G-body" and testing its use in alloimmune responses. The G-body was conceived as a bifunctional molecule with two "business ends" to exploit the potential immunosuppressive properties of the LILRs for use in an allogeneic setting. One business end would comprise HLA-G, the known highest affinity ligand for

LILRB1 and LILRB2 to exploit the immunosuppressive potential of these molecules. The other business end would comprise an anti-HLA mAb portion or whole molecule (HLA-A2 was used in this project for proof of concept) to allow localisation of the G-body to targets bearing the allogeneic HLA. This combined molecule would allow localisation of the immunosuppressive signal delivered through the LILRs by HLA-G to allogeneic cells bearing foreign MHC molecules; hopefully converting an activating response into an inhibitory one and promoting allogeneic tolerance.

Aims and Objectives

The project has two broad aims:

(i) to explore the basic science underlying how genetic polymorphisms affected the expression of LILR molecules and the functional consequences of this; particularly in the context of antigen presenting cells; and

(ii) to develop a therapeutic molecule which targets LILRs (the G-body) and test its effect on functional responses.

The specific objectives of the project are:

1. Establish baseline levels of expression of various LILR molecules on antigen presenting cells
2. Test the function of antigen presenting cells with and without engaging the LILRs
3. Obtain genomic DNA for genetic polymorphism typing of the LILRs
4. Compare the expression levels and functional results with the polymorphisms to determine if any correlations exist
5. To construct the G-body molecule and confirm its characteristics
6. To test the effect of the G-body on functional responses

Figures

Figure 1.1

Members of the leukocyte immunoglobulin-like receptor (LILR) family. Members are divided into activating 'A' receptors with a short cytoplasmic tail and charged arginine residue in the transmembrane region, or inhibitory 'B' receptors with a long cytoplasmic tail and two to four ITIM domains. Members of the LILR family have also been divided into Group 1 and Group 2 receptors on the basis of conserved residues shared with LILRB1. Group 1 members are thought to bind MHC Class I molecules and Group 2 are thought not to.

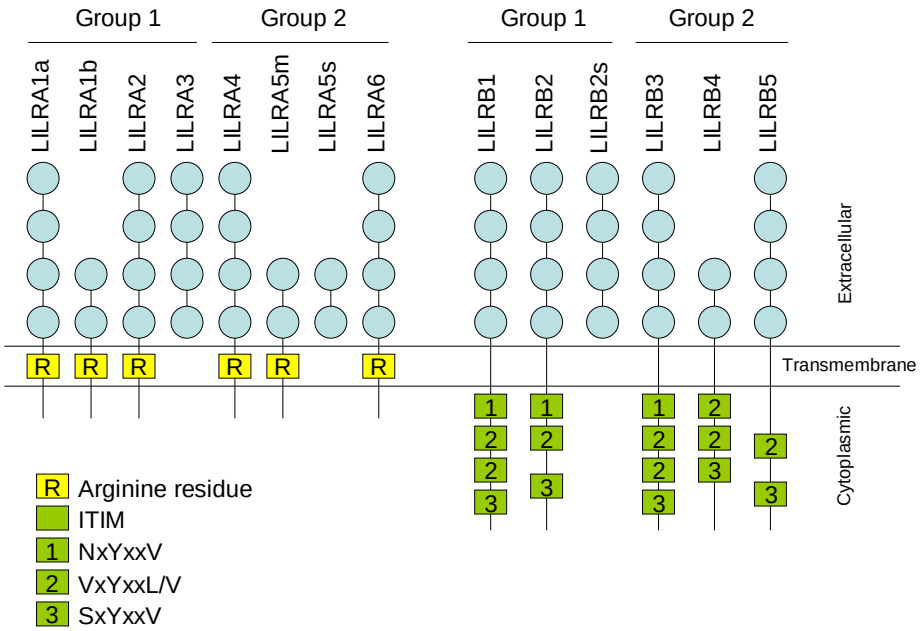

Tables

Table 1.1

A summary of the various LILRs, their alternative names, the number of immunoglobulin (Ig) domains, cytoplasmic tail and ligands they possess and their cellular distribution

	Alternative names	Number of Ig domains	Ig domains and tail	Ligands	Expression
LILRA1	LIR6, CD85i	4	Arginine+TM	HLA Class I, with increased affinity for free heavy chains	Macrophages
LILRA2	ILT1, LIR7, CD85h	4	Arginine+TM	HLA Class I	Monocytes, macrophages, dendritic cells, NK cells, basophils, eosinophils

	Alternative names	Number of Ig domains	Ig domains and tail	Ligands	Expression
LILRA3	ILT6, LIR4, CD85e, HM43, HM31	4	Soluble form only	HLA Class I, with increased affinity for free heavy chains	Only expressed in soluble form, produced by monocytes
LILRA4	ILT7, CD85g,	4	Arginine+TM	Bone marrow stromal cell antigen 2 (BST2)	Plasmacytoid dendritic cells
LILRA5	ILT11, LIR9, CD85f, LILRB7	4	Arginine+TM	Unknown	$CD14^{+}$ monocytes
LILRA6	ILT8, CD85b, LILRB6	4	Arginine+TM	Unknown	Unknown

	Alternative names	Number of Ig domains	Ig domains and tail	Ligands	Expression
LILRB1	ILT2, LIR1, CD85, CD85j, MIR7	4	4 ITIM, Csk	HLA-A, HLA-B, HLA-F, HLA-G HCMV UL18 protein *S. aureus, E. coli*	Monocytes, macrophages, dendritic cells, osteoclasts, eosinophils, B cells, T cells, NK cells, placental stromal cells
LILRB2	ILT4, LIR2 CD85d, MIR10	4	3 ITIM	HLA-A, HLA-B, HLA-F, HLA-G CD1d	Monocytes, macrophages, dendritic cells, osteoclasts, basophils, eosinophils, placental vascular smooth muscle
LILRB3	ILT5, LIR3, CD85a, HL9	4	4 ITIM	*S. aureus*	Monocytes, macrophages, dendritic cells, osteoclasts, basophils, eosinophils

	Alternative names	Number of Ig domains	Ig domains and tail	Ligands	Expression
LILRB4	ILT3, LIR5, CD85k, HM18	2	3 ITIM	Unknown	Monocytes, macrophages, dendritic cells, osteoclasts
LILRB5	LIR8, CD85c	4	2 ITIM	Unknown	Unknown
LILRP1	ILT9, CD85b, LILR6AP	4	Pseudogene		
LILRP2	ILT10, CD85m	4	Pseudogene		

Table 1.2

Known disease associations of various LILRs

LILR	Disease association
LILRA1	The defective function of DCs in patients with progressive HIV infection is correlated with downregulation of LILRA1 (159)
LILRA2	LILRA2 Delta 419-421 isoform associated with increased risk of SLE and microscopic polyangiitis in Japanese individuals (160)
	LILRA2 expression correlates with lepromatous leprosy; functionally LILRA2 suppressed innate defences by skewing monocyte cytokine production from IL12 to IL10 and by blocking TLR induced antimicrobial activity(161)
	LILRA2, B2 and B3 levels in RA synovium was upregulated and decreased in patients who responded to treatment (162)
LILRA3	Homozygous LILRA3 deficiency more prevalent in patients with multiple sclerosis (7.1%) than in healthy blood donors (3.8%) (27) Increase prevalence of LILRA3 deficiency in multiple sclerosis confirmed in further study in Spanish patients. (28)
	Homozygous LILRA3 deficiency is more prevalent in patients with Sjogren's syndrome (8%) compared to healthy controls (3%) (26)
LILRB1	In CMV positive lung transplant recipients, increase in percentage of peripheral blood lymphocytes expressing LILRB1 preceded detection of CMV DNA (163)
	Likely to play a role in HLA-G mediated allograft tolerance (142;164)
	B cells in patients with SLE have reduced expression of LILRB1; in

	addition LILRB1 had reduced inhibitory activity in $CD4^+$ and $CD8^+$ cells (165)
	LILRB1 found to be coexpressed with HLA-G in brain lesions of patients with multiple sclerosis (166)
	Increased expression of LILRB1 on NK cells and $CD8^+$ cells in HIV infection (167;168)
	Proportion of B cells expressing LILRB1 is increased in patients with severe malaria (169)
	Likely to be involved in the mechanism of HLA-G mediated tumour evasion (149;170;171)
	LILRB1 polymorphisms are associated with susceptibility to RA in HLA-DRB1 shared epitope negative subjects in a Japanese population (172)
	HIV-1 'elite controllers' have unique upregulation of LILRB1 and LILRB3, higher than HIV-1 progressors or uninfected subjects (159)
LILRB2	Increased expression on DCs involved in the T cell suppression cascade related to allograft tolerance (23;100)
	Likely to be involved in HLA-G mediated suppression of allo-responses (142;173)
	LILRA2, B2 and B3 levels in RA synovium was upregulated and decreased in patients who responded to treatment (162)
	LILRB2 present in synovial monocytes and T and B cells of patients with spondyloarthritis, and their role as ligands for HLA-B27 homodimers might be relevant to the disease (18)
	LILRB2 upregulated on monocytes in patients with HIV and thought to be due to increased IL10 levels (107)

	HIV-1 viral escape mutant results in increased MHC-peptide binding to LILRB2 and a tolerogenic phenotype of myelomonocytic cells (174)
	LILRB2 and LILRB4 expression increased in B cells of patients with chronic lymphocytic leukaemia and may play a role in T cell suppression (175)
	37.1% of tumour tissue samples from patients with non-small cell lung cancer expressed LILRB2 (176)
	Likely to be involved in the mechanism of HLA-G mediated tumour evasion (149;170;171)
	Infection with *Salmonella typhimurium* or TLR stimulation with Salmonella components results in upregulation of LILRB2 and LILRB4 (177)
	HLA-B*35 Px subtypes increase the rate of HIV-1 disease progression via LILRB2-dependent functional inhibition of DCs (20)
LILRB3	HIV-1 'elite controllers' have unique upregulation of LILRB1 and LILRB3, higher than HIV-1 progressors or uninfected subjects (159)
LILRB4	Increased expression on DCs involved in the T cell suppression cascade related to allograft tolerance (23;100)
	LILRB2 and LILRB4 expression increased in B cells of patients with chronic lymphocytic leukaemia and may play a role in T cell suppression (175)
	LILRB4-Fc construct prevented islet cell allograft rejection in a NOD/SCID mouse model (103)
	Patients with melanoma, and carcinomas of the colon, rectum, and pancreas produce soluble LILRB4 which results in generation of $CD8^+$ T suppressor

	cells and impairs T cell responses in mixed lymphocyte reactions (102)
	Infection with *Salmonella typhimurium* or TLR stimulation with Salmonella components results in upregulation of LILRB2 and LILRB4 (177)

Chapter 2: Materials and methods

In addition to the research materials and experimental protocols used in the project, this chapter also contains results of experiments designed to optimise the assays used as well as confirm data already known.

Cell Lines

The THP-1 (178) cell line was used in both the qPCR and luciferase assays. It is an acute monocytic leukaemia cell line obtained from ATCC. The cells were maintained in RPMI-1640 supplemented with 10% FCS, 300 mg/l L-glutamine and 100U/ml penicillin/ 0.1mg/ml streptomycin (all cell culture media from Sigma).

COS7 (179) and 293T (180) cell lines were used for transient transfection experiments. Both were obtained from ATCC, maintained in DMEM supplemented with 10% FCS, 300 mg/l L-glutamine and 100U/ml penicillin/ 0.1mg/ml streptomycin and passaged with Trypsin-EDTA (Sigma) just prior to reaching confluence. Additionally, COS7 cells were adapted to serum free medium growth by gradual reduction of serum concentration and replacement with VPSFM media (Invitrogen). These cells were passaged using TrypLE (Invitrogen).

The K562 (181;182) cell line is a myelogenous leukaemia cell line growing in suspension obtained from HPA Cultures. Cells were maintained in RPMI 1640 supplemented with 10% FCS, 300 mg/l L-glutamine and 100U/ml penicillin/ 0.1mg/ml streptomycin. K562 cells transfected with HLA-A2, HLA-A24 and HLA-

B8 in a pcDNA3.1(+) vector and selected with G418 at 700 μg/ml were a kind gift from Mark Peakman. Additionally, K562 cells were stably transfected with pcDNA3.1(+) and LILRB1, LILRB2 and HLA-G to be used in further experiments.

The JEG3 cell line (183) is an adherent human placental choriocarcinoma cell line obtained from HPA Cultures and was used as a source of HLA-G mRNA for cloning experiments. It was cultured in EMEM supplemented with 10% FCS, 300 mg/l L-glutamine, non-essential amino acids and 100U/ml penicillin/ 0.1mg/ml streptomycin; and passaged with Trypsin-EDTA (Sigma) just prior to reaching confluence.

BB7.2 (184), W6/32 (185), ZM3.8 (42) and 42D1 (40) are hybridomas producing monoclonal antibodies against HLA-A2, pan-HLA Class I, LILRB4 and LILRB2 respectively. These were maintained in DMEM supplemented with 10% FCS, 300 mg/l L-glutamine and 100U/ml penicillin/ 0.1mg/ml streptomycin. For generation of antibody, hybridomas were left to proliferate in medium for 7 days prior to the supernatant being harvested for antibody purification. BB7.2 and W6/32 were obtained from ATCC. ZM3.8 and 42D1 were a kind gift from Marco Colonna.

Generation of stable K562 transfectants with LILRB1, LILRB2 and pcDNA3.1(+)

K562 cells were transfected with pcDNA3.1(+) vectors containing LILRB1, LILRB2 or empty vector alone as a control using the Attractene transfection reagent (Qiagen) following the manufacturer's instructions. The Attractene reagent is a nonliposomal lipid transfection reagent. Briefly, $3x10^5$ cells were incubated in 2 ml

of RPMI 1640 medium supplemented with 10% FCS, 300 mg/l L-glutamine and 100U/ml penicillin/ 0.1mg/ml streptomycin in 6-well plates. 1.2 μg of plasmid DNA was mixed with 4.5 μl of the Attractene reagent, incubated for 10 to 15 minutes and added to the cells. After 48 hours, the cells were transferred to medium containing G418 700 μg/ml for selection and maintained until the appearance of colonies.

Additionally for LILRB1 and LILRB2 transfectants, cells with a high level of expression were sorted using a BD FACS ARIA cell sorter and single clone colonies were grown by limiting dilution cloning. Briefly, transfectants were diluted to a concentration of 2.5 cells/ml and 200 μl of the cell suspension was transferred to individual wells in 96-well plates. Wells with single colonies were then expanded after several weeks of culture, and cells were assessed for expression of the transfected protein, for selection of the best clones.

Purification of monoclonal antibody from hybridoma supernatant

Monoclonal antibodies were isolated from hybridoma supernatant using the MAbTrap kit (GE Life Sciences) following the manufacturer's instructions. Briefly, this utilised a protein-G column for binding of antibody and subsequent elution. Filtered hybridoma supernatant was injected manually into the column, washed and eluted using a low pH buffer (1M glycine-HCl, pH 2.7) into a neutralising buffer (1M Tris-HCl, pH 9.0).

Isolation and manipulation of primary cells

PBMC separation

Human PBMCs were separated from whole blood or buffy coat (National Blood Service, Tooting) by using Lymphoprep (Axis Shield). Whole blood or buffy coat was diluted 1:1 with RPMI or PBS, layered on Lymphoprep and centrifuged at 800G for 20 minutes at 20^{o}C. The PBMC layer was then harvested and washed with HBSS or medium before being used in experiments or frozen in liquid nitrogen for future use.

Purification of CD14^{+} monocytes

Monocytes were purified from PBMCs using anti-CD14 magnetic beads (Miltenyi Biotec) for positive selection, according to the manufacturer's instructions. Briefly, PBMCs were labelled with anti-CD14 beads, washed and run through a magnetic separation column (LS columns, Miltenyi Biotec) according to the manufacturer's instructions. Monocyte purity was checked by staining with anti-CD14 APC (clone 61D3, eBioscience) and analysis using flow cytometry.

Generation of MoDCs

Monocytes separated from PBMCs by adherence to plastic were used for generation of MoDCs. Prior to use, frozen PBMCs were thawed at 37^{o}C and allowed to adhere

in a 100 mm dish for 2 hours. Non-adherent cells were then removed and frozen in liquid nitrogen prior to subsequent use.

Fresh culture medium, RPMI 1640 (Invitrogen) supplemented with 10% heat-inactivated FCS (Invitrogen or Sigma), 2mM L-glutamine (Sigma), 100U/ml penicillin and 0.1 mg/ml streptomycin (Sigma) was added to the adherent cells. Cells were cultured in a final concentration of IL-4 (R&D Systems) at 20 ng/ml and GM-CSF (R&D Systems) at 3.33 ng/ml. Cytokines were refreshed on day 2 or 3 of cultures by addition of the same amount of cytokine added on day 0. On day 5 of culture, the dendritic cells were washed and resuspended in medium with fresh cytokines at a concentration of $0.5x10^6$ cells/ml in 6-well plates. On day 6 of culture, a maturation stimulus consisting of a final concentration of 5 ng/ml TNF-α, 5ng/ml IL-1β, 150 ng/ml IL-6 and 1 μg/ml prostaglandin E2 was added to the DCs. Dendritic cells were harvested and counted on day 7 for use in downstream experiments.

General molecular biology techniques

The general molecular biology techniques used in different parts of the project are described below:

Transformation of competent E. Coli

Competent E coli (TOP10 from Invitrogen or NEB10beta from New England Biolabs) were transformed with plasmid DNA according to manufacturer's

instructions. E coli were thawed on ice, incubated with plasmid DNA for 30 minutes, heat shocked at 42^{o}C for 30 seconds and the incubated on ice for a further 2 to 5 minutes. 250 or 950 µl of SOC medium (for TOP10 and NEB10beta respectively) were then added to the *E coli* and the mixture incubated at 37^{o}C in a shaking incubator for 60 minutes. Subsequently, 20 and 200 ul of the mixture were plated on to selective LB agar plates and incubated overnight at 37^{o}C.

DNA Minipreps

DNA minipreps were obtained by plating or streaking transformed TOP10 or NEB10 beta E Coli on LB agar plates with selective medium (carbenicillin 100 µg/ml) and incubating overnight at 37^{o}C. Single colonies were then incubated in 6 ml LB broth with carbenicillin and the culture incubated overnight at 37^{o}C in a shaking incubator. 4 ml LB culture was then centrifuged and plasmid DNA was extracted from the pellet using the Qiagen Qiaprep Miniprep kit. The DNA was eluted in dH_2O, the concentration measured using a Nanodrop ND-1000 spectrophotometer and stored at -20^{o}C until needed for use.

DNA Midipreps/Maxipreps

DNA midipreps/maxipreps were obtained by plating or streaking transformed TOP10 or NEB10 beta E Coli on LB agar plates with selective medium (carbenicillin 100 µg/ml) and incubating overnight at 37^{o}C. Single colonies were then incubated in a starter culture of 5 ml LB broth with carbenicillin and the culture incubated for 8 hours at 37^{o}C in a shaking incubator. 1 or 5 ml LB culture

was then added to 50 or 250 ml LB broth with carbenicillin (for midi and maxipreps respectively) and incubated overnight at 37^{o}C in a shaking incubator. The LB broth was centrifuged and plasmid DNA was extracted from the pellet using the Sigma GenElute HP Midiprep or Maxiprep kit. The DNA was eluted in dH_2O, the concentration measured using a Nanodrop ND-1000 spectrophotometer and stored at -20^{o}C until needed for use.

DNA gel extraction

All DNA extractions from agarose gels was performed using the Qiagen Qiaquick Gel Extraction kit. The manufacturer's instructions were followed. The gel slice was solubilised using proprietary buffers, bound in a spin column, washed and eluted with dH_2O or 10 mM Tris-HCL buffer, pH 8.5.

Purification of PCR products

When necessary, PCR products were purified using the Qiagen Qiaquick PCR Purification kit. In principle, the Qiaquick system uses a proprietary silica membrane to bind DNA in a spin-column technology format. Different buffers are used for efficient recovery of DNA and removal of contaminants. DNA is adsorbed to the silica membrane in the presence of high concentrations of salt while contaminants pass through the column. Subsequently contaminants are washed away, and pure DNA is eluted. The manufacturer's instructions were followed. PCR products were diluted in the supplied proprietary buffer, bound in a spin column, washed and eluted with dH_2O or 10 mM Tris-HCl buffer, pH 8.5.

Restriction enzyme digestion

Restriction enzymes used for experiments included ApaI, BamHI, BspEI, HindIII, NheI and XhoI (all from New England Biolabs). Restriction enzymes were used as per manufacturer's instructions and mixed with the DNA to be digested in the provided buffers. Samples were incubated for 1 hour at 37^{o}C or 25^{o}C (for ApaI only).

DNA ligation

All DNA ligation was done using T4 DNA ligase and T4 DNA ligase buffer (from New England Biolabs). Ligation reactions were incubated overnight at 16^{o}C. A vector:insert ratio of 1:3 was used for all ligation reactions.

RNA extraction

Total RNA extraction from either PBMCs or cell lines was extracted using the Qiagen RNEasy Mini extraction kit. In principle, the technology utilised the combination of selective binding of RNA to a silica-based membrane with microspin technology. A proprietary high-salt buffer system allowed up to 100 μg of RNA > 200 bases to bind to the RNeasy silica membrane.

Cells were initially lysed and homogenized in a highly denaturing guanidine-thiocyanate–containing buffer. This was to immediately inactivate RNases to ensure

purification of intact RNA. Ethanol was then added to provide appropriate binding conditions, and the sample applied to a spin column, where the total RNA binds to the membrane and contaminants are washed away. The RNA is then eluted in 50 µl of deionised water.

Reverse transcription

Reverse transcription of mRNA into cDNA was done using the Qiagen Omniscript Reverse transcription reagent. Template RNA was incubated with Omniscript RT, dNTPs, anchored oligo-dT primers and RNase inhibitor according to the manufacturer's instructions at 37^{o}C for 60 minutes. Reaction products were subsequently used in downstream PCR or frozen for storage.

DNA sequencing

All DNA sequencing was done by a commercial company, Geneservice who use Applied Biosystems 3730 DNA analyzers for their work. Standard sequencing primers or custom designed ones on occasion were provided by the company.

PCR amplification

PCR reactions were undertaken using the Phusion High-Fidelity PCR kit (New England Biolabs), which uses an enzyme incorporating a novel *Pyrococcus*-like enzyme with a processivity-enhancing domain, engineered for high fidelity PCR

work. Proprietary buffers and reagents were supplied with the kits, and the manufacturer's recommendations for their use were followed.

Reactions were undertaken in either 20 µl or 50 µl volumes, with a final concentration of 0.5µM forward and reverse primers, 200µM dNTPs, proprietary buffer and template DNA.

DNA Agarose electrophoresis

Agarose electrophoresis for DNA was done on agarose gels, using 0.5X Tris-borate-EDTA buffer to cast the gel and in the tank. DNA was visualized using an ultraviolet transilluminator.

Development of assays to measure variance in LILRs

Measurement of LILR levels on DCs and other immune cells

Whole blood (collected in sodium heparin tubes) was stained with anti-CD1c FITC (AD5-8E7, Miltenyi), anti-ILT1 PE (135.4, eBioscience) or anti-ILT4 PE (42D1, eBioscience), anti-CD14-ECD (RMO52, IOTest, Beckman), anti-ILT2 APC (HP-F1, eBioscience) or anti-ILT3 APC (eBioscience, ZM4.1) and anti-CD19 PC7 (J3-119, IOTest, Beckman). Isotype matched controls were IgG2a (mouse) FITC (S43.10, Miltenyi), IgG2a (rat) PE (eBioscience), IgG2a (mouse) ECD (7T4-1F5, IOTest, Beckman), IgG1 (mouse) APC (eBioscience) and IgG1 (mouse) PC7 (679.1Mc7, IOTest, Beckman). After incubation at 4^{o}C for 30 minutes, stained

blood was lysed with BD PharmLyse solution (Becton Dickinson). Cells were washed twice with wash buffer (PBS/1%BSA/0.1% azide) and fixed with BD CellFix (Becton Dickinson) prior to being analysed on the flow cytometer (Cytomics FC500, Beckman Coulter).

Analysis of the data was done with FlowJo software (Tree Star, USA). Gates for the DC, monocyte and B cell populations were drawn as shown in Figure 1. The FL2 and FL4 median fluorescence intensity (MFI) values for these populations were then obtained and normalized to units of molecules of equivalent fluorochrome (MEF) using normalising fluorospheres (Rainbow Calibration Particles-30-5A, Spherotech) according to manufacturer's protocol. Briefly, normalising fluorospheres were run on each day, and MFI values plotted against the manufacturer provided MEF values to draw a 'standard curve' which was used to convert unknown MFI values into MEF values. This allowed longitudinal comparison of LILR levels on samples taken on different days. (186) To further reduce variation in LILR measurement, all antibodies used were from the same batch. This single batch of antibodies was specifically allocated to the part of the project assessing the variation of the LILRs between different individuals.

Figure 2.1

Flow cytometry plots showing (top row from left to right): forward scatter vs. side scatter (with white cell gate), FL3 (CD14 ECD) vs. side scatter (with the white cell gate applied, and showing the monocyte gate), FL5 (CD19 PC7) vs. FL1 (Cd1c FITC) (showing DC and B cell gates). FL2 and FL4 histogram plots for monocytes, DCs and B cells were drawn to obtain median fluorescence intensity. The FL2 and FL4 overlay histograms are shown for monocytes in the bottom row. The FL2 overlay histogram plot (bottom left) shows the fluorescence intensity for the PE IMC (red), LILRA2 (blue) and LILRB2 (orange) on monocytes. The FL4 overlay histogram plot (bottom right) shows the fluorescence intensity for the APC IMC (red), LILRB1 (blue) and LILRB4 (orange) on monocytes.

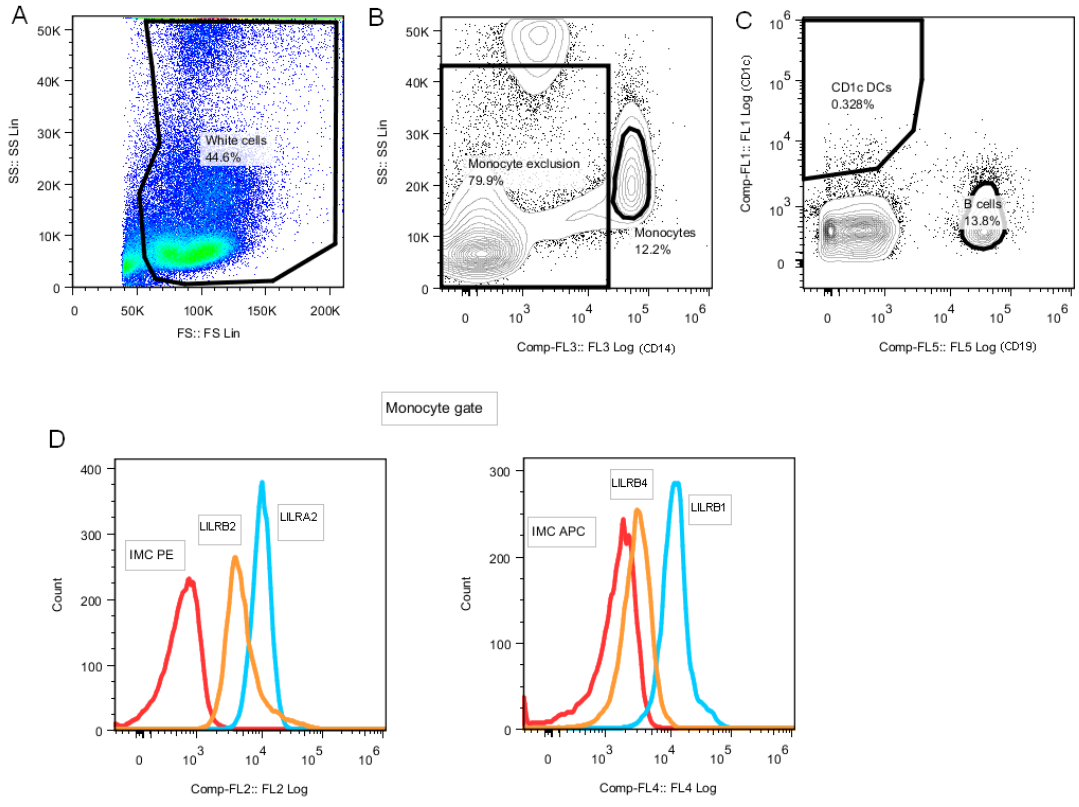

Effect of cytokine stimulation on LILR expression

In optimisation experiments, whole blood was incubated at 37^{o}C for various intervals with or without the addition of IL10, an IL1β/TNFα/PGE2/IL6 cocktail, IL1β, TNFα, IL6 alone or TGF-β was analysed with this assay to determine the effect of LILR expression after whole blood stimulation. The concentration of the cytokines in the cocktail were IL1β 10ng/ml, TNFα 10 ng/ml, PGE2 2μg/ml and IL6 300 ng/ml.

For determination of the change in LILR expression for correlation with genomic variation, whole blood was incubated at 37^{o}C for 21 hours with or without the addition of 50 ng/ml IL-1β or 20 ng/ml TGF-β (both cytokines from Miltenyi Biotec, Germany), and LILR cell surface levels were measured. Culture was performed with undiluted whole blood in loosely capped 12x75 mm polypropylene tubes in a humidified incubator with supplemental 5% CO_2. The endotoxin level in all cytokines used in cell culture were certified to be <0.1 ng/μg cytokine by the manufacturer. For some experiments, the "modulation index" was calculated as the ratio of MEF with cytokine stimulation divided by MEF under baseline conditions.

Sequencing of polymorphisms in the LILRB2 promoter region

DNA extraction

Total genomic DNA was extracted from whole blood using the QIAamp DNA Mini Kit (Qiagen) according to the manufacturer's instructions. Briefly, 200 μl of whole

blood was lysed, incubated at 56^{o}C for 10 minutes and mixed with ethanol. The mixture was run though a spin format column and washed with the proprietary buffers provided; and eluted in 200 µl of Tris EDTA buffer (10 mM Tris Cl, 0.5 mM EDTA, pH 9.0). The concentration of the DNA was measured using a Nanodrop ND-1000 spectrophotometer and stored at -20^{o}C until needed for use.

PCR to amplify the LILRB2 promoter region

Primers to amplify a region of 2306 base pairs containing the putative promoter region for LILRB2 were designed using the PrimerZ web application. (187) The amplified PCR product was designed to be –1925 to +380 bp from the ATG start codon of the LILRB2 sequence (Genome Reference Consortium Human genome build 37, GRCh37:19:54784103-54786408).

PCR reactions were done with the Phusion High-Fidelity PCR kit (New England Biolabs), which uses an enzyme incorporating a novel *Pyrococcus*-like enzyme with a processivity-enhancing domain, engineered for high fidelity PCR work. Proprietary buffers and reagents were supplied with the kits, and the manufacturer's recommendations for their use were followed. Reactions were done in 50 µl volumes, with a final concentration of 0.5µM forward and reverse primers, 200µM dNTPs, proprietary buffer and template genomic DNA.

The amplification primers used were the forward primer, PRO1F (TGCCATGCACTCCATATTGT) and reverse primer, EX2R (CTGGGGACAGACTCACCTGT). Reaction conditions were: initial denaturation

at 98^{o}C for 30 seconds, followed by 35 cycles of denaturation at 98^{o}C for 10 seconds, annealing at 65^{o}C for 30 seconds and elongation at 72^{o}C for 75 seconds; with a final elongation step at 72^{o}C for 8 minutes.

The PCR reactions were then run on an 0.8% agarose gel in 0.5X TBE buffer at 100V for 60 minutes. The 2306 bp band corresponding to the amplified region containing the LILRB2 promoter region was then extracted using the Qiagen QiaQuick Gel Extraction kit according to the manufacturer's instructions.

Sequencing of the amplified PCR fragment

The amplified DNA region was then sent to a commercial company, Geneservice for sequencing using the custom primers designed with the PrimerZ application. The custom primers are detailed below in Table 2.1.

Table 2.1 Primers used for sequencing of amplified LILRB2 promoter region

Primer name	Primer sequence
PRO1F	TGCCATGCACTCCATATTGT
ILT4_PRO1R	AATGACAGTGAGGGGCTCAG
ILT4_PRO2F	ACTGGGCAAGAAGACAAGGA
ILT4_PRO2R	ACAGTGGTTGTGGGGTCAGT
ILT4_PRO3F	TCACCTCTGGCCTCTGTTCT
ILT4_PRO3R	ATGCAGGGAAGTAGGGGAAG
ILT4_PRO4F	GAGGCTCAGTGATGGGACAT

ILT4_PRO4R	TGGTTTCTCCTCGTCTCACC
ILT4_EX1F	ACGACTGCCATGGTAAGGAC
EX2R	CTGGGGACAGACTCACCTGT

Analysis of LILRB2 polymorphisms

The sequenced LILRB2 regions were then analysed using Variant Reporter software (version 1.1, Applied Biosystems) to overlay PCR amplicons, compare to the reference sequence and identify SNPs.

Real time PCR to quantify LILRB2 mRNA levels

Cell types used and experimental conditions

Purified monocytes or THP-1 cells were exposed to various stimuli to confirm that LILRB2 mRNA could be transcriptionally regulated. 5 x 10^5 monocytes or 2.5 x 10^5 THP-1 cells were incubated in 500 μl volumes with IL10 600 ng/ml , an inflammatory cytokine mixture (17.5 ng/ml TNFα, 17.5 ng/ml IL1β, 525 ng/ml IL6 and 3.5 μg/ml PGE_2) or LPS 1 μg/ml for 6 or 22 hours prior to having total RNA harvested. RNA was also harvested at 0 hours prior to addition of stimuli.

RNA extraction and genomic DNA removal

Total RNA was extracted using the RNAqueous-4PCR kit (Applied Biosystems). Briefly, cells were lysed and the lysate run through a spin column to extract the RNA. The RNA underwent wash steps and was subsequently eluted.

Eluted RNA was incubated with DNase 1 (Applied Biosystems) at 37^{o}C to for 15 to 30 minutes to remove any trace of contaminating genomic DNA. The DNase 1 was then inactivated and the RNA converted to cDNA.

Conversion of RNA to cDNA

Total RNA was converted to cDNA using the High Capacity RNA-to-cDNA kit (Applied Biosystems) according to the manufacturer's instructions. Briefly, purified RNA was incubated with the proprietary reverse transcriptase enzyme and buffers for 60 minutes at 37^{o}C. The mixture was then incubated at 95^{o}C to inactivate the enzyme and stored at -20^{o}C prior to use in further experiments.

Real time PCR reaction

The primers used to quantify the amount of LILRB2 mRNA were those recommended by Applied Biosystems (Hs01629548_s1, FAM/MGB probe) with a human GAPD (GAPDH) Endogenous Control (FAM/MGB Probe) primer. An equal amount of cDNA was loaded with each primer set and a no-template control was also set up with each run.

All samples were run in 20µl volumes in triplicates. The real-time PCR reaction was performed on an Applied Biosystems StepOnePlus^{TM} Real-Time PCR System with the following cycling parameters: 50^{o}C for 2 minutes, 95^{o}C for 10 minutes, followed by 40 cycles of 95^{o}C for 15 seconds and 60^{o}C for 1 minute.

Data was analysed using DataAssist software v3.0 (Applied Biosystems). The ΔΔCt method of relative quantification was used to compare the different samples. (188) Briefly, this method allows comparison of the amount of DNA or RNA present in different samples by normalization against a housekeeping gene (GAPDH in these experiments). The Ct (or threshold cycle) value is the number of cycles at which fluorescence based detection of DNA exceeds a pre-set limit above background. The difference between the Ct of the gene of interest and the housekeeping gene gives the ΔCt value. The amount of DNA or RNA present in different samples (normalized to an endogenous reference) can then be compared by calculating the difference between the ΔCt of the target sample and that of a reference sample, giving the ΔΔCt value. The relative quantitation (RQ) is calculated using the formula $2^{-\Delta\Delta Ct}$, allowing the amount of DNA or RNA in the sample (normalized to an endogenous reference) to be expressed as an *x* fold value relative to a reference sample.

Luciferase assay

Dual luciferase assays were undertaken to determine if the different SNPs identified in the LILRB2 promoter region affected transcriptional regulation of the protein.

Briefly, a 1000 bp region upstream of the ATG start codon of the LILRB2 region was cloned into a promoterless firefly luciferase plasmid (pGL4.10, luc2, Promega). This was co-transfected with a Renilla luciferase plasmid with an SV40 promoter (pGL4.73, hRluc/SV40, Promega) into THP-1 cells to allow normalisation of firefly luciferase activity.

Cloning of LILRB2 region upstream of start codon into promoterless luciferase vector for sequencing

A 1000-bp region upstream of the LILRB2 ATG start codon was PCR cloned from the amplified 2306 bp region. NheI and XhoI restriction enzyme sites were added to the start of the PCR primers to allow cloning into the multiple cloning region of the pGL4.10 vector. The primers used were the forward primer ILT4P_1000_NHEF (ATAGCTAGCACCTACAGAATGTGGAGTCC) and reverse primer ILT4P_NOATG_XHOR (ATACTCGAGGGGGTGTTGTCATCTGCAGC); underlined sequences represent the restriction enzyme sites.

PCR reactions were done with the Phusion High-Fidelity PCR kit (New England Biolabs) in 50 µl volumes. Reaction conditions were: initial denaturation at 98^{o}C for 30 seconds, followed by 35 cycles of denaturation at 98^{o}C for 10 seconds and elongation at 72^{o}C for 30 seconds; with a final elongation period at 72^{o}C for 7 minutes.

The PCR products were run on an 0.8% agarose gel in 0.5X TBE buffer at 100V for 60 minutes. Bands of approximately 1000 bp were excised and extracted from the gel using the Qiagen QiaQuick Gel Extraction kit.

The promoterless firefly luciferase vector pGL4.10 and the cloned 1000 bp region of the putative LILRB2 promoter were digested with NheI and XhoI restriction enzymes at 37^{o}C for 60 minutes. The digested product was then run on an agarose gel to confirm that no additional bands were present and then purified using the Qiagen QiaQuick PCR purification kit.

The linearized pGL4.10 vector and digested LILRB2 promoter region were then ligated together overnight at 16^{o}C with T4 DNA ligase (New England Biolabs), at a vector:insert ratio of 1:3. Ligated products were then transformed into NEB10beta competent E coli (New England Biolabs). Selected colonies were screened for presence of the insert by restriction enzyme digestion with NheI and XhoI prior to sequencing to determine the LILRB2 promoter haplotype.

Sequencing of cloned 1000 bp LILRB2 region upstream of start codon

pGL4.10 plasmids containing the 1000 bp LILRB2 promoter region insert were sent to Geneservice for sequencing to determine the haplotype/SNPs contained in the plasmid. The sequencing primers used were RVprimer3 (CTAGCAAAATAGGCTGTCCC) and GLprimer4 (GCCCTTCTTAATGTTTTTG) synthesized by Sigma-Aldrich.

Gene synthesis of LILRB2 promoter region for use in luciferase assay

Based on the haplotypes obtained from sequencing of the cloned 1000 bp LILRB2 region, five different haplotypes of a 633 bp region [-533 to +74 from the putative promoter site identified by Nakajima et al (189)] were synthesized and cloned into pGL4.10 plasmids by a commercial company (Genscript). These five different plasmids were used in further luciferase transfection experiments to determine if SNPs in the LILRB2 promoter affected expression levels.

Transfection of THP-1 cells with luciferase plasmids

THP-1 cells were transfected in 96-well flat-bottom plates. Cells were resuspended in OptiMEM medium (Invitrogen) with 10% FCS and seeded at a density of 10^5 cells per well prior to transfection.

The THP-1 cells were then co-transfected with LILRB2 promoter/luc2 and pGL4.73 plasmids using Lipofectamine 2000 (Invitrogen) according to the manufacturer's instructions. Briefly plasmid DNA and Lipofectamine 2000 were mixed with 25 µl of OptiMEM medium (Invitrogen) each and combined after 5 minutes. Plasmid-lipofectamine complexes were allowed to form for 20 minutes prior to being added to cells.

Cells were harvested after 24 or 48 hours for use in the luciferase assay. Additionally 1 µg/ml LPS was also added to cells at specific time points to determine if luciferase expression could be enhanced.

Measurement of luciferase activity

Measurement of firefly and renilla luciferase activity was undertaken using the Dual Luciferase Reporter system (Promega) according to the manufacturer's instructions. Briefly, transfected cells were lysed with the proprietary lysis buffer. 20 µl of lysate was then incubated with 100 µl of luciferase assay reagent and measured on the luminometer. 100 µl of Stop&Glo reagent was then added to quench firefly luciferase activity and allow measurement of renilla luciferase activity. All readings were done on a Biotek FLX800 luminometer.

The ratio of firefly to renilla luciferase was then calculated to allow for comparison between different LILRB2 haplotypes.

Functional assays with anti-LILRB2 antibodies

Functional assays to determine the effect of LILRB2 ligation were undertaken on anti-$CD14^+$ purified peripheral blood monocytes, isolated with magnetic beads as described in the Section 2.2 on isolation and manipulation of primary cells.

Stimulation with TLR ligands

Purified monocytes were incubated with various TLR ligands including LPS, imiquimod, ssRNA/Lyovec, Pam3CSK4, polyI:C and CpG DNA ODN2006 (LPS

from Sigma, all remaining TLR ligands from Invivogen). Additionally anti-LILRB2 antibodies (clone 42D1 purified from hybridoma supernatant) or a rat IgG2a kappa isotype matched control (clone eBR2a, eBioscience) were added to determine if there would be any functional effect. After overnight incubation at 37^{o}C, supernatant was harvested and frozen at -20^{o}C prior to analysis for cytokine concentration.

ELISA for cytokine secretion

The concentrations of IL6, IL8, IL10 and TNFα in the supernatants of stimulated monocytes were measured using Ready-SET-Go! ELISA kits from eBioscience according to the manufacturer's instructions. Briefly, Corning Costar plates were incubated overnight at 4^{o}C with the appropriate capture antibody. The following day, plates were washed, incubated with blocking buffer, washed and then incubated overnight with supernatant diluted to allow concentration of the cytokines to come within the range of the standard curve.

Following this, plates were washed and incubated with the biotinylated detection antibody. After a further wash step, plates were incubated with HRP-avidin as the detection reagent and washed again. The TMB substrate was then added and sulphuric acid used as the stop reagent. Plates were then read at 450 nm using a Varioskan Flash Multimode Reader (Thermo Fisher Scientific).

Development and testing of the G-Body

Two main approaches were taken to create the bifunctional G-body molecule comprising a HLA-G domain for interaction with the immunosuppressive LILRB1 and LILRB2 and an anti-HLA-A2 domain for localisation to allogeneic cells expressing HLA-A2:

(i) a recombinant DNA approach; and

(ii) a chemical conjugation approach using the biotin-streptavidin interaction

Generation of recombinant G-body and control materials

Hybridoma sequencing

Hybridoma sequencing was performed by a commercial company (Fusion Antibodies Ltd). Briefly, mRNA was extracted from the hybridoma pellets using the company's in-house RNA extraction protocol. cDNA was created from the RNA by reverse-transcription with an oligo(dT) primer. PCR reactions using variable domain primers were used to amplify both the V_H and V_L regions of the monoclonal antibody DNA. The V_H and V_L products were cloned into the sequencing vector pCR2.1 (Invitrogen) and transformed into TOP10 cells (Invitrogen) for positive transformants. Selected colonies were picked and analyzed through sequencing.

DNA synthesis

DNA was chemically synthesised by a commercial company (Genscript, USA) using undisclosed methods. The synthesized gene was then cloned into a pUC57 vector and subcloned into a pcDNA3.1(+) vector (Invitrogen).

Generation of plasmids for transfection

The general molecular biology techniques used to generate various plasmids for different versions of the recombinant G-body and control materials are described previously.

Briefly, the original recombinant G-body was designed in a modular fashion to allow replacement of various segments using appropriate restriction enzymes. Subsequent modifications to the original recombinant G-body were undertaken using a combination of PCR cloning and/or gene synthesis of the segments to be changed.

Minipreps were generated to allow confirmation by gene sequencing that the intended sequence was present. Subsequently, midipreps or maxipreps were generated for transfection purposes.

For control materials, various genes including HLA-G, LILRB1 and LILRB2 were obtained from RNA extracted from PBMCs. These were converted to cDNA,

amplified by PCR and cloned into the pcDNA3.1+ expression vector prior to being used in various transfection experiments.

Transient transfection of cell lines

Transient transfection experiments were undertaken using the Attractene transfection reagent (Qiagen), a proprietary non-liposomal lipid based reagent. The manufacturer's instructions were followed. Briefly, the cells to be transfected were seeded 24 hours before transfection, to achieve 40 – 80% confluence at the time of transfection. Plasmid DNA (inserts were cloned into a pcDNA3.1+ expression vector) and the transfection reagent were mixed in medium according to manufacturer's instructions and incubated for 10 to 15 minutes at room temperature. When co-transfections with two separate plasmids were performed, the amount of DNA used for each plasmid was halved. Subsequently, the mixture was added to the cells to be transfected. Supernatant and cells were harvested at 48 to 72 hours post-transfection for further experiments.

Generation of chemically conjugated G-body

Conjugation of streptavidin to BB7.2

BB7.2 was conjugated to streptavidin using the EZ-Lightning Link kit (Innova Biosciences); at a molar ratio of approximately 1:3. 100 μg of purified mAb in PBS was added to 100 μg of streptavidin after addition of the proprietary reagents. The

conjugate was incubated for 3 hours and then a proprietary quenching reagent was used to stop the reaction.

Measurement of endotoxin levels

Biotinylated HLA-G monomers were purchased from the Fred Hutchinson Cancer Research Centre and tested for endotoxin contamination with the QCL-1000 limulus amebocyte lysate endotoxin measurement kit (Lonza). Briefly, the kit measures endotoxin levels by measuring the colorimetric change after addition of limulus amebocyte lysate (LAL) to samples.

Endotoxin purification of biotinylated HLA-G

bHLA-G monomers were purified using the ToxinEraser Endotoxin Removal Kit (Genscript). Briefly, samples were run through a modified polymixin B resin in a pre-packed column which removed endotoxin. Samples were then buffer exchanged into PBS using the Vivaspin 2 ultrafiltration device (Sartorius). Endotoxin levels were re-measured after this process.

Protein measurement

Protein concentrations were measured using a bicinchoninic acid (BCA) kit (Pierce). Briefly, standards and samples were added to the BCA reagents and absorbance measured at 562 nm after incubation at 37^{o}C for 30 minutes.

Conjugation of biotinylated HLA-G monomers to streptavidin-conjugated BB7.2

The biotinylated HLA-G was mixed with streptavidin-conjugated BB7.2 at various molar ratios and incubated at room temperature for 30 minutes before being ready for use.

Generation of controls for chemically conjugated G-body

Controls for the cG-body were generated using the same processes above but substituting BB7.2 with MPC11 (mouse IgG2b isotype matched control) and bHLA-G with biotinylated BSA (Pierce) in various combinations.

Testing of constructs

Immunoprecipitation

30 µl of streptavidin agarose or protein G sepharose beads (Sigma Aldrich) were washed with 1 ml of PBS and incubated with 1 µg of biotinylated HLA-A2 (purchased from the Fred Hutchinson Cancer Research Centre) or 1 µg mAb in 250 µl PBS for 1 hour and washed twice with PBS. Beads were then incubated with culture supernatant or lysates for 3 hours and then washed a further 3 times. The beads were then used for SDS-PAGE and Western blotting. The primary antibodies used for immunoprecipitation included the conformational anti-HLA-G antibodies 87G (BioLegend) and MEM-G/9 (AbD Serotec), and the pan-HLA I antibody W6/32 (generated from hybridoma supernatant).

SDS-PAGE

The Laemmli buffer system with discontinuous polyacrylamide gels and Tris-glycine-SDS buffer was used for SDS-PAGE experiments. Gels were cast in house with the Bio-Rad Mini Protean gel casting stands. Samples were run using the Bio-Rad Mini-Protean Tetra cell. Laemmli reducing buffer was added to the samples and boiled for 5 minutes at 95 to 100^{o}C before loading on to the gels for electrophoresis.

Western blotting

Protein transfer from SDS-PAGE gels to PVDF membranes (Hybond-P, GE Life Sciences) was performed using the Bio-Rad Trans-Blot SD Semi-Dry Electrophoretic Transfer Cell. The Bjerrum and Schafer-Nielsen transfer buffer was used (48 mM Tris. 39 mM glycine, 20% methanol). Transfer times were as the manufacturer's recommendations.

Membranes were then incubated in TBS-T (Tris buffered saline-Tween) buffer with 5% skimmed milk for 60 minutes, followed by a wash, and then incubated overnight at 4^{o}C with the primary antibody in TBS-T/2.5%BSA. The membranes were then washed 2 times with TBS-T and incubated with the secondary antibody [goat anti-mouse IgG (Fc specific) HRP (Sigma)] in TBS-T for 60 minutes at room temperature. The membrane was then washed a further 3 times before imaging.

ECL reagent (GE Life Sciences) was then added to the membrane for 1 minute before the membrane was exposed to autoradiography film (Hyperfilm ECL, GE Life Sciences). Exposure times ranged between 2 to 60 minutes to obtain the best quality images and the film was developed in an automated film processor.

Primary antibodies used for Western blotting included anti-denatured HLA-G (4H84, Santa Cruz Biotech), anti-β2m (B2M-01, Abcam), anti-His(C-term) and anti-myc (both from Invitrogen).

For some Western blotting experiments, biotinylated anti-denatured HLA-G (4H84, Abcam) was used as the primary antibody with streptavidin-HRP (eBioscience) as the secondary layer. This was done for immunoprecipitation experiments where a monoclonal antibody was bound to protein G sepharose beads to avoid detection of this antibody in Western blots.

HLA-G ELISA

The amount of HLA-G or G-body present in the supernatant of transfected cells was measured using a HLA-G sandwich ELISA kit (US Biological).

Flow cytometry

LILRB2 and HLA-A2 transfected K562 cells were used as targets to test G-body binding to its ligands. Cells were incubated with the chemical G-body or supernatant from G-body transfected cells for 30 to 60 minutes at 4^{o}C. Cells were

then washed twice and incubated with a secondary layer, either goat-anti-mouse IgG FITC (Invitrogen) or anti-HLA-G (87G-PE, eBioscience) for 30 to 60 minutes at 4^{O}C. Cells were then washed twice and fixed prior to flow cytometric analysis.

Functional testing of G-Body

Lymphocytes proliferation experiments

PBMCs were incubated with anti-CD3/28 beads (Invitrogen), anti-CD3 (OKT3, eBioscience) or SEB (Sigma-Aldrich) in the presence of the chemically conjugated G-body (at a concentration containing 2.5μg/ml of the mAb component) or its controls to determine if there was any effect on proliferative responses as measured by tritiated thymidine incorporation. 10^5 PBMCs were incubated with anti-CD3/28 beads at a ratio of 1 bead:5 cells, or anti-CD3 at a concentration of 0.5 μg/ml, or SEB at a concentration of 1 ng/ml in 96-well round bottom plates in 200 μl total volume.

PBMCs were incubated for 4 days and pulsed with 0.5μCi of tritiated thymidine18 hours prior to harvesting or freezing for later harvest. Cells were harvested with a Perkin Elmer Filtermate harvester. The filter membranes were then dried and counted using a Packard Matrix 9600 Direct β counter.

Mixed lymphocyte reactions

MoDCs or isolated PBMCs were used as stimulator cells. MoDCs were used "as is" after generation and PBMCs were treated with mitomycin-C (MMC) (Merck Chemicals) to prevent proliferation. PBMCs were incubated at a concentration of $2x10^6$/ml with 25 μg/ml MMC for 1 hour at 37°C. PBMCs were washed three times with medium prior to being used for experiments. PBMCs from another donor were used as responder cells.

MoDCs or MMC-treated PBMCs were incubated with 10^5 allogeneic PBMCs per well in 250 μl total volume in 96-well round bottom plates at a ratio of 1:10 or 1:1 for 5 to 7 days with various concentrations of the chemically conjugated G-body or its controls. 75μl of supernatant was removed for cytokine measurement and cells were pulsed with 0.5μCi of tritiated thymidine18 hours prior to harvesting or freezing for later harvest.

Cells were harvested with a Perkin Elmer Filtermate harvester. The filter membranes were then dried and counted using a Packard Matrix 9600 Direct β counter.

Cytokine measurements

IFN-γ, IL2, IL4 and IL10 were measured in culture supernatants using the FlowCytomix kit (Bender Medsystems), which used a bead-based flow cytometric method. Briefly, various cytokine capture beads and a biotin conjugate antibody

were incubated with culture supernatants, washed and incubated with PE-streptavidin. Cytokine capture beads were differentiated by light scatter and FL4 fluorescence; and cytokine concentration determined by FL2 fluorescence on flow cytometry.

Statistical analysis

Statistical analysis was undertaken using either Sigmastat (Systat Software Inc) or SPSS (IBM) software. The student's t-test, paired t-test, one-way ANOVA, ANOVA by ranks, Mann-Whitney U test or Kruskal-Wallis test were used to test for differences between various groups as appropriate depending on whether the data was parametric or non-parametric and whether two group or multiple group comparison was being undertaken. Correlation analyses were undertaken using parametric or non-parametric tests depending on the distribution of the data.

Generation of control materials

Cloning of green fluorescent protein (GFP) into pcDNA3.1 for use as transfection control

An EGFP (enhanced GFP) containing vector was used as a positive transfection control to determine if the transfection process was effective. An EGFP insert extracted using a BamHI/XhoI digest (a kind gift from Lucas Chan) was cloned into pcDNA3.1(+) linearized with BamHI/XhoI. The ligated insert and vector were transformed into TOP10 cells. The sequence of the EGFP (GenBank reference AM181664.2) was confirmed by gene sequencing.

When transfected into COS7 cells, these showed GFP expression confirming effectiveness of the transfection process. (Figure 2.2)

Figure 2.2

Histograms showing expression of GFP in vector transfected COS7 cells (above) or vector-EGFP transfected cells (below)

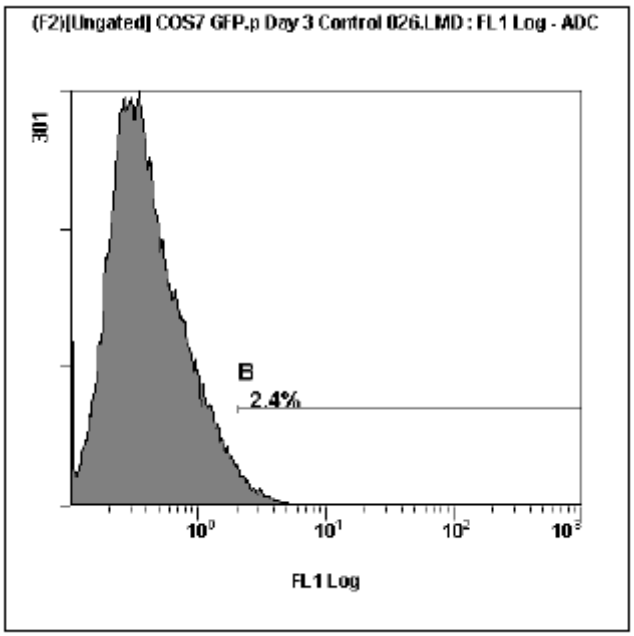

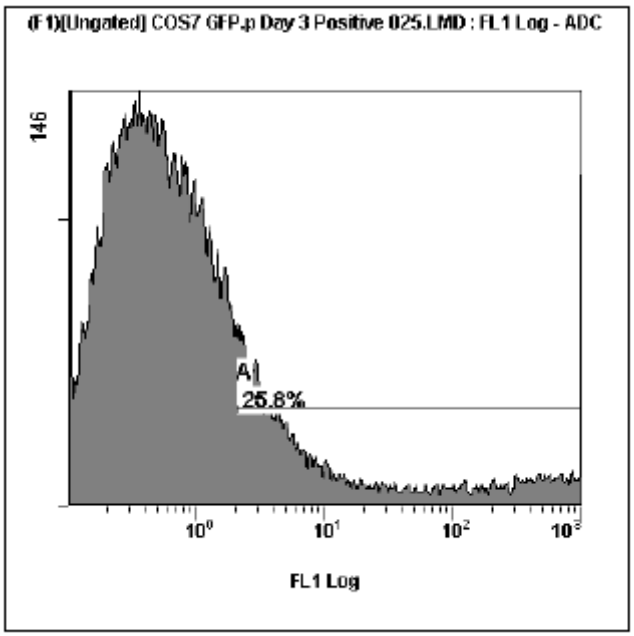

Cloning of full-length HLA-G, soluble HLA-G, β2-microglobulin into pcDNA3.1 for use as experimental controls

To generate controls for the recombinant G-body, HLA-G and β2m were all cloned into the same expression plasmid used for the G-body.

Full-length HLA-G (NCBI reference sequence NM_002127.5) was PCR cloned from cDNA extracted from JEG3 cells. The primers used were 5'-CACCATGGTGGTCATGGCACCCCG and 3'-TCAATCTGAGCTCTTCTTCCTCC. The PCR product was run on an agarose gel and extracted before being cloned into pcDNA3.1 using the directional TOPO cloning system (Invitrogen). TOP10 cells were transformed with the vector, and the sequence for the gene confirmed by DNA sequencing and maxipreps generated.

Soluble HLA-G was PCR cloned from the recombinant G-body plasmid using the primers 5'- ATAGGATCCACCATGGTGGTCATGGC and 3'-ATACTCGAGTCAGGAAGACTGCTTCC which had 5'-BamHI and 3'-XhoI restriction sites (underlined) built in to allow cloning into pcDNA3.1. The PCR products and the pcDNA 3.1 vector were digested with BamHI/XhoI. PCR products were purified using the Qiagen Qiaquick PCR purification kit and the digested pcDNA3.1 was extracted after agarose electrophoresis. The vector and insert were ligated, and TOP10 cells were transformed to allow DNA sequencing and maxiprep generation after confirmation of sequence.

β2 microglobulin (NCBI reference sequence NM_004048.2)was PCR cloned using from the β2M Mammalian Gene Collection (ATCC) clone. Primers 5'-AAAGGATCCACCATGTCTCGCTCCGTG and 3'-AAACTCGAGTTACATGTCTCGATCCC were designed with 5'-BamHI and 3'-XhoI restriction enzyme sites (underlined) and subsequently cloned into pcDNA3.1 using the same process as the soluble HLA-G clone.

DNA sequencing confirmed that all the clones had the correct sequence.

Cloning of LILRB1 and LILRB2 for use in ligand binding experiments

LILRB1 and LILRB2 were cloned as these are the natural ligand for HLA-G and were meant for the purpose of testing binding of the G-body.

LILRB1 and LILRB2 receptors were PCR cloned using cDNA extracted from human PBMCs. A 2-stage nested PCR process was used. For LILRB1, the first set of primers were 5'- GCTCATCCATCCACAGAGC and 3'-ATGGAGTGTGGGGTCTGC; for LILRB2 the first set of primers were 5'-CTCATCCATCCGCAGAGC and 3'- GAGTGTGGAGTCTGCGTACC; and the second set of primers were 5'- ATAAAGCTTGACGCCATGACCCCC and 3'-ATACTCGAGCTAGTGGATGGCCAG with 5'-HindIII and 3'-XhoI restriction sites (underlined) at either ends. The PCR products were then inserted into pcDNA3.1 using the same process as described for soluble HLA-G with HindIII and XhoI enzymes. Gene sequencing confirmed the PCR products as LILRB1,

transcript variant 2 (NCBI reference NM_001081637.1) and LILRB2, transcript variant 2 (NCBI reference NM_001080978.1).

The pcDNA3.1 plasmids with LILRB1 and LILRB2 were then stably transfected into K562 cells with G418 selection. Single clones were generated with limiting dilution cloning as described and FACS analysis confirmed expression of the transfected gene. (Figure 2.3a and 2.3b) This was to generate a stable clone of cells to allow testing of binding of the G-body.

Figure 2.3a

Histogram overlay showing staining of a K562-LILRB1 transfectant after sorting and limiting dilution cloning stained with anti-LILRB1 mAb. The pink histogram represents the isotype matched control and the green histogram is with the staining antibody.

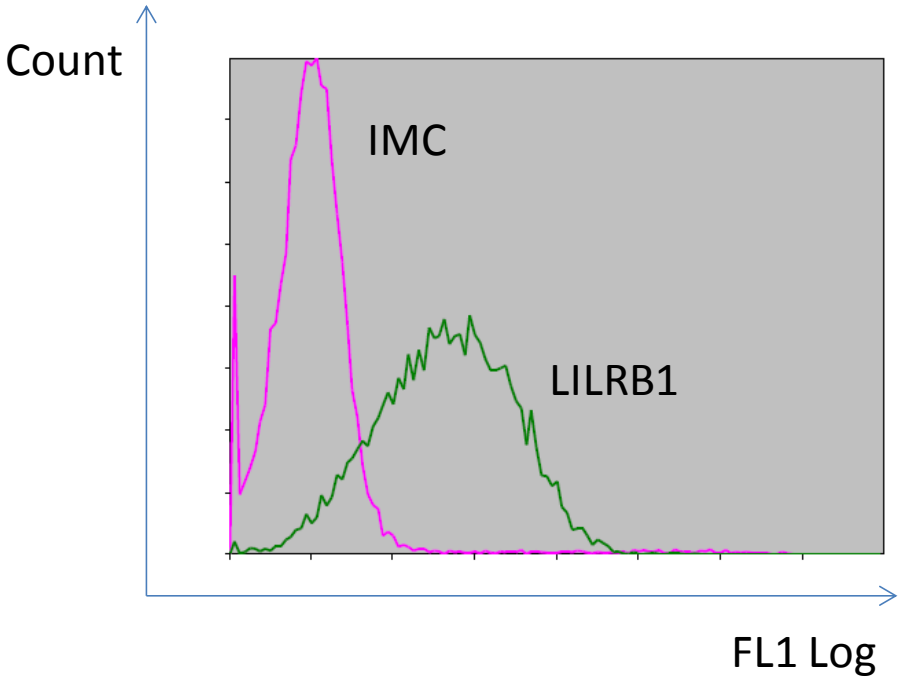

Figure 2.3b

Histogram overlay showing staining of a K562-LILRB2 transfectant after sorting and limiting dilution cloning stained with anti-LILRB2 mAb. The red histogram represents the isotype matched control and the blue histogram is with the staining antibody.

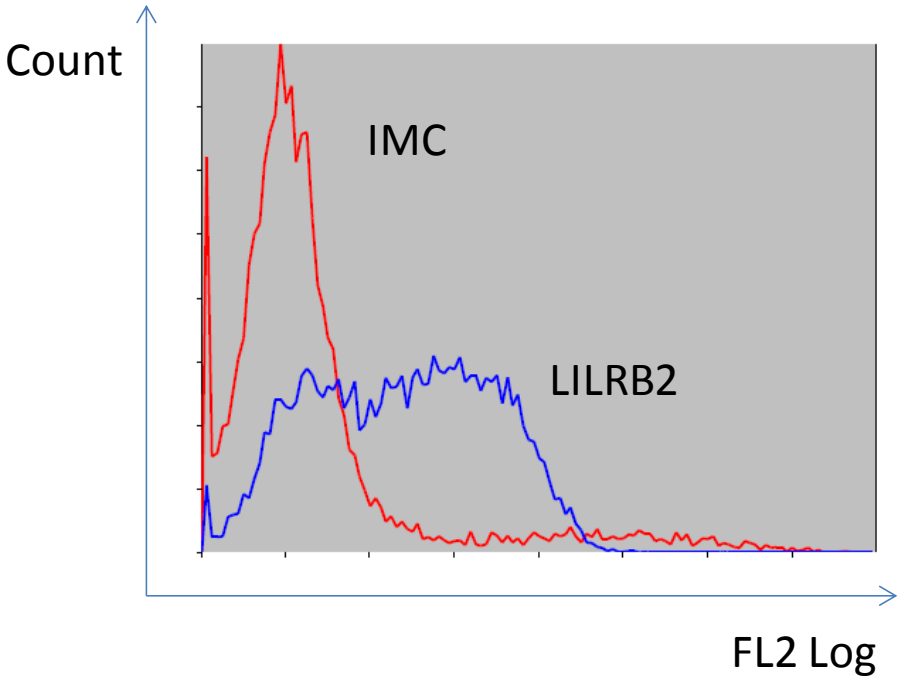

Chapter 3: Characterisation of expression levels of LILR molecules in healthy individuals

Background

In view of the hypothesis that the expression level of LILR molecules is (at least in part) influenced by genetic variation, and could affect immunological responses, the first step in the project was to develop a method for accurately quantifying expression levels on different cell types. This forms the prelude to further experiments to determine if genetic variation does affect LILR expression and also if the differences in LILR levels have functional consequences.

Furthermore, in view of the data suggesting that expression levels of some of the LILR molecule are associated with certain haplotypes, (172) which in turn have an association with certain diseases, the development of a straightforward, robust flow cytometric assay to characterise these molecules would also be a useful tool to study their expression in various disease states. The same tool could be used to compare changes before and after treatment which could give an idea how these molecules are affected by various therapeutic modalities.

In this chapter, the development of 5-colour flow cytometric method to quantify cellular surface protein expression of LILRA2, LILRB1, LILRB2 and LILRB4 on $CD1c^+$ DCs, monocytes and B cells is described. This is then used to quantify the LILR levels in 26 healthy individuals at baseline and after stimulation with different cytokines. In addition, these results are also normalized over time to allow

comparison between samples obtained on different days. The differences between various individuals, various cell types and response to different stimuli are then analysed for statistical differences.

Optimisation of whole blood LILR expression assay

Determination of antibody concentrations to be used

Initial optimisation experiments were performed to determine the correct amount of antibody required for staining for LILR expression as well as to determine the inherent variability of the assay.

Saturating amounts of the anti-LILR antibodies were determined by titration experiments staining 50µl whole blood and with different amounts of staining antibody - at 2x, 1x, 0.5x and 0.25x the amount recommended by the manufacturer (Figure 3.1a and 3.1b). At double the manufacturer recommended amount, there was still a degree of increase in MFI; however, these amounts of antibody were used as the optimum balance between detection and economy. The manufacturer recommended amount of antibody was 20µl for the PE conjugated antibodies (anti-LILRA2 0.5µg in 20µl, 0.025 mg/ml and anti-LILRB2 1µg in 20µl, 0.05 mg/ml) and 5µl for the APC conjugated antibodies (anti-LILRB1 0.25µg in 5µl, 0.05 mg/ml and anti-LILRB4 0.125µg in 5µl, 0.025 mg/ml). Figure 3.1a and 3.1b use antibody volume as the *x* axis as the manufacturer recommended amounts were given by volume.

Determination of assay characteristics

The inherent variation of the assay was then determined by analysing 5 repeat measurements of the same sample. This showed that intra-assay variability for the MFIs for the various LILRs was very good, with the highest coefficient of variation being less than 6%. (Table 3.1)

These findings suggest that the assay is highly reproducible and that differences observed between individuals are likely to result from inherent differences rather than being due to assay variability. It also suggests that the assay would be a useful tool for measuring LILR expression for correlation with SNP differences.

Intra-individual variation was also determined by measuring LILR levels on 2 different individuals at 5 distinct time points. This showed that the greatest variability was seen in LILRB2 (CV of 44% and 37% for DCs and monocytes, respectively), whereas other molecules showed little variation from day to day, e.g. the other LILRs expressed on DCs and monocytes had a CV range between 9.6 to 16% and 4.4 to 13.4% respectively (Table 3.2).

Optimisation of whole blood stimulation assay to measure LILRs

In addition to testing basal expression levels of the LILRs, a functional assay was developed to further determine if regulatory genetic polymorphisms could affect not just basal levels, but also the LILR response to stimulation with different cytokines.

A whole blood assay was developed in the first instance to allow a relatively quick tool to test large numbers of subjects for genotype-expression correlation.

Experiments incubating whole blood overnight at 37^{o}C without addition of any stimuli showed changes in the expression level of the LILRs on monocytes and DCs. (Figure 3.2) There were marked increases in the expression levels of LILRB1, LILRB4 and LILRB2 on monocytes, which increased the longer the cells were incubated at 37^{o}C. There was also a rise in the expression of LILRB1 and LILRB2 on DCs although not as marked. LILRA2 levels increased slightly on monocytes although there was no change on DCs. In contrast, expression levels of LILRB1 on B cells did not change.

Subsequently, various different cytokines were tested to identify one cytokine each that could result primarily in upregulation or downregulation of the LILR molecules. This was to allow correlation with genotype to determine if any variation was related to the magnitude of change in LILR expression levels.

A mixture of inflammatory cytokines (IL1β, IL6, TNFα and PGE_2), IL10 or TGFβ were added to whole blood to determine their effect on LILR expression levels of APCs. This showed that the inflammatory cytokines and IL10 generally resulted in upregulation of the LILRB molecules (particularly on monocytes but also LILRB2 and LILRB4 on DCs) whereas TGFβ prevented the upregulation associated with overnight incubation. (Figure 3.3)

To allow for better discrimination during subsequent correlation with genotype, IL1β, IL6 and TNFα were individually tested in the overnight whole blood stimulation assay. (Figure 3.4) This showed that all the individual inflammatory cytokines increased LILRB expression although to varying degrees. From this data, IL1β at a dose of 50 ng/ml was chosen as the stimulus for use in the genetic correlation part of the project.

LILR expression levels in 26 healthy individuals at baseline and after stimulation with cytokines

Differential LILR cell surface patterns on monocytes and DCs at baseline

After optimisation work was complete, LILR expression levels on antigen-presenting cells in 26 healthy individuals were measured. This showed different patterns of expression of the four receptors tested (Figure 3.5, monocytes and DCs express all the LILRs tested whereas B cells only express LILRB1). In addition, different cell types expressed different levels of individual LILRs. DCs expressed higher levels of LILRB4 compared to monocytes ($p<0.001$). Conversely monocytes had higher expression of LILRB2 compared to DCs ($p<0.001$). DCs and monocytes had similar expression levels of LILRA2 and LILRB1, although B cells had significantly lower levels of expression of LILRB1. As the whole blood assay showed good reproducibility with an intra-assay CV between 1.7 and 5.7%, most of the variability seen is likely to arise due to difference between individuals or cell type rather than assay performance.

Incubation of whole blood ex vivo alters LILR expression on monocytes and DCs

For the same 26 individuals, whole blood was incubated for 21 hours at 37^{o}C without any manipulation to determine the amount of change without stimulation. Monocytes upregulated all the LILR molecules tested (Figure 3.7) whereas DCs only upregulated LILRB1 and LILRB2 to a lower extent (Figure 3.6). Conversely, DCs downregulated LILRA2 and LILRB4 expression (Figure 3.6).

Monocytes were then compared to DCs with respect to their ability to modulate LILR levels. When cultured in whole blood *ex vivo*, there were significant differences in the change of LILRs between DCs and monocytes for all molecules tested (Figure 3.8). Monocytes always upregulated all four LILRs tested to a greater extent than DCs. In contrast, DCs showed a slight downregulation of LILRA2 and LILRB4, but upregulated both of LILRB1 and LILRB2.

LILRs are upregulated on monocytes and DCs by inflammatory cytokines

The change in LILR expression in response to the inflammatory cytokine, IL1-β was then tested in the group of 26 healthy individuals. This showed a marked increase of LILRB1, LILRB2 and LILRB4 on monocytes above the levels seen without stimulation (Figure 3.10). On DCs, only LILRB2 showed marked upregulation, whereas the other two molecules showed less upregulation, although still statistically significant (Figure 3.9). The activating receptor LILRA2 did not show much change on either monocytes or DCs (Figures 3.9 and 3.10). Monocytes significantly upregulated LILRB1 and LILRB4 more than dendritic cells. A

significant difference in the change of LILRA2 expression levels between monocytes and DCs was observed as well, although the magnitude of difference was less. Both monocytes and DCs upregulated LILRB2 to a similar degree (Figure 3.11).

LILRs are downregulated on monocytes and DCs by stimulation with TGF-β

Subsequently, the response to the inhibitory cytokine TGF-β at a dose of 20 ng/ml was tested to determine the responses in the 26 individuals. This showed significant downregulation in all molecules tested on monocytes and DCs. The downregulation was most pronounced for LILRA2 on DCs and LILRB2 on DCs and monocytes (Figures 3.12 and 3.13). There was a more moderate downregulation in the remaining LILRs. Comparison of the modulation index showed significant differences in the degree of downregulation seen in all 4 LILRs tested between DCs and monocytes (Figure 3.14). Monocytes showed greater downregulation of LILRB1 and LILRB2 compared to DCs whereas the converse was true for LILRA2 and LILRB4. These findings again further confirm that LILRs are regulated differently on different cell types of APCs.

Discussion

These findings show that the LILRs, despite being relatively non-polymorphic express some variation between different individuals and on different cell types. This appears to be true for LILR baseline as well as IL-1β and TGF-β mediated changes (a summary of all results is found in Table 3.3). However, the pattern of

LILR regulation is remarkably similar between the 26 individuals studied. Such variation may play a significant functional role as published data have demonstrated that expression of some of the inhibitory LILRs on cells *in vitro* has resulted in functional consequences such as the generation of tolerogenic DCs. (23;101)

It is possible that the variation of the different LILRs on the cells surface may just represent natural biological variation and be of no functional consequence. There is relatively little data on how much variability normally exists for most cell surface molecules, so it is difficult to be certain what the significance of the variation in LILR levels is. However, with the advent of genome-wide association studies, there has been increasing need to assess genotype-phenotype correlations. One approach has been to use standardised flow cytometry to compare protein expression levels with genetic variation. (190) Dendrou *et al* compared alleles in the *IL2RA* (or *CD25*) gene (that has been shown to have an association with type 1 diabetes and multiple sclerosis) with CD25 expression on CD4+ T cells. (190) They found that subjects with the a certain protective allele (against type 1 diabetes, rs12722495) had 27% higher mean CD25 expression on CD4+ memory T cells, compared to patients with susceptibility alleles or other protective alleles. Although there was variability in CD25 expression for subjects with different alleles, there was a significant difference in mean expression levels. In addition, they noted a gene dosage effect with heterozygous and homozygous individuals having a 22% and 33% higher mean CD25 level respectively. This data examining a different cell surface molecule does lend support to the hypothesis that variation in cell surface expression could have functional consequences and is worth investigating in other molecules.

The phenomenon of LILR upregulation primarily on monocytes but not DCs with incubation ex vivo is intriguing. The function of these molecules is still not completely understood, although it is likely that they represent some form of sensor for 'self' given that they bind to MHC class I. One possible explanation could be that monocytes *ex vivo* respond to deprivation of an *in vivo* suppressive signal, perhaps from vascular endothelial cells. Another possible explanation for LILR upregulation on monocytes *ex vivo* could be the presence of stimulatory unidentified factor(s) in culture. Endotoxin contamination has been ruled out (see materials and methods).

It is also interesting to note the direction of change of the so-called 'inhibitory' LILRB molecules in response to stimulation with IL1-β and other 'inflammatory' cytokines. It would be expected that an inflammatory stimulus would depress levels of inhibitory molecules; whereas the converse occurred. In keeping with the expectation that inhibitory cytokines should upregulate inhibitory LILRB molecules, IL-10 has been shown to upregulate LILRB1, LILRB2 and LILRB4 on monocyte-derived dendritic cells *in vitro* (23;104) and in these experiments as well. Addition of inflammatory cytokines resulted in increase of all of the LILRB molecules on monocytes but mainly LILRB2 on DCs. LILRB1 and LILRB4 showed less change on DCs. Interestingly, levels of the 'activating' LILRA2 did not show much change in response to IL-1β.

The reduction in most of the LILRs on monocytes and DCs (and particularly LILRB2 on monocytes) with incubation with TGF-β also stands in contrast to the

findings with IL-10, indicating that different ‘inhibitory’ cytokines can regulate the LILR molecules in different ways. Although it would be predicted that an inhibitory cytokine would reduce the levels of the activating LILRA2, the reduction in the inhibitory LILRB molecules as well is worthy of further attention.

These findings clearly indicate that the regulation of these molecules is likely to be more complex than just simple inhibition or activation of immune cells. It is also possible that differential expression of the LILRs could result in variable cell signals quantitatively and/or qualitatively. This might provide a potential mechanism to explain the diversity of interaction between APCs and ‘self’.

The similar direction of change in the LILRs in response to stimuli seen in different healthy individuals implies that they are tightly regulated and further suggests that these molecules could have evolved to discriminate between innate self and non-self and play a fundamental role in determining the way immune responses develop.

It should be noted that there is the possibility that the effect of overnight culture or cytokines on LILR expression may be due to other cells being affected and subsequently influencing DCs and monocytes to modify their expression of the LILRs.

In summary, the whole blood assay to measure LILR levels on antigen-presenting cells is robust and can be used to accurately quantify these molecules in different individuals. This could represent a useful tool for translational research as LILRs are likely to gain greater prominence. At present, there are multiple studies showing

an association of various LILRs with rheumatologic diseases, infection, autoimmunity, transplantation and malignancy. (1) Various *in vitro* and *in vivo* attempts have been made to harness HLA-G (the highest affinity natural ligand for LILRB1 and LILRB2) and other stimuli that affect LILRB levels for therapeutic purposes. (24;133;191;192) These have made a difference and proposals for potential use in patients have been suggested.

Potentially, the expression levels of these molecules *in vivo* might have functional consequences as well. Consequently, the use of the whole blood assay clinically could be important for two reasons: (i) as understanding of the LILRs increases, their contribution to many diseases will be better delineated and (ii) a reliable method for assessing their expression levels will be useful for translation of this knowledge into useful clinical application. LILR levels could be used to accurately categorise high or low-risk patients for a particular outcome based on their LILR expression levels; to more precisely direct therapy by selecting patients who would be more likely to benefit from interventions using the LILRs; or for monitoring disease progression.

As yet, the whole blood assay has not been used to compare healthy individuals with those with diseases states; or between individuals before and after some form of therapeutic intervention. There is some data suggesting that LILRB2 and LILRB4 levels can be altered with venom immunotherapy (193) although there is limited other data looking at LILR levels during various immunological manipulations. Consequently, this represents an area (in addition to characterizing baseline levels in different diseases) where the whole blood assay could be utilised.

Tables

Table 3.1

Mean, standard deviation and coefficient of variation of the MFI of LILRA2, LILRB1, LILRB4 and LILRB2 on DCs, monocytes and B cells for 5 replicates of one sample

	B cell LILRB1	DC LILRA2	DC LILRB1	DC LILRB2	DC LILRB4	Monocyte LILRA2	Monocyte LILRB1	Monocyte LILRB2	Monocyte LILRB4
Mean	5.63	11.9	12.2	1.21	8.60	11.3	11.7	3.27	2.63
SD	0.095	0.471	0.369	0.060	0.488	0.264	0.285	0.138	0.074
CV	1.70	3.96	3.03	4.96	5.68	2.33	2.43	4.22	2.83

Table 3.2

Intra-individual variation in LILRs in 2 different individuals sampled at 5 different time points. The coefficient of variation for the 4 LILR molecules tested is shown.

		B cells	DCs				Monocytes			
		LILRB1	LILRA2	LILRB1	LILRB2	LILRB4	LILRA2	LILRB1	LILRB2	LILRB4
Individual 1	Mean	3.04	16.6	7.60	3.23	2.79	12.4	5.34	5.77	1.05
	SD	0.117	1.59	0.937	0.475	0.220	0.914	0.234	1.78	0.0814
	CV	3.85	9.6	12.3	14.7	7.9	7.3	4.4	30.8	7.8
Individual 2	Mean	3.41	17.9	8.50	1.89	4.48	17.2	7.57	4.48	1.73
	SD	0.165	1.82	1.36	0.838	0.673	1.45	0.871	1.65	0.232
	CV	4.82	10.2	16.0	44.3	15.0	8.5	11.5	36.8	13.4

Table 3.3

Change in LILR levels at 21 hours of culture on different APCs following stimulation with IL-1β or TGF-β compared to baseline.

	B cells	DCs				Monocytes			
	LILRB1	LILRA2	LILRB1	LILRB2	LILRB4	LILRA2	LILRB1	LILRB2	LILRB4
Cultured vs. baseline	NC	NC	NC	↑	NC	↑	↑	↑↑	↑
IL-1β vs. medium alone	NC	NC	↑	↑↑	NC	NC	↑↑	↑↑	↑↑↑
TGF-β vs. medium alone	NC	↓	NC	↓	↓	NC	NC	↓↓↓	NC

NC (no change) = between 50% increase and 33% reduction compared to baseline/unstimulated cells, ↑ = 50 to 200% increase compared to baseline/unstimulated cells, ↑↑ = 200 to 400% increase compared to baseline/unstimulated cells, ↑↑↑ = > 400% increase compared to baseline/unstimulated cells, ↓ = 33% to 66% reduction compared to baseline/unstimulated cells, ↓↓ = 66% to 80% reduction compared to baseline/unstimulated cells, ↓↓↓ = > 80% reduction compared to baseline/unstimulated cells)

Figures

Figure 3.1a

Median fluorescence intensity of monocyte staining with various amounts of anti-LILRA2 and anti-LILRB2

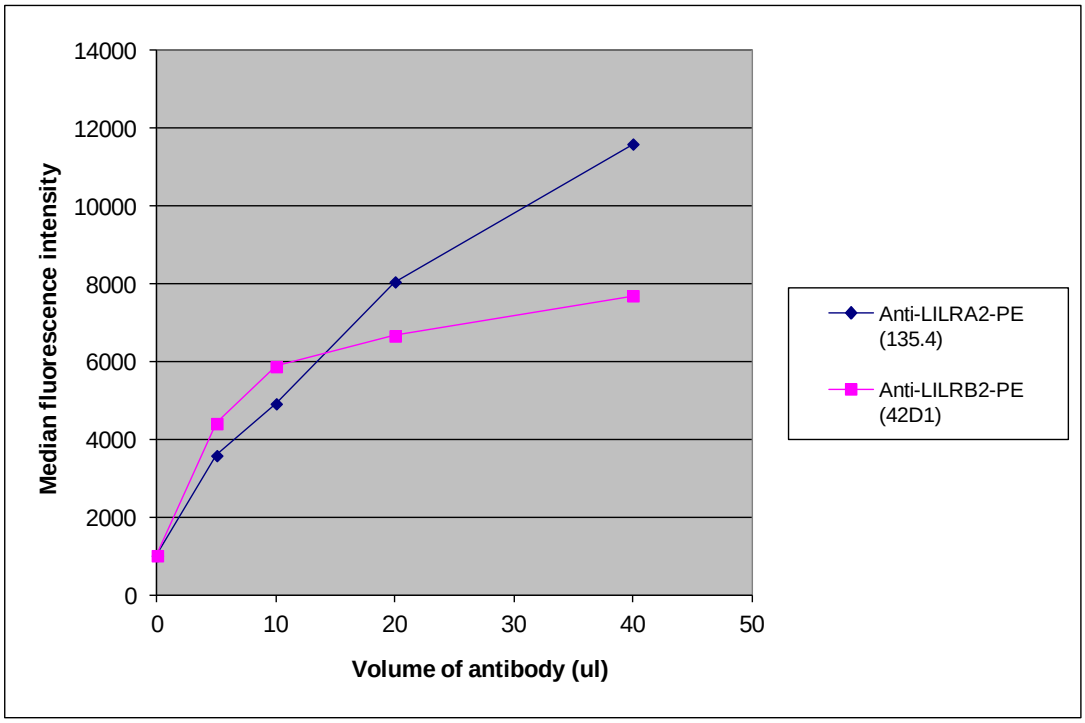

Figure 3.1b

Median fluorescence intensity of monocyte staining with various amounts of anti-LILRB1 and anti-LILRB4 monoclonal antibodies

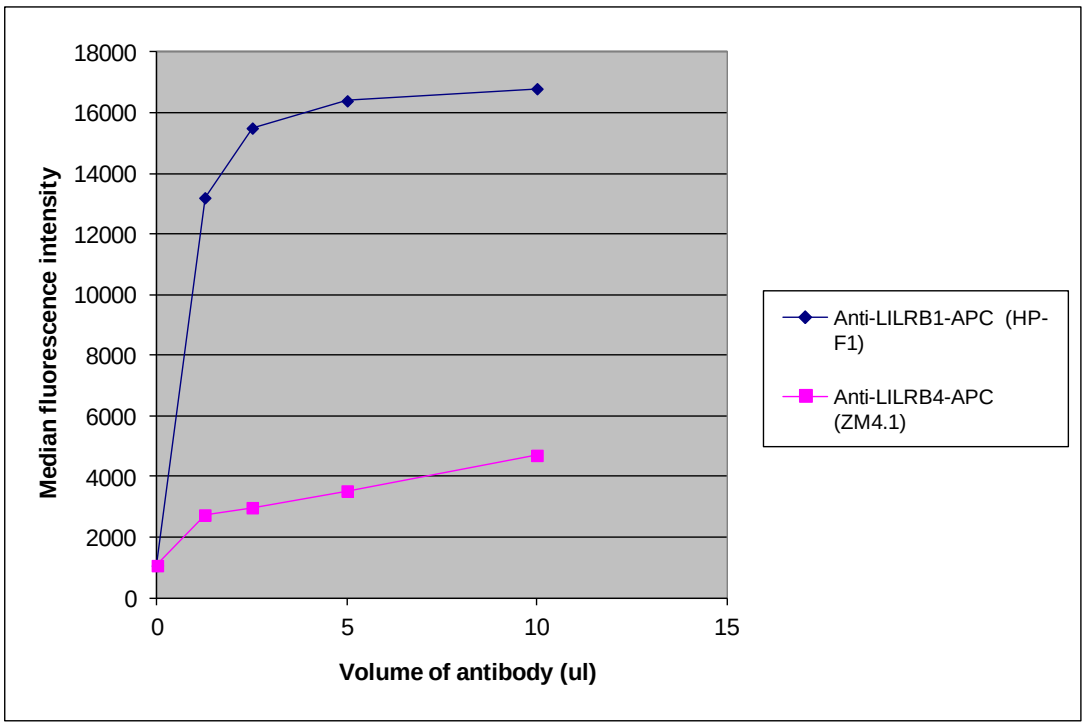

Figure 3.2

Change in the levels of LILR molecules on B cells, DCs and monocytes at baseline, 3, 6 and 22 hours incubation at 37^{o}C in whole blood without addition of any stimuli

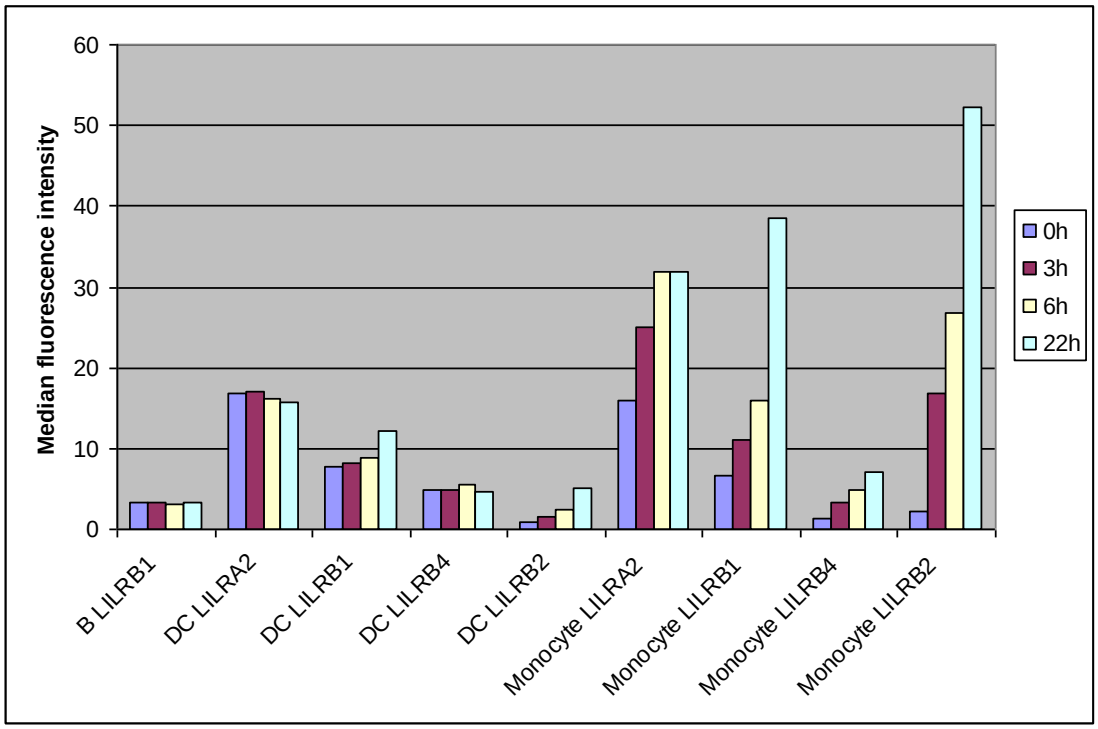

Figure 3.3

Differential response of LILRs after addition of inflammatory cytokines MCM (IL1β, IL6, TNFα and PGE_2), IL10 or TGFβ on B cells, monocytes and dendritic cells. Modulation index (ratio of the median fluorescence intensity of LILR expression after 21 hours incubation at 37°C with stimulus over LILR expression at 21 hours without stimulation) for B cells, DCs and monocytes. B cells only express LILRB1.

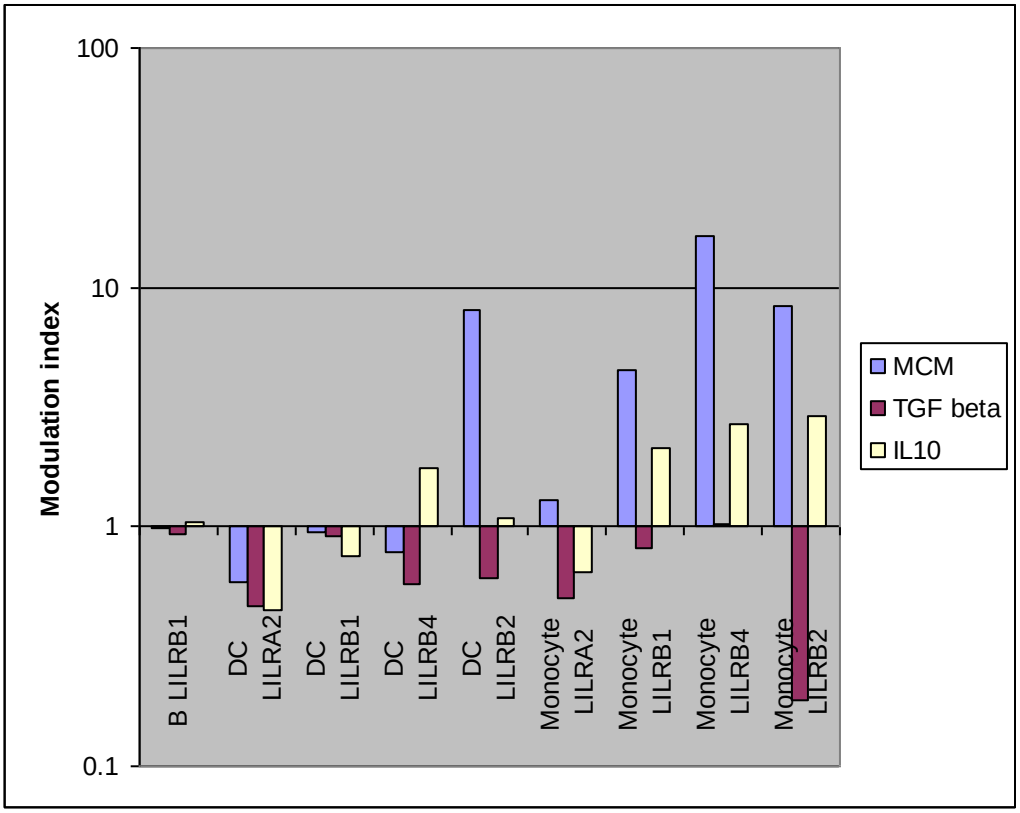

Figure 3.4

Modulation index (ratio of the median fluorescence intensity of LILRB1, LILRB4 and LILRB2 expression after 21 hours incubation at 37°C with stimulus over expression at 21 hours without stimulation) for monocytes, after stimulation with a cocktail of inflammatory cytokines (MCM = IL1β, IL6, TNFα and PGE_2) or individually with IL1β, IL6 or TNFα at 3 different doses.

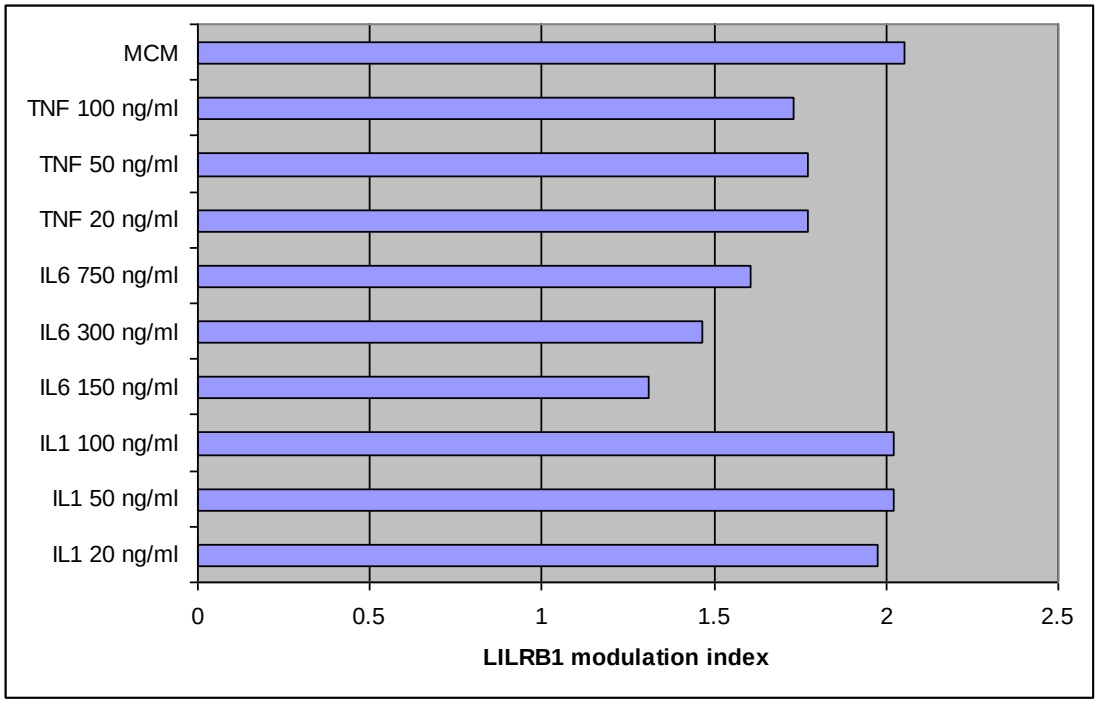

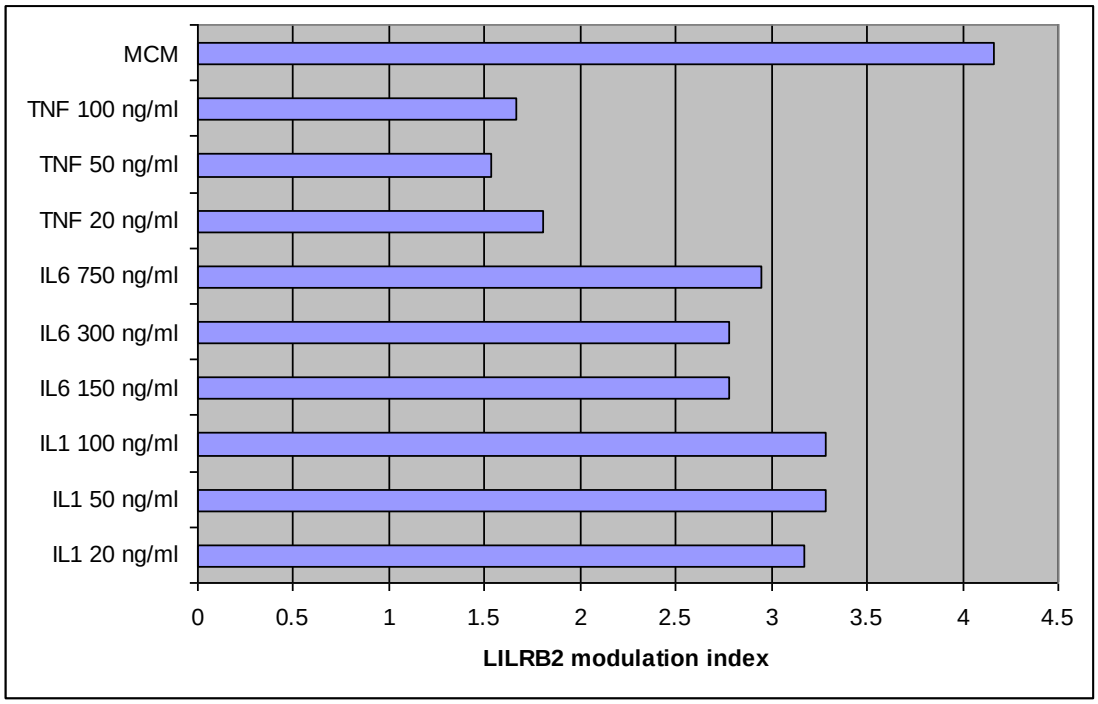
MCM
TNF 100 ng/ml
TNF 50 ng/ml
TNF 20 ng/ml
IL6 750 ng/ml
IL6 300 ng/ml
IL6 150 ng/ml
IL1 100 ng/ml
IL1 50 ng/ml
IL1 20 ng/ml
0
0.5
1
1.5
2
2.5
3
3.5
4
4.5
LILRB2 modulation index

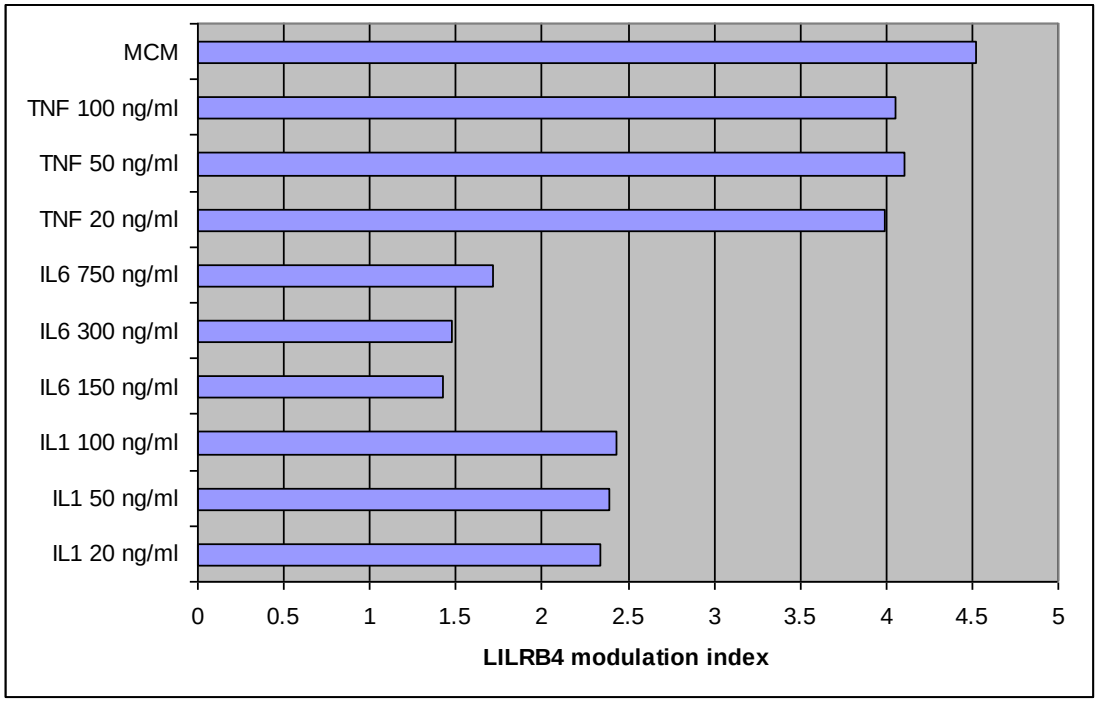
MCM
TNF 100 ng/ml
TNF 50 ng/ml
TNF 20 ng/ml
IL6 750 ng/ml
IL6 300 ng/ml
IL6 150 ng/ml
IL1 100 ng/ml
IL1 50 ng/ml
IL1 20 ng/ml
0
0.5
1
1.5
2
2.5
3
3.5
4
4.5
5
LILRB4 modulation index

Figure 3.5

Differential baseline LILR expression between monocytes and dendritic cells. Molecules of equivalent fluorochrome (MEF) of LILRA2, LILRB1, LILRB2 and LILRB4 on B cells (grey circles), DCs (white circles) and monocytes (black circles) on healthy individuals (n=26). B cells only express LILRB1. The diamonds represent the mean value and error bars represent 1 standard deviation.

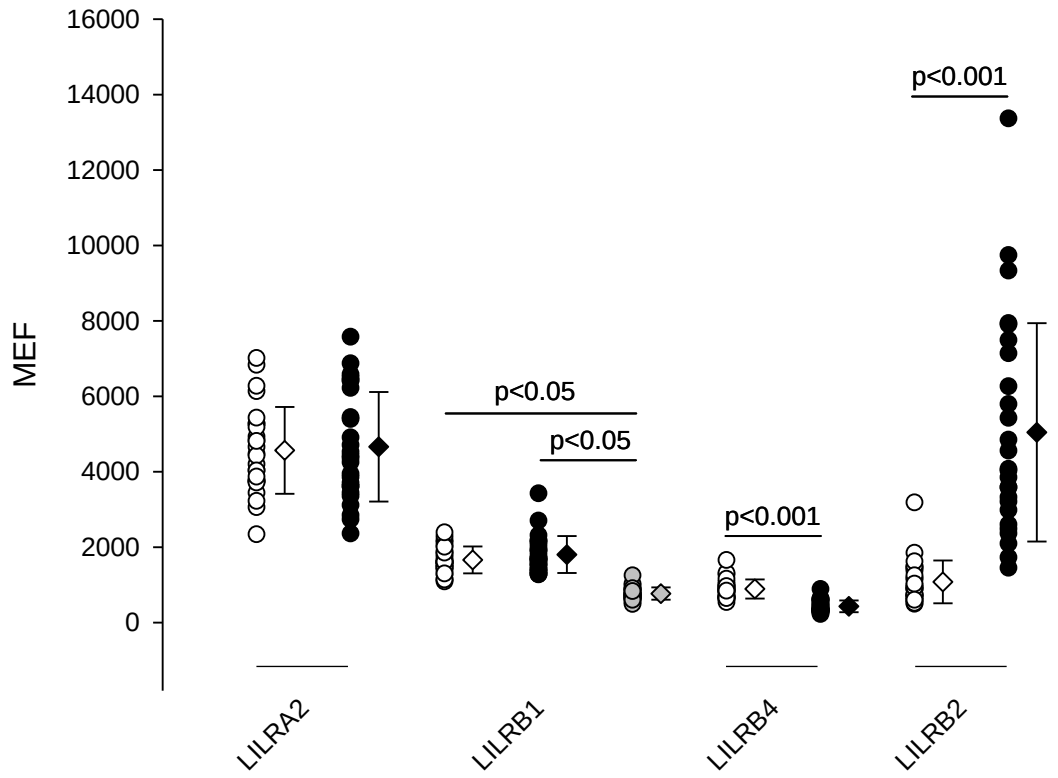

Figure 3.6

Change in LILR expression on dendritic cells by *ex vivo* incubation in healthy individuals (n=26). Difference in molecules of equivalent fluorochrome (MEF) of LILRs on B cells and DCs between cells at 0 hours and 21 hours incubation unstimulated at 37^{o}C.

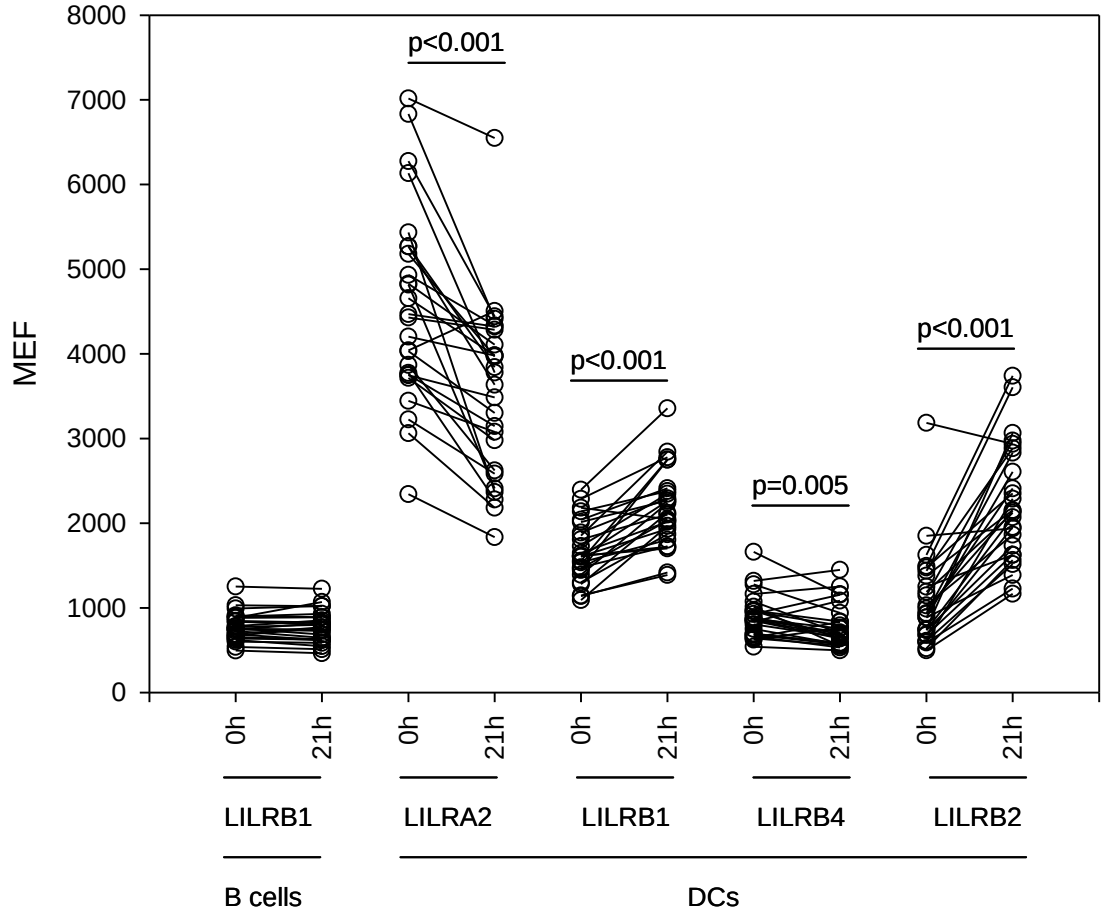

Figure 3.7

Change in LILR expression on monocytes by *ex vivo* incubation in healthy individuals (n=26). Difference in molecules of equivalent fluorochrome (MEF) of LILRs on monocytes between cells at 0 hours and 21 hours incubation unstimulated at 37^{o}C.

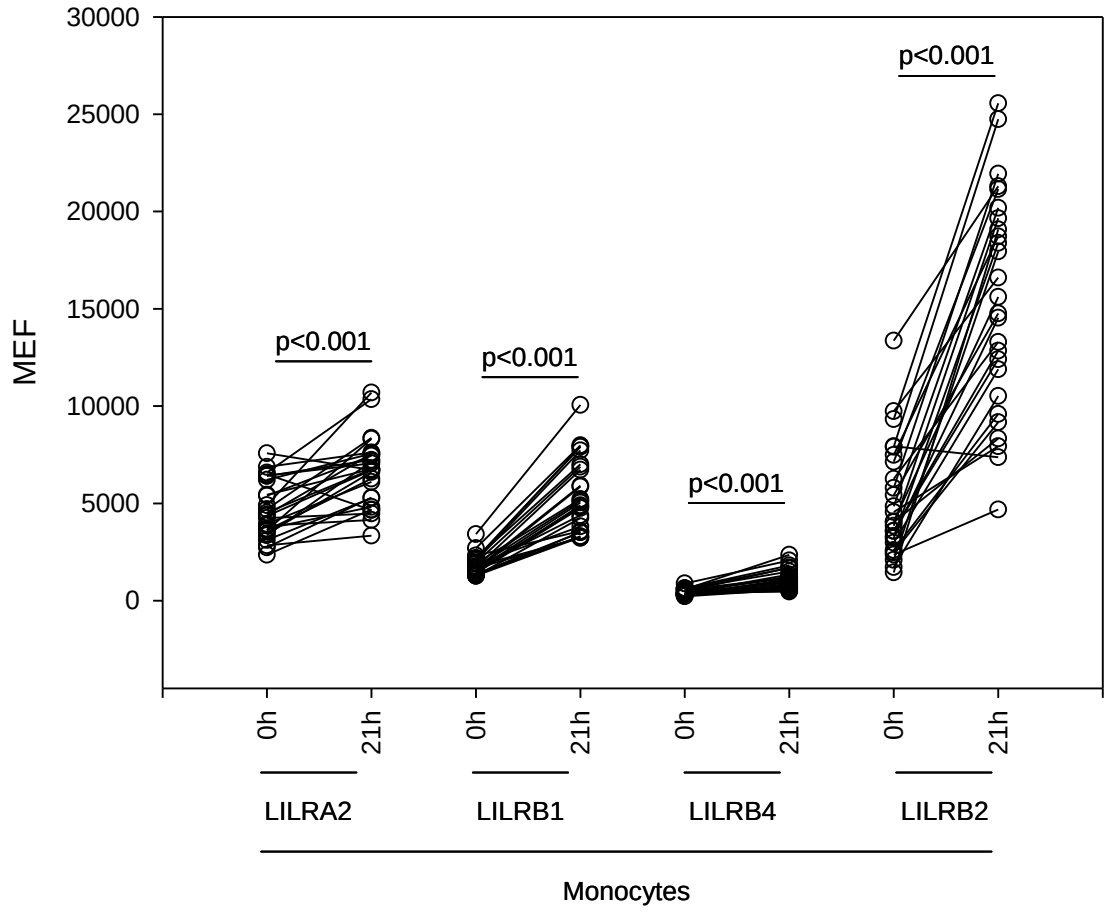

Figure 3.8

Differential upregulation of LILRs by *ex vivo* incubation between monocytes and dendritic cells. Modulation indices (ratio of the molecules of equivalent fluorochrome of LILR staining after 21 hours incubation at 37^{o}C over LILR expression at 0 hours) for B cells (grey circles), DCs (white circles) and monocytes (black circles) of 26 healthy individuals are shown. B cells only express LILRB1. The diamonds represent the mean and the error bars represent 1 standard deviation.

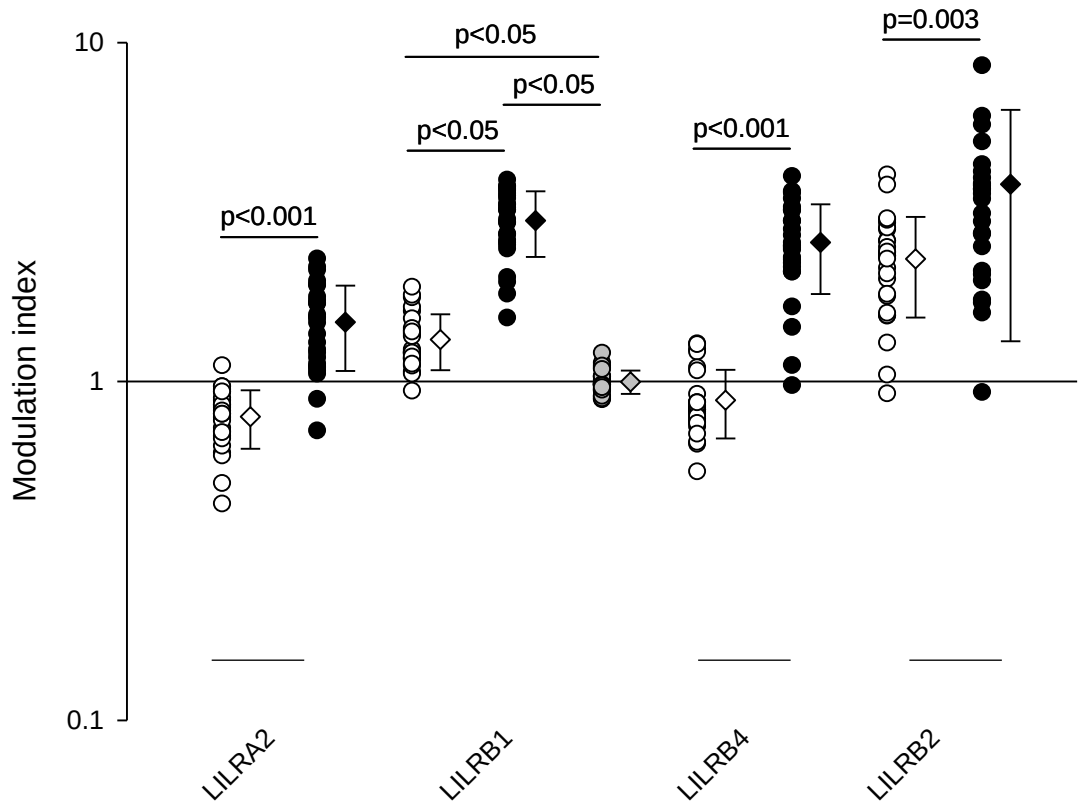

Figure 3.9

Change in LILR expression on dendritic cells by stimulation with IL-1β in healthy individuals (n=26). Difference in molecules of equivalent fluorochrome (MEF) of LILRs on B cells and DCs between cells at 21 hours incubation at 37^{o}C unstimulated and cells incubated with 50 ng/ml IL-1β.

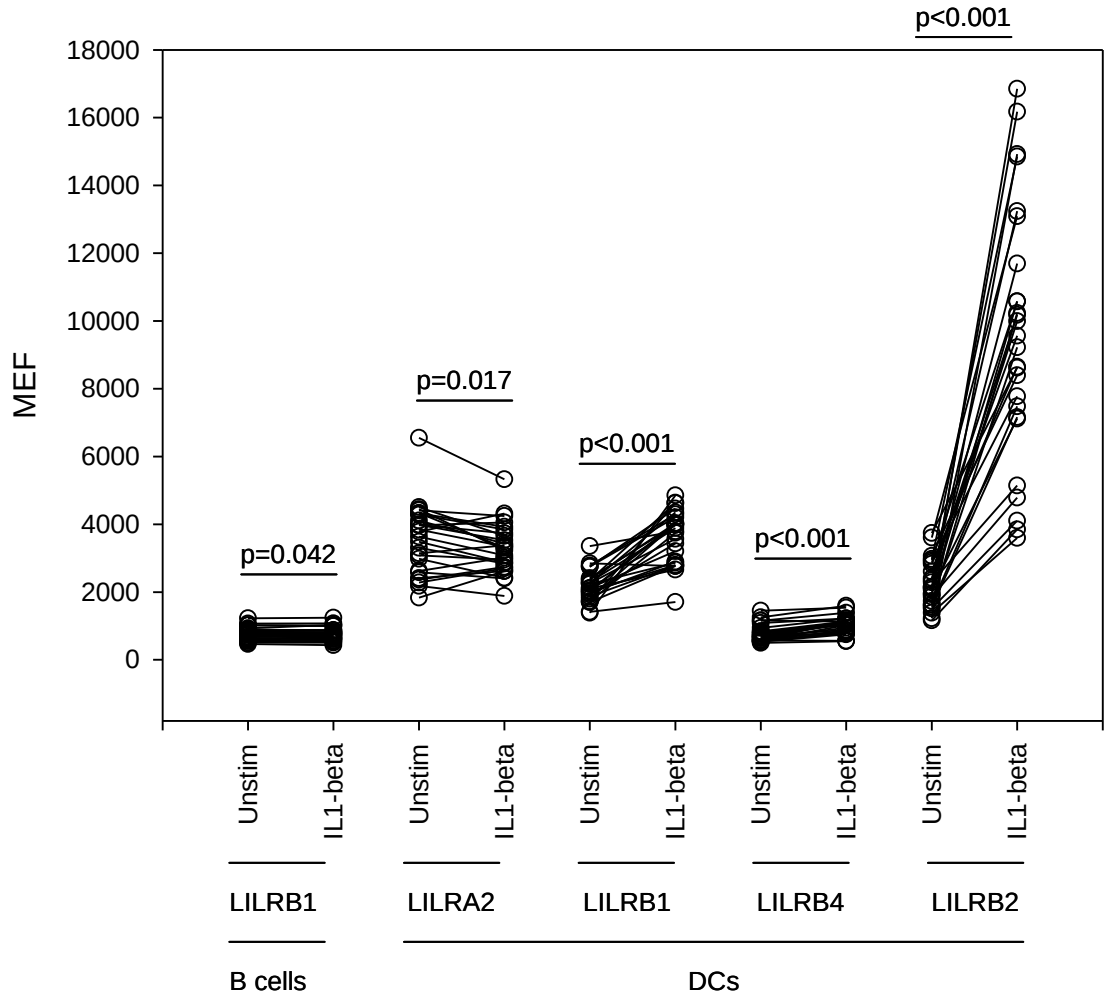

Figure 3.10

Change in LILR expression on monocytes by stimulation with IL-1β in healthy individuals (n=26). Difference in molecules of equivalent fluorochrome (MEF) of LILRs on monocytes between cells at 21 hours incubation at 37°C unstimulated and cells incubated with 50 ng/ml IL-1β.

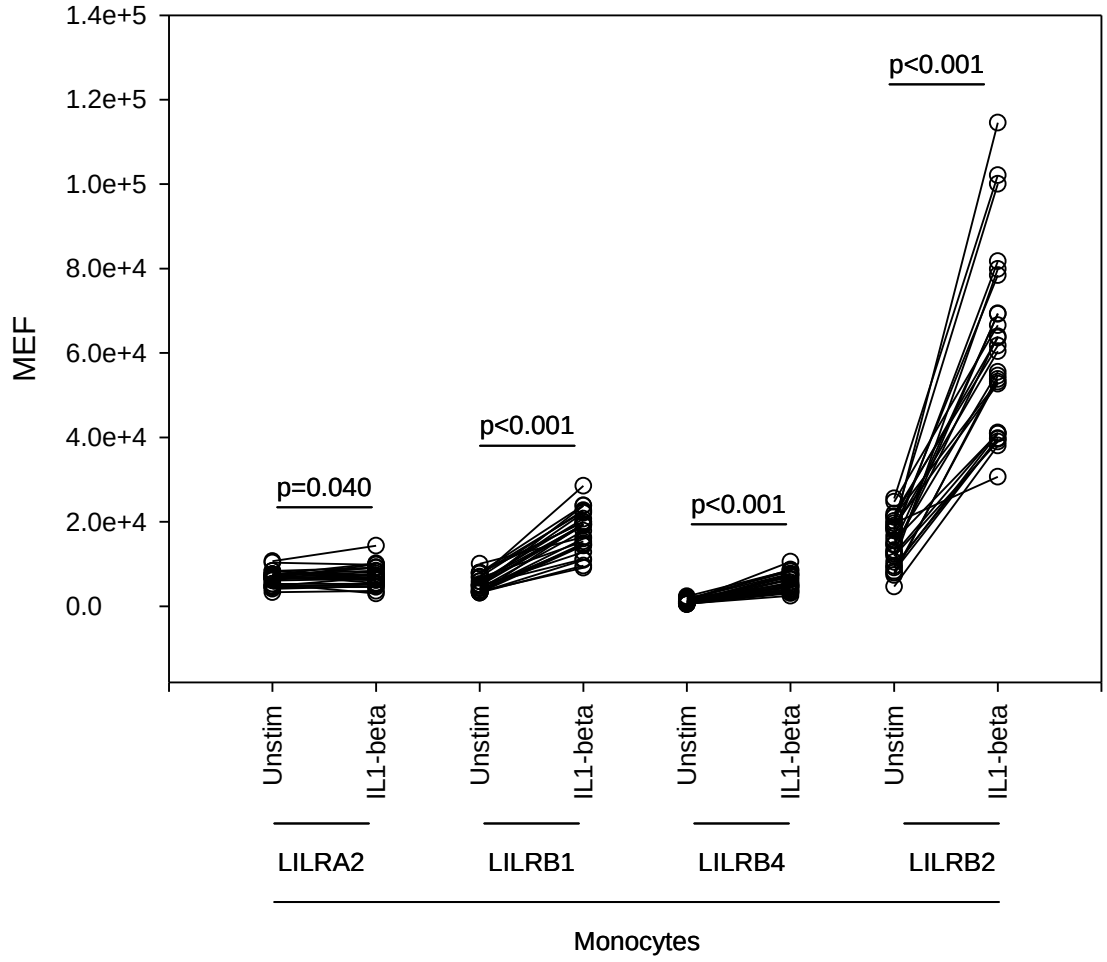

Figure 3.11

Differential upregulation of LILRs by IL-1β between monocytes and dendritic cells. Modulation index (ratio of the molecules of equivalent fluorochrome of LILR expression after 21 hours incubation at 37°C with 50 ng/ml IL-1β over LILR expression at 21 hours without stimulation) for B cells (grey circles), DCs (white circles) and monocytes (black circles) of 26 healthy individuals. B cells only express LILRB1. The diamonds represent the mean and the error bars represent 1 standard deviation.

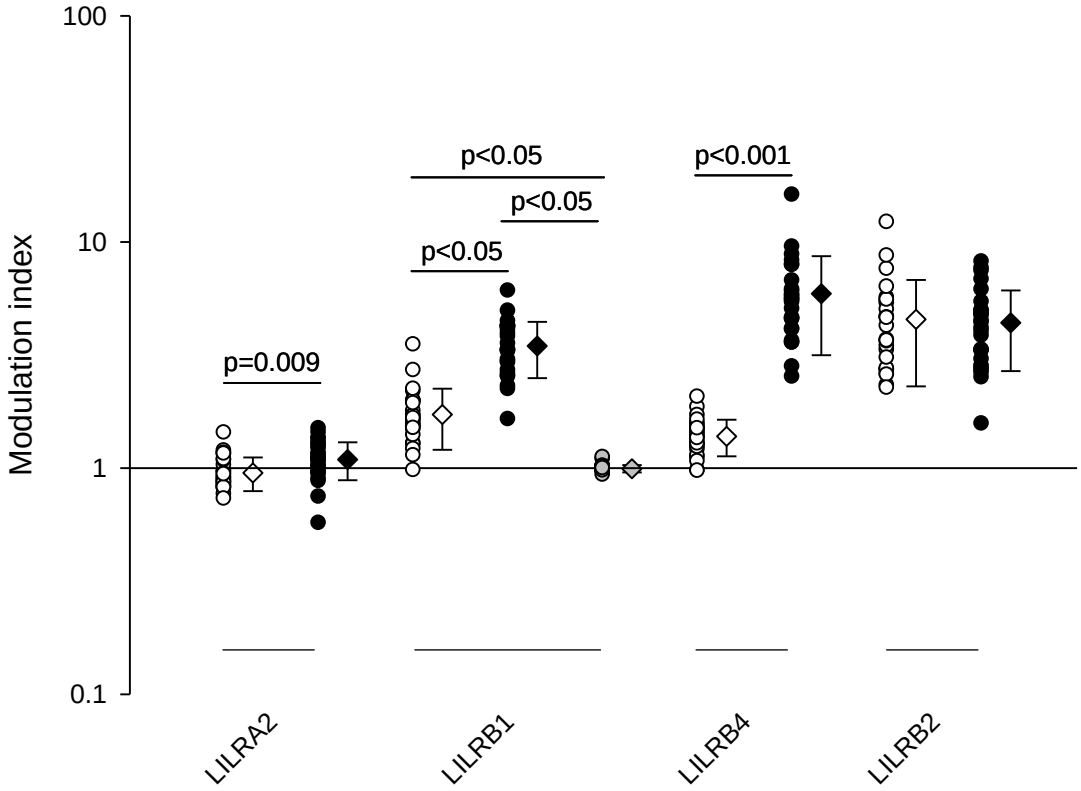

Figure 3.12

Change in LILR expression on dendritic cells by stimulation with TGF-β in healthy individuals (n=26). Difference in molecules of equivalent fluorochrome (MEF) of LILRs on B cells and DCs between cells at 21 hours incubation at 37^{o}C unstimulated and cells incubated with 20 ng/ml TGF-β.

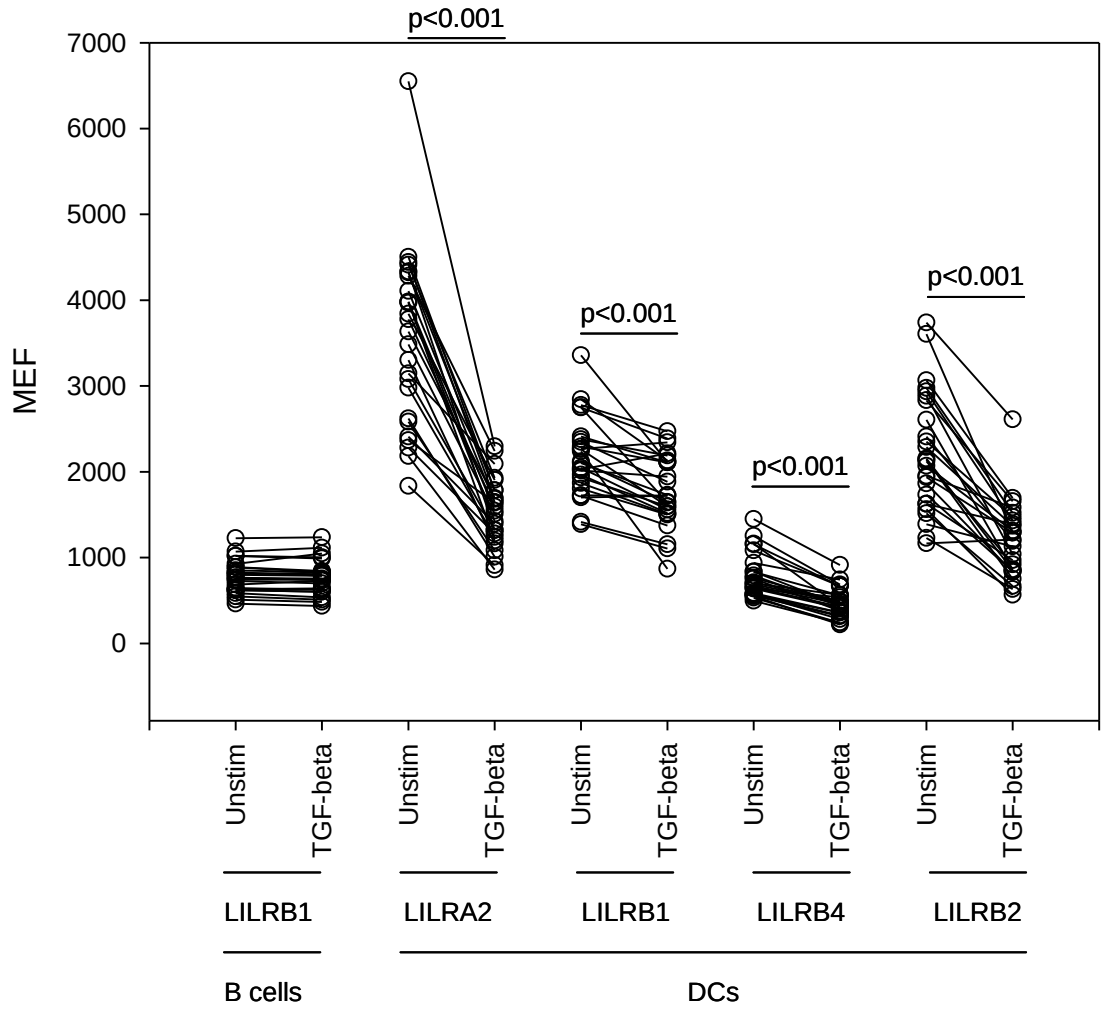

Figure 3.13

Change in LILR expression on monocytes by stimulation with TGF-β. Difference in molecules of equivalent fluorochrome (MEF) of LILRs on monocytes between cells at 21 hours incubation at 37^{o}C unstimulated and cells incubated with 20 ng/ml TGF-β.

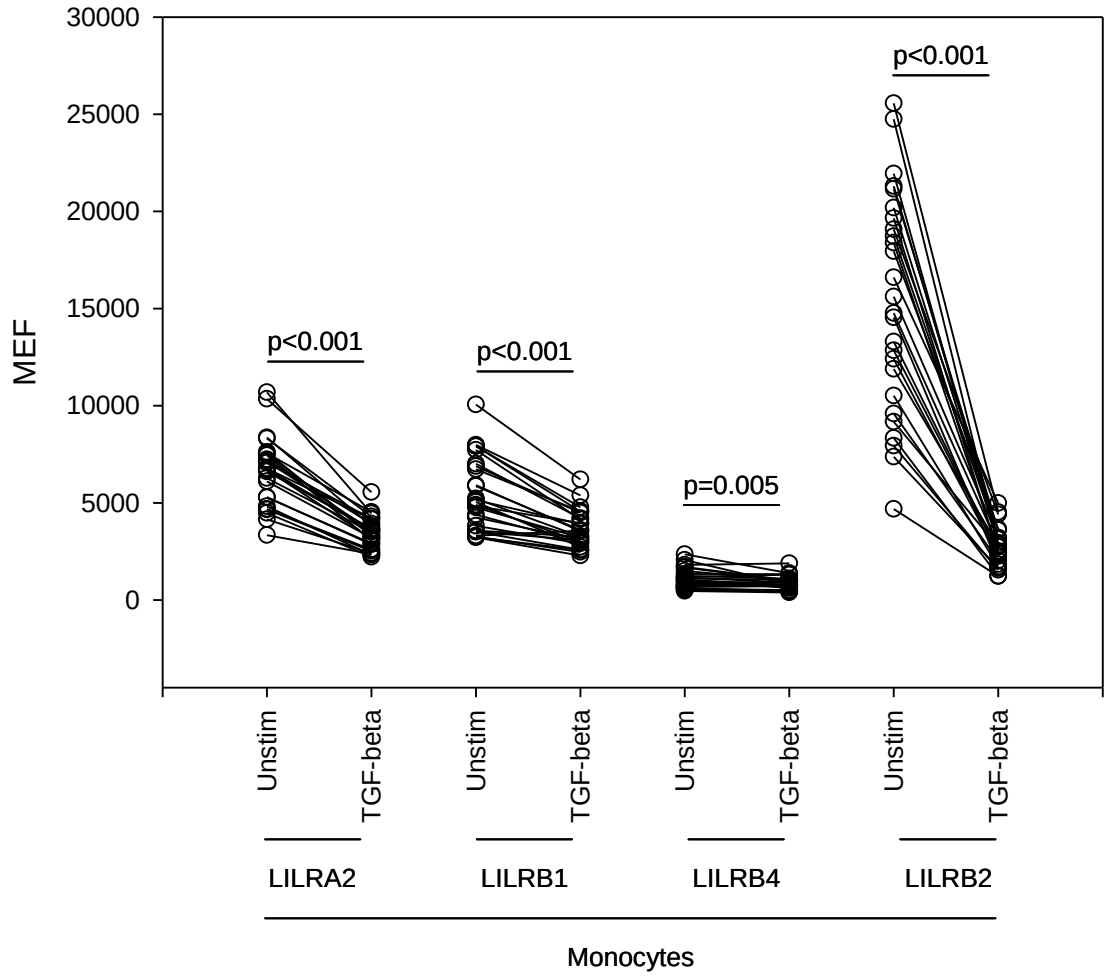

Figure 3.14

Differential downregulation of LILRs by TGF-β between monocytes and dendritic cells. Modulation index (ratio of the molecules of equivalent fluorochrome of LILR expression after 21 hours incubation at 37°C with 20 ng/ml TGF-β over LILR expression at 21 hours without stimulation) for B cells (grey circles), DCs (white circles) and monocytes (black circles) of 26 healthy individuals. B cells only express LILRB1. The diamonds represent the mean and the error bars represent 1 standard deviation.

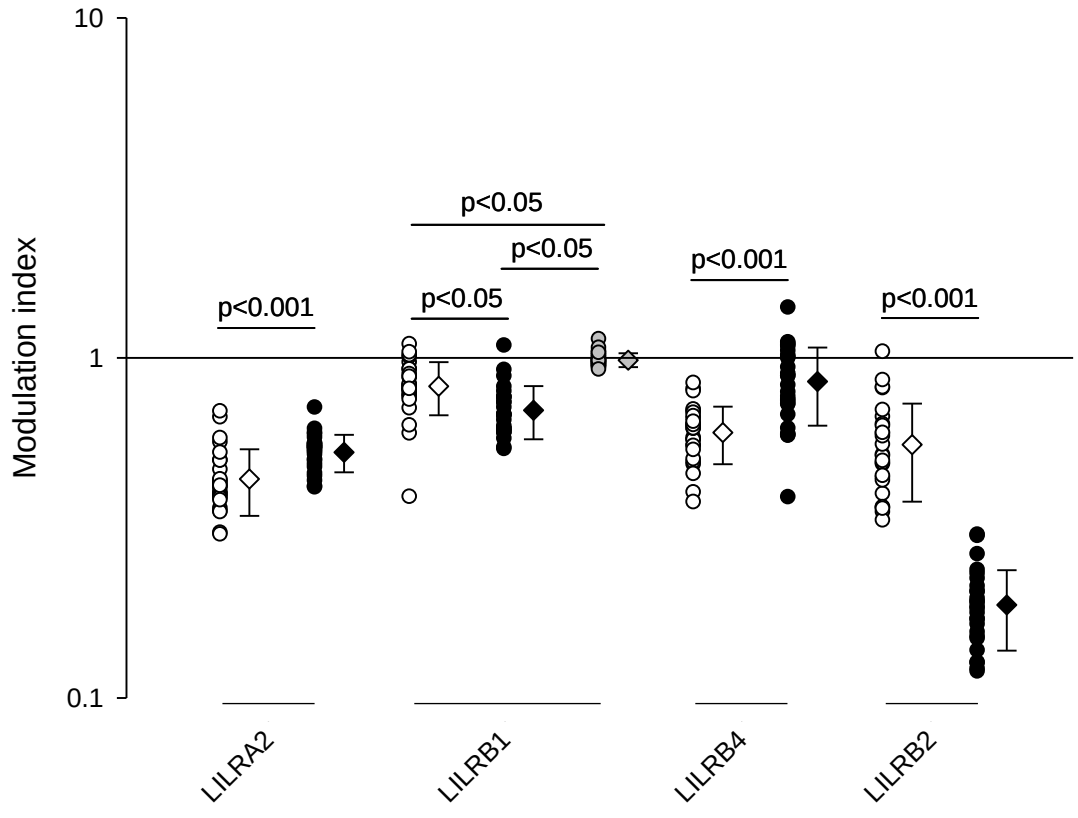

Chapter 4: Genomic variation in the LILRB2 promoter and its effect on protein expression

Background

There is a limited amount of previously published data showing that LILR polymorphisms are associated with either expression levels on the cell surface or with various immunological diseases. The most well described example of a LILR deficiency being associated with disease is homozygous LILRA3 deficiency which has been shown to have an association with multiple sclerosis and Sjogren's syndrome. (26;27) A polymorphism in LILRA2 resulting in an isoform lacking 3 amino acids in the linker region (Delta 419-421) has been shown to be more prevalent in microscopic polyangiitis and systemic lupus. (160) In addition to the data showing that polymorphisms in the LILR molecules can affect expression or be linked to disease, there is data showing that polymorphisms in HLA molecules, the ligands for some of the LILRs can affect both binding affinity to the LILRs and have an association with disease. (5)

Most of the other studies showing differences in LILR levels in various pathological conditions have not investigated whether this is due to genetic polymorphism or other disease-related or non-genetic factors. There are two published studies that have looked at the effect of polymorphisms on expression levels of the LILRs; and one of these studies looked at the association of polymorphisms with a disease (rheumatoid arthritis). However, some of the polymorphisms described affected the coding region of the LILR molecules and potentially might have effects on the

binding/functional properties of the molecules (rather than their expression levels) to account for their association with disease states.

Kuroki et al have shown that for LILRB1, a certain haplotype (described as LILRB1.PE01) with two SNPs present in the promoter region (not present in the other 2 haplotypes described) was associated with lower level of LILRB1 by flow cytometry both on lymphocytes and monocytes .(172) No differences were noted in crystal structure, binding affinities or thermostability in any of the three haplotypes described. It should be noted, however, that there were also non-synonymous polymorphisms present in the coding regions of the molecule, although they did show that this did not affect the affinity of the detection antibody used in the flow cytometric assay. They did not find a significant association with rheumatoid arthritis or systemic lupus. However, on analysis of patients who did not carry the RA-associated HLA-DRB1 shared epitope, patients homozygous for LILRB1.PE01/01 were more likely to have rheumatoid arthritis (with an odds ratio of 2.05). These data suggest that LILRB1 promoter polymorphisms can affect expression levels of the molecule and subsequently increase propensity to rheumatoid arthritis (at least in the absence of an HLA type strongly associated with the disease).

Hirayasu *et al* identified 3 LILRB2 polymorphisms (two in the 5'-UTR and one in the signal sequence region, c.59A→G, p.H20R) which had an effect on expression levels on monocytes. (194) Individuals with the c.59GG phenotype had a significantly lower level of cell surface expression of LILRB2 compared to those with the c.59AA phenotype. The remaining two polymorphisms c.-169A and c.-

153A showed the same effect but were in absolute linkage disequilibrium with c.59G. Hence, it is possible that the signal sequence region polymorphism is solely responsible for the differences in expression levels. Their study did not investigate whether any of these alleles were more likely to be associated with any particular diseases.

Consequently, the data on whether promoter region polymorphisms affect the expression levels of the LILR molecules (and potentially affect susceptibility to illness) is not conclusive. To test the hypothesis, the putative LILRB2 promoter region was chosen for sequencing to focus effort and resources; in particular, given that there was availability of large amounts of anti-LILRB2 antibody from hybridoma stock to allow for further functional testing of this particular molecule.

In this chapter, the sequencing results of the LILRB2 promoter region in the 26 individuals had previously had LILR expression levels measured are described. The different polymorphisms are then compared to determine if any of these have an effect on LILRB2 expression levels. Transcriptional regulation of LILRB2 in response to various stimuli is confirmed both in monocytes and the human acute monocytic leukaemia cell line, THP-1. Finally, a 607 bp region (-533 to +74) around the putative transcription initiation site for LILRB2 (189) is cloned into the pGL4.10/luc2 firefly luciferase vector to determine if any effect for the promoter polymorphisms can be found in a transcriptional luciferase reporter gene assay.

Sequencing of the putative LILRB2 promoter region

PCR amplification of 2306 bp region containing the LILRB2 promoter

Genomic DNA was extracted from heparinised whole blood of the 26 individuals (designated C1 to C26) who had previously had their LILR expression levels measured. This yielded a genomic DNA concentration in the range of 11.8 to 43.6 ng/µl. (Table 4.1) A 2306 bp region corresponding to –1925 to +380 bp from the ATG start codon (with A being designated as position 0) was then amplified with primers designed using the PrimerZ web application. (195) In the Genome Reference Consortium Human genome build 37 this corresponds to GRCh37:19:54784103-54786408. Agarose gel electrophoresis demonstrated successful amplification of the product (Figure 4.1). The 2306 bp band was then extracted from the gel and sent off for sequencing.

Sequencing of amplified PCR product and identification of SNPs contained in the amplified PCR region

The amplified PCR product was then sequenced with 5 overlapping primer pairs (Figure 4.2) and the sequence data analysed with Variant Reporter 1.1 software (Applied Biosystems). Individual traces showing the various polymorphisms for the 26 healthy individuals tested is shown are Figure 4.3. This identified 15 SNPs present in the 26 individuals that were sequenced. (Table 4.2) The public SNP database (dbSNP build 135) was then checked to determine if these SNPs had been previously identified. 13 of these SNPs had previously been identified; the dbSNP

ID and GRCh37 chromosome 19 positions for the SNPs identified are noted in Table 4.2. Two new SNPs were identified – GRCh37 chromosome 19, position 54786194 with a G/A polymorphism in one individual (C9) and position 54784798 with a C/T polymorphisms in another individual (C22).

Relationship between SNPs identified and LILRB2 protein expression levels

The expression levels of LILRB2 protein on flow cytometry (Figures 2.1, 3.5, 3.8, 3.11 and 3.14) were then compared for differences between groups of individuals with different SNPs. Figure 4.4 shows the values for LILRB2 expression (at baseline and as a modulation index after incubation with or without cytokines at 22 hours) divided by genotype. Although there was some variation in expression levels by different genotype, no statistically significant differences were found between the different groups. The statistical tests used for parametric data was the t-test (when there were 2 genotypes for the SNP) or one way ANOVA with the Bonferroni correction (when there were 3 genotypes for the SNP). Non-parametric data was compared using the Mann-Whitney U test (when 2 SNP genotypes were present) or the Kruskal-Wallis test (when 3 SNP genotypes were present).

Previously published data has shown that individuals with a homozygous haplotype of AA at the rs448092 and rs448083 SNPs (associated with G at the rs383369 SNP) have lower levels of LILRB2 expression on monocytes. (194) Unfortunately, it was not possible to demonstrate this as there was only one individual with the AA haplotype at the rs448092 SNP present in the 26 individuals tested. (Table 4.2) Statistical comparison did not show any significant differences.

Demonstration of the transcriptional regulation of LILRB2

In order to confirm that expression levels of LILRB2 are transcriptionally regulated, real time PCR was performed on purified monocytes (Figure 4.5a) and THP1 cells (Figure 4.5b) at baseline and after stimulation with IL10, an inflammatory cytokine mixture (MCM = IL1β, IL6, TNFα and PGE_2) or unstimulated.

Published data had shown that addition of IL10 resulted in upregulation of LILRB2 mRNA in THP-1 cells (196) and that addition of *Salmonella thyphimurium* LPS results in upregulation of LILRB2 (and LILRB4) mRNA in *in vitro* cultured macrophages. (177)

The experiments were performed to confirm some of these findings and also to determine if the changes in the LILRB2 protein expression seen in monocytes in the whole blood stimulation assay could possibly occur due to transcriptional regulation of LILRB2.

Real time PCR for LILRB2 in monocytes and THP1 cells with different stimuli

Total mRNA was harvested from both purified monocytes and THP-1 cells at baseline and after 6 and 24 hours with or without stimulation with IL10, MCM or E Coli LPS. Following conversion of the mRNA to cDNA, the samples were then run through a real time PCR reaction. The monocyte experiments were done on two different individuals and the THP-1 experiments were repeated on two occasions.

For purified monocytes, the greatest amount of increase in LILRB2 mRNA was seen at 6 hours after stimulation with LPS (with a relative quantitation, RQ value of 17.9, using the ΔΔCt method of calculation). (Figure 4.5a) There was a more modest increase in IL10 (RQ of 6.7) and with inflammatory cytokines at 6 hours (RQ of 3.1). By 24 hours, the amount of increase in LILRB2 mRNA had almost returned to baseline.

For THP-1 cells, there was an increase in LILRB2 mRNA with both LPS and inflammatory cytokines (RQ of 9.4 and 6.7 respectively), with similar change at both 6 and 24 hours after addition of stimuli (RQ of 4.8 and 5.1 respectively). (Figure 4.5b) There was a more modest increase with addition of IL10. (RQ of 4.2 at 6 and 24 hours)

These findings confirm that the change in expression levels of LILRB2 is, at least in part, transcriptionally regulated.

Dual luciferase reporter assay to determine if LILRB2 promoter SNPs affect protein expression levels

In view of the fact that no significant differences were found in LILRB2 expression levels in individuals with different SNPs, cloning of individual LILRB2 promoter haplotypes into a firefly luciferase plasmid was undertaken. This was done in case other factors could have masked any significant effect the individual SNPs would

have had on expression levels in primary cells; potential reasons for this are discussed further below.

Cloning of the 1000 bp region upstream of the ATG start codon to determine individual LILRB2 promoter region haplotypes

A 1000 bp region upstream of the ATG start codon was PCR cloned into the pGL4.10/luc2 promoterless firefly luciferase plasmid (Promega). This was done from the amplified 2306 bp region containing the LILRB2 promoter from 5 out of the 26 individuals (C2, C3, C11, C13 and C25) to obtain a selection of LILRB2 promoter haplotypes for testing in the luciferase assay.

PCR cloning was done using primers which had the addition of NheI at the 5' end and XhoI at the 3' end of the sequence to allow directional cloning into the pGL4.10 vector. Four clones from each individual were selected for sequencing to allow identification of both haplotypes present in each individual; DNA agarose gel of the restriction enzyme digest of each of the clones is shown in Figure 4.6.

Sequencing of cloned promoter regions and identification of the LILRB2 promoter haplotype

Sequencing of the 1000 bp region upstream of the ATG start codon for each of the 5 clones from each of the 5 individuals was undertaken by a commercial sequencing service (Geneservice). This identified 5 different haplotypes, shown in Table 4.3.

Gene synthesis of a region from -533 to +74 from the putative transcription initiation site for LILRB2 and cloning into pGL4.10/luc2 vector

Previously work undertaken by Nakajima et al. indicated that the transcription initiation site for LILRB2 most likely lay 600 bp upstream of the ATG start codon. (189) Based on the data obtained from sequencing of the 1000 bp region, a region from -533 to +74 of the putative transcription initiation site identified by Nakajima et al. was sent for gene synthesis and subcloning into the pGL4.10/luc2 vector for use in the luciferase assay. (Figure 4.7) This region encompassed the first 482 bp of the sequenced 1000 bp region and a further 125bp upstream of this which did not contain any SNPs on sequencing of the amplified PCR product.

This region was chosen as it included a more than sufficient amount of the promoter region for expression of luciferase (189) as well as a short segment after the putative transcription initiation site that was particularly rich in SNPs, to increase the probability of identifying polymorphisms that might affect protein expression.

Effect of LILRB2 promoter SNPs on luciferase expression

The LILRB2p/pGL4.10 plasmids were transfected into THP-1 cells based on the data that LILRB2 was transcriptionally regulated and behaved in a similar way to monocytes. In addition, there was also published data indicating that THP-1 cells could be used in a luciferase assay. (189;196)

Luciferase expression between the 5 different haplotypes showed a degree of variation although the differences did not meet statistical significance. (Figure 4.8) The greatest variation was seen between haplotype C2-2 and C3-1, with a 2.15-fold difference. However, the coefficient of variation for the assay was large with values between 10 and 59% for the luciferase:renilla ratios, despite quadruplicate data. This could potentially have contributed to the lack of any statistically significant differences seen.

Discussion

The purpose of the experiments described in this chapter is primarily to demonstrate that genomic variation (including SNPs) in LILR promoter regions can affect their transcriptional regulation and the expression levels of the molecules on the cell surface. For practical considerations, LILRB2 was used in this exercise as there was comparatively more (if limited) data published on the molecule and a suggestion from one study that genomic variation (within the 5' UTR and signal sequence) could affect its expression levels. (194) In addition, experiments in the previous chapter had shown greater variability in LILRB2, which would hopefully have made it easier to identify genomic differences resulting in variation in expression levels. Availability of the anti-LILRB2 hybridoma also influenced the choice of molecule investigated as this provided large amounts of antibody for use in subsequent functional experiments to determine if there was any relationship between LILRB2 expression levels and functional responses to LILRB2 engagement. (Experiments and results for this described in Chapter 6)

Sanger sequencing of the 2306 bp upstream of the LILRB2 ATG start codon identified 15 SNPs in this region, of which 2 had not previously been documented in the reference database (dbSNP build 135). The identification of 13 previously known SNPs served to confirm the validity of the sequencing data. Although the 2 previously unidentified SNPs require confirmation, their identification in a group of 26 individuals does indicate that the non-coding regions for LILRB2 (and potentially the other LILR molecules as well) are not extensively mapped. This represents an area for future potential research, especially as these molecules are known to be linked to disease and more detailed mapping could identify further linkages with immunological disease.

Despite the number of SNPs identified, there was no statistically significant difference between the various SNP genotype founds when compared with LILRB2 expression levels. This included the differences seen in the haplotype previously described by Hirayasu *et al*. (194) They described a c.59GG homozygous genotype (corresponding to dbSNP reference rs383369 and position 2279 on the 2306 bp sequence described in this data) which had lower expression levels of LILRB2 compared to the c.59AA and c.59AG genotypes. The c.59GG genotype was particularly common in North East Asian populations. (194) However, in this study, there were 23 participants with the AA genotype, 3 with the AG genotype; and none with the GG genotype shown to have lower LILRB2 expression levels, possibly due to the different ethnic composition of subjects. This is the most likely explanation as to why there were no observed differences between the different genotypes for SNP rs383369.

In addition to this, Hirayasu *et al*. also found that two other SNPs, which they describe as c.-153 and c.-169 (corresponding to rs448083/position 1489 and rs448092/position 1473) were in absolute linkage disequilibrium with c.59 in their sample of subjects tested for LILRB2 expression. They concluded that these additional SNPs might also be responsible for the differences in LILRB2 expression seen although this was not tested in their study. Again, there were no statistically significant differences between the different genotypes for these two SNPs seen in the data described here.

Some of the possible reasons why there were no statistically significant differences identified between the different LILRB2 genotypes include:

1. Insufficient numbers of each genotype to demonstrate a significant difference - although there were SNPs identified, the proportion of each genotype present often resulted in small numbers of the variant genotype
2. Other genetic factors (outside of the LILRB2 promoter region) having a greater effect on LILRB2 expression levels and masking any effect of promoter genomic variation
3. Other non-genetic factors that could have influenced LILR levels - e.g. subclinical infection or other undeclared disease states in the subjects tested
4. The effect of heterozygosity vs. homozygosity for each genotype, as differences might have been more obvious with sufficient numbers of two different homozygous genotypes, which often was not the case due to the relatively small sample size

To attempt to address some of the issues that might have resulted in no significant differences between the various genotypes when assessed in human subjects, a dual luciferase reporter assay was performed with cloning of different haplotypes of LILRB2 promoter regions into a luciferase vector for transfection into cell lines. This would help eliminate most of the difficulties described above. Initially, qPCR experiments were performed to confirm that LILRB2 expression could be transcriptionally regulated. Exposure of monocytes and the THP-1 cell line to different cytokines and LPS did indeed confirm this. In addition, it also demonstrated that monocytes and the THP-1 cell line responded to the same stimuli in a similar fashion, indicating that the THP-1 cell line would be reasonable to use in this experimental model.

However, although there were some differences in luciferase activity between the various promoter haplotypes seen in the experiment, these were not statistically significant. It is possible that this indicates that there is no actual difference between the difference promoter haplotypes; however, it should be noted that the luciferase assay demonstrated a marked amount of variability (despite the experiments being run in quadruplicate) which could have accounted for the lack of statistical significance. In addition, addition of the LPS failed to result in augmentation of luciferase activity in THP-1 cells despite the fact that LPS resulted in an increase in LILRB2 mRNA in both monocytes and THP-1 cells. For future work, further optimisation of this experimental system would be undertaken to improve the performance characteristics of this assay as well as determine the optimum time to detect LPS enhancement of LILRB2 promoter activity.

In summary, these experiments have demonstrated that there is significant genomic variability in the non-coding regions of the LILRB2 gene. There were also differences in expression of LILRB2 levels seen when these were separated by genotype as well as luciferase activity by LILRB2 promoter haplotype. However, none of the correlations between genomic variation and LILRB2 expression were statistically significant, which is most likely a result of insufficient numbers to achieve this, although a lack of a true difference cannot be ruled out.

To take forward the work in this chapter, next generation sequencing of the genomic regions for all the LILRs measured in the previous chapter (i.e. LILRA2, LILRB1, LILRB2 and LILRB4) should be performed on a larger sample of the population. The large amount of data generated could then be subjected to more thorough bioinformatics analysis to determine what effect genomic variation in both the non-coding and coding regions of the LILR molecules would have on their expression levels. In addition, it would also serve to confirm some of the SNPs identified in this small scale pilot study as well as help determine whether genomic variation in one LILR molecule can affect expression of another LILR molecule.

It would also be important to obtain a larger sample size of subjects to allow enrichment of rarer LILR SNPs to allow more meaningful comparison of different genotypes. With regard to the luciferase assay as a means to demonstrate *in vitro* that genomic variation in the LILR promoters could affect expression levels, it might be useful to clone a longer region of the LILR promoter region in case SNPs further upstream might play a role in determining expression levels. In addition, further optimisation of the luciferase assay (e.g. with different transfection

conditions or reagents) might provide less intra-assay variability making it easier to demonstrate any true differences in luciferase activity due to genomic variation in the LILR promoter insert.

Tables

Table 4.1

Concentration of genomic DNA from 26 healthy controls (C1 to C26). 200 µl blood was processed, resulting in 200 µl of solution containing the DNA.

Individual	Concentration of genomic DNA (ng/µl)
C1	12.15
C2	11.91
C3	20.42
C4	29.07
C5	34.74
C6	20.79
C7	17.14
C8	38.45
C9	21.02
C10	21.56
C11	23.76
C12	27.76
C13	33.28
C14	35.3
C15	22.12

C16	11.02
C17	22.26
C18	27.02
C19	43.64
C20	14.58
C21	23.88
C22	18.1
C23	14.27
C24	23.48
C25	15.47
C26	15.47

Table 4.2

SNPs identified in the putative LILRB2 promoter region of the 26 individuals sequenced. Yellow boxes indicate where the genotype is different from the reference sequence.

Position on PCR	GRCh37 position	Reference SNP ID	**Reference nucleotide (GRCh37 build)**	C1	C2	C3	C4	C5	C6	C7	C8	C9	C10	C11	C12	C13	C14	C15	C16	C17	C18	C19	C20	C21	C22	C23	C24	C25	C26
215	54786194		**G**	G	G	G	G	G	G	G	G	R	G	G	G	G	G	G	G	G	G	G	G	G	G	G	G	G	G
387	54786022	rs4112253	**C**	C	C	C	S	S	C	C	C	G	C	S	S	S	S	S	C	S	S	C	S	C	C	C	S	C	S
546	54785863	rs113412095	**G**	G	G	G	G	G	G	G	K	G	G	G	G	G	G	G	G	G	G	G	G	G	G	G	G	G	G
630	54785779	rs7260261	**G**	G	G	R	G	G	R	G	A	R	G	G	G	G	G	G	A	G	G	R	R	G	R	R	G	G	R
816	54785593	rs380573	**T**	Y	C	Y	Y	Y	Y	T	C	C	Y	C	C	C	C	Y	C	Y	T	Y	C	C	C	Y	Y	C	C
1444	54784965	rs73938625	**G**	G	G	G	G	G	G	G	G	G	G	G	G	G	G	G	G	G	G	G	G	G	G	G	G	S	G
1473	54784936	rs448092	**G**	G	A	G	G	G	G	G	G	G	R	R	R	R	G	G	G	G	G	G	G	G	G	G	G	R	G
1481	54784928	rs13347079	**A**	R	A	R	A	A	R	A	G	A	A	A	A	A	A	A	G	A	R	R	R	A	R	R	A	A	R

1487	54784922	rs13347078	**A**	R	A	R	A	A	R	A	G	A	A	A	A	A	A	A	A	G	A	R	R	R	A	R	R	A	A	R
1489	54784920	rs448083	**G**	G	A	G	G	G	G	G	G	G	R	R	R	R	G	G	G	G	G	G	G	G	G	G	G	G	G	G
1501	54784908	rs13345069	**G**	K	G	K	K	K	K	G	T	T	G	K	K	K	T	K	T	K	T	K	T	G	K	K	K	G	T	
1511	54784898	rs13345054	**T**	K	T	K	K	K	K	T	G	G	T	K	K	K	G	K	G	K	G	K	G	T	K	K	K	T	G	
1611	54784798		**C**	C	C	C	C	C	C	C	C	C	C	C	C	C	C	C	C	C	C	C	C	C	C	Y	C	C	C	C
1788	54784621	rs188025641	**G**	G	G	G	G	G	G	G	G	G	G	G	G	G	G	G	G	G	G	G	G	G	G	R	G	G	G	
2279	54784130	rs383369	**A**	A	A	A	A	A	A	A	A	A	R	R	R	A	A	A	A	A	A	A	A	A	A	A	A	A	A	A

Table 4.3

SNP haplotypes identified in the 1000 bp region upstream of the ATG start codon of LILRB2

Position of SNP on 2306 bp product	1444	1473	1481	1487	1489	1501	1511
Reference sequence	**G**	**G**	**A**	**A**	**G**	**G**	**T**
C2-1, C2-2, C2-3, C2-4, C11-3, C11-4, C13-1, C13-2, C13-3	G	A	A	A	A	G	T
C3-1	G	G	G	G	G	T	G
C3-2, C3-3, C3-4, C25-2	G	G	A	A	G	G	T
C11-1, C11-2, C13-4	G	G	A	A	G	T	G
C25-1, C25-3, C25-4	C	A	A	A	G	G	T

Figures

Figure 4.1

Agarose gel showing PCR products of the 2306 bp region containing the putative LILRB2 promoter region. The 2306 bp product is visible between the 2.0 and 3.0 kb markers on the ladder in all 26 healthy individuals (C1 to C26). The cloning primers used to amplify the 2306 bp region were the forward primer, PRO1F (TGCCATGCACTCCATATTGT) and reverse primer, EX2R (CTGGGGACAGACTCACCTGT).

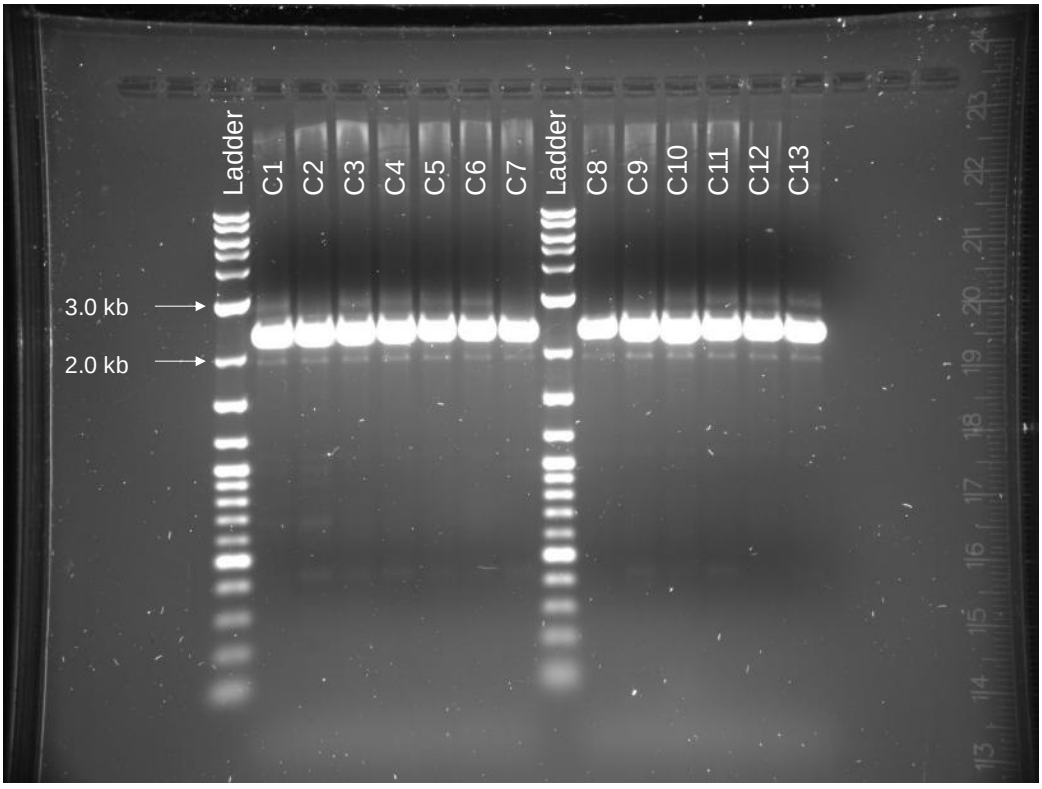

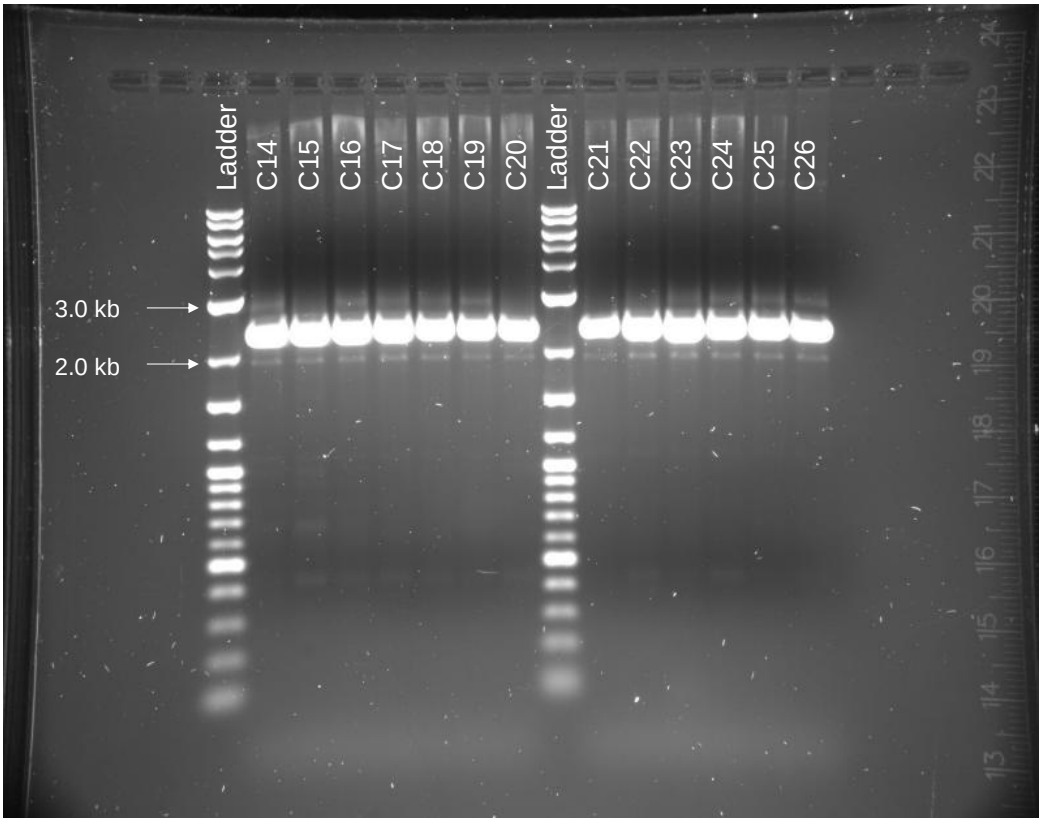
Ladder
C14
C15
C16
C17
C18
C19
C20
Ladder
C21
C22
C23
C24
C25
C26
3.0 kb
2.0 kb

Figure 4.2

Diagram showing the regions covered by the 5 primer pairs used to sequence the 2306 bp region upstream of the LILRB2 ATG start codon. The green bars (labelled PRO1, PRO2, PRO3, PRO4 and EX1+2) represent the areas of the 2306 bp product covered by the 5 primer pairs. The blue arrows represent the direction and length of sequence obtained from each individual primer and the yellow areas represent areas where data from both forward and reverse primers overlap. This data is shown for all subjects in the study (C1 to C26). The sequencing primers used are detailed in Table 2.1.

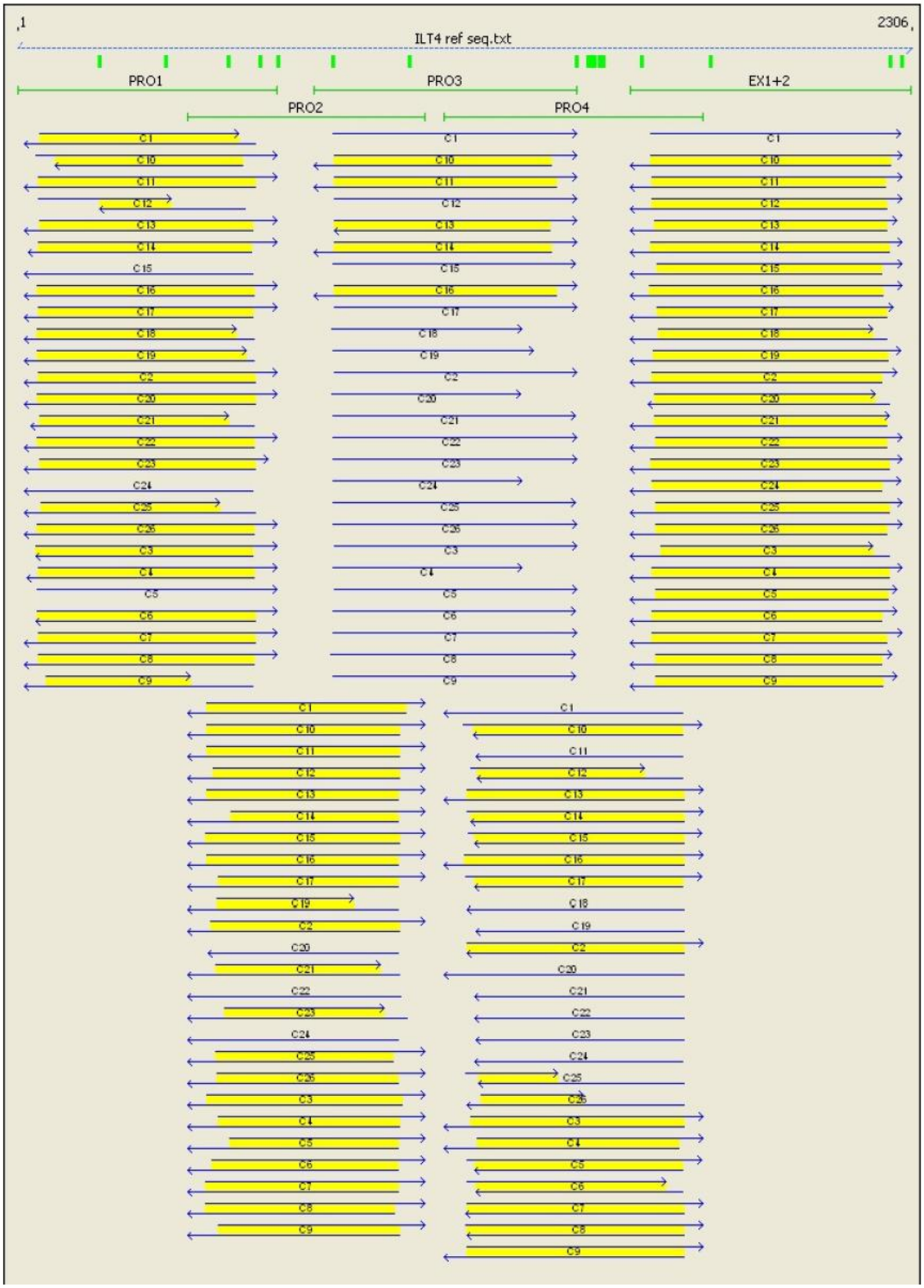
1
2306
ILT4 ref seq.txt
PRO1
PRO2
PRO3
PRO4
EX1+2

Figure 4.3

DNA sequencing data showing the individual SNPs identified in the 26 healthy subjects (C1 to C26). The numerical positions identified correspond to that on the 2306 bp region upstream of the LILRB2 ATG start codon, with the reference nucleotide identified first, followed by the SNP present. Green peaks represent adenine, red peaks represent thymidine, blue peaks represent cytosine and black peaks represent guanine.


215G>R
387C>S
387C>S
387C>S
387C>G
387C>S
387C>S
387C>S
387C>S
387C>S
387C>S
387C>S
387C>S
387C>G

546G>K

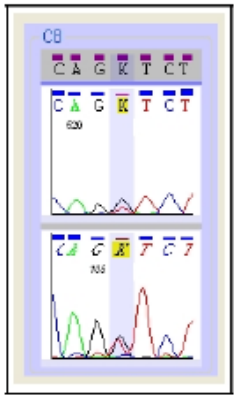

630G>A

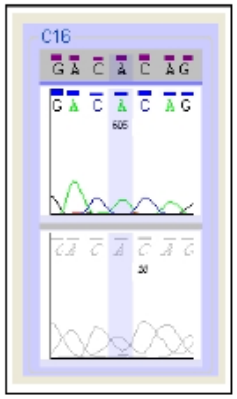

630G>R

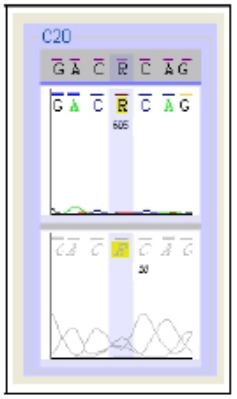

630G>R

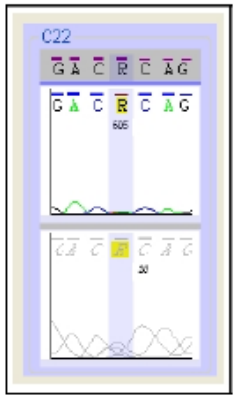

630G>R

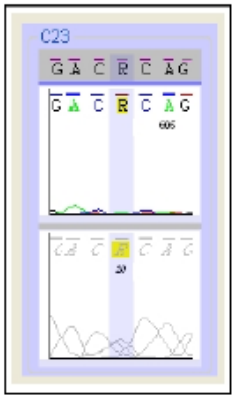

630G>R

630G>R

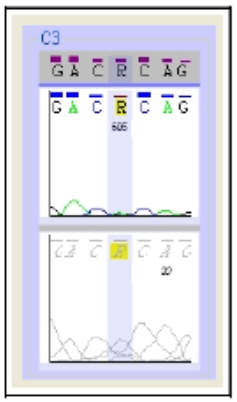

630G>R

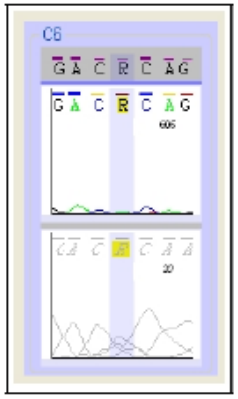

630G>A

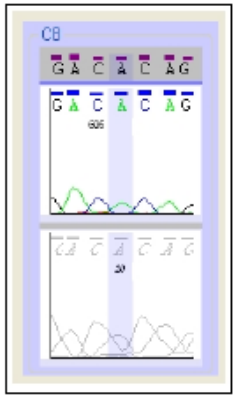

674T>W

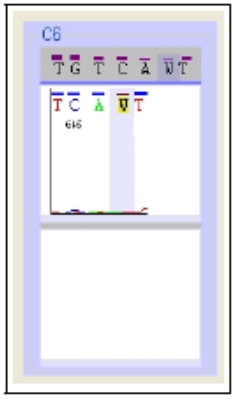


546G>K
630G>A
630G>R
630G>R
630G>R
630G>R
630G>R
630G>R
630G>R
630G>A
630G>R
816T>Y
816T>Y
816T>C


816T>C
C12
816T>C
C13
816T>C
C14
816T>Y
C15
816T>C
C16
816T>Y
C17
816T>Y
C19
816T>C
C2
816T>C
C20
816T>C
C21
816T>C
C22
816T>Y
C23
816T>Y
C24
816T>C
C25


816T>C
816T>Y
816T>Y
816T>Y
816T>Y
816T>C
816T>C
816T>Y
816T>C
816T>C
816T>C
1014G>R
1444G>S


1444G>S
1473G>R
1473G>R
1473G>R
1473G>R
1473G>A
1473G>R
1481A>R
1481A>G
1481A>R
1481A>R
1481A>R
1481A>R


1481A>R
1481A>R
1481A>R
1481A>G
1487A>R
1487A>G
1487A>R
1487A>R
1487A>R
1487A>R
1487A>R
1487A>R
1487A>R
1487A>R


1487A>G
1489G>R
1489G>R
1489G>R
1489G>R
1489G>A
1501G>K
1501G>K
1501G>K
1501G>K
1501G>T
1501G>K
1501G>T
1501G>K


1501G>T
C18
1501G>K
C19
1501G>T
C20
1501G>K
C22
1501G>K
C23
1501G>K
C24
1501G>T
C26
1501G>K
C3
1501G>K
C4
1501G>K
C5
1501G>K
C6
1501G>T
C8
1501G>T
C9
1511T>K
C1


1511T>K
C11
1511T>K
C12
1511T>K
C13
1511T>G
C14
1511T>K
C15
1511T>G
C16
1511T>K
C17
1511T>G
C18
1511T>K
C19
1511T>G
C20
1511T>K
C22
1511T>K
C23
1511T>K
C24
1511T>G
C26


1511T>K
1511T>K
1511T>K
1511T>K
1511T>G
1511T>G
1611C>Y
1611C>Y
1788G>R
2250T>C
2279A>R
2279A>R
2279A>R

Figure 4.4

Graph showing mean LILRB2 expression levels (in molecules of equivalent fluorochrome of LILR staining, MEF) at 0 hours, and modulation indices without addition of cytokines (ratio of the MEF after 21 hours incubation at 37^{o}C over LILR expression at 0 hours), with addition of IL-1β (ratio of the MEF after 21 hours incubation at 37^{o}C with 50 ng/ml IL-1β over LILR expression at 21 hours without stimulation) or addition of TGF-β (ratio of the MEF after 21 hours incubation at 37^{o}C with 20 ng/ml TGF-β over LILR expression at 21 hours without stimulation). Monocytes are represented by the red bars and dendritic cells by the blue bars; expression levels are shown for each individual genotype present at different loci along the 2306 bp sequence upstream of the LILRB2 ATG start codon. There was no statistical difference found between any of the groups. The error bars represent one standard deviation; where no error bars are shown, there was only one subject with that particular genotype. The genotype symbols used are International Union of Pure and Applied Chemistry (IUPAC) codes for nucleotides (detailed in Appendix 1).

	LILRB2 at 0 hours	LILRB2 index at 21h without addition of cytokines	LILRB2 index after stimulation with IL-1β at 21h	LILRB2 index after stimulation with TGF-β at 21h
p215	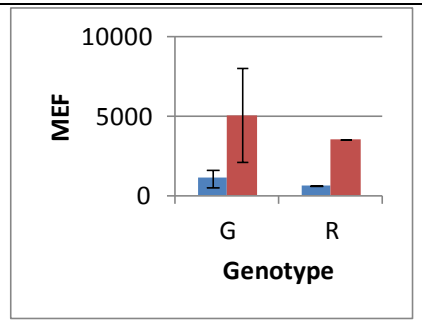	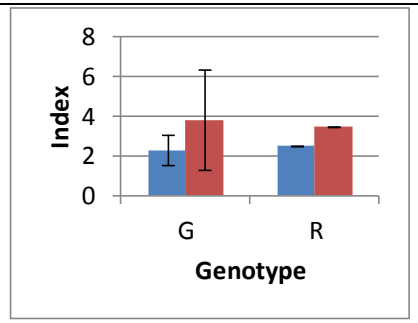	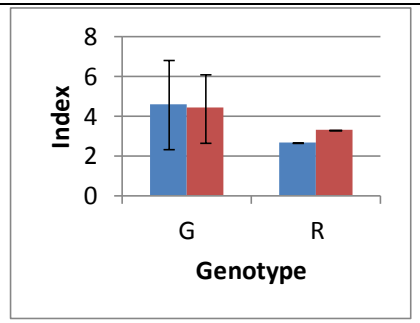	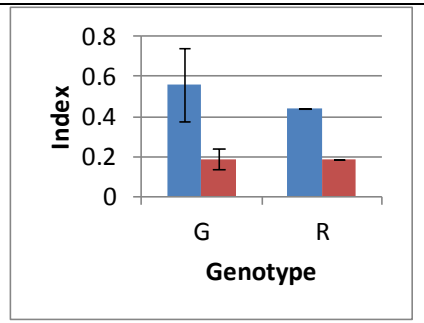
p387	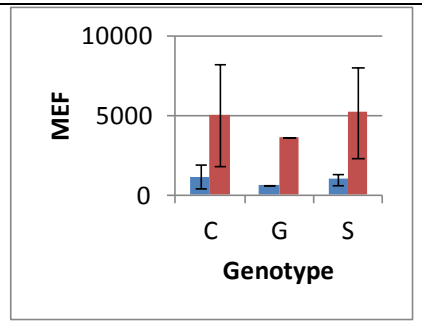	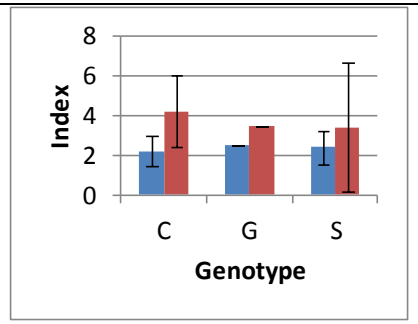	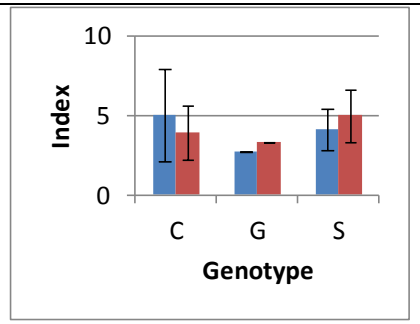	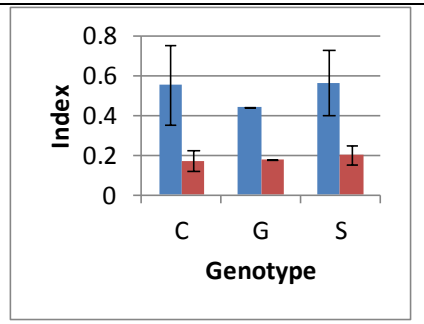

	LILRB2 at 0 hours	LILRB2 index at 21h without addition of cytokines	LILRB2 index after stimulation with IL-1β at 21h	LILRB2 index after stimulation with TGF-β at 21h
p546	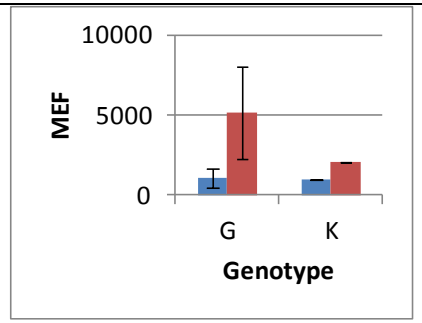	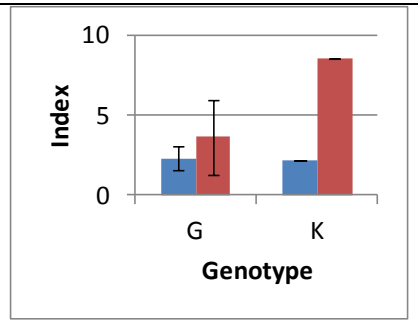	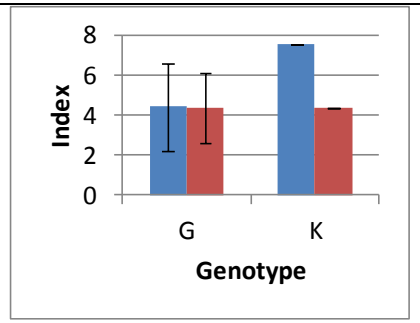	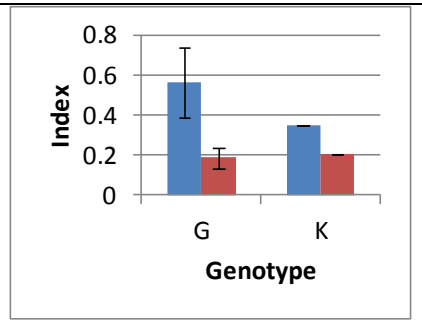
p630	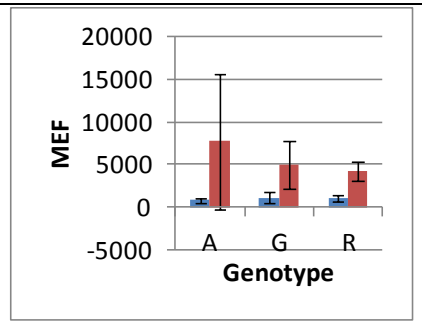	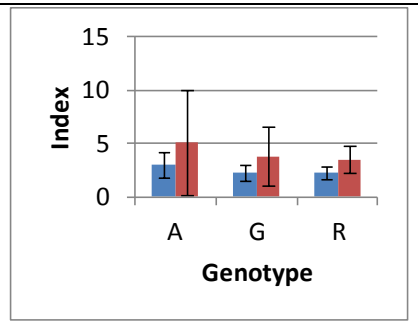	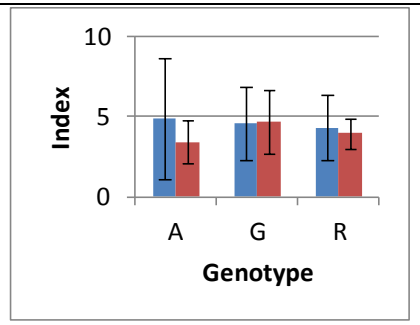	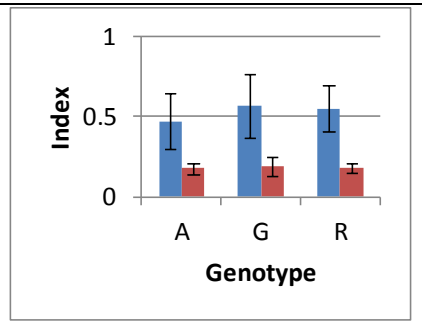

	LILRB2 at 0 hours	LILRB2 index at 21h without addition of cytokines	LILRB2 index after stimulation with IL-1β at 21h	LILRB2 index after stimulation with TGF-β at 21h
P674	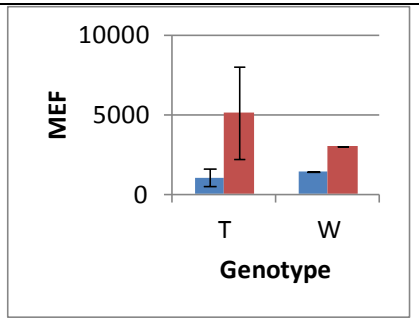	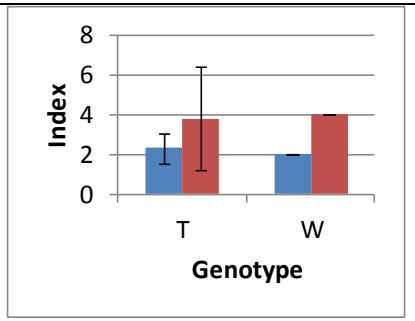	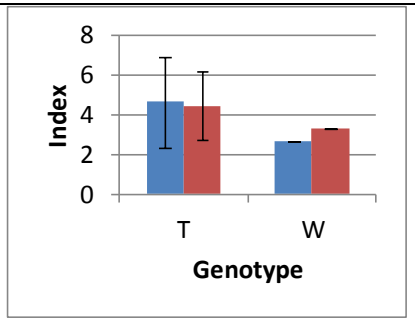	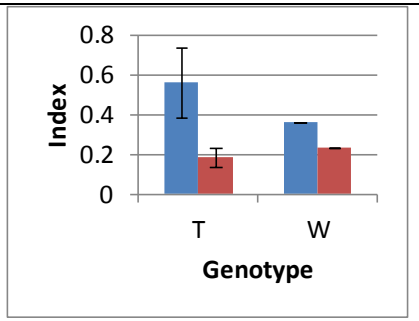
p816	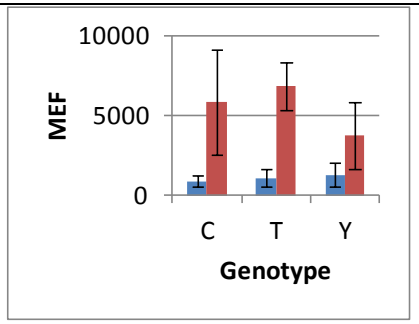	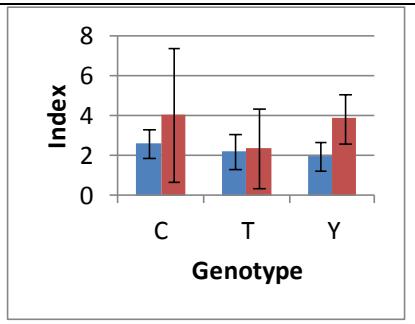	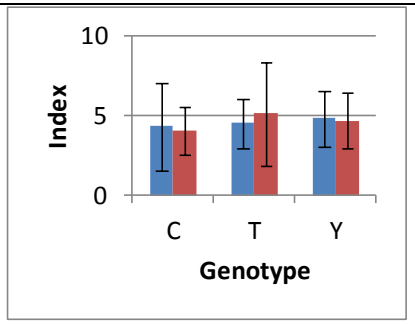	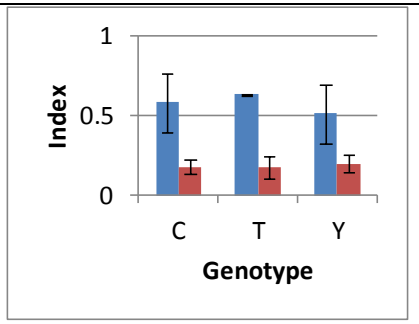

	LILRB2 at 0 hours	LILRB2 index at 21h without addition of cytokines	LILRB2 index after stimulation with IL-1β at 21h	LILRB2 index after stimulation with TGF-β at 21h
p1014	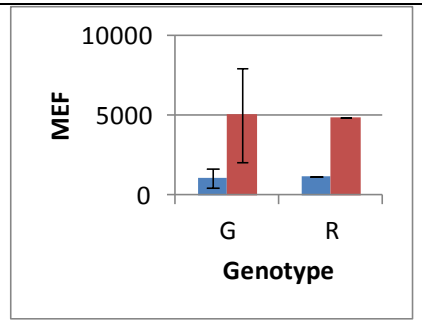	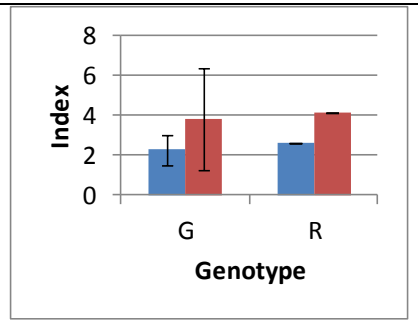	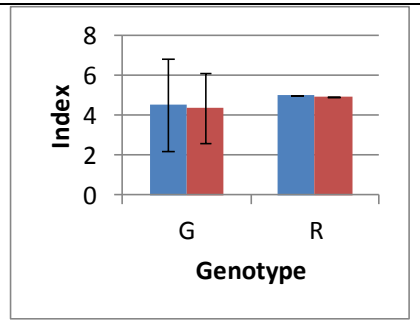	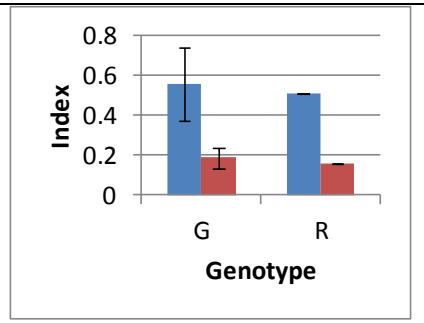
p1444	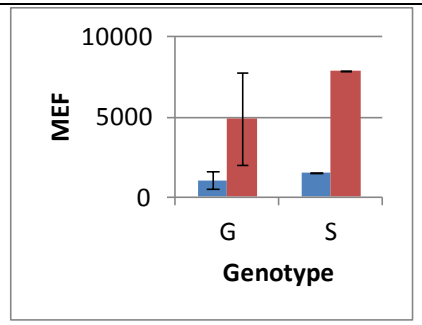	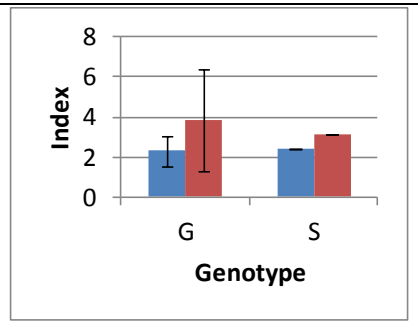	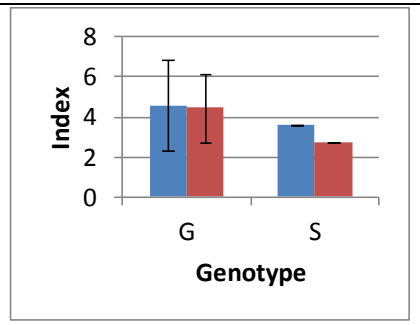	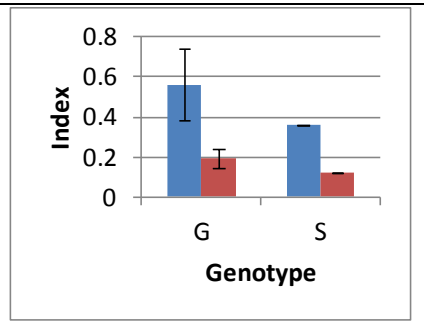

	LILRB2 at 0 hours	LILRB2 index at 21h without addition of cytokines	LILRB2 index after stimulation with IL-1β at 21h	LILRB2 index after stimulation with TGF-β at 21h
p1473	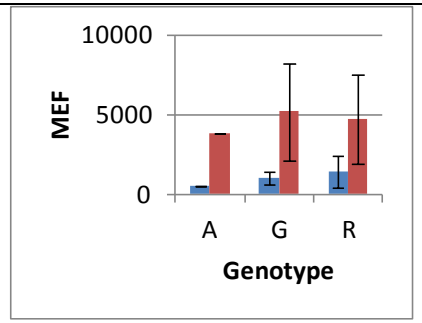	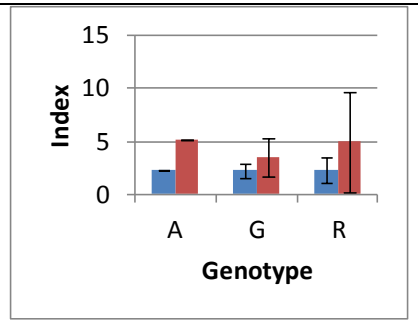	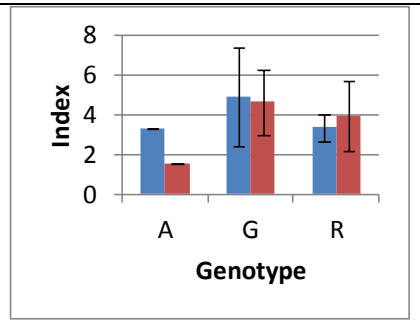	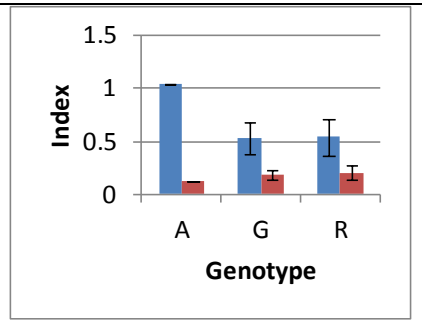
p1481	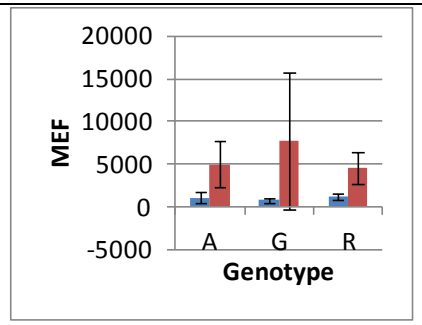	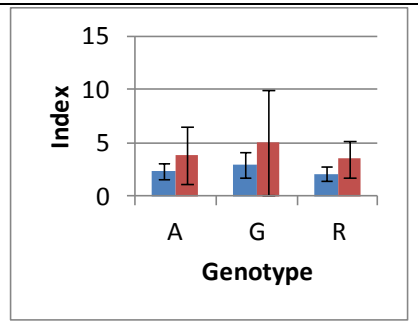	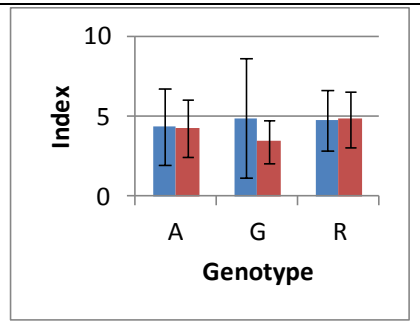	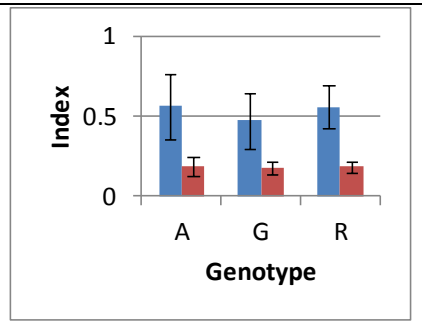

	LILRB2 at 0 hours	LILRB2 index at 21h without addition of cytokines	LILRB2 index after stimulation with IL-1β at 21h	LILRB2 index after stimulation with TGF-β at 21h
p1487	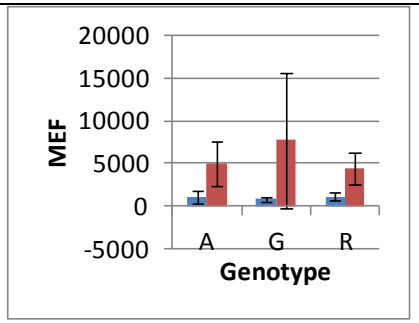	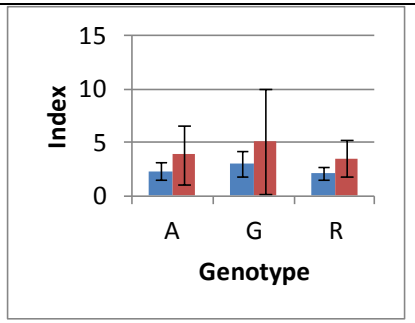	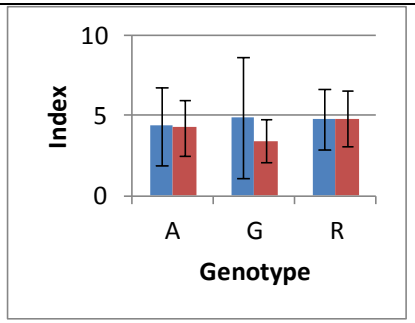	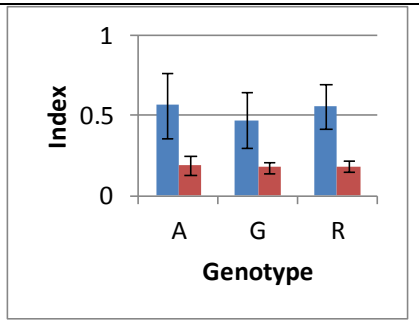
p1489	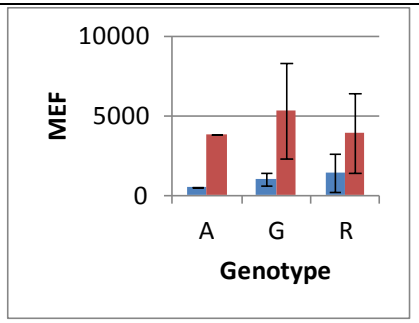	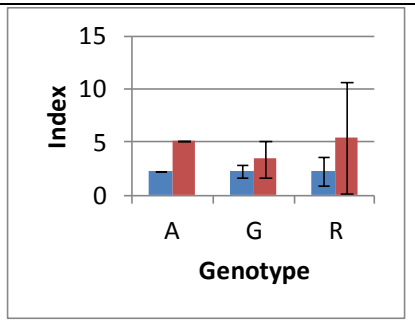	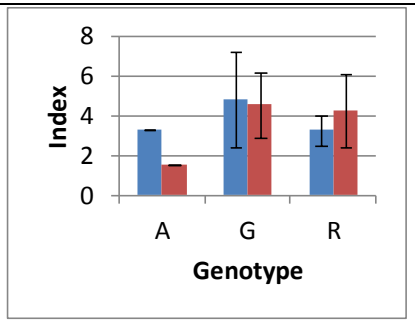	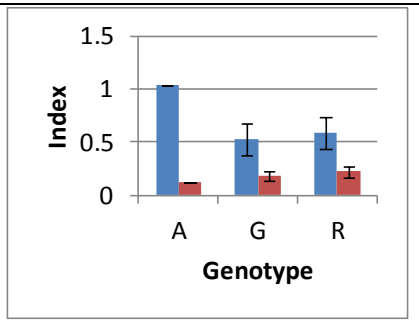

	LILRB2 at 0 hours	LILRB2 index at 21h without addition of cytokines	LILRB2 index after stimulation with IL-1β at 21h	LILRB2 index after stimulation with TGF-β at 21h
p1501	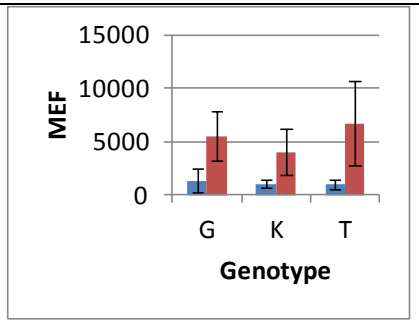	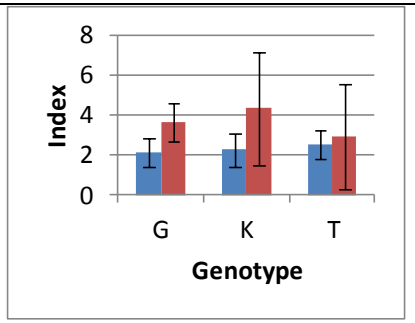	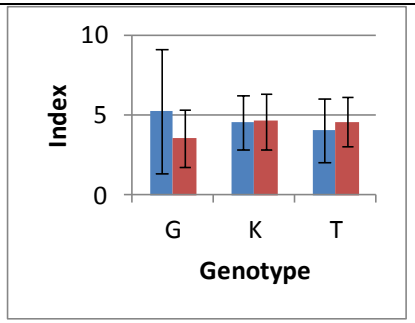	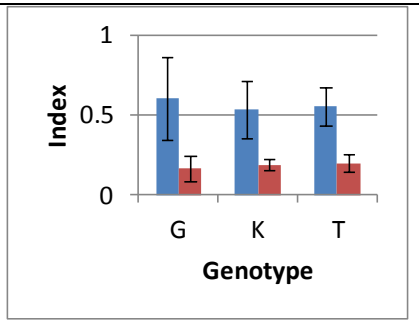
p1511	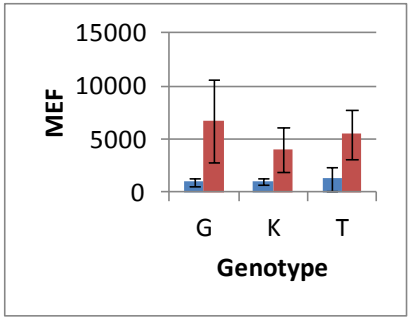	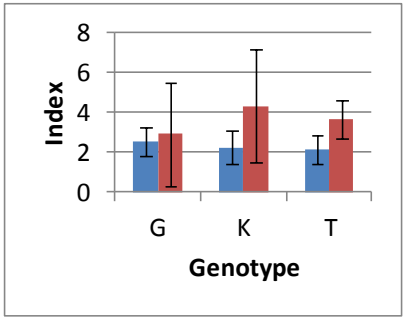	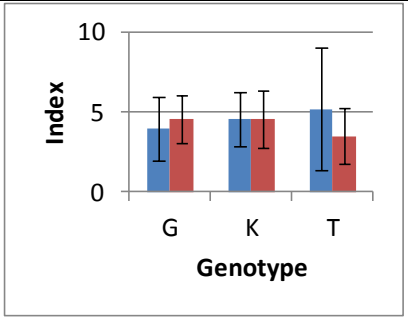	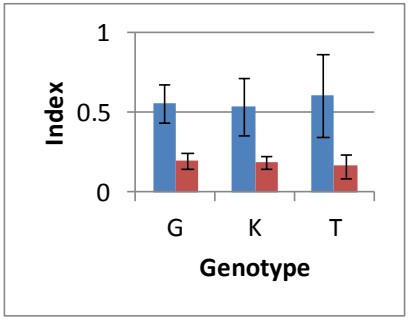

	LILRB2 at 0 hours	LILRB2 index at 21h without addition of cytokines	LILRB2 index after stimulation with IL-1β at 21h	LILRB2 index after stimulation with TGF-β at 21h
p1611	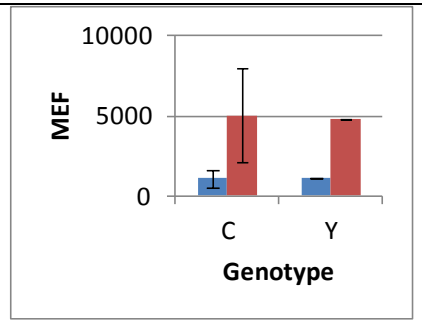	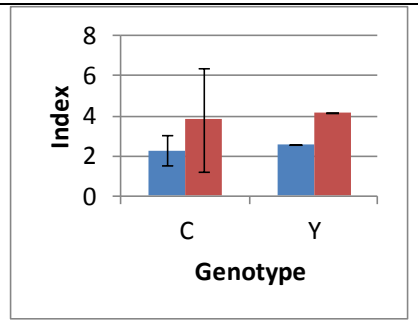	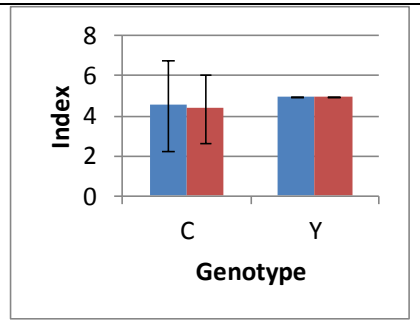	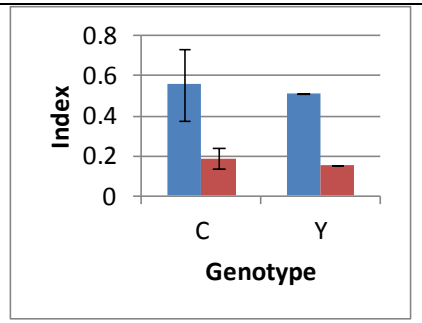
p1788	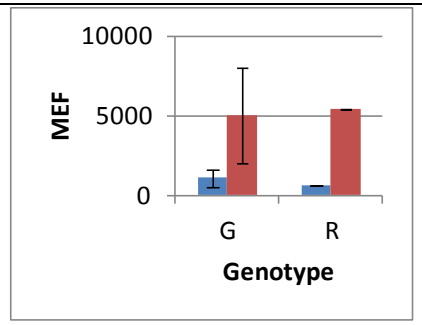	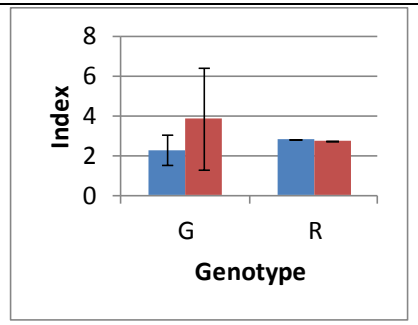	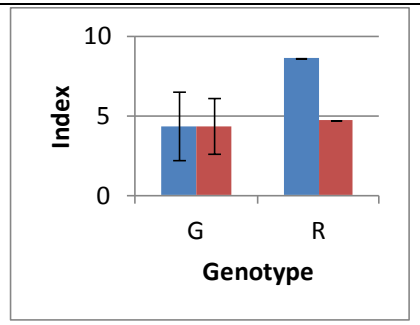	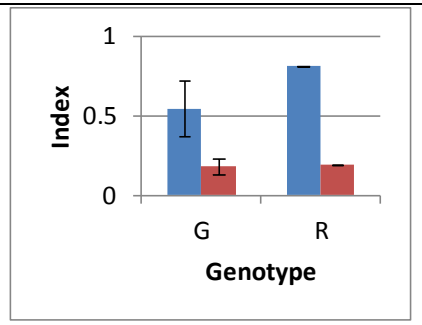

	LILRB2 at 0 hours	LILRB2 index at 21h without addition of cytokines	LILRB2 index after stimulation with IL-1β at 21h	LILRB2 index after stimulation with TGF-β at 21h
p2250	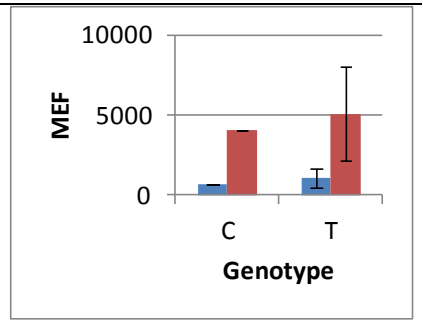	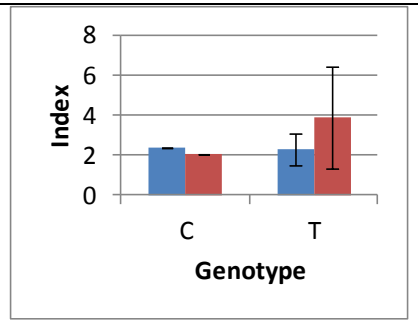	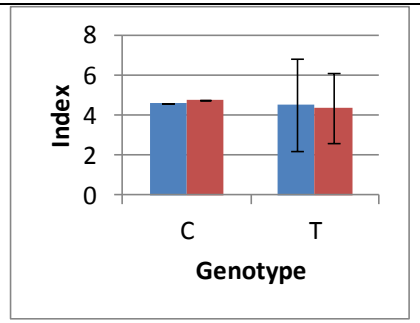	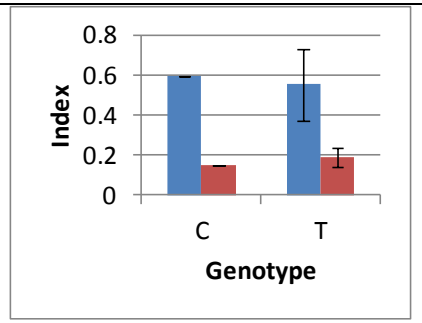
p2279	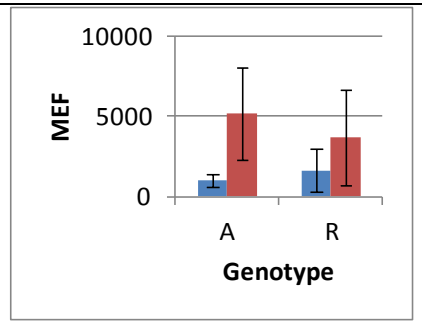	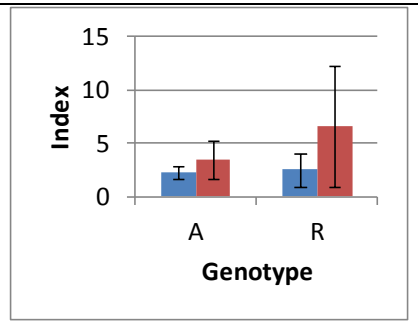	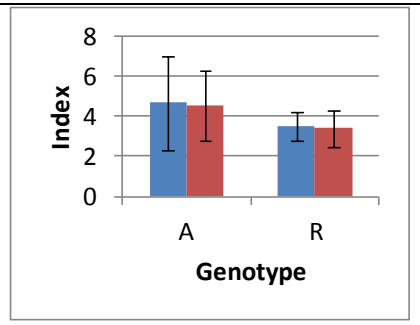	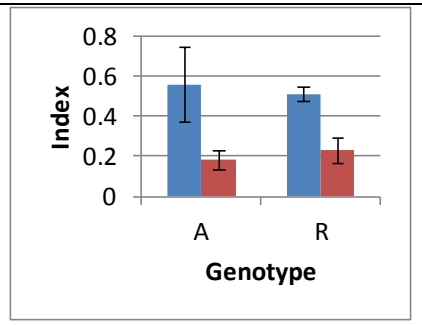

Figure 4.5a

LILRB2 mRNA in monocytes at 0 hours, and after 6 and 24 hours incubation at 37^{o}C with no cytokines, IL10, an inflammatory cocktail of cytokines (MCM = IL-1β, TNF-α, IL-6 and PGE_2) or LPS. mRNA was quantified using qPCR and the ΔΔCt method to obtain relative quantitation by using the 0h sample for normalization.

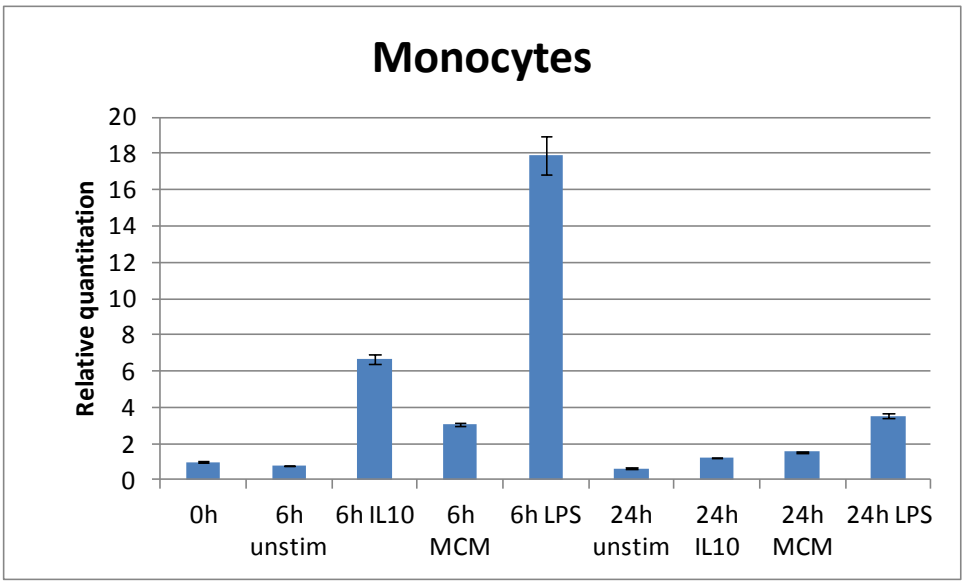

Figure 4.5b

LILRB2 mRNA in THP-1 cells at 0 hours, and after 6 and 24 hours incubation at 37^{o}C with no cytokines, IL10, an inflammatory cocktail of cytokines (MCM = IL-1β, TNF-α, IL-6 and PGE_2) or LPS. mRNA was quantified using qPCR and the ΔΔCt method to obtain relative quantitation by using the 0h sample for normalization.

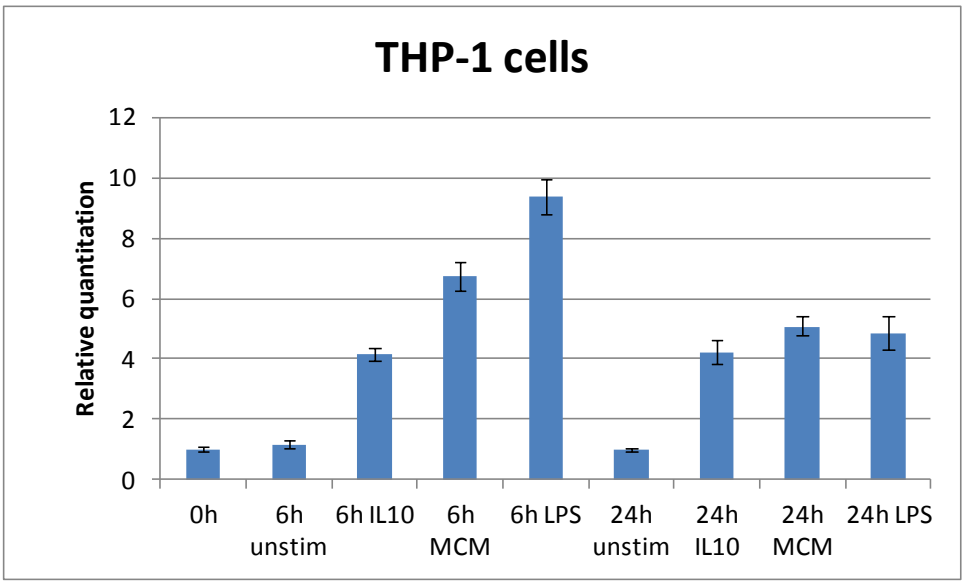

Figure 4.6

Agarose gel showing restriction enzyme digest of a 1000 bp product region upstream of the LILRB2 ATG start codon, cloned into pGL4.10 vector. 4 clones for each of the healthy subject C2, C3, C11, C13 and C25 were sent for DNA sequencing to determine the haplotypes present in these individuals.

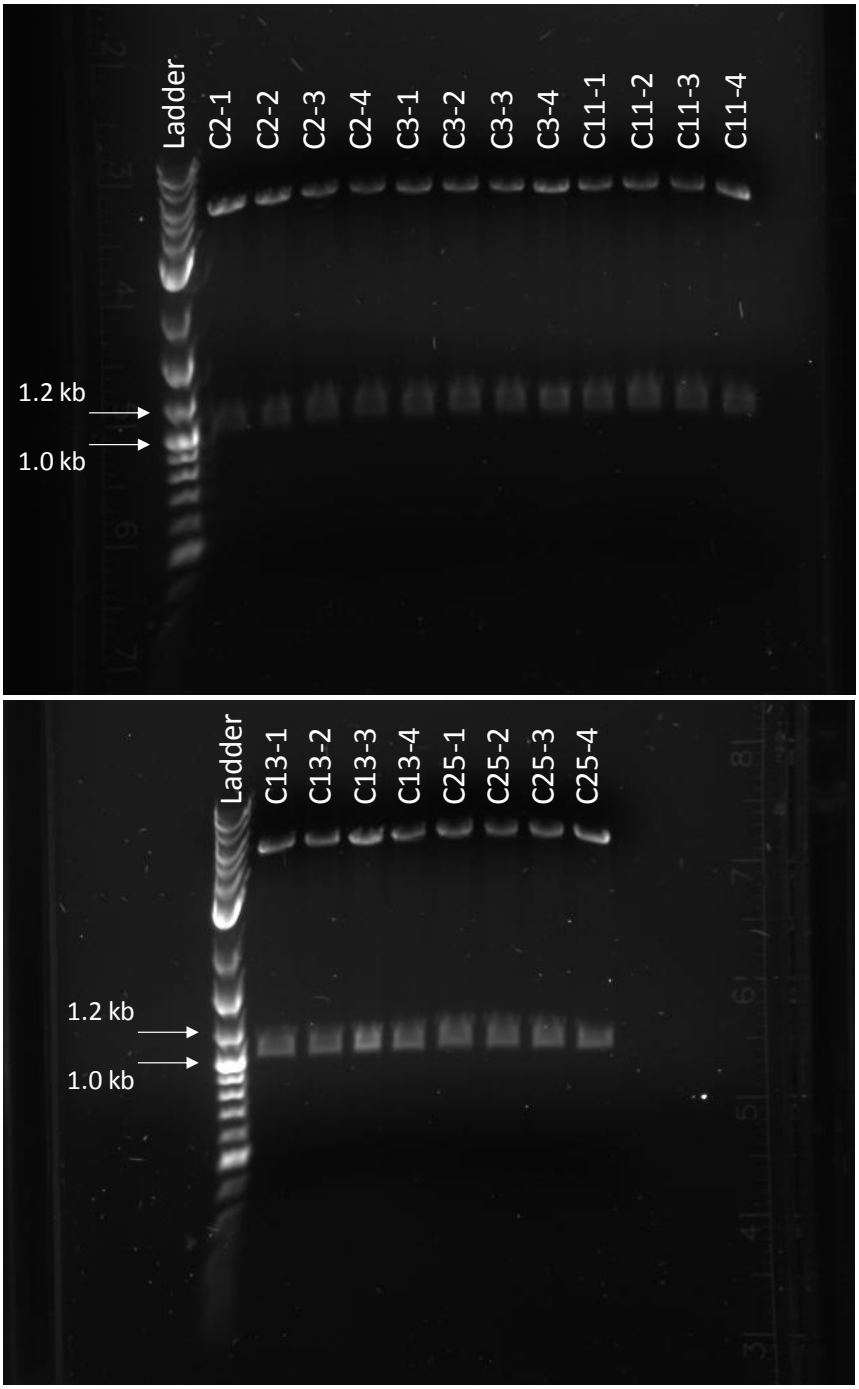

Figure 4.7

DNA sequences of the 5 different haplotypes (C2-2, C3-1, C3-2, C13-4 and C25-3) used for cloning into pGL4.10/luc2 for dual luciferase experiments. The sequence is -533 to +74 bp from the putative promoter start site for LILRB2. Green characters represent SNPs in the DNA sequence with C3-2 being identical to the GRCh37 build reference sequence.

C2-2

GAATGTGGAGTCCAACAGCAAGATCCTCTCACGTCCCAAAGCCTCAGGTCTTAC

CCTGGTCTGGAAATCAAGCACAAATGAGCCCCTCCCAATGTCCCAGGCACCACT

GACCCCACAACCACTGTGACGAGTGGGATTCATGACAACAATCTGCAAAGGAAG

AAACTGAGGCTCAGTGATGGGACATTACAAACCAAGGTCACGTAGGCAGCGGAT

GATAACCAGTCATCAAATAAATATCAACTCCCTCCCCCACTCCCCAAATCAAAG

CTCAAACATAAGTCATTGTTCCCAAAATGTTGACCAGGAATTGAGGTGCAGAGG

GACGGCTAAGGACGCAATGGGCACCGAGGAGGCAGGAAAGACTCAGAGGTTTCT

TCCCGGGGGGGAGGGAGTGGACGCTGGAGCAAAAACATTTAAAAAGGGGAAGTT

AAGAGGGGACTATTTGGTTGAAAGAAAACCCACAATCCAGTGTCAAGAAAGAAG

TCAACTTTTCTTCCCCTACTTCCCT**G**CATTTCTCCTCTGTGCTCACTGCCACAC

ACAGCTCA**A**CCTGG**A**C**A**GCACAGCCAGA**G**GCGAGATGC**T**TCTCTGCTGATCTGA

GTCTGCCTGCAGC

C3-1

GAATGTGGAGTCCAACAGCAAGATCCTCTCACGTCCCAAAGCCTCAGGTCTTAC

CCTGGTCTGGAAATCAAGCACAAATGAGCCCCTCCCAATGTCCCAGGCACCACT

GACCCCACAACCACTGTGACGAGTGGGATTCATGACAACAATCTGCAAAGGAAG

AAACTGAGGCTCAGTGATGGGACATTACAAACCAAGGTCACGTAGGCAGCGGAT

GATAACCAGTCATCAAATAAATATCAACTCCCTCCCCCACTCCCCAAATCAAAG

CTCAAACATAAGTCATTGTTCCCAAAATGTTGACCAGGAATTGAGGTGCAGAGG

GACGGCTAAGGACGCAATGGGCACCGAGGAGGCAGGAAAGACTCAGAGGTTTCT

TCCCGGGGGGGAGGGAGTGGACGCTGGAGCAAAAACATTTAAAAAGGGGAAGTT

AAGAGGGGACTATTTGGTTGAAAGAAAACCCACAATCCAGTGTCAAGAAAGAAG

TCAACTTTTCTTCCCCTACTTCCCTGCATTTCTCCTCTGTGCTCACTGCCACAC

GCAGCTCAGCCTGGGCGGCACAGCCAGATGCGAGATGCGTCTCTGCTGATCTGA

GTCTGCCTGCAGC

C3-2 (reference)

GAATGTGGAGTCCAACAGCAAGATCCTCTCACGTCCCAAAGCCTCAGGTCTTAC

CCTGGTCTGGAAATCAAGCACAAATGAGCCCCTCCCAATGTCCCAGGCACCACT

GACCCCACAACCACTGTGACGAGTGGGATTCATGACAACAATCTGCAAAGGAAG

AAACTGAGGCTCAGTGATGGGACATTACAAACCAAGGTCACGTAGGCAGCGGAT

GATAACCAGTCATCAAATAAATATCAACTCCCTCCCCCACTCCCCAAATCAAAG

CTCAAACATAAGTCATTGTTCCCAAAATGTTGACCAGGAATTGAGGTGCAGAGG

GACGGCTAAGGACGCAATGGGCACCGAGGAGGCAGGAAAGACTCAGAGGTTTCT

TCCCGGGGGGGAGGGAGTGGACGCTGGAGCAAAAACATTTAAAAAGGGGAAGTT

AAGAGGGGACTATTTGGTTGAAAGAAAACCCACAATCCAGTGTCAAGAAAGAAG

TCAACTTTTCTTCCCCTACTTCCCTGCATTTCTCCTCTGTGCTCACTGCCACAC

GCAGCTCAACCTGGACGGCACAGCCAGAGGCGAGATGCTTCTCTGCTGATCTGA

GTCTGCCTGCAGC

C13-4

GAATGTGGAGTCCAACAGCAAGATCCTCTCACGTCCCAAAGCCTCAGGTCTTAC

CCTGGTCTGGAAATCAAGCACAAATGAGCCCCTCCCAATGTCCCAGGCACCACT

GACCCCACAACCACTGTGACGAGTGGGATTCATGACAACAATCTGCAAAGGAAG

AAACTGAGGCTCAGTGATGGGACATTACAAACCAAGGTCACGTAGGCAGCGGAT

GATAACCAGTCATCAAATAAATATCAACTCCCTCCCCCACTCCCCAAATCAAAG

CTCAAACATAAGTCATTGTTCCCAAAATGTTGACCAGGAATTGAGGTGCAGAGG

GACGGCTAAGGACGCAATGGGCACCGAGGAGGCAGGAAAGACTCAGAGGTTTCT

TCCCGGGGGGGAGGGAGTGGACGCTGGAGCAAAAACATTTAAAAAGGGGAAGTT

AAGAGGGGACTATTTGGTTGAAAGAAAACCCACAATCCAGTGTCAAGAAAGAAG

TCAACTTTTCTTCCCCTACTTCCCTGCATTTCTCCTCTGTGCTCACTGCCACAC

GCAGCTCAACCTGGACGGCACAGCCAGATGCGAGATGCGTCTCTGCTGATCTGA

GTCTGCCTGCAGC

C25-3

GAATGTGGAGTCCAACAGCAAGATCCTCTCACGTCCCAAAGCCTCAGGTCTTAC

CCTGGTCTGGAAATCAAGCACAAATGAGCCCCTCCCAATGTCCCAGGCACCACT

GACCCCACAACCACTGTGACGAGTGGGATTCATGACAACAATCTGCAAAGGAAG

AAACTGAGGCTCAGTGATGGGACATTACAAACCAAGGTCACGTAGGCAGCGGAT

GATAACCAGTCATCAAATAAATATCAACTCCCTCCCCCACTCCCCAAATCAAAG

CTCAAACATAAGTCATTGTTCCCAAAATGTTGACCAGGAATTGAGGTGCAGAGG

GACGGCTAAGGACGCAATGGGCACCGAGGAGGCAGGAAAGACTCAGAGGTTTCT

TCCCGGGGGGGAGGGAGTGGACGCTGGAGCAAAAACATTTAAAAAGGGGAAGTT

AAGAGGGGACTATTTGGTTGAAAGAAAACCCACAATCCAGTGTCAAGAAAGAAG

TCAACTTTTCTTCCCCTACTTCCCTCCATTTCTCCTCTGTGCTCACTGCCACAC

ACAGCTCAACCTGGACGGCACAGCCAGAGGCGAGATGCTTCTCTGCTGATCTGA

GTCTGCCTGCAGC

Figure 4.8

Dual luciferase assay data showing luciferase and renilla activity and the luciferase:renilla ratio for THP-1 cells transfected with the pGL4.10 firefly luciferase vector containing 5 different haplotypes (C2-2, C3-1, C3-2, C13-4 and C25-3) of the LILRB2 promoter region. Luciferase activity was measured 24 hours after transfection with or without the addition of LPS at 6 hours. The bars show the mean of quadruplicate experiments and the error bars indicate 1 standard deviation from the mean. There were no statistically significant differences between the various groups.

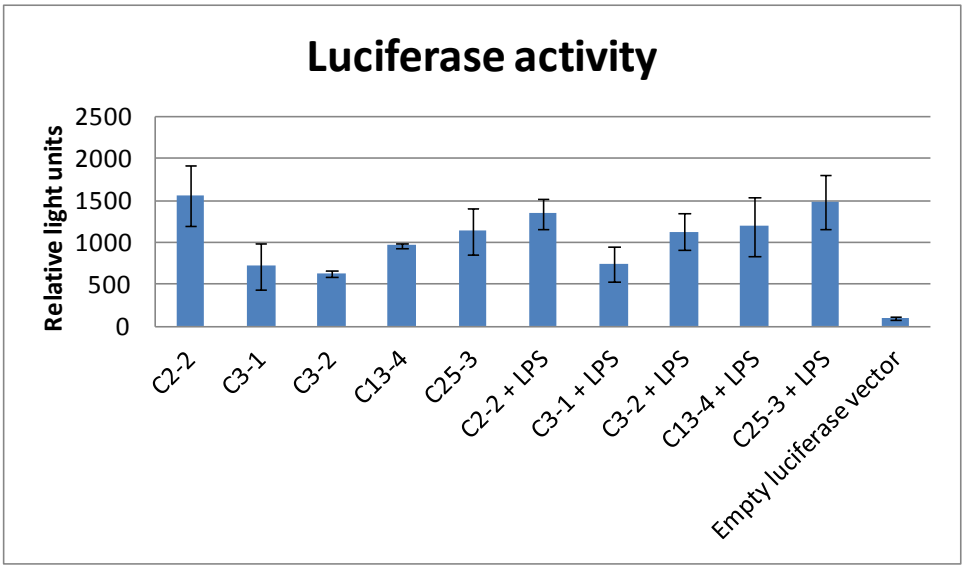

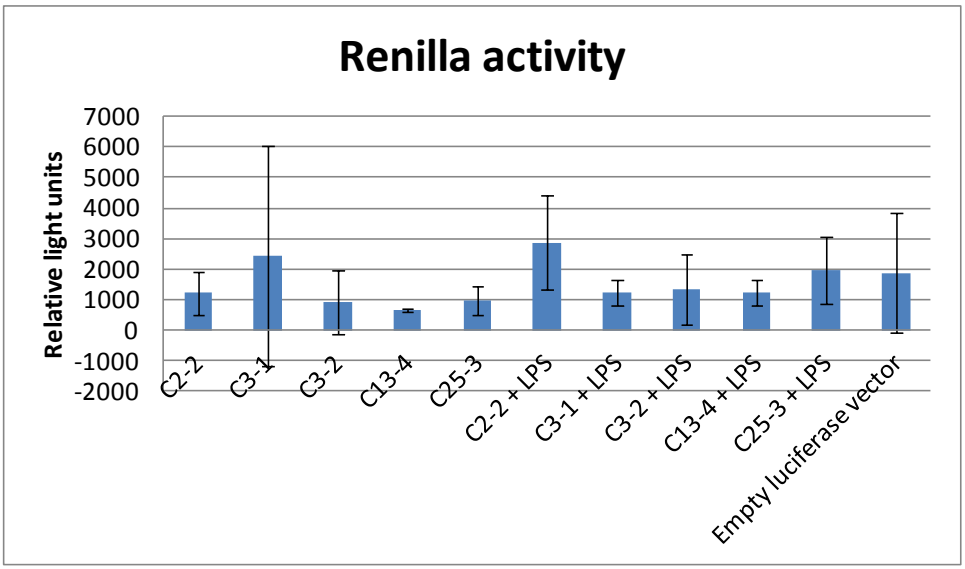
Renilla activity
Relative light units
7000
6000
5000
4000
3000
2000
1000
0
-1000
-2000
C2-2
C3-1
C3-2
C13-4
C25-3
C2-2 + LPS
C3-1 + LPS
C3-2 + LPS
C13-4 + LPS
C25-3 + LPS
Empty luciferase vector

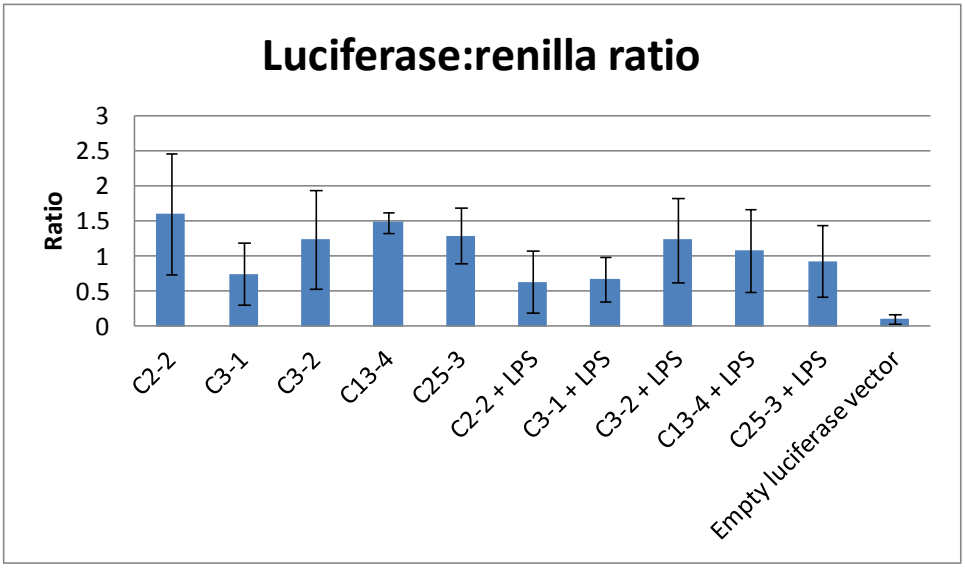
Luciferase:renilla ratio
Ratio
3
2.5
2
1.5
1
0.5
0
C2-2
C3-1
C3-2
C13-4
C25-3
C2-2 + LPS
C3-1 + LPS
C3-2 + LPS
C13-4 + LPS
C25-3 + LPS
Empty luciferase vector

Chapter 5: Development of a therapeutic product utilising the LILR molecules

Background

In view of the immunosuppressive properties of the LILRB molecules, their potential use in therapeutic applications has been considered. In particular, HLA-G, the high-affinity natural ligand for LILRB1 and LILRB2 has been suggested as a potential therapeutic molecule. Engagement of the LILRB molecules *in vitro* by HLA-G has been shown to result in various tolerogenic or immunosuppressive effects on NK cells, $CD4^+$ and $CD8^+$ T cells, antigen presenting cells as well as whole PBMC fractions and endothelial cells. In addition, HLA-G also binds to KIR2DL4, CD8 and CD160, and mediates some of its functions through these molecules.

HLA-G has been shown to inhibit NK cell cytotoxicity, (121;197) NK cell proliferation (198) and transendothelial cell migration via LILRB2. (199) In addition, through its interaction with KIR2DL4, HLA-G also inhibits NK cytotoxicity. (121;197) Conversely, interaction with KIR2DL4 results in increased proliferation and IFN-γ production by uterine NK cells. (200;201) Binding to endocytosed KIR2DL4 results in increased secretion of pro-angiogenic factors. (202) HLA-G induces apoptosis in $CD8^+$ T cells and NK cells (135;203) and inhibits cytotoxic T cell activity through interaction with CD8. (135) Indirectly, HLA-G can also inhibit NK cell cytotoxicity through

stabilisation of HLA-E via CD94/NKG2A. (204) Expression of HLA-G by target cells prevents polarization of cytolytic granules at the immune synapse. (205)

HLA-G inhibits alloreactivity via LILRB1 and LILRB2 in $CD4^+$ helper T cells, (206;207) and inhibits proliferation through LILRB1 in $CD4^+$ and $CD8^+$ T cells. (208;209) HLA-G inhibits the cytotoxic function of $CD8^+$ T cells (210;211) and results in the generation of $CD4^{low}$ and $CD8^{low}$ regulatory T cells. (146;206)

Dendritic cells exposed to HLA-G have reduced maturation, antigen presenting ability and trafficking (by downregulation of chemokine receptors), and result in the induction of regulatory T cells. (24;212) HLA-G also upregulates inhibitory receptors LILRB1, LILRB2, LILRB4 and KIR2DL4 in APCs, NK and T cells. (156) PBMCs exposed to HLA-G *in vitro* secrete Th2 cytokines. (213)

In addition to its effect on immune cells, HLA-G has also been shown to result in apoptosis of endothelial cells via CD160. (214) More recently, it has been demonstrated that HLA-G can also be acquired from other cells via trogocytosis resulting in a novel means of immunological escape. (198;209)

There is more limited data on *in vivo* use of HLA-G resulting in a tolerogenic effect, although there is some evidence in mouse models that exogenous administration of HLA-G results in benefit in transplantation and autoimmunity. In allogeneic skin transplants in mice, both HLA-G transgenic mice and injection of microbeads coated with tetrameric HLA-G (or other HLA-G fusion proteins) resulted in delayed skin allograft rejection. (70;215;216) Some of the HLA-G

fusion proteins shown to improve allograft tolerance included β2m linked to HLA-G1-IgG Fc, β2m linked to HLA-G5 and the HLA-G α1 domain linked to IgG Fc. (216)

HLA-G5-β2m microbeads have also been used in a mouse model of lupus nephritis (MRL/lpr mice). (217) Injection of microbeads for 10 weeks (from week 12 of age) resulted in attenuation of disease with reduced renal inflammation, reduced $CXCR3^+$ T cells in the kidney, reduced IFN-γ producing cells, reduced infiltration and activation of DCs and macrophages in the kidney; and lower levels of rheumatoid factor, IL12p40, TNF-α and IL17.

Most of the immunosuppressive effects of HLA-G have been studied with either the full HLA-G molecule (either as membrane bound HLA-G1, shed HLA-G1 or soluble HLA-G5). However, there is less data on the function of the other HLA-G isoforms (which lack some of the α domains). HLA-G2, G3 and G4 have been shown to inhibit NK and cytotoxic T cell cytolysis in vitro. (210)

In view of its multiple immunosuppressive and tolerogenic effects, the use of HLA-G as a therapeutic molecule represents an attractive option with potential use in transplantation and autoimmune disease. However, theoretically there would be little specificity with the use of HLA-G and this would carry with it the consequent risk of generalised immunosuppression and susceptibility to infection and/or malignancy.

As a result, the G-body was developed to determine if the known immunosuppressive properties of the LILRs could be manipulated for therapeutic purposed by combining one of their natural ligands with another molecule to allow localisation to an allogeneic target. Both a more "elegant" recombinant product and a chemically conjugated molecule comprising both "business ends" that would make up the G-body were generated.

Conceptually, the G-Body was designed as a bifunctional molecule to be used in the setting of transplantation and alloimmune responses. It would consist of two parts; one "business end" would be HLA-G, used for its known immunosuppressive properties and the other "business end" would enable specific localization of the HLA-G to donor cells/tissues to prevent alloimmune responses and generate allospecific tolerance. To this end, HLA-A2 was used as the allogeneic target for a proof-of concept model. This would allow localisation of HLA-G to donor HLA-A2 positive cells in a HLA-A2 negative recipient for suppression of alloimmune responses.

Two approaches were concurrently taken to develop the G-body. This was to allow more rapid development of a product that would be suitable for functional testing and proof-of-concept. The first was a more elegant recombinant technology approach that sought to combine HLA-G and the ScFv fragment of an anti-HLA-A2 monoclonal antibody within a single expression plasmid, and transfected into mammalian cells for protein production. This approach, although likely to take longer and be more complex was used with the longer term view of using the molecule in *in vivo* studies.

The second approach involved chemically conjugating biotinylated HLA-G monomers to an anti HLA-A2 monoclonal antibody that had been labelled with streptavidin. Although this approach would result in a mixture of molecular species, it was expected that this method would more quickly generate a bifunctional product that could be used in functional studies for proof of concept.

Design of the recombinant G-body

The recombinant G-body was intended to be created as two polypeptide chains; one with the HLA-G heavy chain and the V_L fragment of a monoclonal antibody directed against HLA-A2 and one with β2m and the V_H fragment of the same monoclonal antibody. Each of the parts of the two separate molecule would be linked by using a repeating $(G_4S)_{n=1-3}$ linker (Figure 5.1), to allow a degree of flexibility for the portions of the two polypeptide chains to fold correctly, resulting in a HLA-G/β2m molecule and an anti-HLA-A2 ScFv on two separate ends of the recombinant molecule. Four different recombinant constructs were designed to achieve this goal. (Figures 5.2 to 5.4)

Recombinant G-Body version 1 (ORIGBv1)

The recombinant G-body was first designed as a single polypeptide chain with a furin cleavage site in the middle that would allow generation of the two polypeptide chains (Figure 5.2). In addition, c-myc and 6x His tags were added to allow detection and purification of the molecule.

The HLA-G sequence (NCBI reference sequence NM_002127.5) was truncated to remove the intracytoplasmic tail to allow the protein product to be secreted into supernatant. The genetic sequence for the anti-HLA-A2 ScFv was obtained by sequencing of the BB7.2 hybridoma by a commercial company. The two sequences were then combined such that the genetic sequences were in the following order: HLA-G signal peptide, HLA-G heavy chain, $(G_4S)_1$ linker, V_L mAb fragment, c-myc tag, furin cleavage site, V_H mAb fragment, $(G_4S)_3$ linker, β2m. Synonymous substitutions were made in the coding DNA to generate specific restriction enzyme sites to allow subsequent modular modification of the molecule as necessary. (Figure 5.5) The gene was synthesized and cloned into the pcDNA3.1+ expression vector by Genscript.

COS7 cells were chosen as the transfection system to utilize the large T antigen-SV40 interaction to allow episomal replication of the transfected plasmid and facilitate large amounts of transient protein production. These cells were transfected with this plasmid with and without co-transfection with a pRC furin plasmid (a kind gift from Joop Gaken). The presence of protein of the correct molecular size was detectable in unconcentrated supernatant with Western blotting using the anti-denatured HLA-G antibody, 4H84. (Figure 5.6) However, staining with the anti-β2m, anti-myc and anti-His antibodies failed to detect protein. (Figure 5.6) The reasons for the non-binding of these antibodies was not completely clear although might possible have been due to refolding of the entire G-body molecule on the PVDF membrane resulting in epitopes for these antibodies being “hidden”.

In addition, immunoprecipitation experiments failed to show demonstrable binding to HLA-A2, either in the furin-cleaved or uncleaved molecule. (Figure 5.6) The lack of binding of OGBv1 to HLA-A2 could have been due to insufficient affinity in its monomeric form, errors in the sequencing of the hybridoma or problems in folding of the ScFv domain.

Recombinant B11 G-body (B11GBv1)

To overcome the problem of ORIGBv1 not binding to HLA-A2, the ORIGBv1 molecule was modified with removal of the V_L mAb fragment, c-myc tag, furin cleavage site and V_H mAb fragment to be replaced with an alternative anti-HLA-A2 sequence proven to bind to its target when expressed as an ScFv fragment. (Figure 5.7) The sequence for the ScFv fragment was obtained from a published anti-HLA-A2 ScFv sequence, B11 developed using phage display technology and light-chain shuffling to enhance avidity. (218;219)

Sequencing of B11 plasmid

Sequencing of the B11pUC119 plasmid was undertaken to confirm that it matched the published sequence. The original B11 pUC119 plasmid (a kind gift from Dr Ouwehand and Dr Watkins) was transformed into TOP10 cells and plasmid DNA minipreps were made. Plasmid DNA was sent to a commercial company, Geneservice for sequencing with stock M13F, M13R and a custom

"AGGCGAGTCAGGACATTAGC" primer. Sequence data was compared with the published sequence, which confirmed a match.

Synthesis of B11 insert to replace BB7.2 fragment

The B11 ScFv insert was designed following the published sequence with $(G4S)_3$ linker arms at both ends and in between the two variable domains and with BspEI and BamHI restriction enzymes sites at the 5' and 3' ends to allow cloning into the original G-body. (Figure 5.7a) The design was submitted to Genscript, who further optimized the codons for expression in COS7 cells (using in-house software) and synthesized the B11 insert with cloning into a pUC57 vector. (Figure 5.7b)

Cloning of the B11 insert into ORIGBv1

The B11 pUC57 vector was transformed into TOP10 cells and plasmid minipreps generated. Both the ORIGBv1 and the B11 pUC57 plasmids were digested with BspEI and BamHI and run on an 0.8% agarose gel. (Figure 5.8) The digested G-body fragment (without the BB7.2 portion) and the B11 insert were extracted from the gel and ligated. The ligated products were then used to transform TOP10 cells and plasmid minipreps were generated.

DNA sequencing confirmed that the B11 insert had correctly replaced the original BB7.2 sequence in the ORIGBv1 plasmid. Sequencing primers used were T7F, bGHR and "ATGGAACCTTCCAGAAGTGG". After confirmation

of the sequence, a plasmid maxiprep of the B11-Gbody version 1 (B11GBv1) construct was generated for transfection.

Binding characteristics of B11GBv1

Immunoprecipitation experiments showed that B11GBv1 was capable of binding HLA-A2. (Figure 5.9) Due to the relatively poor binding affinity of the monomeric HLA-G portion for its ligand, its conformational state was assessed by binding to anti-HLA-G mAbs. However, B11GBv1 was only bound weakly or not at all in repeat experiments by the conformational mAbs (87G, MEM-G9 and W6/32). Figure 5.10a to 5.10d shows faint binding of B11GBv1 with the 87G mAb; there was possibly better binding by MEMG/9 and the binding pattern for W6/32 was similar to that of 87G.

In conclusion, these results showed that the B11GBv1 could bind HLA-A2 but it was not certain if the HLA-G portion was definitely in the correct conformational state. One possible explanation for this was that the expression of β2m at the end of the polypeptide chain attached to the anti-HLA-A2 ScFv was interfering with proper folding of the HLA-G heavy chain.

Original G-Body version 2 (ORIGBv2) and B11 G-Body version 2 (B11GBv2)

Due to uncertainty of the HLA-G portion of the B11GBv1 not being in the correct conformational state, both ORIGBv1 and B11GBv1 were recloned

without the β2m portion of the molecule; with the intention of co-transfecting β2m separately in the expression system to determine if this would enable correct folding of the HLA-G portion.

PCR cloning of ORIGBv2 and B11GBv2

Further versions of the recombinant G-body without the β2m segment (and 6xHis tag) "version 2" were generated by PCR cloning. (Figure 5.4) The ORIGBv1 and B11GBv1 plasmids were used as the template for PCR cloning. The new constructs were designed with 5' NheI and 3' BamHI restriction enzyme sites (underlined) to allow cloning into a pcDNA3.1(+) vector. The primers used for ORIGBv2 cloning were 5'-CTGGCTAGCACCACCATGGTGGTC and ATAGGATCCTCACGGGGGTGTCGTACGGGCTG-3'; whereas the primers used for B11GBv2 cloning were 5'-CTGGCTAGCACCACCATGGTGGTC and ATAGGATCCTCACCCGAGCACTGTCAGCTTGG -3'.

PCR conditions for the reaction were: denaturation at 98^{o}C for 2 minutes, 30 cycles of denaturation at 98^{o}C for 10 seconds and extension at 72^{o}C for 60 seconds, and a final extension at 72^{o}C for 5 minutes. PCR products were run on an 0.8% agarose gel and bands corresponding to the expected size were extracted from the gel (Figure 5.11a and 5.11b) and incubated with NheI and BamHI restriction enzymes prior to being purified with the Qiagen PCR product purification kit.

pcDNA3.1(+) plasmid was also incubated with NheI and BamHI restriction enzyme prior to being run on an 0.8% agarose gel. The corresponding linearized plasmid was extracted from the gel. The linearized vector and RE digested inserts were ligated and transformed into TOP10 cells.

DNA sequencing confirmed that the ORIGBv1 and B11GBv1 plasmids had the intended sequence. Sequencing primers used were stock T7F and bGHR.

Binding characteristics of ORIGBv2 and B11GBv2

Immunoprecipitation experiments confirmed binding of B11GBv2 to HLA-A2. (Figure 5.9) Of interest, ORIGBv2 also showed weak binding to HLA-A2 unlike ORIGBv1. One possible explanation for this difference is that expression of β2m attached to the ScFV in the ORIGBv1 could have affected the conformational state of the anti-HLA-A2 ScFV portion of the molecule.

In addition, both ORIGBv2 and B11GBv2 showed binding with the conformational monoclonal antibodies 87G and MEM-G/9 (Figure 5.10a to5.10d), although arguably the binding intensity was similar to that of the B11GBv1. The original Western blotting experiment was done with an unconjugated primary antibody (4H84) and a goat anti-mouse Fc HRP antibody as secondary layer. This resulted in some difficulty clearly identifying the GBv2 bands as the secondary antibody also bound to the monoclonal antibodies used for immunoprecipitation, which has a similar molecular weight to the GBv2

products. Hence, the Western blot portion of the experiment was repeated using a biotinylated primary detection antibody (4H84) and streptavidin-HRP as the secondary layer to avoid the problem of the immunoprecipitation antibody being seen on the Western blot.

In summary, the B11GBv2 showed binding to HLA-A2 and had a HLA-G portion that had the correct conformational state. The ORIGBv2 had an HLA-G portion in the correct conformational state and probably had a degree of binding to HLA-A2 as well.

Measurement of recombinant G-body concentrations

Concentrations of the recombinant G-body were then measured using an ELISA kit to determine how much protein was actually being generated to allow planning of downstream experiments. This showed that the concentrations of the G-Body in the supernatant were all <20 ng/ml. (Table 5.1) Published literature suggested that it should be possible to obtain up to 1 μg/ml of protein using a COS7 expression system. (220) The reason for this discrepancy is not completely understood, although the expression system has not been fully optimised yet. In addition, it is possible that the signal peptide used for the G-body is not ideal for the purpose of secreting a soluble protein product.

Design of the chemically conjugated GBody

In view of the difficulty in generating a recombinant G-body, a chemically conjugated G-body (cGBOD) with both the requisite business ends was generated as described to allow quicker testing in functional experiments. Another advantage of the chemically conjugated molecule is that it would allow multimerisation of HLA-G, with potential to increase its effects. The chemically conjugated G-body was generated by exploiting the effectively irreversible biotin-streptavidin interaction. In summary, the anti-HLA-A2 antibody BB7.2 was conjugated to streptavidin using a commercial kit. Biotinylated HLA-G was purchased and the two reagents were mixed to allow biotinylated HLA-G-BB7.2-streptavidin complexes to form.

However, biotinylated HLA-G purchased from the vendor was found to have significantly elevated levels of endotoxin. (Table 5.2) Consequently, this was removed to prevent interference with functional assays and the endotoxin levels remeasured. After buffer exchange, there was still some degree of endotoxin contamination although this was significantly less and expected to be lower still after dilution in culture medium prior to use in functional experiments.

Binding characteristics of cGBOD

K562 stably transfected with HLA-A2 (a kind gift from Mark Peakman) and LILRB2, the ligand with the highest affinity for HLA-G, were used in FACS experiments to test cGBOD binding. This confirmed that the conjugation process

had not affected the binding properties of both molecules. (Figure 5.12a and 5.12b)

Binding of the cGBOD was also tested on PBMCs of HLA-A2 positive and HLA-A2 negative individuals. (Figure 5.12c) This showed binding to monocytes, assumed to be due to the myeloid-specific expression of HLA-G receptors LILRB1 and LILRB2, but not lymphocytes in HLA-A2 negative individuals. This is consistent with published flow cytometric data investigating the binding properties of HLA-G tetramers. (221) cGBOD binding was seen in both lymphocytes and monocytes of HLA-A2 positive subjects as expected due to interaction of the anti-HLA-A2 (BB7.2) portion of the construct with HLA-A2 present on all cells. This confirmed that in addition to transfectants, the cGBOD could also interact with human cells that were to be used in functional experiments.

An optimisations experiment with different molar ratios (4:1, 8:1 and 12:1) of biotinylated HLA-G to BB7.2 was performed (Figure 5.12d) to determine the best ratio for the cGBOD. This showed that there was greatest staining of LILRB2 transfectants with a ratio of 4:1. There was slightly less staining of HLA-A2 transfectants at this ratio compared to the other ratios. However, the MFI for LILRB2 staining at the other ratios were relatively close to the MFI for the IMC and hence the ratio of 4:1 was chosen for subsequent experiments.

Discussion

The results above indicate that both the recombinant and chemically conjugated G-bodies have been successfully generated. This represents the first step required for proof of concept that localisation of the HLA-G signal to the site of an allogeneic immune response confers additional immune suppression compared to just HLA-G alone. Functional experiments utilising the G-body are described in the following chapter.

The recombinant G-body has been shown to bind to HLA-A2 unequivocally. As expected there is particularly strong affinity when the B11 ScFv sequence is used (218;219) but also some degree of binding with the original BB7.2 sequence is used. Additionally, this indicates that the ScFv fragment has folded correctly, at least for the ORIGBv2, B11GBv1 and B11GBv2 constructs. The addition of β2m with one shorter $(G_4S)_1$ segment may have resulted in the ORIGBv1 construct not folding in the correct conformational state and binding to HLA-A2.

Proving that the HLA-G portion of the recombinant G-body bound to its target was more of a challenge. Monomeric HLA-G, despite being the highest affinity ligand for LILRB1 and LILRB2 still binds relatively weakly to its ligand (especially compared to antibody-antigen interactions). Surface plasmon resonance has been required to demonstrate binding (130) and additionally tetramerised HLA-G can also bind to its target. (222) As a surrogate to check whether the HLA-G portion of the recombinant G-body was folded correctly, binding to two different conformational anti-HLA-G antibodies was checked.

This showed that both the ORIGBv2 and the B11GBv2 bound two different conformational monoclonal antibodies, making it likely that the HLA-G portion in these two constructs had folded correctly. This does not necessarily constitute proof that the HLA-G portion would bind to its ligand but is sufficient evidence to try the molecule in functional experiments.

Unfortunately, the transient transfection system did not generate sufficient quantities of protein for use in functional experiments. For future work, potential ways of addressing this would be generating the recombinant protein in large-scale mammalian cell transfection systems, which would have the benefits of both ensuring appropriate folding of the protein in the cell machinery as well as glycosylation. The signal peptide used in the recombinant G-body was native human HLA-G and modification to an alternative signal peptide more suited to the cells used in the expression system (or using cells that might be more suited for a human signal peptide as COS7 cells are derived from monkey kidney tissue) might have increased the protein yield. A more economical way of producing the recombinant protein might be to use yeast or bacterial protein expression systems. However, it is likely in this instance that additional steps would need to be taken to obtain correct folding of the protein product.

With additional time and resources, testing of different constructs using alternative HLA-G isoforms (i.e. HLA-G2, HLA-G3 or HLA-G4) instead of the full HLA-G1/G5 molecule would be useful to undertake. Another possibility for a molecule incorporating full length HLA-G with β2m and the ScFv portion as a single polypeptide chain might be to design the gene sequence as β2m-HLA-G-

ScFv. β2m-HLA-G fusion protein constructs have recently been demonstrated to have functional tolerogenic effects in murine allogeneic skin graft model. (216) These approaches might have allowed for both easier production and re-folding of the recombinant protein without sacrificing immunosuppressive potential.

The chemically conjugated G-body, on the other hand, can be generated in sufficient quantity for functional experiments. Additionally the flow cytometric data confirms that both portions of the molecule bound to their respective targets, both in transfectants and primary cells. The process for generation of this is relatively quick and allows for production of large quantities of the G-body, with the only limitation being cost. On the negative side, however, the process used to make the chemically conjugated G-body does result in a variety of molecular species as it is not possible to control the exact stoichiometries of monoclonal antibody to streptavidin to biotinylated HLA-G. It might be possible that certain particular stoichiometries result in greater functional consequences although a means of separating or isolating the different species generated by the conjugation process would need to be undertaken. For future work, potentially mass spectrometry could be used to determine the make-up of the chemically conjugated G-body as well as isolating the fraction which is likely to have the greatest biological activity.

The development of both the G-body products is exciting as it gives a new set of tools to test the therapeutic potential of manipulating the LILR molecules via HLA-G. The chemically conjugated G-body, although a crude mixture of different molecules allows rapid testing for proof-of-concept; the results of which

are described in the next chapter. The recombinant molecule on the other hand holds more potential as a therapeutic that might eventually have *in vivo* use, although further development is required to maximise its production prior to *in vitro* testing.

Tables

Table 5.1

Concentration of HLA-G/G-body in the supernatant of various transfectants

Supernatant from transfectant:	**HLA-G concentration (ng/ml)**
pcDNA3.1(+)	1.2
Soluble HLA-G/β2m	6.8
ORIGBv1	18.4
ORIGBv2/β2m	8.4
B11GBv1	14
B11GBv2/β2m	4.4

Table 5.2

Endotoxin levels in biotinylated-HLA-G before and after endotoxin removal and after buffer exchange into PBS

Sample	**Endotoxin concentration (EU/ml)**
Biotinylated HLA-G, from supplier	>250
Biotinylated HLA-G, post ET removal	0.107
Biotinylated HLA-G, post buffer exchange	11.20
Biotinylated BSA	1.135
Streptavidin conjugated BB7.2	21.95
Streptavidin conjugated MPC13	15.03
Sterile PBS (as control)	0.087

Figures

Figure 5.1

The conceptual design for the recombinant G-body which would incorporate two polypeptide chains, consisting of HLA-G heavy chain-VLA and β2m-VHA

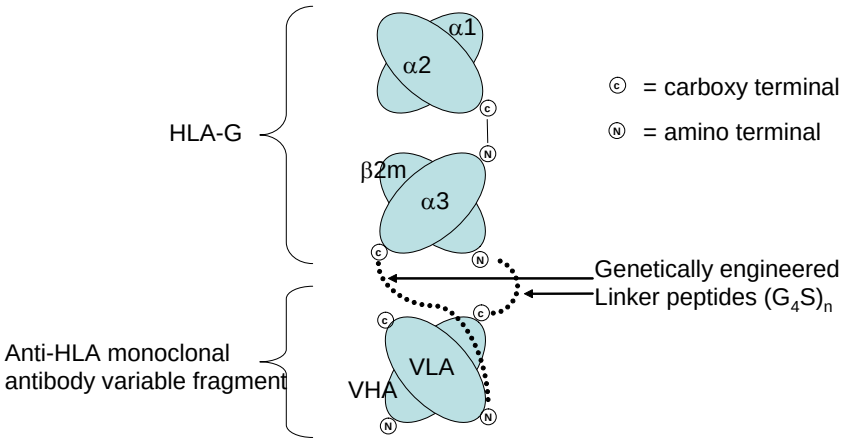

G-body design

Figure 5.2

The ORIGBv1 construct consisting of a single polypeptide chain with a furin linker that would be cleaved in vitro, as well as c-myc and 6xHis tags

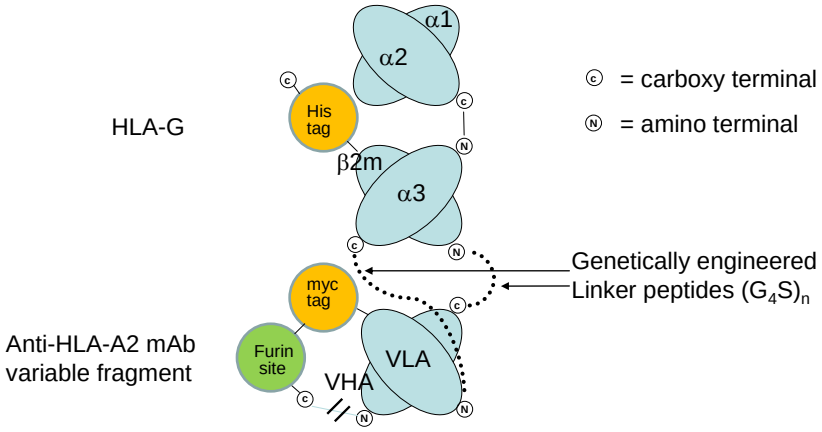

G-body design

Figure 5.3

The B11GBv1 construct consisting of a single polypeptide chain with the B11 ScFv fragment inserted in place of the BB7.2 ScFv fragment, and 6xHis tag at the C-terminal

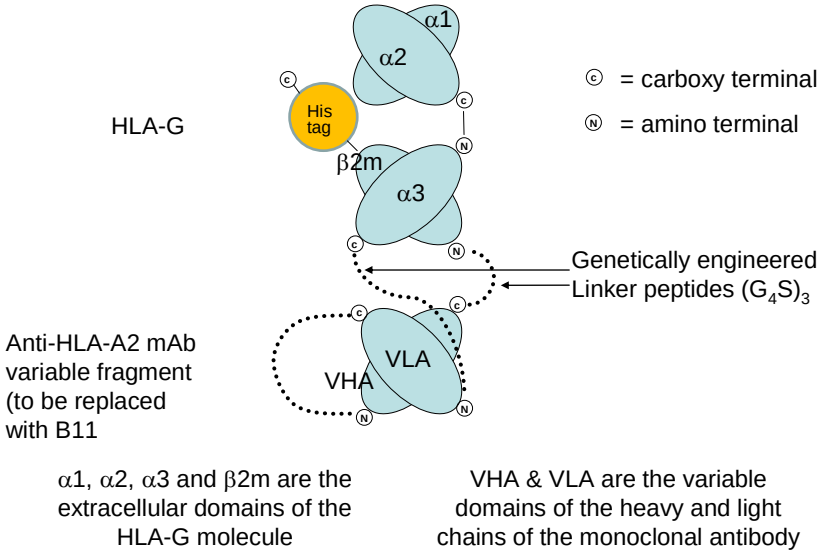

Figure 5.4

Schematic for the ORIGBv2 and B11GBv2 constructs which consist of the HLA-G heavy chain linked to the anti-HLA-A2 ScFv fragment; with the β2m being co-transfected on a separate plasmid

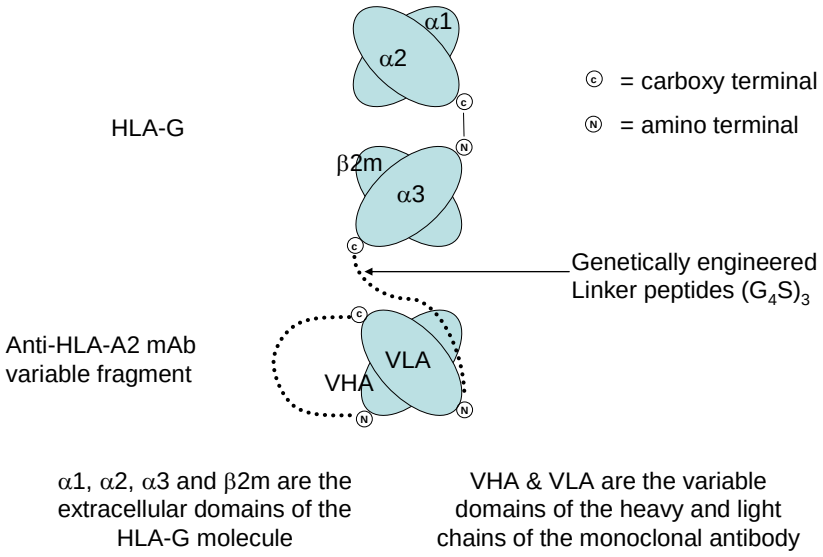

Figure 5.5

DNA sequence for the ORIGBv1 construct cloned into pcDNA3.1(+).

Underlined sequences represent a deliberate restriction enzyme cutting site

gctagcACCACCATGGTGGTCATGGCGCCCCGAACCCTCTTCCTGCTGCTCTCG

GGGGCaCTGACCCTGACCGAGACCTGGGCGGGCTCCCACTCCATGAGGTATTTC

AGCGCCGCCGTGTCCCGGCCCGGCCGCGGGGAGCCCCGCTTCATCGCCATGGGC

TACGTGGACGACACGCAGTTCGTGCGGTTCGACAGCGACTCGGCGTGTCCGAGG

ATGGAGCCGCGGGCGCCGTGGGTGGAGCAGGAGGGGCCGGAGTATTGGGAAGAG

GAGACACGGAACACCAAGGCCCACGCACAGACTGACAGAATGAACCTGCAGACC

CTGCGCGGCTACTACAACCAGAGCGAGGCCAGTTCTCACACCCTCCAGTGGATG

ATTGGCTGCGACCTGGGGTCCGACGGACGCCTCCTCCGCGGGTATGAACAGTAT

GCCTACGATGGCAAGGATTACCTCGCCCTGAACGAGGACCTGCGCTCCTGGACC

GCAGCGGACACTGCGGCTCAGATCTCCAAGCGCAAGTGTGAGGCGGCCAATGTG

GCTGAACAAAGGAGAGCCTACCTGGAGGGCACGTGCGTGGAGTGGCTCCACAGA

TACCTGGAGAACGGGAAGGAGATGCTGCAGCGCGCGGACCCCCCCAAGACACAC

GTGACCCACCACCCTGTCTTTGACTATGAGGCCACCCTGAGGTGCTGGGCaCTG

GGCTTCTACCCTGCGGAGATCATACTGACCTGGCAGCGGGATGGGGAGGACCAG

ACCCAGGACGTGGAGCTCGTGGAGACCAGGCCTGCAGGGGATGGAACCTTCCAG

AAGTGGGCAGCTGTGGTGGTGCCTTCTGGAGAGGAGCAGAGATACACGTGCCAT

GTGCAGCATGAGGGGCTGCCGGAGCCCCTCATGCTGAGATGGAAGCAGTCTTCC

CTGCCCACCATCCCCtcCGGAGGTGGAGGTTCTGGAGGTGGAGGTTCcGGAGGT

GGAGGTTCTGATGTTTTGATGACCCAAACTCCACTCTCCCTGCCTGTCAGTCTT

GGAGATCAAGTCTCCATCTCTTGCAGATCTAGTCAGAGCATTGTACATAGTAAT

GGAAACACCTATTTAGAATGGTACCTGCAGAAACCAGGCCAGTCTCCAAAGCTC

CTGATCTACAAAGTTTCCAACCGATTTTCTGGGGTCCCAGACAGGTTCAGTGGC

AGTGGATCAGGGACAGATTTCACACTCAAGATCAGCAGAGTGGAGGCTGAGGAT

CTGGGAGTTTATTACTGCTTTCAAGGTTCACATGTTCCTCGGACGTTCGGTGGA

GGCACCAAGCTcGAgATCAAACGGGCTGATGCTGCAGAACAAAAgCTtATCTCA

GAAGAGGATCTGCATCACCATCGTGCTCGATACAAGAGACAGGTCCAGCTGCAG

CAGTCTGGgCCcGAGCTGGTGAAGCCTGGGGCCTCAGTGAAGATGTCCTGCAAG

GCTTCTGGCTACACCTTCACAAGCTACCATATACAGTGGGTGAAGCAGAGGCCT

GGACAGGGACTTGAGTGGATTGGATGGATTTATCCTGGAGATGGTAGTACTCAG

TACAATGAGAAGTTCAAGGGCAAGACCACACTGACTGCAGACAAATCCTCCAGC

ACAGCCTACATGTTGCTCAGCAGCCTGACCTCTGAGGACTCTGCGATCTATTTC

TGTGCAAGGGAGGGGACCTACTATGCTATGGACTACTGGGGTCAAGGAACCTCA

GTCACCGTCTCCTCAGCCCgtACgACACCCCCgGGAGGTGGAggatccATCCAG

CGTACTCCAAAGATTCAGGTTTACTCACGTCATCCAGCAGAGAATGGAAAGTCA

AATTTCCTGAATTGCTATGTGTCTGGGTTTCATCCATCCGACATTGAAGTTGAC

TTACTGAAGAATGGAGAGAGAATTGAAAAAGTGGAGCATTCAGACTTGTCTTTC

AGCAAGGACTGGTCTTTCTATCTCTTGTACTACACTGAATTtACCCCCACTGAA

AAAGATGAGTATGCCTGCCGTGTGAACCATGTGACTTTGTCACAGCCCAAGATA

GTTAAGTGGGATCGAGACATGaccggtcatcatcaccatcaccatTAAaccggt

tgagttt

Kozak sequence, Sig pep of HLA-G h chain, HLA-G alpha-1,2 and 3 domains, HLA-G connecting stalk, Linker peptide (3X), VLA, Connecting peptide of Ig domain, C-myc tag (10aa), 3X His tag, Furin site, VHA, Connecting peptide of Ig domain, Linker peptide (1X), Beta 2 m, 6X His tag, STOP CODON

Figure 5.6

Western blot showing immunoprecipitation using biotinylated HLA-A2 bound to streptavidin beads (Lanes 1 and 2); and detection of ORIGBv1 in neat supernatant using different detection antibodies (Lanes 3 to 6). The primary detection antibody used in the immunoprecipitation experiments is 4H84 (non-conformational anti-HLA-G). No binding of ORIGBv1 to biotinylated HLA-A2 is visible in lane 2. For lanes 3 to 6, detection of the ORIGBv1 (predicted molecular weight of 73 kDa) in neat supernatant is noted only when 4H84 is the detection antibody (Lane 3). No detection is noted with anti-β2m, anti-c-myc or anti-His antibodies (Lanes 4 to 6).

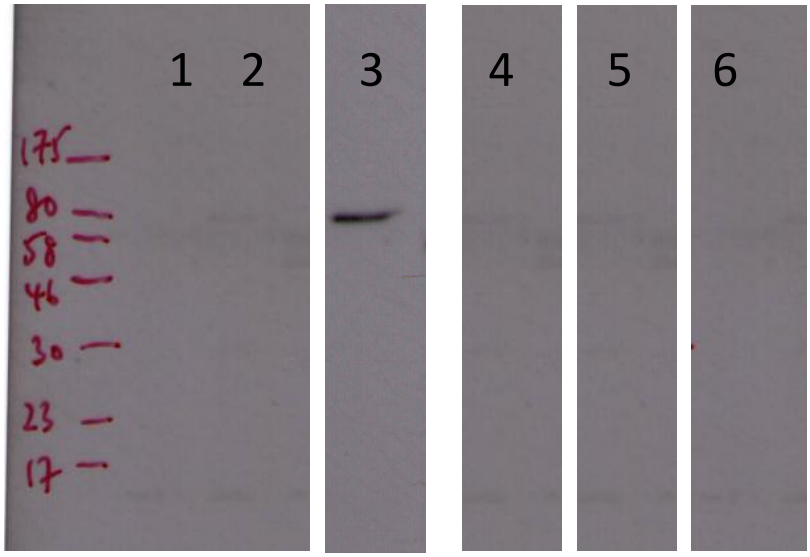

Lane	bHLA-A2	Material	Detection antibody
1	-	ORIGBv1 sup	4H84
2	+	ORIGBv1 sup	4H84
3	Neat ORIGBv1 supernatant		4H84
4	Neat ORIGBv1 supernatant		Anti-β2m
5	Neat ORIGBv1 supernatant		Anti-c-myc
6	Neat ORIGBv1 supernatant		Anti-His

Figure 5.7a

Original anti-HLA-A2 sequence derived from B11 ScFv clone used to replace the BB7.2 sequence in ORIGBv1, prior to optimisation for COS7 cells. Underlined sequences are the 5' BspEI and 3' BamHI restriction enzyme sites

tcCGGAGGTGGAGGTTCTGGAGGTGGAGGTTCTGGAGGTGGAGGTTCTCAGGTG
CAGCTGGTGCAGTCTGGGGGAGGCGTGGTCCAGCCTGGGGGGTCCCTGAGAGTC
TCCTGTGCAGCGTCTGGGGTCACCCTCAGTGATTATGGCATGCATTGGGTCCGC
CAGGCTCCAGGCAAGGGGCTGGAGTGGATGGCTTTTATACGGAATGATGGAAGT
GATAAATATTATGCAGACTCCGTGAAGGGCCGATTCACCATCTCCAGAGACAAC
TCCAAGAAAACAGTGTCTCTGCAAATGAGCAGTCTCAGAGCTGAAGACACGGCT
GTGTATTACTGTGCGAAAAATGGCGAATCTGGGCCTTTGGACTACTGGTACTTC
GATCTCTGGGGCCGTGGCACCCTGGTCACCGTGTCGAGTGGTGGAGGCGGTTCA
GGCGGAGGTGGCTCTGGCGGTGGCGGATCGGATGTTGTGATGACTCAGTCTCCA
TCCTCCCTGTCTGCATCTGTAGGAGACAGAGTCACCATCACTTGCCAGGCGAGT
CAGGACATTAGCAACTATTTAAATTGGTATCAGCAGAAACCAGGGAAAGCCCCT
AAGCTCCTGATCTACGATGCATCCAATTTGGAAACAGGGGTCCCATCAAGGTTC
AGTGGAAGTGGATCTGGGACAGATTTTACTTTCACCATCAGCAGCCTGCAGCCT
GAAGATATTGCAACATATTACTGTCAACAGTATGATAATCTCCCTCCCACTTTC
GGCGGAGGGACCAAGCTGACCGTCCTAGGTGGAGGTGGAGGTTCTGGAGGTGGA
GGTTCTGGAGGTGGAggatcc

Linker arms,B11 sequence

Figure 5.7b

Anti-HLA-A2 sequence derived from B11 ScFv clone used to replace the BB7.2 sequence in ORIGBv1, after optimisation for expression in COS7 cells. Underlined sequences are the 5' BspEI and 3' BamHI restriction enzyme sites

tcCGGAGGCGGGGGCTCTGGGGGCGGGGGCTCCGGGGGCGGGGGCAGCCAGGTG
CAGCTGGTCCAGTCTGGGGGCGGGGTGGTCCAGCCCGGCGGGTCCCTGCGCGTG
AGCTGCGCTGCTAGTGGCGTCACCCTCTCCGACTACGGCATGCACTGGGTGCGG
CAGGCTCCAGGGAAAGGCCTGGAGTGGATGGCTTTCATCCGCAACGACGGCTCT
GACAAATACTATGCCGACTCCGTCAAGGGCCGCTTCACCATCTCTAGGGACAAC
TCCAAGAAAACAGTGAGCCTGCAGATGTCTTCCCTCAGGGCCGAGGACACCGCT
GTCTACTATTGCGCTAAGAACGGCGAGTCCGGGCCACTGGACTACTGGTATTTC
GACCTGTGGGGGAGGGGCACCCTCGTCACAGTCAGCAGTGGCGGGGGCGGGAGT
GGCGGGGGCGGGTCTGGCGGGGGCGGGTCCGACGTGGTCATGACCCAGTCTCCA
TCTTCCCTGTCTGCCTCCGTGGGCGACAGGGTCACCATCACATGCCAGGCCTCT
CAGGACATCAGTAACTACCTGAACTGGTATCAGCAGAAGCCCGGCAAAGCCCCA
AAGCTGCTCATCTACGACGCCTCTAACCTCGAGACCGGCGTGCCCAGTAGGTTC
AGCGGGAGTGGCTCTGGGACAGACTTCACCTTCACAATCAGCAGTCTGCAGCCA
GAGGACATCGCCACCTACTATTGCCAGCAGTATGACAACCTGCCCCCAACCTTC
GGCGGCGGCACCAAGCTGACAGTGCTCGGGGGCGGGGGCGGGAGCGGCGGGGGC
GGGAGTGGCGGGGGCggatcc

Linker arms,B11 sequence

Figure 5.8

0.8% agarose gel of ORIGBv1 and B11 pUC57 plasmids digested with BspEI and BamHI showing two bands of approximately 800 bp corresponding to the cut ScFv fragments and the remainder of the plasmid

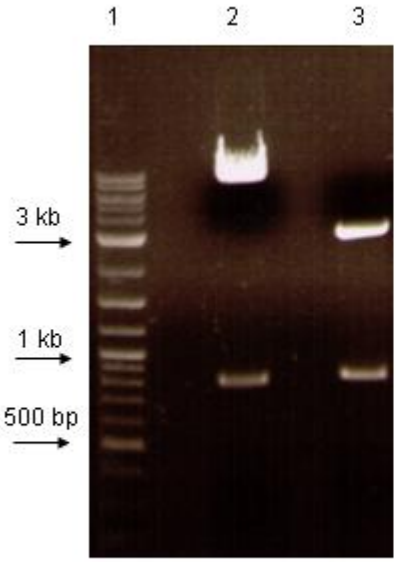

Lane	
1	DNA ladder
2	ORIGBv1 plasmid digested with BspEI and BamHI
3	B11 pUC57 plasmid digested with BspEI and BamHI

Figure 5.9

Western blot showing immunoprecipitation using biotinylated HLA-A2 bound to streptavidin beads. The primary detection antibody is 4H84 (non-conformational anti-HLA-G). Faint binding of ORIGBv2 (predicted molecular weight of 62 kDa) and stronger binding of B11GBv1 (predicted molecular weight of 73 kDa) and B11GBv2 (predicted molecular weight of 60 kDa) is seen.

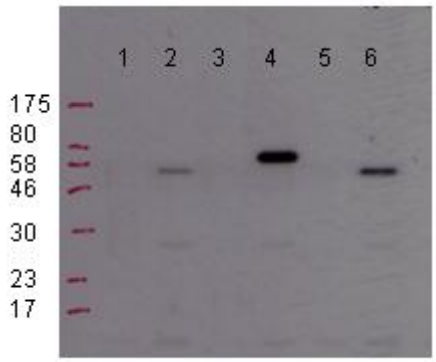

Lane	bHLA-A2	Transfectant supernatant
1	-	OriGBv2
2	+	OriGBv2
3	-	B11GBv1
4	+	B11GBv1
5	-	B11GBv2
6	+	B11GBv2

Figure 5.10a

Western blot showing immunoprecipitation using anti-HLA-G (87G) bound to protein G beads. The primary detection antibody is 4H84 (non-conformational anti-HLA-G). and the secondary antibody is goat-anti mouse Fc-HRP. Faint binding of B11GBv1 (predicted molecular weight of 73 kDa) and very faint binding of ORIGBv1; stronger binding of ORIGBv2 and B11GBv2/β2m (predicted molecular weight of 62 and 60 kDa respectively) is seen in the region of the yellow box.

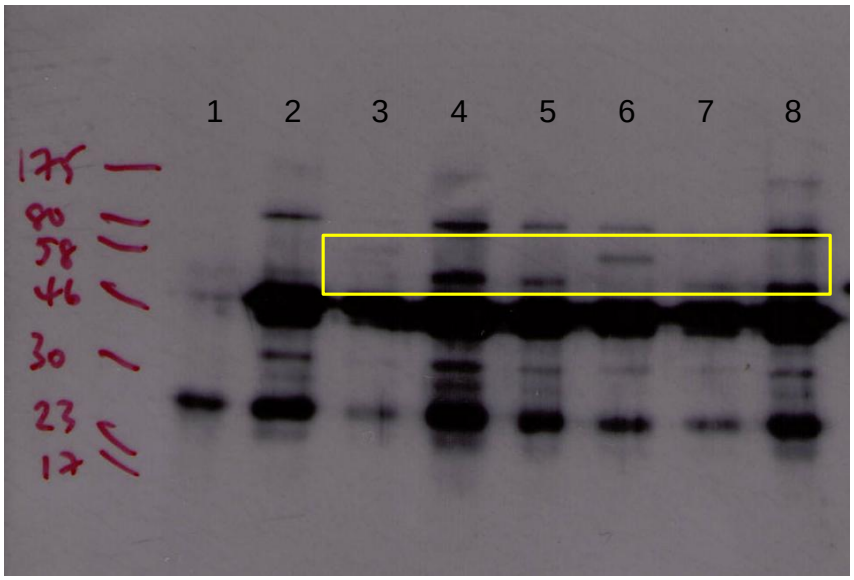

Lane	Protein G	87G	Supernatant
1	+	-	OriGBv2
2	+	+	-
3	+	+	OriGBv1
4	+	+	OriGBv2
5	+	+	OriGBv2/β2m
6	+	+	B11GBv1
7	+	+	B11GBv2
8	+	+	B11GBv2/ β2m

Figure 5.10b

Western blot showing immunoprecipitation using anti-HLA-G (MEMG/9) bound to protein G beads. The primary detection antibody is 4H84 (non-conformational anti-HLA-G). and the secondary antibody is goat-anti mouse Fc-HRP. Binding of B11GBv1 (predicted molecular weight of 73 kDa) and very faint binding of ORIGBv1is seen in the region of the yellow box. Binding of GBv2 by MEMG/9 is less certain due to proximity to IgG heavy chain band.

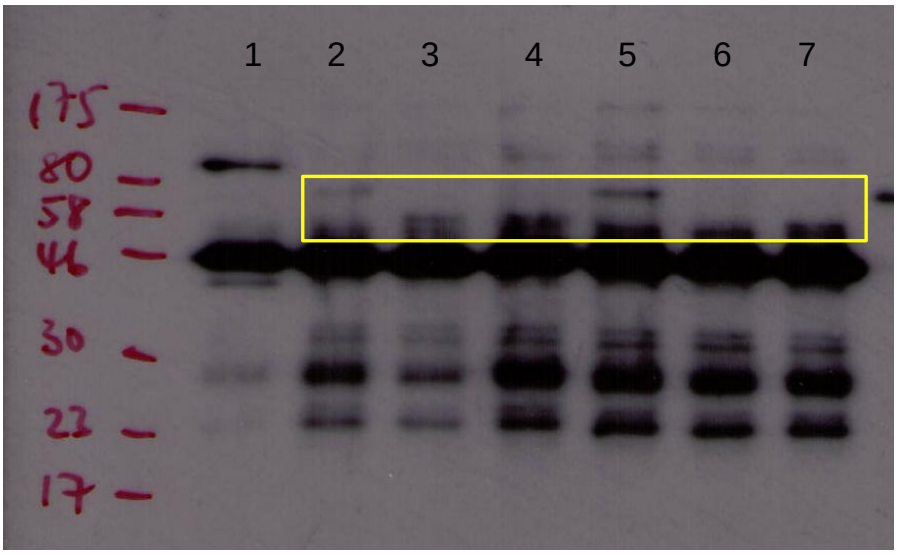

Lane	Protein G	MEMG9 mAb	Supernatant
1	+	+	-
2	+	+	OriGBv1
3	+	+	OriGBv2
4	+	+	OriGBv2/β2m
5	+	+	B11GBv1
6	+	+	B11GBv2
7	+	+	B11GBv2/ β2m

Figure 5.10c

Western blot showing immunoprecipitation using anti-HLA-G (87G) bound to protein G beads. The primary detection antibody is biotinylated 4H84 (non-conformational anti-HLA-G). and the secondary antibody is streptavidin-HRP. Binding of B11GBv1 (predicted molecular weight of 73 kDa); and of ORIGBv2 and B11GBv2 proteins (predicted molecular weight of 62 and 60 kDa respectively) is seen. There is also very faint binding of ORIGBv1.

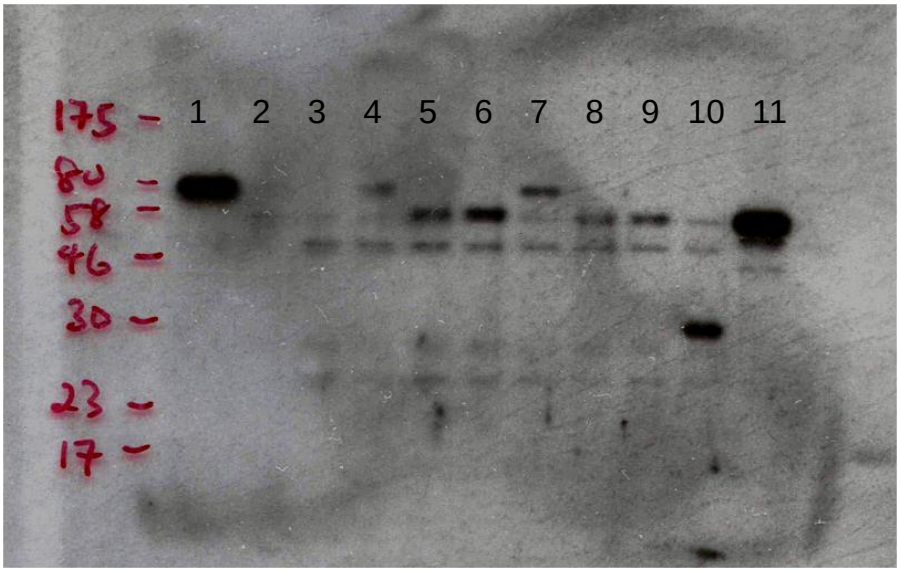

Lane	Protein G	87G	Supernatant
1	Neat OGBv1 supernatant		
2	+	-	B11GBv2/b2m
3	+	+	-
4	+	+	OGBv1 250ul
5	+	+	OGBv2
6	+	+	OGBv2/b2m
7	+	+	B11GBv1
8	+	+	B11GBv2
9	+	+	B11GBv2/b2m
10	+	+	sol HLA-G/b2m
11	Neat B11GBv2/b2m supernatant		

Figure 5.10d

Western blot showing immunoprecipitation using anti-HLA-G (MEMG/9) bound to protein G beads. The primary detection antibody is biotinylated 4H84 (non-conformational anti-HLA-G). and the secondary antibody is streptavidin-HRP. Binding of B11GBv1 (predicted molecular weight of 73 kDa); and of ORIGBv2 and B11GBv2 proteins (predicted molecular weight of 62 and 60 kDa respectively) is seen.

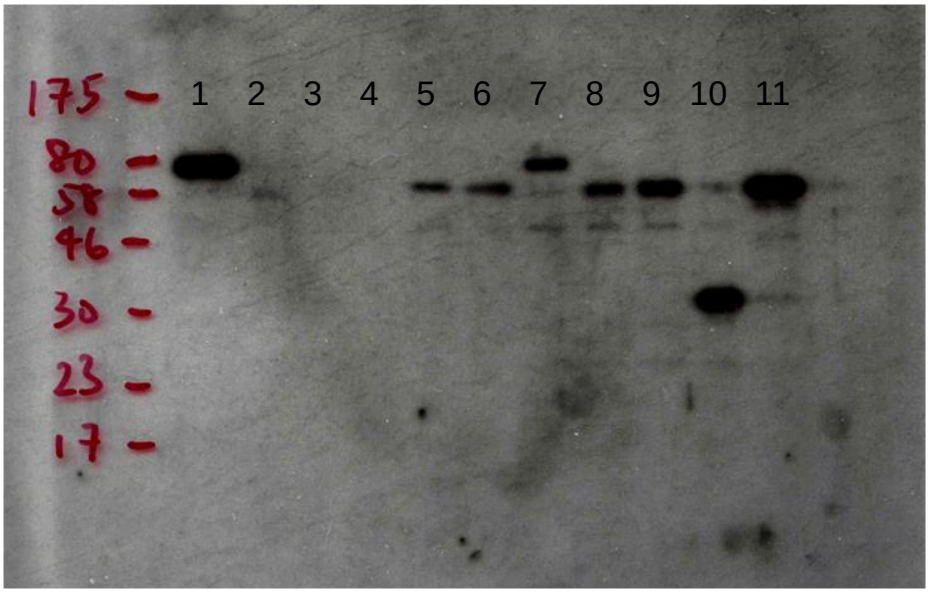

Lane	Protein G	MEMG/9	Supernatant
1	Neat OGBv1 supernatant		
2	+	-	B11GBv2/b2m
3	+	+	-
4	+	+	OGBv1 250ul
5	+	+	OGBv2
6	+	+	OGBv2/b2m
7	+	+	B11GBv1
8	+	+	B11GBv2
9	+	+	B11GBv2/b2m
10	+	+	sol HLA-G/b2m
11	Neat B11GBv2/b2m supernatant		

Figure 5.11a

0.8% agarose gel showing the products of the ORIGBv2 PCR reaction. The expected product of 1761 bp can be seen in lanes 2 and 3.

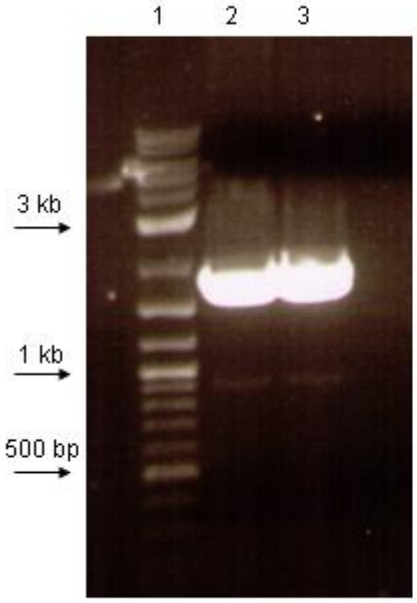

Lane	
1	DNA ladder
2	Products of ORIGBv2 PCR reaction
3	

Figure 5.11b

0.8% agarose gel showing the products of the B11GBv2 PCR reaction. The expected product of 1758 bp highlighted by the yellow box, was extracted from the gel for further cloning.

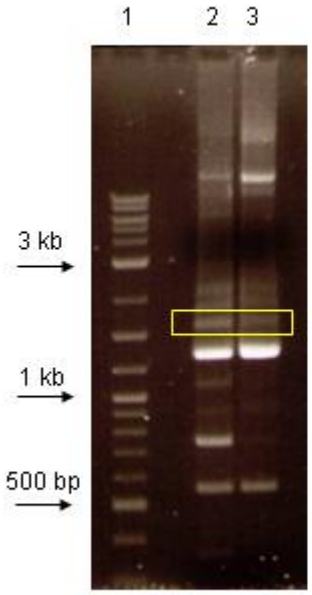

Lane	
1	DNA ladder
2	B11GBv2 PCR reaction, standard buffer
3	B11GBv2 PCR reaction, GC rich buffer

Figure 5.12a

Overlay histogram showing binding of cGBOD to LILRB2 transfected K562 cells. The detection antibody is goat anti-mouse FITC. The red histogram is detection antibody alone and the blue histogram is staining with cGBOD followed by detection antibody.

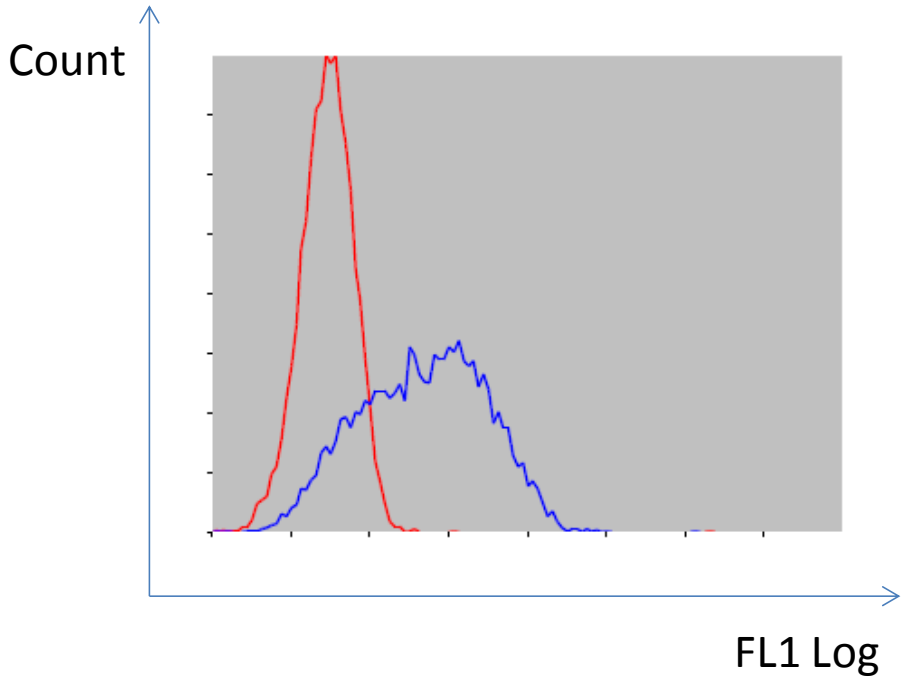

Figure 5.12b

Overlay histogram showing binding of cGBOD to HLA-A2 transfected K562 cells. The detection antibody is anti-HLA-G (87G) PE. The red histogram is detection antibody alone and the blue histogram is staining with cGBOD followed by detection antibody.

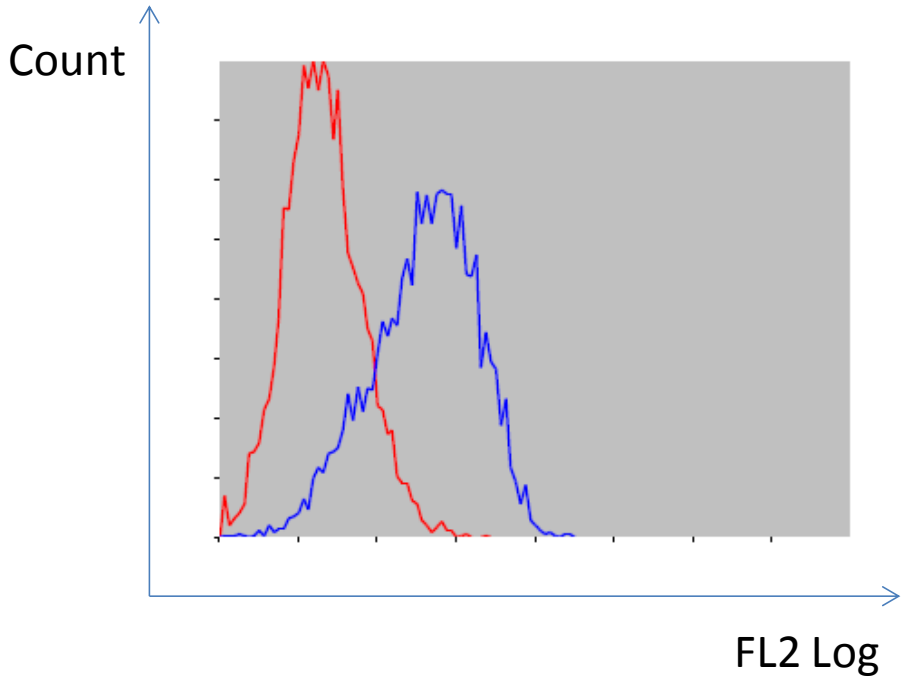

Figure 5.12c

Overlay histograms showing binding of cGBOD to lymphocytes and monocytes (identified by light scatter on flow cytometry) in PBMCs of HLA-A2 positive and HLA-A2 negative subjects. The red histogram represents detection antibody alone and the blue histogram represents addition of cGBOD followed by detection antibody. Binding was seen to monocytes in both HLA-A2 positive and negative subjects, as monocytes express the ligands for HLA-G. cGBOD binding was only seen in lymphocytes of HLA-A2 positive individuals due to interaction of the anti-HLA-A2 portion of the molecule.

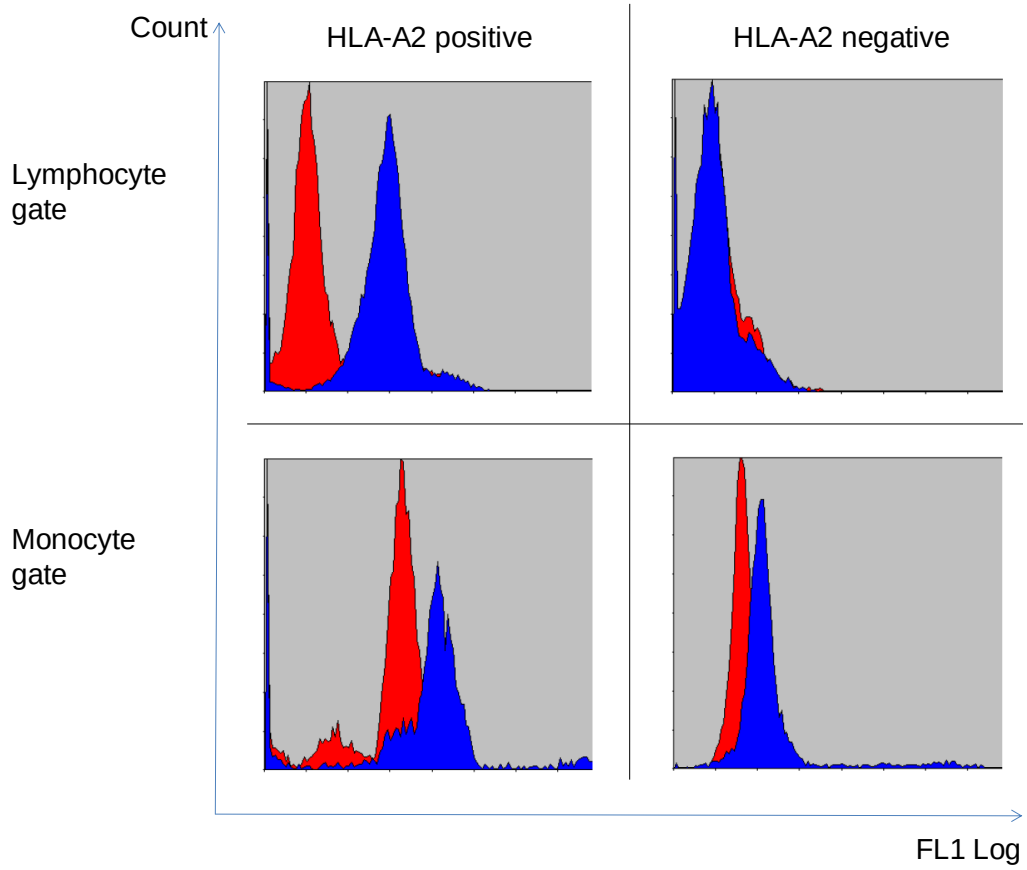

Figure 5.12d

Overlay histograms showing cGBod (at different ratios) binding to K562-HLA-A2 transfectants (top) with an 87G-PE detection antibody; and binding to K562-LILRB2 transfectants (bottom) with an goat anti-mouse FITC detection antibody

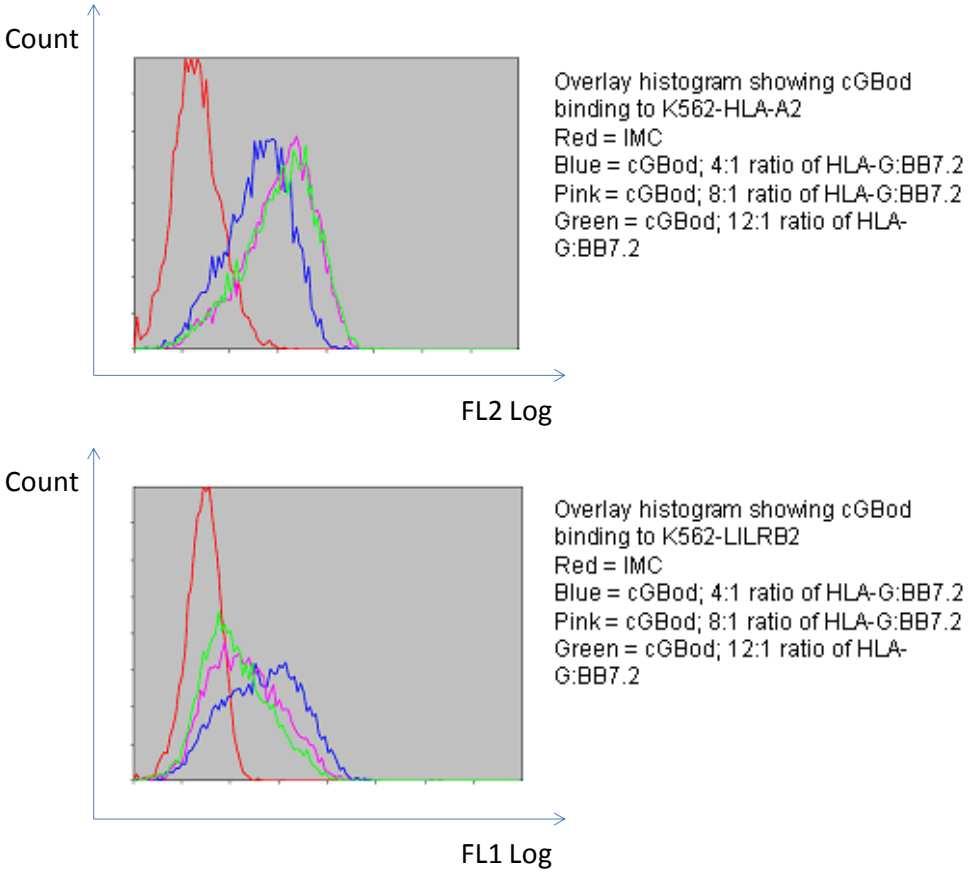

Chapter 6: Functional assays to determine the effect of ligation of LILRB2 on cellular responses

Background

Engagement of the LILR molecules has been shown to influence the development of dendritic cells, early activation events in monomyelocytic cells, T cell responses and NK cell cytotoxicity. Some of these effects have been demonstrated with monoclonal antibodies directed against LILRB1, LILRB2 and LILRB4. (39;40;42) In addition, HLA-G (in various formats) has also been shown to have an effect on immune responses following engagement of its cognate ligands (which include LILRB1 and LILRB2). (39;40)

In the original paper describing LILRB1, Colonna et al showed that LILRB1 was involved in downregulation of intracellular calcium mobilisation in monocytes and B cells, reduction in NK and T cell cytotoxicity as well as reduction in serotonin release from LILRB1-trasnfected rat basophilic leukaemia (RBL) cells. (39) Cytosolic calcium was measured using Indo-1 AM and calcium released was triggered by cross-linking of MHC I on B cells (using the mAb HP-1F7) or MHC II on monocytes (using the mAb 3.8B1). Co-cross linking of LILRB1 (using the mAb HP-F1) resulted in downregulation of calcium mobilisation.

Fanger *et al* have also shown that co-ligation of CD64 (FcγRI, using the mAb 32.2) and LILRB1 (using the mAbs M402 and M405) resulted in inhibition of intracellular calcium mobilisation and tyrosine phosphorylation of associated Fc

receptor γ chain and Syk molecules, compared with crosslinking of CD64 alone. (44)

LILRB1-transfected RBL cells were activated to release serotonin using plate bound mouse IgE (acting through FcεRI). Co-cross linking of LILRB1 using HP-F1 bound to the plate resulted in clear reduction in serotonin release. (39)

Addition of HP-F1 (directed against LILRB1) resulted in restoration of lysis of HLA transfected 721.221 cells by an NK cell line (NKL). (39) Lysis was restored in HLA-B*2702, B*2705 and B*5101 transfectants with addition of HP-F1 and restored in HLA-A*0301, B*0702 and G1 transfectants in combination with an anti-CD94 mAb. These data were further tested in reverse ADCC experiments, where the FcR^+ murine mastocytoma cell line P815 was killed by NKL in the presence of an anti-CD16 mAb which binds FcR on the target cell line and CD16 on the effector cell line. Addition of HP-F1 resulted in reduction of target lysis, hence acting as a ligand for LILRB2 in this instance and blocking CD16 activation.

$CD8^+$ T cell cytotoxicity was also restored by addition of HP-F1. HP-$F1^+$ T cells were sorted and cloned and then selected for expression of Vβ2 which binds the toxic shock syndrome toxin-1 (TSST-1) superantigen. Cytotoxicity was tested using 721.221 cells with or without a HLA-B*2705 transfection, pulsed with different concentrations of TSST-1. One of the T cell clones efficiently killed TSST-1 pulsed 721.221 cells but not the HLA transfected 721.221 cells.

Cytotoxicity against the transfected cells was restored by addition of HP-F1 mAb Fab fragments. (39)

Addition of the anti-LILRB1 mAb, HP-F1 has also been shown to result in an increase of interferon-γ production by NK-92 $CD56^{+}$ cells after binding to HLA transfected 721.221 cells presumably by inhibition of the LILRB1-HLA interaction. (223) Fresh NK cells were also shown to downregulate interferon-γ production after exposure to polyI:C and suboptimal doses of IL-12 , when incubated in HP-F1 coated wells, although this effect was not seen with NK-92 cells. (223)

The anti-LILRB1 mAb, GHI/75 has been shown to block the interaction of recombinant HLA-G5 and G6 with LILRB1 on U937 cells resulting in reduction in TGFβ secretion. (224) However, a similar effect was not demonstrated when the anti-LILRB2 mAb, 27D6 was used, although LILRB2 is expressed on U937 cells.

LILRB1 ligation (with HP-F1 and protein G for cross linking) during the development of GM-CSF/IL-4 monocyte derived DCs *in vitro* has been shown to result in modulation of DC maturation and function. (99) DCs treated with anti-LILRB1 had high levels of CD14 and low levels of CD1a, no CD83 and low levels of CD86. In addition, they also resulted in a reduced MLR when incubated with CFSE labelled allogeneic lymphocytes. (99)

Similar to LILRB1, co-ligation of LILRB2 (with the mAb 42D1) has also been shown to reduce intracellular calcium mobilisation in DCs triggered by FcγRII (CD32, with mAb IV.3) and HLA-DR (mAb 3.8B1). (40) Ligation of LILRB2 on transfected RBL cells also resulted in a reduction of serotonin release, although the RBL cells were activated by incubation with HLA I transfected or untransfected 721.221 cells coated with TNP and mouse anti-TNP IgE. (40)

Co-ligation of LILRB4 on monocytes and macrophages also resulted in a reduction in intracellular calcium mobilisation. (42) In this instance, calcium flux was triggered by engagement of CD11b (with mAb 44aabc), MHC II (with mAb B73.1) or (CD16, with mAb 3.8B1). Cella *et al* also showed that tyrosine phosphorylation in monocytes stimulated with anti-HLA DR was reduced with co-ligation with anti-LILRB4. (42) Lu *et al* confirmed a similar finding in THP-1 cells, where co-ligation of CD64 (FcγRI) with LILRB4 using mAbs resulted in a 80to 90% reduction in protein tyrosine phosphorylation seen on Western blot. (225) They further established that LILRB4 co-ligation specifically reduced protein tyrosine phosphorylation of the proximal signalling molecules, Lck and Syk, the downstream signalling molecules, LAT and ERK as well as the adaptor protein c-Cbl. However, protein tyrosine phosphorylation of α-actinin-4 was not reduced, indicating selectivity in LILRB4 mediated regulation of tyrosine dephosphorylation.

Engagement of LILRB4 has also been demonstrated to possibly have downstream functional effects on monomyelocytic cells. Lu et al also showed inhibition of TNF-α production by LILRB4 co-ligation in both THP-1 cells and

monocytes activated by engagement of CD64. (225) Brown *et al* showed that ligation of LILRB4 (with the mAb ZM3.8 and protein G) during the development of GM-CSF/IL-4 monocyte derived DCs (both immature and LPS-matured) resulted in upregulation of CD86. (177) There was no change in CD1a, CD80 or CD83. However, this had no effect on a MLR with allogeneic $CD4^+$ naïve T cells. LILRB4 ligation also resulted in increased IL-10 and reduced IL-8 production by macrophages.

HLA-G has also been shown to have various immunosuppressive properties both *in vivo* and *in vitro*. As previously discussed, HLA-G binds to LILRB2 and LILRB4 and is the highest affinity natural ligand known for these molecules. (14) It also interacts with KIR2DL4 and CD8. (134;135)

HLA-G has been shown *in vitro* to have effects on allo-proliferative responses, cytotoxicity and cytokine secretion. Experiments have been done both by transfecting cells with HLA-G or by addition of some form of soluble HLA-G to culture medium, which is more directly comparable to the experiments performed in this chapter.

In various published experiments, HLA-G has been transfected into 721.221, K562 or C1R cells. Riteau *et al* transfected HLA-G into 721.221 and K652 cell lines. (207) HLA-G transfected 721.221 cells were used as stimulator cells with PBMCs as responder cells; and reduced allo-proliferation when compared to vector only transfectants. Furthermore, HLA-G transfected K562 cells were able to reduce all-proliferation in an MLR with 721.221 cells as the stimulators and

PBMCs as the responders. (207) Bainbridge et al demonstrated that C1R cells transfected with HLA-G (rather than HLA-A2) also reduced the allo-proliferative response of PBMCs in an MLR. (226) Apps *et al* further extended this work to try to determine which cells were primarily affected by HLA-G in the reduction of allo-proliferative responses. (133) They tested the effect of co-culturing HLA-G transfected 721.221 with MoDCs. This did not inhibit the upregulation of HLA-DR, co-stimulatory molecules (CD40, CD80, CD86) or the activation marker CD83, but did result in an increase in IL-6 and IL-10 (but not IL-8 or TNF-α) secretion. Additionally, they did one-way MLR reactions with PBMCs as responders and 721.221 cells as stimulators. HLA-G transfection resulted in reduced proliferation, which could be reversed with the addition of anti-LILRB1/LILRB2 antibodies (HP-F1, M401 and M402). They then tested this again with depletion of HLA-DR^+ cells (to remove APCs) and found that there was no additional inhibitory effect with HLA-G transfected stimulator cells, suggesting that most of the HLA-G effect was on the indirect stimulation of T cells by responder APCs. (133)

Soluble HLA-G has also been shown to have immunomodulatory effects, similar to cell membrane-bound HLA-G, consistent with the hypothesis underpinning development of the G-body. Kapasi *et al* showed that HLA-G (isolated from placental tissue using anti-HLA-G, 4H84 mAb and anti-β2m affinity columns) modulated cytotoxic T lymphocyte activity at different doses, although in their experiments allo-proliferative responses were not affected by HLA-G. (227) Low doses of HLA-G (0.01 to 0.05 μg/ml) resulted in increased cytolytic activity whereas higher doses (>1 μg/ml) had a suppressive effect. There was however,

no effect seen when HLA-G was added to cells that had already been primed. They also found that IL-10 was increased and TNF-α and IFN-γ were reduced with decreased allo-CTL responses and that the converse was true when there was increased allo-responses. (227)

Le Friec *et al* generated soluble HLA-G by transfecting HLA-G5 into LCL cells, and purified the supernatant using anti-HLA I (W6/32 mAb) columns. (228) The purified HLA-G5 was then incubated with MoDCs during their development and incubated with allogeneic $CD3^+$ T cells. Again, there was no change in maturation markers with addition of HLA-G5, but there was a reduction in allo-proliferation in a proportion of MLR responses (4/17 cases showed a strong reduction in proliferation, 5/17 showed a weak reduction and 8/17 showed no reduction). (228) Naji *et al* used recombinant HLA-G5 produced in SF9 insect cells, supernatant from M8 cells transfected with HLA-G1 or G5 or HLA-G5 isolated from liver-kidney transplant patient's plasma; they also demonstrated a reduction in allo-proliferative MLRs (using LCL as stimulator and PBMCs as responder cells) which could be blocked with addition of anti-LILRB1 or anti-LILRB2 antibodies. (146) In addition, they demonstrated that blocking FasL restored HLA-G induced inhibition, suggesting that this pathway was important in the process.

Addition of HLA-G tetramers has been shown to affect the development of MoDCs *in vitro*. Liang et al have shown a reduction in HLA-DR and costimulatory molecules (CD80, CD86) with addition of HLA-G tetramers. (229) Subsequent to that, Ristich *et al* demonstrated that addition of HLA-G tetramer

treated MoDCs to a MLR resulted in the generation of anergic and immunosuppressive T cells, with a reduced population of $CD4^+CD25^+$ T cells and raised CTLA-4^+ cells in that population. (24) These cells were also more likely to produce IL-10. $CD4^+$ T cells also showed a reduction in spontaneous and anti-CD3 induced proliferation. There was also an increased population of immunoregulatory $CD8^+CD28^-$ T cells with an increased capacity for IL-10 production. Ristich *et al* also looked at gene profiles in HLA-G treated MoDCs and found that 11 genes (most of which were downregulated) were specifically affected. (24) These genes were mainly involved in remodelling of specialized antigen-processing compartments and in MHC Class II restricted antigen presentation.

Experiments have also been done to try to improve the potency of soluble HLA-G as an immunosuppressive molecule. In view of the increased potency of dimeric HLA-G, Zhong *et al* made a construct comprising IgG-Fc and soluble HLA-G in place of the variable regions of the IgG molecule, resulting in a divalent molecule. (230) They then demonstrated that compared to monomeric HLA-G, the divalent molecule had a greater inhibitory effect on both $CD4^+$ and $CD8^+$ T cells in an MLR using irradiated T1 cells as stimulators and non-adherent PBMCs as responders. Additionally, the dimeric HLA-G molecule was also shown to suppress cytotoxic responses more than monomeric HLA-G, thought to be due to upregulation of LILRB1 on cytotoxic $CD8^+$ T cells. (230)

In summary, it is reasonably clear that engagement of the LILRB molecules does result in inhibition of cellular responses – although the magnitude of the

responses does vary between the subjects tested. The published data, however, has yet to address exactly how these molecules vary the magnitude of their influence on cellular immune responses. As these molecules are relatively non-polymorphic structurally, one possible explanation is that the cell surface density of expression is responsible for modulating their immunological influence.

The experiments in this chapter were undertaken to determine if the magnitude of response to LILR engagement was influenced by the density of surface expression of these molecules. First of all, experiments were undertaken to confirm that engagement of the LILR molecules did modulate immunological responses. Subsequently, the magnitude of LILR expression on the cell surface was compared with the effect on the immunological response being tested to determine if there was any relationship between the two.

In this chapter, development of the assays used to test the effect of LILR engagement (by anti-LILRB2 monoclonal antibodies and by the G-body) is described. LPS (E Coli) and ssRNA are used to induce cytokine secretion from purified monocytes and the effect of modulation with anti-LILRB2 antibodies tested. Additionally, modulation of lymphocyte proliferation by anti-CD3/28 beads, anti-CD3 or SEB is also used to determine if the G-body has any functional effect and whether there is a difference between HLA-A2 positive and HLA-A2 negative individuals.

The variation in the effect on the functional assays is then tested in different individuals; and the effect of the anti-LILRB2 monoclonal antibodies correlated with the cell surface expression of LILRB2.

The anti-LILRB2 monoclonal antibody 42D1 was used for these experiments as proof of principle that LILR ligation would have functional immune effects as there was availability of a large amount of this particular antibody from the hybridoma. Although, there is more published functional data available on the effects of LILRB1 engagement, the hybridoma for this was not available and obtaining significant quantities of an anti-LILRB1 mAb for functional experiments was not feasible. In addition, despite there being more published data on LILRB1 compared to LILRB2, overall there was still a relative paucity.

It should be noted that the exact functional effect (with regard to whether they are agonistic or blocking) of these antibodies is not completely certain. In the original paper describing the discovery of LILRB2 and generation of 42D1, these antibodies were shown to abolish intracellular calcium flux when co-ligated (using a secondary antibody) with the stimulatory anti-FcγRII or anti-HLA-DR monoclonal antibodies in dendritic cells. (40) The 42D1 antibody has also been shown to enhance HLA-G tetramer staining. (221) However, the same antibody has also been shown to have blocking properties, in that addition of 42D1 to LILRB4^{+} LILRB2^{+} tolerogenic DCs results in return of their stimulatory capacity. (23) Similar results have been seen with anti-LILRB1 mAbs where the same mAb could result in activation or blockade of receptor function, depending on how it was used.

Effect of anti-LILRB2 antibodies on LPS and ssRNA induced cytokine secretion

The effect of LILR ligation on TLR-induced responses was tested as both sets of molecules function as part of innate immunity, with the TLRs primarily recognising microbial products and the LILRs probably recognising self. In addition, the LILR (and PIR) pathway has been shown to have effects on TLR stimulation. LILR and PIR-B receptors have been shown to bind *S aureus* with TLR2 and result in IL-10 release. (7) Inhibition of TLR2 signalling has also been shown to be impaired in PIRB-/- mice with exaggerated Th2 responses and impaired DC maturation. (60) The importance of LILR and PIR signalling as a counterbalance to TLR activation is also seen in PIRB-/- mice which are more prone to lethal Salmonella infection; interestingly, due to enhanced susceptibility rather than an excessive immune response. (81) Engagement of LILRA2 has been shown to result in reduced IL-12 production by TLRs in the context of leprosy. (161) Signalling through TLRs has also been shown to affect LILR expression. (177;231) Exposure to live and heat-inactivated Salmonella results in upregulation of LILRB4, thought to be mediated by LPS. (177) LILRA2 has been shown to inhibit TLR4 activity (232) and LILRA4 has been demonstrated to regulate TLR7/9 function in PDCs. (29)

Purified monocytes were chosen as the cellular target as these cells expressed LILRB2 and were abundant, allowing easy testing in multiple individuals. Another consideration in design of the assay was the selection of an assay that

had a quantitative (or at least semi-quantitative) readout to allow more significant comparison with the cell surface expression levels of the LILR molecules. For this reason, ELISA measurement of cytokines was chosen.

Optimisation of the concentration of antibody and stimulus for use in the assay

A range of TLR ligands were initially tested to determine if they resulted in secretion of IL-6 from monocytes. The range of stimuli used included poly-I:C (TLR3), LPS (TLR4), imiquimod (TLR7), ssRNA40/LyoVec (TLR8) and CpG (ODN2006, TLR9). This showed that only LPS and ssRNA induced secretion of IL-6. (Figure 6.1)

In view of this, LPS and ssRNA were then chosen for use in further optimisation experiments. Experiments were initially conducted to determine if there was any reduction in cytokine secretion when 42D1 was added compared to a rat IgG2a isotype matched control. This was done with a single stimulus (LPS) with cytokine levels measured for a single cytokine (IL-6) as a pilot experiment. This showed that there was a reduction in IL-6 secretion with addition of anti-LILRB2 antibody compared to the rat IMC. There was a ~20% reduction in IL-6 secretion at a mAb concentration of 1 μg/ml, with a reduction of 40 to 45% at concentrations between 10 to 50 μg/ml. (Figure 6.2) This confirmed that engagement of LILRB2 with the 42D1 antibody did result in suppression of IL-6 concentration.

Subsequently, experiments with a range of concentrations of antibody, TLR ligand and monocyte numbers were conducted to determine the optimum conditions for testing of the effect of 42D1 in a larger group of individuals. On the basis of these experiments (Figure 6.3), the experimental conditions for use in a larger group of individuals was set at 20,000 purified monocytes per well, with addition of 50 μg/ml of anti-LILRB2 or IMC and stimulated with either 1ng/ml of LPS or 1 μg/ml of ssRNA.

Results of anti-LILRB2 antibodies on TLR ligand-induced cytokine secretion in 5 individuals

The assay was then performed on five healthy individuals, and this showed variation in levels of cytokine suppression with addition of 42D1 between different cytokines, different stimuli and between the individuals tested. (Figures 6.4 and 6.5)

There was suppression of all cytokines tested (IL-6, IL-8, IL-10 and TNF-α) when LPS was used as the stimulus. (Figure 6.4a) However, when ssRNA was used as the stimulus, there was no suppression of TNF-α, unlike the other 3 cytokines tested. (Figure 6.4b)

When comparing the different individuals tested, it can also be seen that there was quite a wide degree of variation both in the baseline cytokine secretion and in the reduction of cytokine secretion if 42D1 had been added. (Figure 6.5b)With LPS stimulation and addition of 42D1, there was a reduction in IL-6 of 13 to

68% (mean 41%), in IL-8 of 5 to 31% (mean 18%), in IL-10 of 39 to 90% (mean 66%) and in TNF-α of 6 to 54% (mean 28%). When ssRNA was used as the stimulus, there was a similar reduction in IL-6 (mean 45%, range 25 to 58%) and a slightly greater reduction in IL-8 (mean 25%, range 10 to 37%). There was slight less reduction in IL-10 (mean 52%, range 43 to 80%, after exclusion of one significant outlier). A more significant difference seen was the lack of any suppression of TNF-α secretion by 42D1 when ssRNA was used as the stimulus, suggesting that an alternative pathway (not affected by LILRB2 inhibition) of activation compared to LPS might be involved.

These findings confirmed that there was variation in a functional response following engagement of LILRB2; and consequently, it would be useful to determine if the expression levels of LILRB2 correlated with this functional response.

Relationship to LILRB2 expression levels

Cellular surface expression levels of LILRB2 were also measured on purified monocytes at baseline. Following this, the amount of cytokine suppression by 42D1 was correlated with monocyte cell surface expression levels. (Figure 6.6) This, however, did not show any significant relationship. Baseline monocyte LILRB2 expression levels were similar for 4 of the subjects with one subject having markedly lower levels (<50% compared to the rest). However, the single subject with lower LILRB2 expression levels did not have functional data results significantly different from the rest of the group.

Part of the reason for the lack of relationship between LILRB2 expression levels and functional effects might be due to the small numbers of subjects used; and consequently, it would have been interesting to determine if a correlation would have been detectable in a larger group of subjects.

Effect of the chemically conjugated G-body in functional studies

Effect of the chemically conjugated G-body on lymphocyte proliferation assays

In order to determine if the chemically conjugated G-body had any effect on lymphocyte proliferation, initially more straightforward experiments using single defined stimuli on isolated PBMCs were undertaken. The cGBOD and appropriate controls (i.e. HLA-G tetramers, BB7.2, HLA-G tetramers and BB7.2 combined without streptavidin linking, and mouse IgG2b as isotype matched control for BB7.2) were added to PBMCs (isolated from buffy coats) stimulated with an anti-CD3 monoclonal antibody (OKT3), anti-CD3/CD28 beads or SEB. PBMCs were incubated for 4 days and tritiated thymidine was added 18 hours prior to the cells being harvested. To test whether the localisation by the anti-HLA-A2 monoclonal antibody had any effect, both cells that were HLA-A2 positive and HLA-A2 negative were used. In total, five HLA-A2 positive donors and two HLA-A2 negative donors were tested.

Effect of the chemically conjugated G-body in lymphocytes stimulated with anti-CD3/CD28 beads

When stimulated with anti-CD3/28 beads, addition of the cGBOD resulted in suppression of lymphocyte proliferation compared to untreated cells, although this effect was only seen in individuals who were HLA-A2 positive. This result was statistically significant compared to untreated cells and with the addition of HLA-G tetramers. (Figures 6.7) A similar suppression of proliferation was not seen in HLA-A2 negative individuals. (Figures 6.8) There was not much difference in proliferation seen when any of the other reagents (anti-HLA-A2, HLA-G tetramers or a combination of those two) were used in both HLA-A2 positive and negative individuals

Effect of the chemically conjugated G-body in lymphocytes stimulated with SEB

When stimulated with SEB, addition of the cGBOD resulted in more marked suppression of proliferation compared to that seen when cells were stimulated with anti-CD3/CD28 beads (average of 48% vs. 75% proliferation compared to control). Again, this finding was present in HLA-A2 positive individuals but not HLA-A2 negative individuals. (Figure 6.7 and 6.8)

With SEB stimulation, suppression of proliferation was also seen with HLA-G tetramers and HLA-G tetramers + anti-HLA-A2. The amount of suppression was slightly less than that seen with the cGBOD, although the differences were not

significant. Again, this suppression was only seen in HLA-A2 positive individuals.

Effect of the chemically conjugated G-body in lymphocytes stimulated with anti-CD3 mAbs

When stimulated with the anti-CD3 monoclonal antibody, addition of the cGBOD resulted in a similar degree of suppression of proliferation compared to stimulation with SEB, in HLA-A2 positive individuals. (Figure 6.7) There was also a similar effect with addition of HLA-G tetramers or HLA-G tetramers + anti-HLA-A2. In the HLA-A2 negative individuals tested, there was slight reduction in proliferation with addition of cGBOD, HLA-G tetramers or HLA-G tetramers + anti-HLA-A2, although less than that seen in HLA-A2 positive individuals, and not statistically significant. (Figure 6.8)

These experiments have been performed in a larger group of 26 HLA-A2 positive and HLA-A2 negative individuals each by Pedro Vieira, a post-doctoral researcher in the same laboratory. These results are similar to the ones done in a smaller group of samples and indicate that the cGBOD results in suppression of proliferation with all 3 stimuli (anti-CD3/CD28 beads, anti-CD3 and SEB). The reduction in proliferation was greater than that seen with HLA-G tetramers or HLA-G tetramer + anti-HLA-A2, and only present in HLA-A2 positive individuals. In the larger group of HLA-A2 negative individuals, suppression of the proliferative response was seen with the cGBOD, HLA-G tetramers and HLA-G tetramers + anti-HLA-A2, although these were a similar level with no

added suppression seen with the cGBOD (data not shown). These findings confirmed the added effect of combining anti-HLA-A2 into the same construct as HLA-G.

Effect of the chemically conjugated G-body on allo-proliferation reactions

As the cGBOD was shown to bind to the appropriate ligands on both ends (Chapter 5, Figure 5.12a to 5.12d), the molecule was tested in an MLR to determine if it had any functional properties. However, addition of the cGBOD (or its controls) did not have any difference in an MLR with HLA-A2 positive MoDCs as the stimulator population with two different sets of HLA-A2 negative responder PBMCs as the responder population. (Figure 6.9, representative of both experiments) It can be concluded that at least with this set of conditions, the cGBOD did not affect thymidine incorporation by T cells although various other parameters (e.g. whether different concentrations of G-body have an effect or whether cytokine production is different) remain to be tested.

Effect of anti-LILRB2 antibodies on lymphocyte proliferation assays

In view of the effect of the cGBOD and HLA-G tetramers on lymphocyte proliferation induced by anti-CD3/CD28 beads, anti-CD3 and SEB, the effect of anti-LILRB2 in the system was tested, both using the monoclonal antibody alone or with the addition of protein G as a cross linker. However, this did not show any significant reduction in proliferation (Figure 6.10).

Discussion

Cytokine suppression by anti-LILRB2 antibodies

The data showed that there was no significant relationship (in the 5 individuals tested) in the amount of cytokine suppression following ligation with anti-LILRB2 antibodies and the cell surface expression of these molecules. The most likely explanation for this is that there were an insufficient number of individuals to demonstrate any effect. Ideally, it would be preferable to conduct the analysis on a larger number of samples to increase the power of the study, but this was not plausible/practical/feasible.

It should be noted, however, that although there was significant variability in the suppression of cytokine secretion between the various individuals, there was a lot more homogeneity in the expression levels of LILRB2. This raises the possibility that cell surface density of the LILRB2 molecules does not play that significant a role in influencing downstream immune responses. Alternatively, the limited number of structural polymorphisms that exist may play a larger role than expected. Differences in the downstream signalling pathway or the TLRs being stimulated may also be involved in these differences.

In addition, although previously thought that these molecules interact with the non-polymorphic portions of the HLA molecule (the distal D1 and D2 regions of LILRB1 and LILRB2 interacting with the α3 domain of the MHC and β2m),

there is data showing that the LILR molecules possess different binding affinities for different HLA species. (5) The difference in the binding affinity was thought to be due to LILR interactions with the peptide groove on the MHC. These more recent findings suggest that the LILR molecules do interact with the polymorphic regions in the HLA molecule and that HLA haplotype might well influence the subsequent immunological responses following binding to the LILRs. (5) It is possible that *in vivo* this represents a more important mechanism by which the magnitude of the LILR response is controlled.

In the set of experiments involving cytokine secretion, purified monocytes rather than dendritic cells were used. It is possible that the effect of the anti-LILRB2 antibodies on dendritic cells (purified from whole blood) or monocyte-derived dendritic cells (using GM-CSF and IL4) might have been different to purified monocytes. This is potentially relevant as dendritic cells are the most potent antigen presenting cells and have the greatest influence on subsequent immune responses.

Although it is uncertain if the 42D1 clone used to bind the LILRB2 receptor is an agonistic or blocking antibody, the reduction in inflammatory cytokines (e.g. IL-6, IL-8 and TNF-α) would suggest that it is most likely agonistic, at least in the set of experiments here. However, it should also be noted that there was a concomitant reduction in IL10, which is typically seen as an immunosuppressive cytokine. In addition, there is data indicating that engagement of LILR molecules on DCs by HLA-G resulted in increased IL10 production. (133) The reason for these differences is not entirely clear although there are a number of differences

in the experiments conducted. The experiments done here used monocytes whereas published data was with monocyte-derived DCs. Furthermore, in this set of experiments, only LILRB2 was engaged, whereas the published data mainly used HLA-G, which would engage other molecules apart from LILRB2. Also, IL10 has been reported to result in secretion of proinflammatory cytokines when administered to humans. (233) Taken together, in this context, it is most likely that the anti-LILRB2 mAb is suppressing the total cytokine response to the TLR stimulus via LILRB2.

In addition, it should be noted that this set of experiments have not yet addressed the downstream effect of monocytes exposed to LILRB2 engagement during TLR ligand stimulation on the T cell compartment. In terms of next steps, further experiments exploring the effect of exposure of anti-LILRB2 treated monocytes or dendritic cells on T cells should be done.

Effect of the G-body on lymphocyte proliferation

The assays used to investigate the effect of the G-body on proliferation were used initially chosen for simplicity to gauge if more complicated experiments would be useful. These have shown that binding of the G-body to its ligands does reduce lymphocyte proliferative responses particularly in HLA-A2 positive individuals. In addition, the G-body had a greater suppressive effect in proliferation compared to either HLA-G tetramers alone or HLA-G tetramers mixed with anti-HLA-A2, suggesting that localisation of the G-body to the surface of HLA-A2 positive cells had added effects. The effects due to the G-

body were not seen in HLA-A2 negative individuals. Although only 5 HLA-A2 positive and 2 HLA-A2 negative individuals were tested in this set of experiments, a postdoctoral researcher working in the same laboratory (Pedro Vieira) has carried out the same set of experiments on a larger group of samples (26 each HLA-A2 positive and negative). These experiments have confirmed the findings in this small set of results.

The particularly exciting finding is that localisation of the G-body by means of the anti-HLA-A2 portion of the molecule significantly enhances its immunosuppressive effect, consistent with the hypothesis. The reasons and means by which this occurs is not clear, although several different mechanisms may be involved, with both cis- and trans- effects.

It is possible that the G-body binding to dendritic cells and other APCs may influence the stimulatory capacity of the APC by interaction with LILRB1 and LILRB2 on the cell surface in a cis- fashion. There could also be trans- interactions with T cells which express LILRB1; as suggested by the fact that stimulation with anti-CD3/28 beads which only rely on the T cell is also suppressed. The G-body binding to T cells is also likely to play a role as well both through a trans- interaction with APCs as well as cis- interactions with LILRB1 on the same cell.

Interestingly, the same effect is not seen in cells which are HLA-A2 negative suggesting that there is an additional benefit to localisation via the anti-HLA-A2 portion as opposed to the effect of pure HLA-G alone. It is possible that binding

of multiple G-body molecules on the cell surface allows localisation and delivery of a significantly greater immunosuppressive HLA-G signal. To an extent, this possibility is supported by the published data indicating that HLA-G multimers possess a greater effect compared to HLA-G monomers. (130;230)

However, when the G-body was tested in an allo-proliferative MLR, it had no effect when HLA-A2 positive MoDCs were used as stimulator cells with 2 different sets of HLA-A2 negative PBMCs as the responder populations. The reasons for this are not clear – although it should be noted that in published data, not all individuals have suppressed allo-proliferative and in one paper, approximately half the individuals tested did not show any reduction in an MLR when HLA-G was added. (228) In addition, a lower concentration of G-body was used in the allo-proliferation experiments (Gbody containing a concentration of 0.5 μg/ml mAb) compared to those used in the non-allo lymphocyte proliferation (Gbody containing a concentration of 2.5 μg/ml mAb) and anti-LILRB2 experiments (10μg/ml of anti-LILRB2 mAb). This might have contributed to the lack of suppression of the proliferative response. Furthermore, MoDCs are inherently an extremely potent stimulus and it might be that this was too strong for the G-body to overcome.

To further the work and test the potential usefulness of the G-body in a therapeutic setting, more complicated experiments involving different alloreactive donors should be performed to determine if there is any effect on proliferation, cytokine secretion, formation of memory T cells and the development of regulatory cells. It would also be useful to determine if exposure

to the G-body resulted in modification of antigen-presenting cells/T cells once the original stimulus was no longer present.

Experiments looking at the functional effect of the G-body on NK cytotoxicity and function, $CD8^+$ T cell cytotoxicity and early signalling events (e.g. calcium flux and protein tyrosine phosphorylation) would also be worth doing to fully elucidate the properties of the construct.

Summary

In summary, the data presented in this chapter does support published literature indicating that engagement of LILRB2 receptors results in immunosuppressive effects. The exact mechanisms underlying this remain to be fully worked out. However, the effect on TLR signalling pathways in monocytes has not been explored previously and the data showing cytokine suppression in purified monocytes does provide additional information about how LILRB2 influences immunological outcomes. The data showing differential suppression of cytokine secretion (due to TLR agonists) on engagement of LILRB2 has also not been described in published literature and warrants further exploration.

The data from the G-body experiments is also encouraging although further experiments (particularly involving allogeneic systems) need to be done to confirm its immunosuppressive properties. Initial data does suggest that the compound (and the theoretical concept) has significant translational potential. Although these G-body experiments were done with the chemically conjugated

compound, with more resources it would also be useful to determine the functional properties of the recombinant G-body although larger quantities would need to be produced prior to this being undertaken.

Figures

Figure 6.1

IL-6 secretion by purified monocytes after addition of a variety of TLR ligands. Bars represent the mean of 3 replicates and the error bars represent one standard deviation from the mean. The data represents the results of one experiment in one individual.

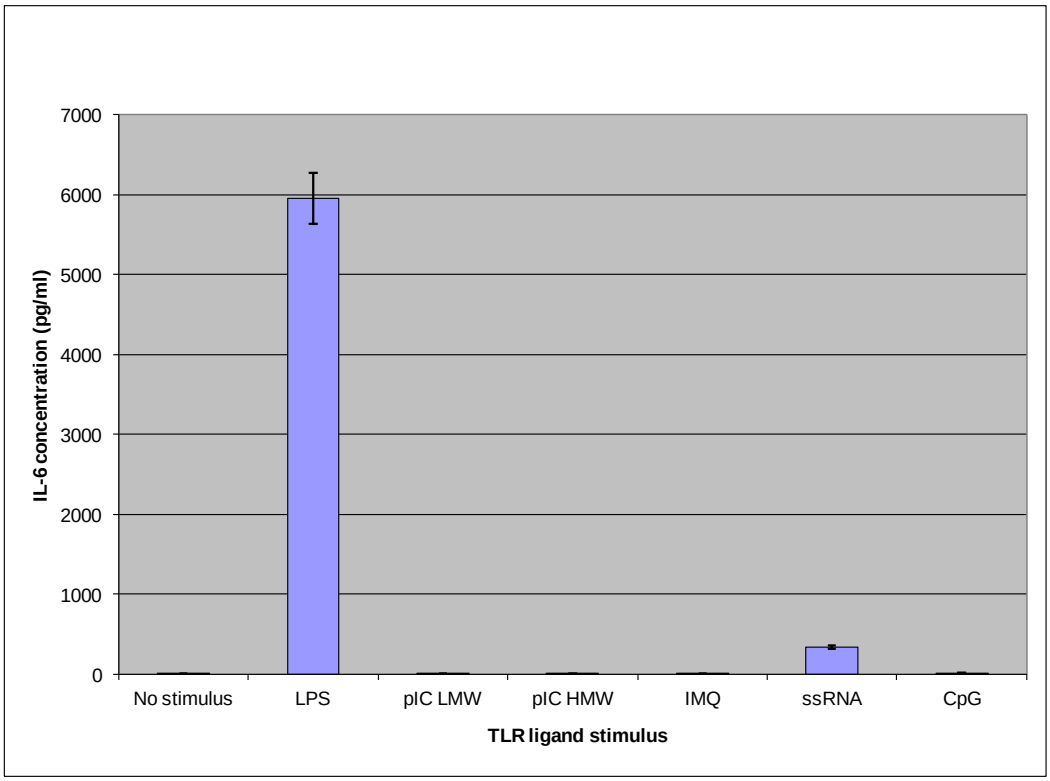

Figure 6.2

Effect of addition of anti-LILRB2 vs. rat IgG2a (as IMC) to IL-6 concentration secreted by purified monocytes stimulated with LPS.

The data represents the results of one experiment in one individual.

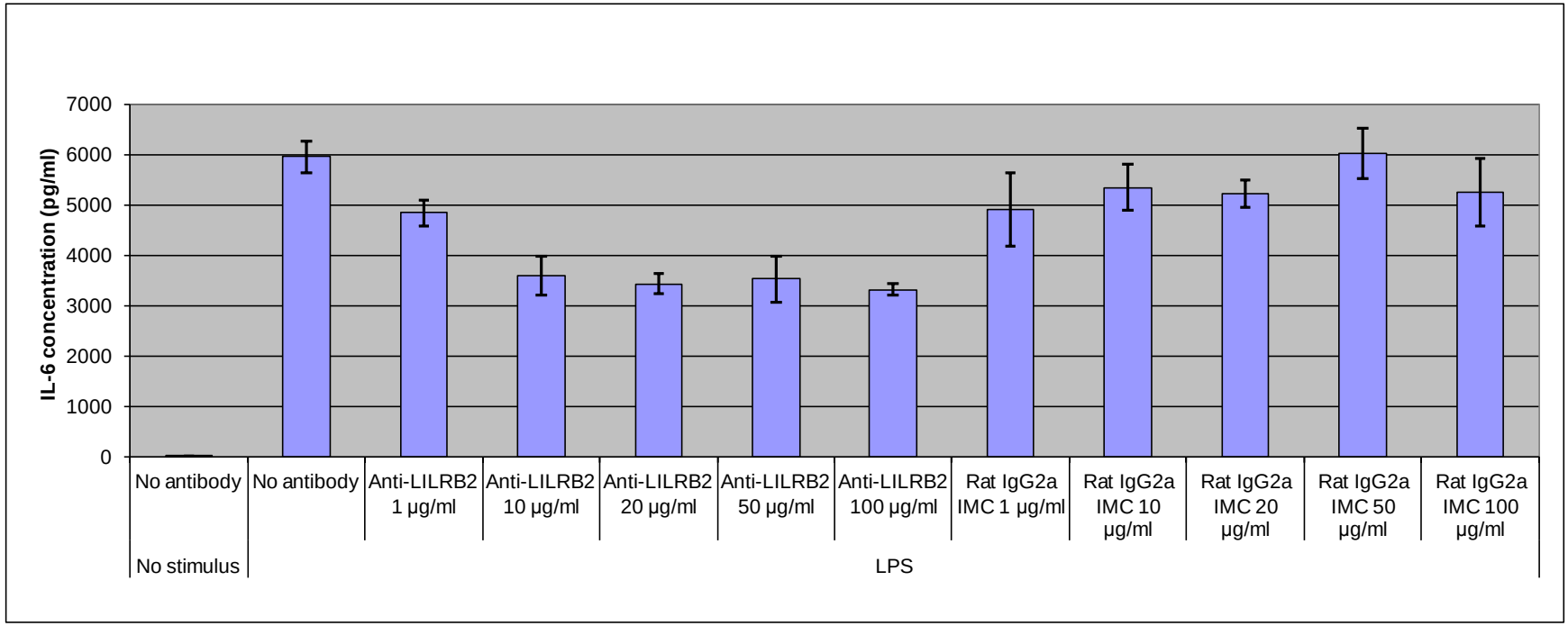

Figure 6.3

Titration experiments showing the effect of varying the dose of TLR ligand (LPS), antibody concentration and monocyte numbers on cytokine secretion (IL-6, IL-8, IL-10, TNF-α). The data represents the results of one experiment in one individual.

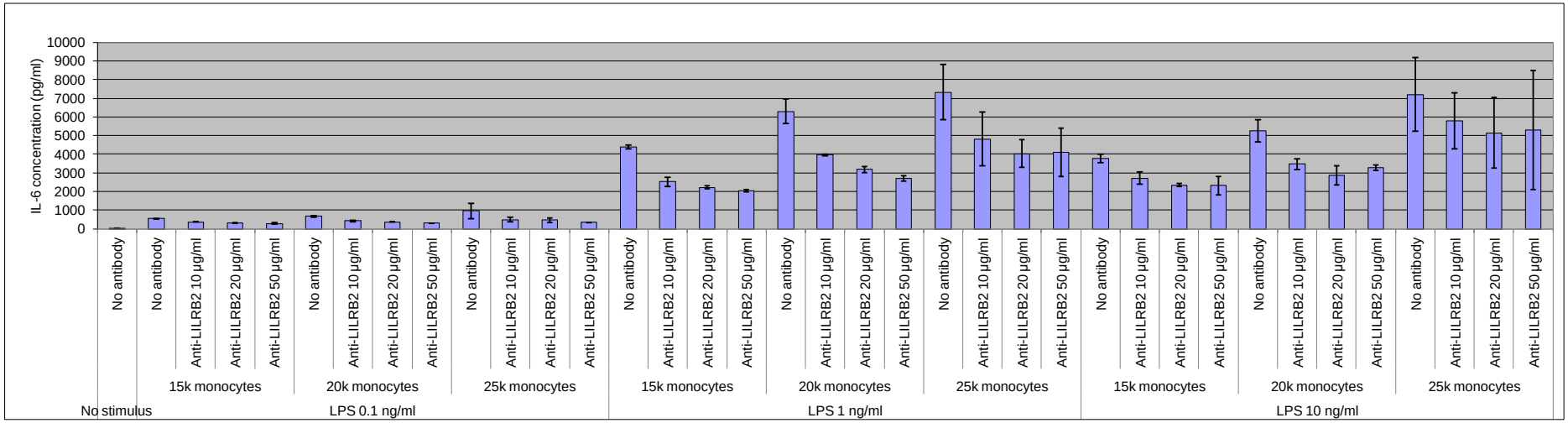
IL-6 concentration (pg/ml)
10000
9000
8000
7000
6000
5000
4000
3000
2000
1000
0
No antibody
Anti-LILRB2 10 µg/ml
Anti-LILRB2 20 µg/ml
Anti-LILRB2 50 µg/ml
15k monocytes
20k monocytes
25k monocytes
No stimulus
LPS 0.1 ng/ml
LPS 1 ng/ml
LPS 10 ng/ml

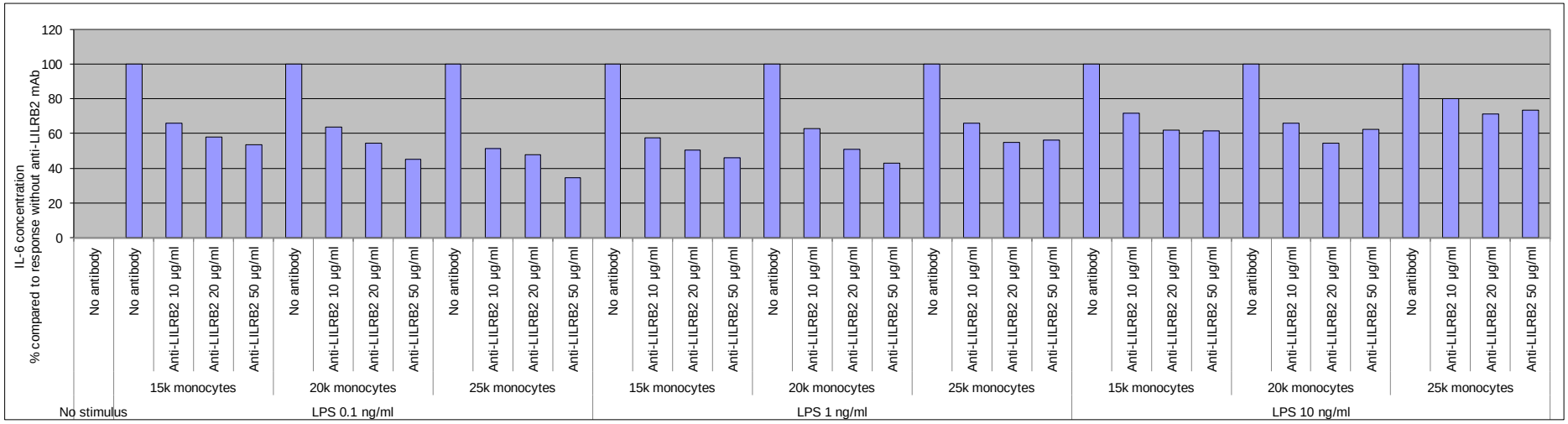
IL-6 concentration
% compared to response without anti-LILRB2 mAb
120
100
80
60
40
20
0
No antibody
Anti-LILRB2 10 µg/ml
Anti-LILRB2 20 µg/ml
Anti-LILRB2 50 µg/ml
15k monocytes
20k monocytes
25k monocytes
No stimulus
LPS 0.1 ng/ml
LPS 1 ng/ml
LPS 10 ng/ml

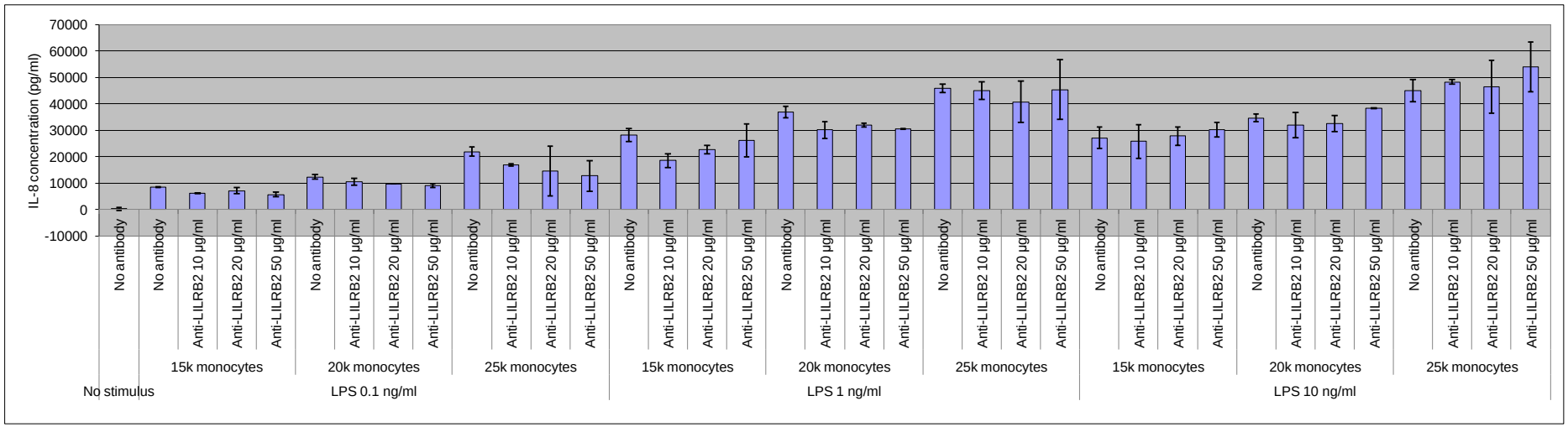
IL-8 concentration (pg/ml)
70000
60000
50000
40000
30000
20000
10000
0
-10000
No antibody
Anti-LILRB2 10 µg/ml
Anti-LILRB2 20 µg/ml
Anti-LILRB2 50 µg/ml
15k monocytes
20k monocytes
25k monocytes
No stimulus
LPS 0.1 ng/ml
LPS 1 ng/ml
LPS 10 ng/ml

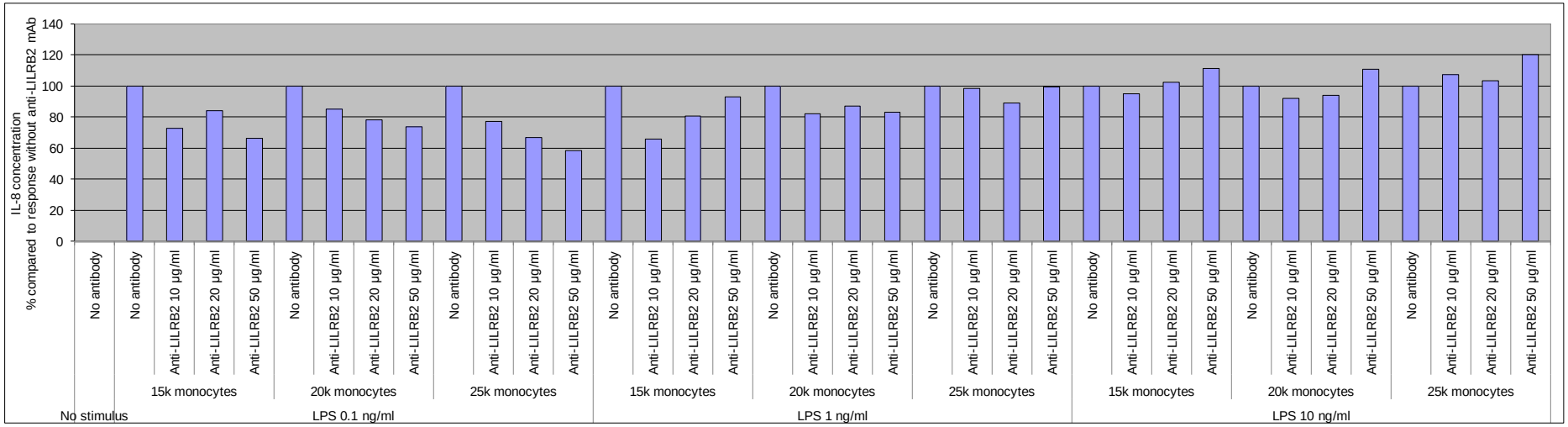
IL-8 concentration
% compared to response without anti-LILRB2 mAb
140
120
100
80
60
40
20
0
No antibody
Anti-LILRB2 10 µg/ml
Anti-LILRB2 20 µg/ml
Anti-LILRB2 50 µg/ml
15k monocytes
20k monocytes
25k monocytes
No stimulus
LPS 0.1 ng/ml
LPS 1 ng/ml
LPS 10 ng/ml

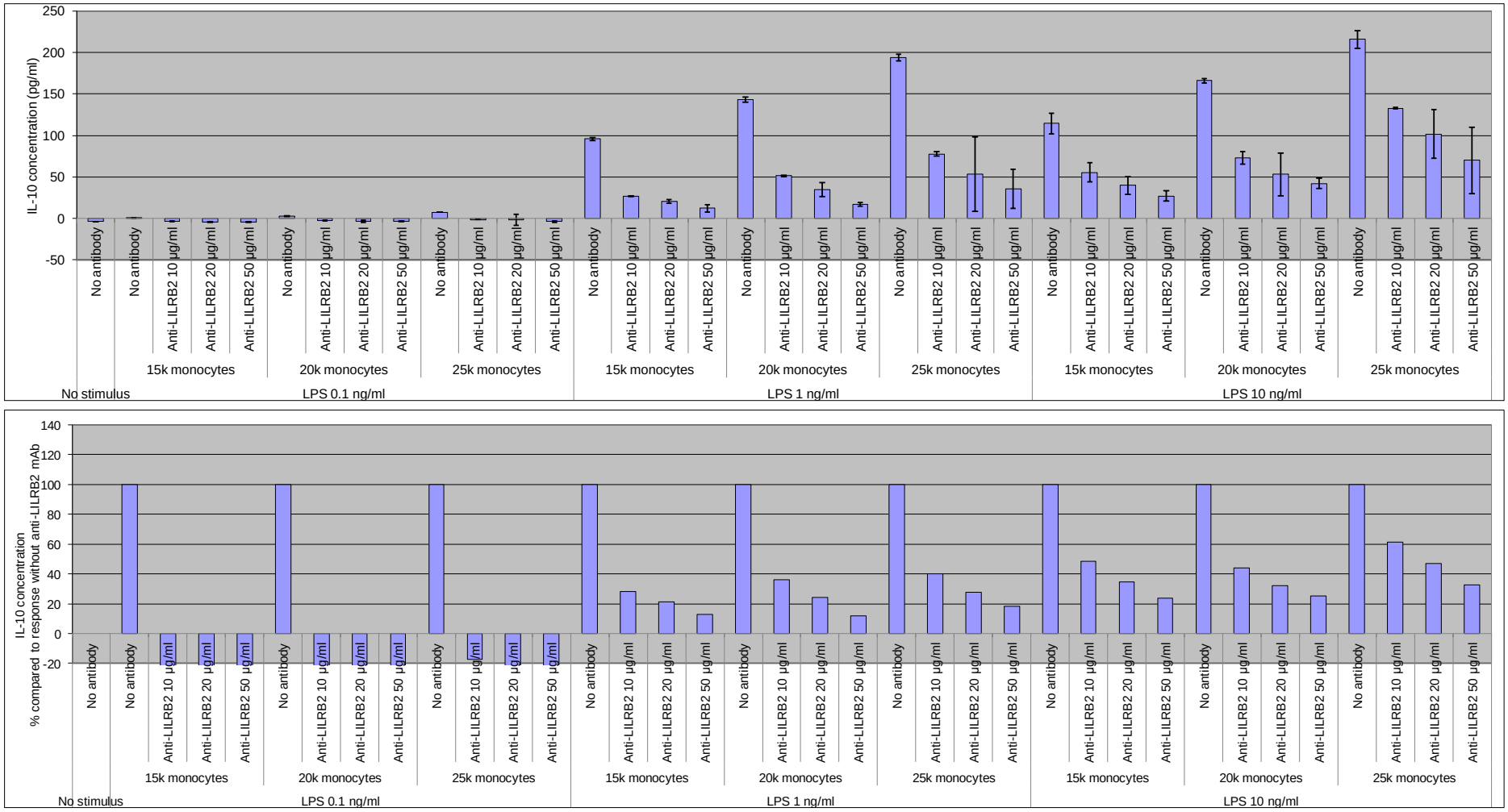
IL-10 concentration (pg/ml)
250
200
150
100
50
0
-50
No antibody
Anti-LILRB2 10 µg/ml
Anti-LILRB2 20 µg/ml
Anti-LILRB2 50 µg/ml
15k monocytes
20k monocytes
25k monocytes
No stimulus
LPS 0.1 ng/ml
LPS 1 ng/ml
LPS 10 ng/ml
IL-10 concentration
% compared to response without anti-LILRB2 mAb
140
120
100
80
60
40
20
0
-20

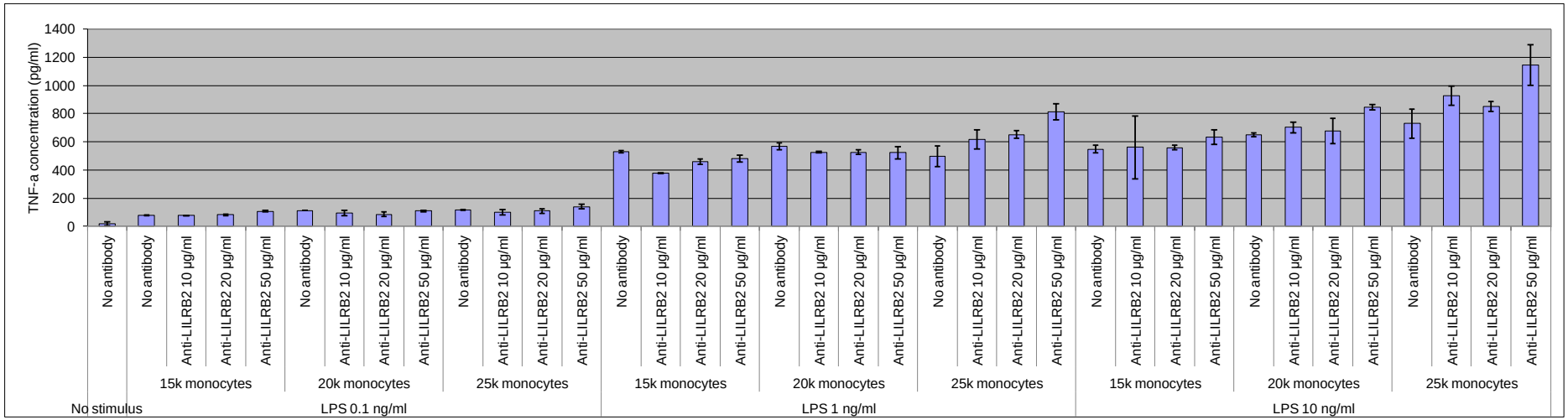
TNF-a concentration (pg/ml)
1400
1200
1000
800
600
400
200
0
No antibody
Anti-LILRB2 10 µg/ml
Anti-LILRB2 20 µg/ml
Anti-LILRB2 50 µg/ml
15k monocytes
20k monocytes
25k monocytes
No stimulus
LPS 0.1 ng/ml
LPS 1 ng/ml
LPS 10 ng/ml

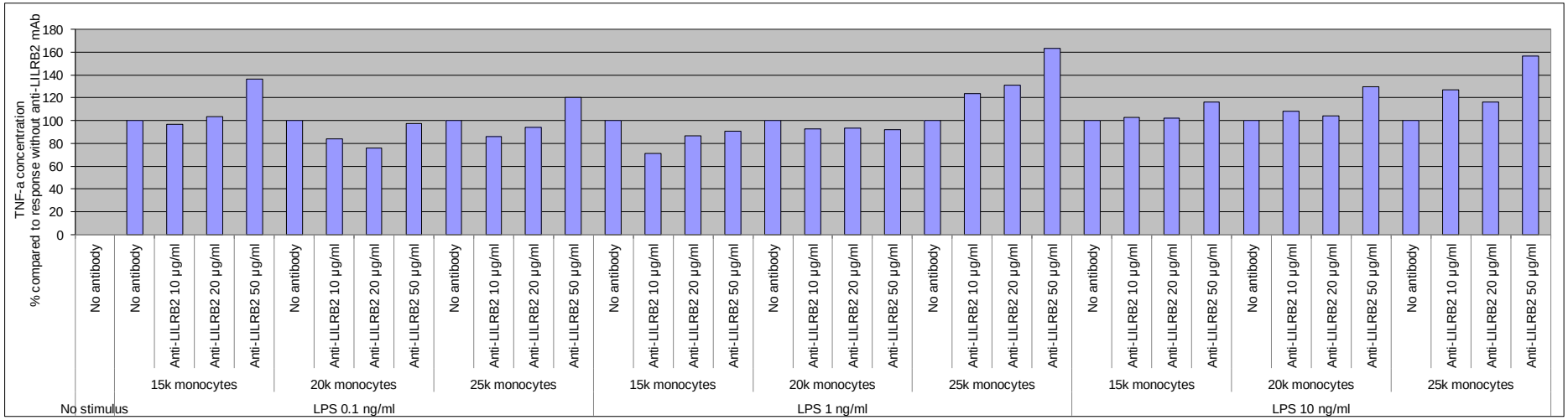
TNF-a concentration
% compared to response without anti-LILRB2 mAb
180
160
140
120
100
80
60
40
20
0
No antibody
Anti-LILRB2 10 µg/ml
Anti-LILRB2 20 µg/ml
Anti-LILRB2 50 µg/ml
15k monocytes
20k monocytes
25k monocytes
No stimulus
LPS 0.1 ng/ml
LPS 1 ng/ml
LPS 10 ng/ml

Figures 6.4a

Percentage reduction in cytokine (IL-6, IL-8, IL-10 and TNF-α) secretion of purified monocytes stimulated with LPS after addition of anti-LILRB2 mAb compared to addition of a rat IgG2b IMC in healthy individuals (n=5). The diamonds represent the mean value and error bars represent 1 standard deviation.

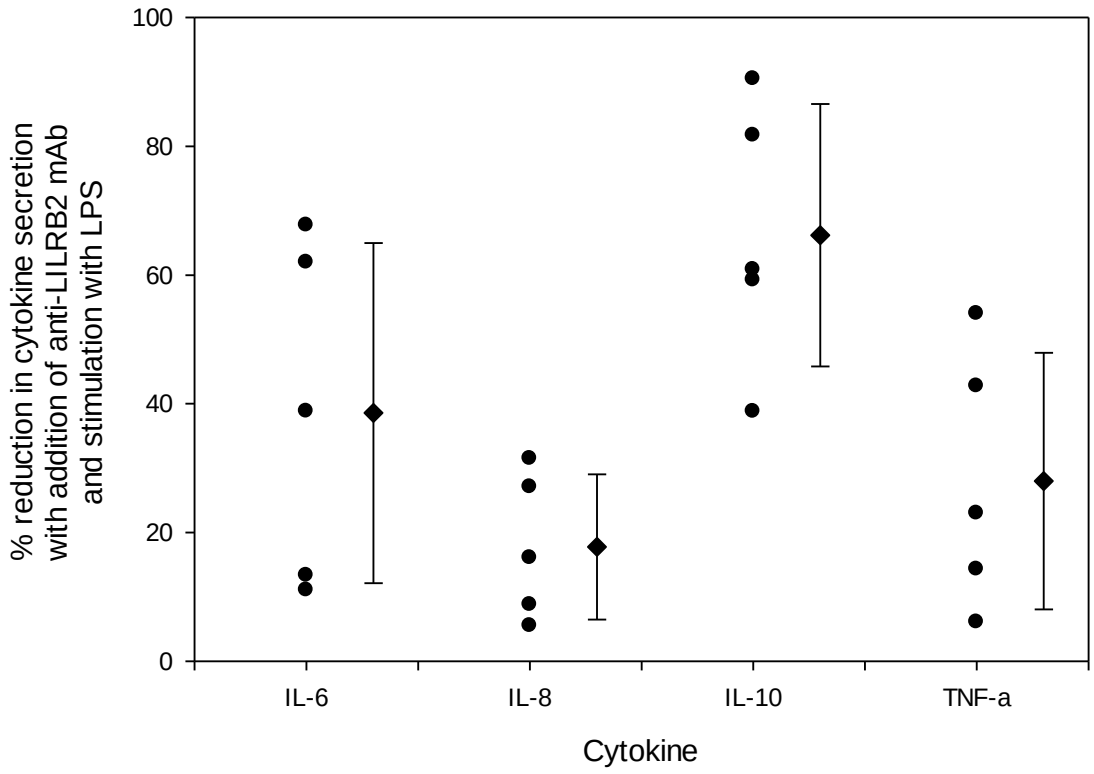

Figures 6.4b

Percentage reduction in cytokine (IL-6, IL-8, IL-10 and TNF-α) secretion of purified monocytes stimulated with ssRNA after addition of anti-LILRB2 mAb compared to addition of a rat IgG2b IMC in healthy individuals (n=5). The diamonds represent the mean value and error bars represent 1 standard deviation.

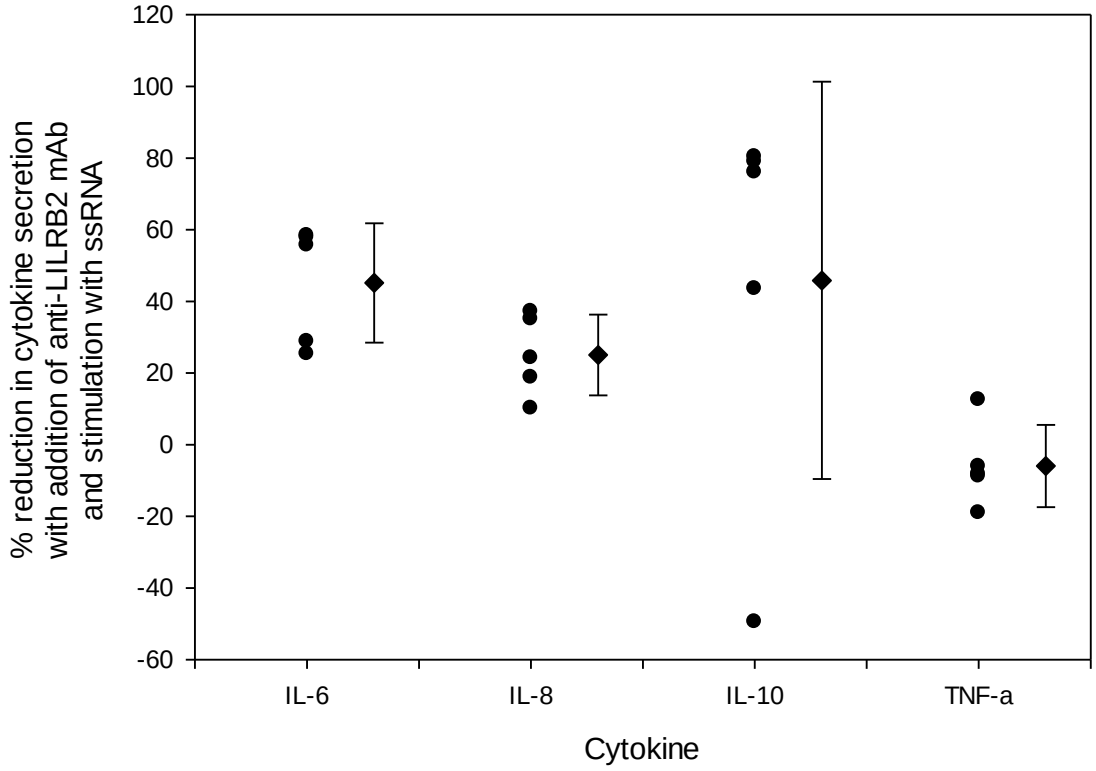

Figure 6.5

Difference in cytokine (IL-6, IL-8, IL-10 and TNF-α) secretion by purified monocytes after stimulation with LPS or ssRNA in healthy individuals (n=5). Cytokine secretion is compared between addition of a rat IgG2b IMC or anti-LILRB2 mAb.

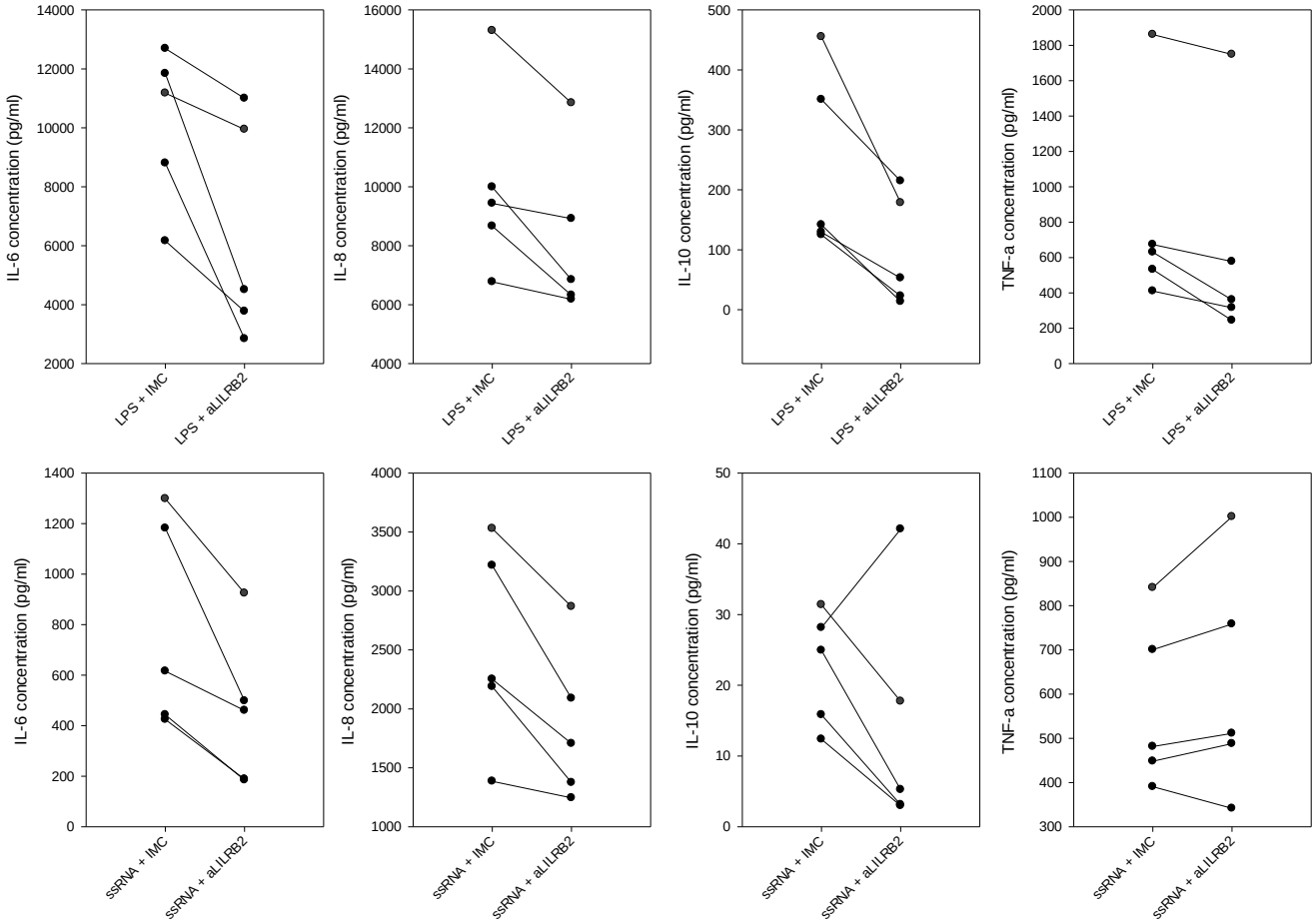
IL-6 concentration (pg/ml)
14000
12000
10000
8000
6000
4000
2000
LPS + IMC
LPS + aLILRB2
IL-8 concentration (pg/ml)
16000
14000
12000
10000
8000
6000
4000
LPS + IMC
LPS + aLILRB2
IL-10 concentration (pg/ml)
500
400
300
200
100
0
LPS + IMC
LPS + aLILRB2
TNF-a concentration (pg/ml)
2000
1800
1600
1400
1200
1000
800
600
400
200
0
LPS + IMC
LPS + aLILRB2
IL-6 concentration (pg/ml)
1400
1200
1000
800
600
400
200
0
ssRNA + IMC
ssRNA + aLILRB2
IL-8 concentration (pg/ml)
4000
3500
3000
2500
2000
1500
1000
ssRNA + IMC
ssRNA + aLILRB2
IL-10 concentration (pg/ml)
50
40
30
20
10
0
ssRNA + IMC
ssRNA + aLILRB2
TNF-a concentration (pg/ml)
1100
1000
900
800
700
600
500
400
300
ssRNA + IMC
ssRNA + aLILRB2

Figure 6.6

Correlation between suppression of cytokine secretion (IL-6. IL-8, IL-10 and TNF-α) by stimulation with LPS and ssRNA after addition of anti-LILRB2 mAb compared to addition of a rat IgG2b IMC; and LILRB2 expression levels (in median fluorescence intensity, MFI) for 5 different individuals. No significant correlations were found.

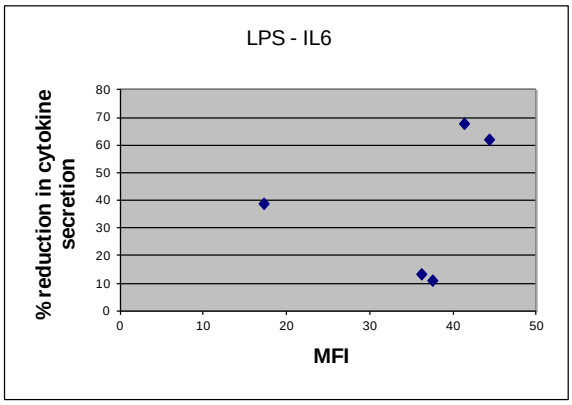
LPS - IL6
% reduction in cytokine secretion
MFI

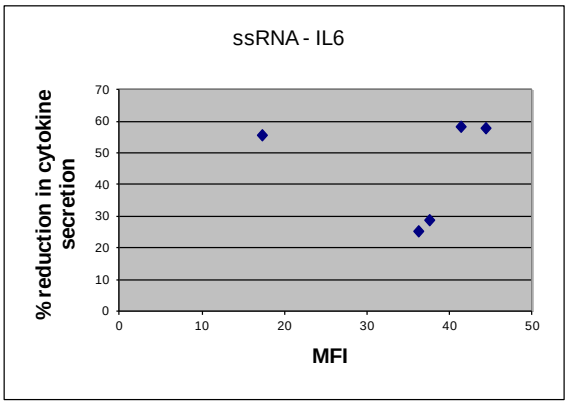
ssRNA - IL6
% reduction in cytokine secretion
MFI

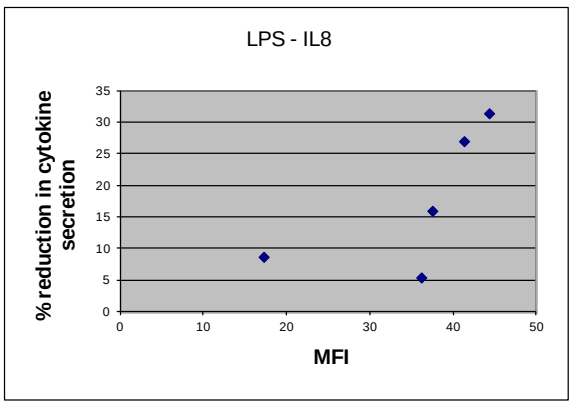
LPS - IL8
% reduction in cytokine secretion
MFI

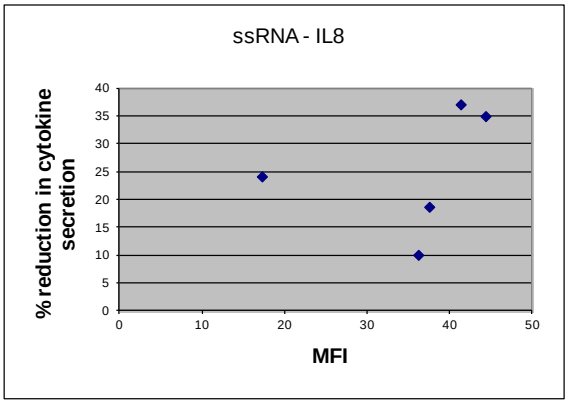
ssRNA - IL8
% reduction in cytokine secretion
MFI

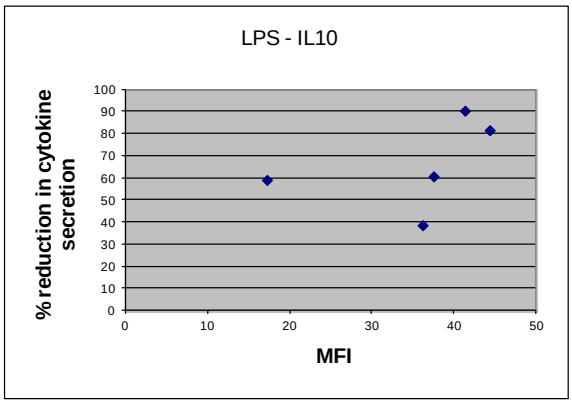
LPS - IL10
% reduction in cytokine secretion
MFI

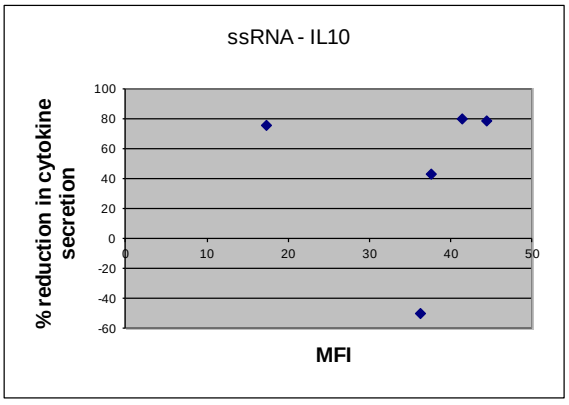
ssRNA - IL10
% reduction in cytokine secretion
MFI

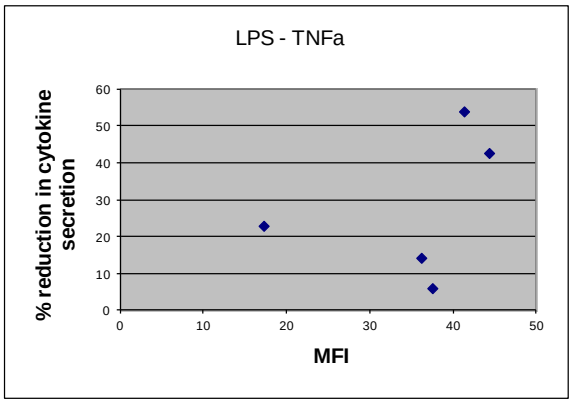
LPS - TNFa
% reduction in cytokine secretion
MFI

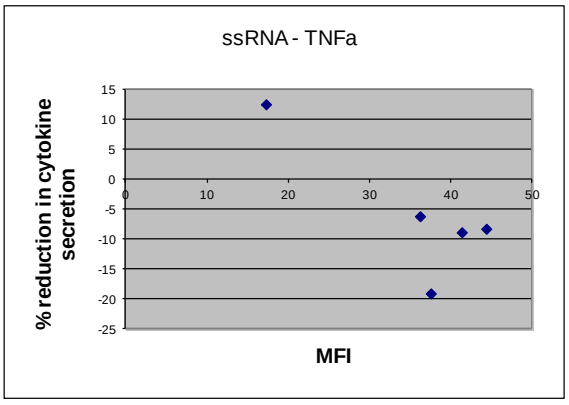
ssRNA - TNFa
% reduction in cytokine secretion
MFI

Figure 6.7

Percentage proliferation compared to control of lymphocytes from buffy coats of healthy HLA-A2 positive donors (n=5). Cells were stimulated with either anti-CD3/CD28 beads, SEB or anti-CD3 mAb. An anti-HLA-A2 isotype matched control (IMC), anti-HLA-A2 mAb, G-body, HLA-G tetramers or HLA-G tetramers and anti-HLA-A2 mAb were added to culture medium to determine if any of these reagents resulted in suppression of proliferation. The circles with the bars represent the mean and one standard deviation respectively. The red horizontal bars indicate a statistically significant difference at $p<0.05$.

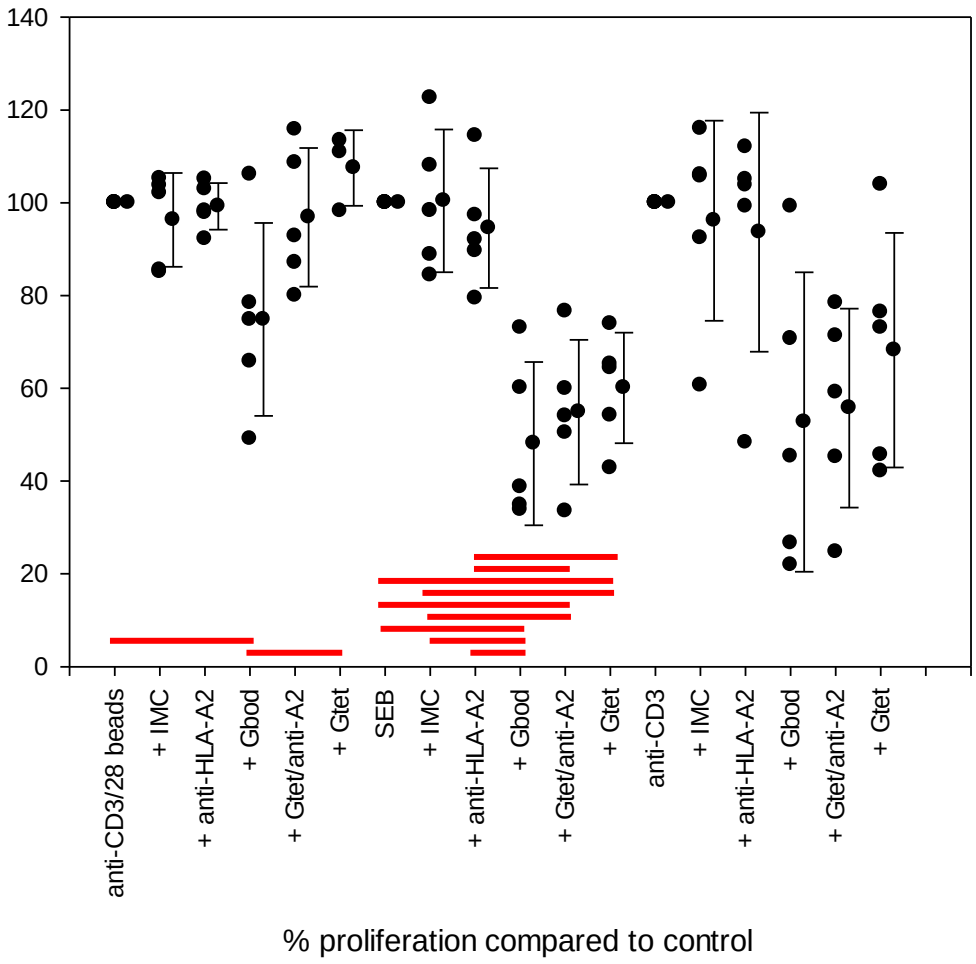

Figure 6.8

Percentage proliferation compared to control of lymphocytes from buffy coats of healthy HLA-A2 negative donors (n=2). Cells were stimulated with either anti-CD3/CD28 beads, SEB or anti-CD3 mAb. An anti-HLA-A2 isotype matched control (IMC), anti-HLA-A2 mAb, G-body, HLA-G tetramers or HLA-G tetramers and anti-HLA-A2 mAb were added to culture medium to determine if any of these reagents resulted in suppression of proliferation. The circles with the bars represent the mean and one standard deviation respectively. There were no statistically significant difference between the groups.

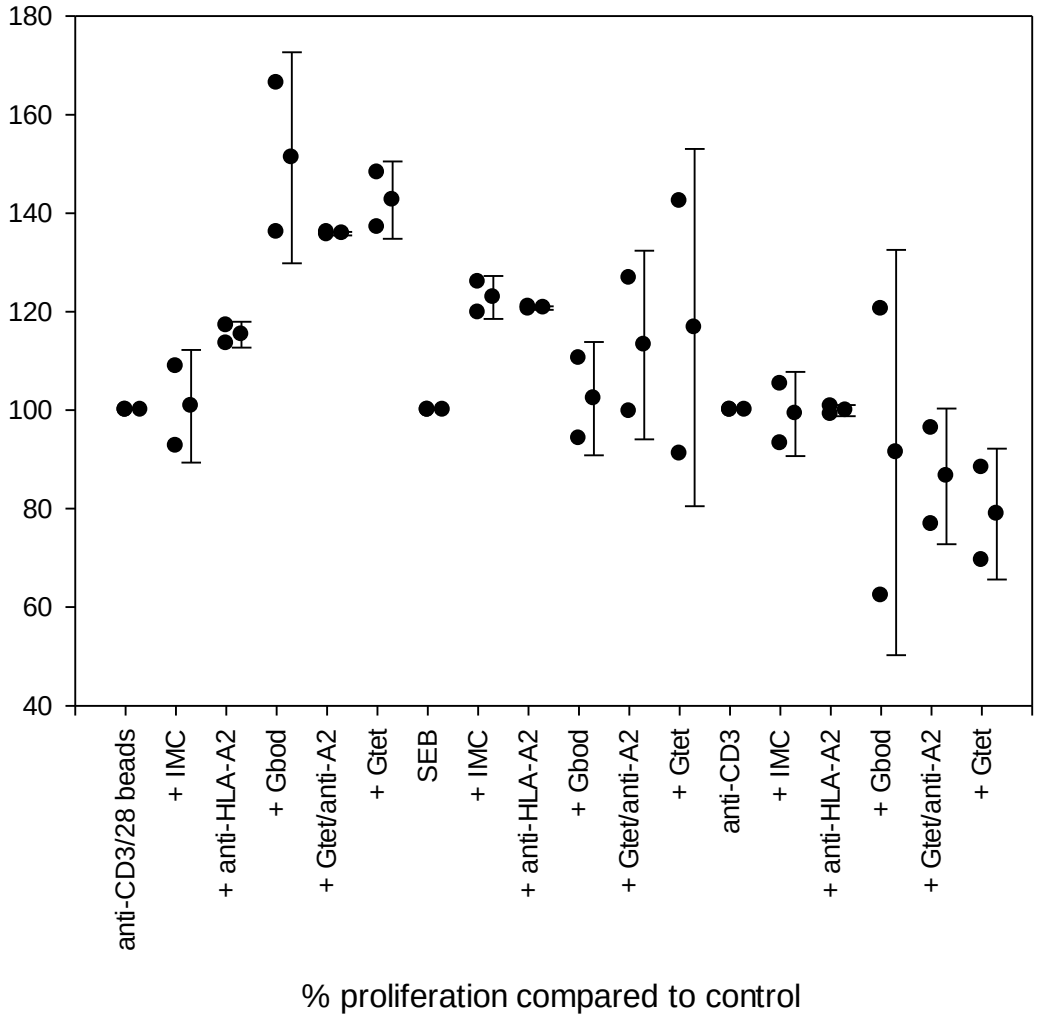

Figure 6.9

Mixed lymphocyte reaction with MoDC "C" as the stimulator cells and PBMCs "F" as the responder population; the cGBod and its controls were added at 3 fold successive dilutions (C1 being the highest concentration containing 0.5µg/ml mAb). The beads are anti-CD3 anti-CD28 microbeads (Invitrogen). Samples were repeated in triplicate and the error bars represent one standard deviation. No significant difference was seen between any of the groups with addition of the cGBod or any of the control reagents. MPC11 is a mouse IgG2b isotype matched control for the anti-HLA-A2 mAb, BB7.2.

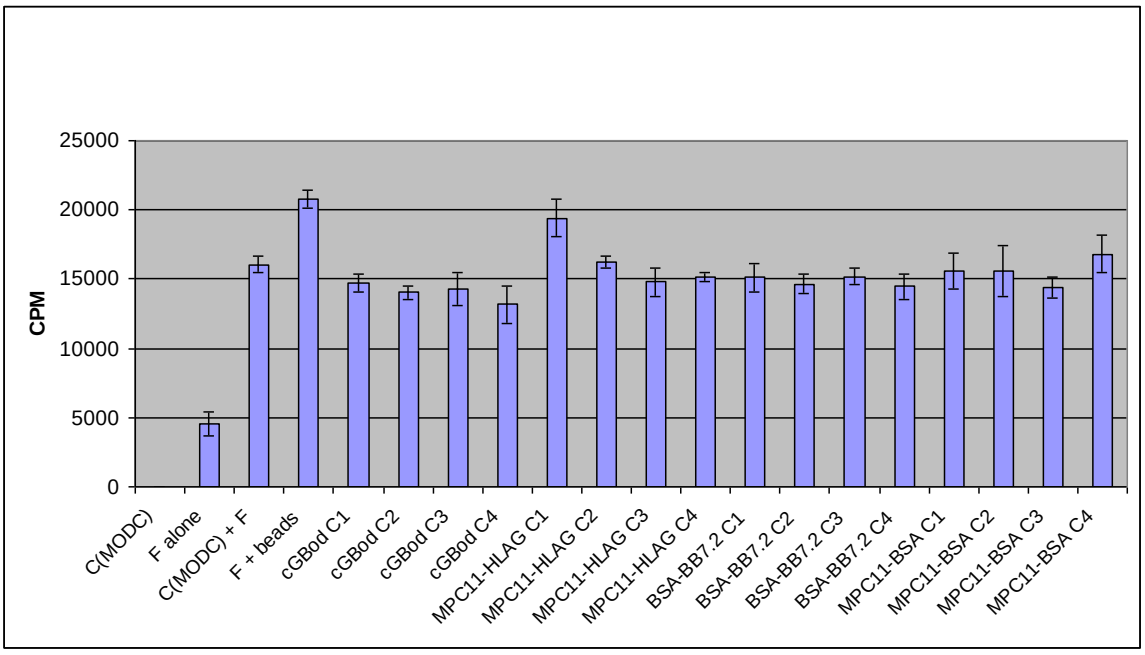

Figure 6.10

Absolute counts per minute (cpm) and percentage of maximum proliferation on addition of anti-LILRB2, protein G (pG) or anti-LILRB2 and protein G to lymphocytes stimulated with either SEB, anti-CD3/CD28 beads or anti-CD3.

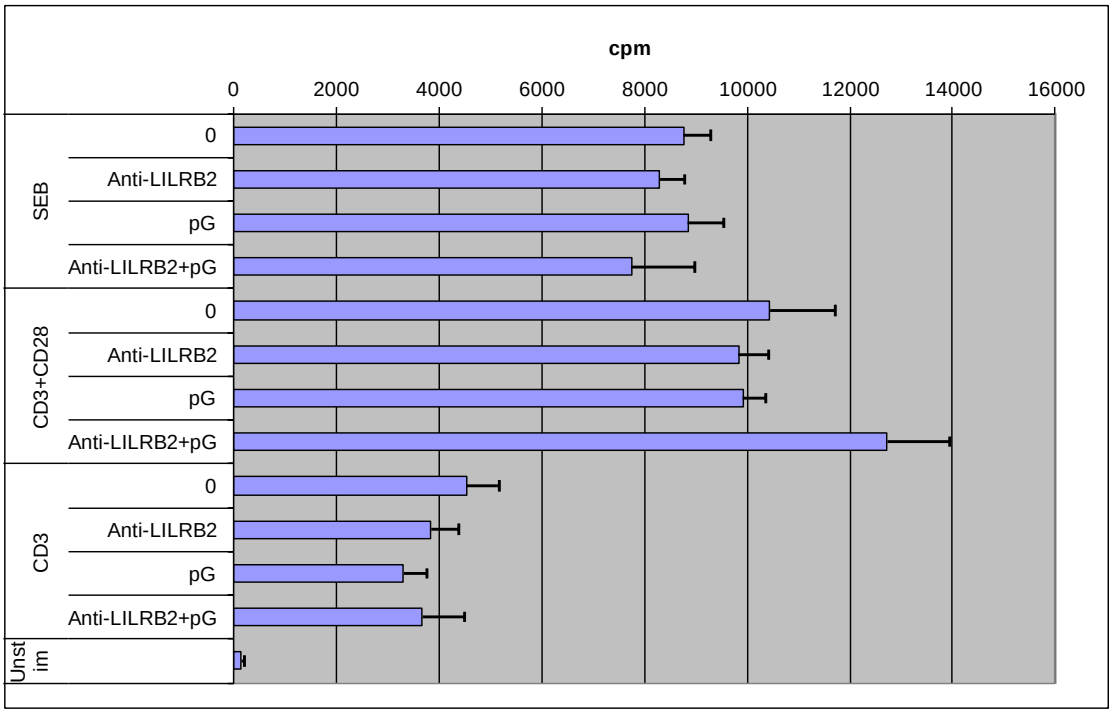

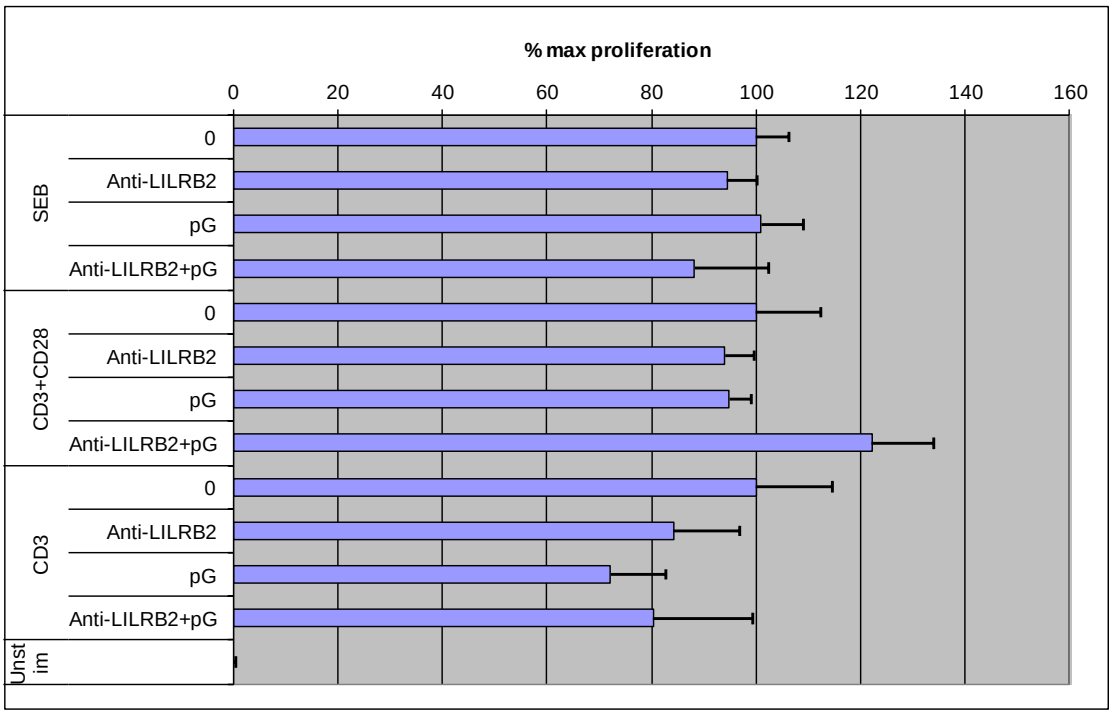

Chapter 7: Discussion

At present, the LILR molecules represent a potentially exciting area of as yet untapped discovery. Their presence and conservation on many different immune cells indicate that they are likely to play a significant role in regulating immune responses. In particular, myelomonocytic antigen presenting cells, including DCs express many different members of the family of these molecules. This suggests that they may well play a significant role in fine tuning and controlling immune responses, particularly as DCs are the most potent 'professional' antigen-presenting cells.

Despite this inference, relatively little research has been conducted since these molecules were first identified more than 15 years ago. These have largely been *in vitro* studies and have demonstrated that the LILR molecules play a role in early calcium signalling events, (39;40;42) protein tyrosine phosphorylation, (42;225) NK and $CD8^+$ T cell cytotoxicity, (39) DC maturation and allostimulatory capacity. (99) There have also been a limited number of *in vivo* murine studies showing that LILR molecules (and the PIR homologues) have roles in transplantation (68;79) and infection. (7;81) However, most of the studies have not been repeated and are relatively few in number.

In addition to laboratory data, there is also some published clinical data showing that the LILR molecules are associated or might a play a role in immune-mediated disease.

These have particularly been in the field of transplantation (142;173) and more recently, in infectious disease and HIV. (20;159) There is also data showing the significance of the LILR molecules in auto-immune and rheumatological disease. (28;172)

There have also been a few authors who have suggested the use of the LILR system as a therapeutic target. (122;230) However, most experiments looking to manipulate the LILR system in the laboratory have utilised HLA-G (as the high affinity ligand for LILRB1 and LILRB2); there have also been a few papers using monoclonal antibodies against specific LILRs. The majority of the experiments have been *in vitro*, with far fewer efforts to develop *in vivo* models. Murine experiments have utilised the homologous PIR system, although there have also been some experiments conducted in mice transfected with HLA-G and LILRs.

Given the widespread distribution of this family of molecules and the data emerging that they do play a role in a multitude of clinical conditions, it is important that steps are taken to increase our understanding. In particular, there is currently limited knowledge of their function, role in the immune response and potentially whether these molecules do represent a suitable target for therapeutic manipulation. To this end, this project has focused on trying to improve understanding of this potentially important group of molecules; in particular, the work described in earlier chapters has focused on understanding non-coding genomic variation in these molecules and their functional impact, as well as attempting to harness the LILR molecules for therapeutic purposes.

Experimental results

The first set of experiments conducted was to assess the variability in expression of a subset of these molecules and explore whether this variation might be due to differences in non-coding DNA. The data showed that there was significant variability in expression levels of the LILR molecules. There were differences in mean expression levels between different cell types, as well as differences in the variability of the same receptor on different cell types. Additionally, variation in expression between different individuals was also evident. The response to a dynamic stimulus (different cytokines were used in this project) was also tested and this too, showed differences between different cell types and between different individuals.

A degree of biological variation in the expression of any receptor is not surprising; however, the differences in variability on the surface expression of the same receptor on different cell types does suggest that expression levels can be varied and may potentially have a role to play in determining immune responses. The variability in expression levels between different individuals also has implications for any therapeutic modality that might be developed in the future to utilize this group of molecules.

Subsequently, following measurement of protein expression levels in a larger group of individuals, DNA sequencing of the non-coding region of LILRB2 was undertaken as proof of principle that genomic variation in this region could affect

LILR expression levels. Published data had shown that different haplotypes or SNPs for LILRB1 and LILRB2 could affect receptor expression levels. (172;194) However, in these studies, some of the variation occurred within coding regions of the protein. In this project, several SNPs were identified, although no significant relationships were found between expression levels of LILRB2 (either at baseline or following cytokine stimulation) and any of the SNPs. The reason for this remains to be determined, but is most likely due to the relatively small number of subjects tested. In a larger group looking at SNPs in more of the LILRs, it is likely that associations between genomic variation and LILR expression levels might become more apparent.

In an attempt to address the relatively small numbers in the study, the putative promoter region for LILRB2 was cloned into luciferase expression vectors to determine if the SNPs present in different haplotypes would affect luciferase activity. This too did not identify any relationship between SNPs/haplotypes or protein expression levels. Possible explanations for this include the small number of haplotypes tested and non-inclusion (in the cloned promoter region) of SNPs that might have effects on protein expression. In addition, the luciferase assay had a large amount of inherent variability which could have hidden small differences due to SNPs.

In addition to looking at relationships between genomic variation and LILR expression levels, the relationship between surface expression levels of LILRB2 and functional effects was also explored. In the process of developing assays to test the effect of LILR expression, it was discovered that ligation of LILRB2

resulted in suppression of cytokine secretion due to TLR4 and TLR8 engagement (by LPS and ssRNA/LyoVec respectively). This finding has not been previously demonstrated and would suggest that LILRB2 ligation can affect both signalling initiated by surface receptors and intracellular receptors. In addition, the suppression of cytokine responses varies between the two TLR receptors, suggesting that there are alternate pathways for secretion of some of the cytokine that are less affected by LILRB2 inhibition.

Despite this, however, no relationship between the magnitude of surface expression of LILRB2 and functional effect due to its ligation were seen. This might have potentially been due to the small numbers of subjects tested in this set of experiments and it would be important to repeat this on a larger number of subjects to determine if LILR expression levels do affect functional outcomes as hypothesized.

The assay for testing LILR expression levels is robust, and given more resources, it would have been interesting to measure values in patients with specific disease states, both at baseline and in response to stimuli, to determine how these molecule are affected in various immunological (and non-immunological) conditions. Additionally, there also remains scope to test if particular SNPs (or haplotypes) are associated with disease as well. This has been demonstrated in a few clinical conditions (Table 1.2) but by and large, remains unascertained for most immune-related disease.

In parallel to the experiments done to evaluate LILR expression levels and their relationship with genomic variation, work was also carried out to develop constructs that could be used to harness the therapeutic potential of these molecules. Both a 'crude' conjugation of biotinylated HLA-G to streptavidin-coated anti-HLA-A2 mAbs and a more elegant recombinant single polypeptide molecule were created. Binding of both constructs to their cognate ligands was demonstrated, showing that these constructs were fit for use in downstream functional experiments. Unfortunately, it was not possible to generate sufficient quantities of the recombinant construct within the resources of the project and hence, the chemically conjugated molecule was used for further experiments. However, it would be important to upscale production of the recombinant molecule for functional testing, as this format would be more directly applicable for use as a therapeutic product.

What is quite promising is the data that the G-body does have an effect in functional experiments. Although the effect was only seen in single population of cells rather than an MLR, it is noteworthy that was significant additional suppression of proliferation with addition of the G-body in the presence of HLA-A2 positive cells. This strongly suggests that localisation of HLA-G to the cell surface by binding to HLA-A2 does confer added immunosuppressive properties.

However, further work with the G-body needs to be done in experiments with an allo-specific stimulus. Although initial experiments in a small number of subjects did not show any significant effect with addition of the G-body, it might be that

an effect would be seen if a larger number of subjects were tested and/or the experimental conditions were modified.

The *in vitro* data also suggests that there is merit in progressing on to mouse experiments. This would possibly be best tested in some form of murine allo-transplantation model e.g. skin grafting. In support of this, a similarly constructed molecule comprising an avidin-linked mAb (33D1, which binds to DCIR2 on conventional DCs) bound to biotinylated K^d monomer has been used in a mouse model of allogeneic skin transplantation. (234) The idea behind this construct was to allow targeting of intact MHC molecules to quiescent dendritic cells, which inhibited the indirect alloresponse against allo-mismatched skin grafts. The authors managed to induce indefinite skin graft survival by using this along with temporary abrogation of the direct alloresponse by depletion of $CD8^+$ T cells.

The conjugate molecule used by Tanriver *et al* is similar in principle to the concept underpinning the G-body in that it combines two properties. However, Tanriver *et al* delivered the mismatched class I MHC combined with a targeting antibody for immature DCs. This allowed the localisation of the high concentration of a target antigen to immunosuppressive cells. Additionally, the conjugation system used by Tanriver *et al* is much the same as the technology employed for generation of the chemically conjugated G-body, thus providing further evidence that this molecule would be suitable for testing in murine experiments.

In summary, this project has shown that LILR expression levels can be accurately quantified on different cell types. Furthermore, engagement of LILRB2 modulates the cytokine response generated by TLR4 and TLR8 signalling, which is a novel finding.

The generation of a construct combining the immunosuppressive properties of HLA-G and the targeting function of an anti-HLA-A2 mAb has been successful. This has also been shown to have effects on lymphocyte proliferation, particularly more so in individuals who are HLA-A2 positive compared with those who are HLA-A2 negative; confirming that there is additional immunosuppressive potential to be gained by target-specific localisation of the HLA-G.

So far, however, it has not been possible to prove the hypothesis that genomic variation affects the expression levels of the LILR molecules, or that the magnitude of expression of the LILR molecules has functional significance. However, this set of experiments was done on relatively small numbers of subjects, which might not have been sufficiently powered to detect a true difference.

Future work

Several areas in this project merit further exploration based on the data generated. In particular, the next set of experiments continuing on from the work would include:

1. Sequencing of the coding and non-coding regions for all 4 LILR molecules assessed in this study
2. Use of bioinformatics to analyse the genetic data generated to determine the effect of various SNPs on LILR expression levels
3. Comparison of LILR expression levels between different disease groups with healthy controls
4. Testing the effect of engagement of LILRB2 on other parameters
    a. Activation markers on cells
    b. Ability of APCs to stimulate a T-lymphocyte response, in an autologous and allogeneic setting
5. Testing the effect of engagement of other LILR molecules on cytokine secretion and other functional properties as described above
6. Up-scaling production of the recombinant G-body for use in *in vitro* and *in vivo* experiments
7. Further testing of the G-body
    a. To determine its effect on other parameters apart from proliferation e.g. cell activation markers, calcium flux, tyrosine phosphorylation, cytokine secretion
    b. In MLR reactions
    c. *In vivo* experiments using transplantation models

Conclusions

In conclusion, this project has generated some exciting data – in particular, the development of a robust method for quantifying the expression of LILR molecules on different cell types, demonstration that engagement of LILRB2 can affect functional effects due to cell surface and intracellular TLR signalling; and development of the G-body and proof of principle that the construct does have an HLA-A2-specific immunosuppressive effect.

However, more work does remain to be done, both in terms of basic science and its potential clinical application. The regulation, function and role of the LILR molecules remain poorly understood, despite their widespread expression on many immune cells. They had been previously thought to act as innate sensors for 'self' especially with their recognition of MHC molecules; however, their recognition of bacteria (7) suggests that they may have additional roles in the recognition and response to microbial pathogens as well. From the point of view of this project, the G-body represents a novel development in using MHC molecules for localisation of an immunosuppressive/tolerogenic signal and this concept may yet prove useful, particularly in the transplantation setting. In this regard, further development of the G-body is likely to be rewarding with the potential for a therapeutic molecule that is localised with limited systemic toxicity.

In summary then, the LILR molecules do indeed represent an area rich with potential for future discovery, both in terms of helping us to better understand innate immune responses as well as manipulation for therapeutic benefit; and hopefully some of the data generated from this project would have contributed to this.

References

(1) Anderson KJ, Allen RL. Regulation of T-cell immunity by leucocyte immunoglobulin-like receptors: innate immune receptors for self on antigen-presenting cells. Immunology 2009; 127(1):8-17.

(2) Barten R, Torkar M, Haude A, Trowsdale J, Wilson MJ. Divergent and convergent evolution of NK-cell receptors. Trends Immunol 2001; 22(1):52-57.

(3) Wende H, Volz A, Ziegler A. Extensive gene duplications and a large inversion characterize the human leukocyte receptor cluster. Immunogenetics 2000; 51(8-9):703-713.

(4) Willcox BE, Thomas LM, Bjorkman PJ. Crystal structure of HLA-A2 bound to LIR-1, a host and viral major histocompatibility complex receptor. Nat Immunol 2003; 4(9):913-919.

(5) Jones DC, Kosmoliaptsis V, Apps R et al. HLA class I allelic sequence and conformation regulate leukocyte Ig-like receptor binding. J Immunol 2011; 186(5):2990-2997.

(6) Li D, Wang L, Yu L et al. Ig-like transcript 4 inhibits lipid antigen presentation through direct CD1d interaction. J Immunol 2009; 182(2):1033-1040.

(7) Nakayama M, Underhill DM, Petersen TW et al. Paired Ig-like receptors bind to bacteria and shape TLR-mediated cytokine production. J Immunol 2007; 178(7):4250-4259.

(8) Chapman TL, Heikeman AP, Bjorkman PJ. The inhibitory receptor LIR-1 uses a common binding interaction to recognize class I MHC molecules and the viral homolog UL18. Immunity 1999; 11(5):603-613.

(9) Navarro F, Llano M, Bellon T, Colonna M, Geraghty DE, Lopez-Botet M. The ILT2(LIR1) and CD94/NKG2A NK cell receptors respectively recognize HLA-G1 and HLA-E molecules co-expressed on target cells. Eur J Immunol 1999; 29(1):277-283.

(10) Lepin EJ, Bastin JM, Allan DS et al. Functional characterization of HLA-F and binding of HLA-F tetramers to ILT2 and ILT4 receptors. Eur J Immunol 2000; 30(12):3552-3561.

(11) Shiroishi M, Kuroki K, Rasubala L et al. Structural basis for recognition of the nonclassical MHC molecule HLA-G by the leukocyte Ig-like receptor B2 (LILRB2/LIR2/ILT4/CD85d). Proc Natl Acad Sci U S A 2006; 103(44):16412-16417.

(12) Shiroishi M, Kuroki K, Tsumoto K et al. Entropically driven MHC class I recognition by human inhibitory receptor leukocyte Ig-like receptor B1 (LILRB1/ILT2/CD85j). J Mol Biol 2006; 355(2):237-248.

(13) Chui CS, Li D. Role of immunolglobulin-like transcript family receptors and their ligands in suppressor T-cell-induced dendritic cell tolerization. Hum Immunol 2009; 70(9):686-691.

(14) Shiroishi M, Tsumoto K, Amano K et al. Human inhibitory receptors Ig-like transcript 2 (ILT2) and ILT4 compete with CD8 for MHC class I

binding and bind preferentially to HLA-G. Proc Natl Acad Sci U S A 2003; 100(15):8856-8861.

(15) Ryu M, Chen Y, Qi J et al. LILRA3 binds both classical and non-classical HLA class I molecules but with reduced affinities compared to LILRB1/LILRB2: structural evidence. PLoS One 2011; 6(4):e19245.

(16) Apps R, Murphy SP, Fernando R, Gardner L, Ahad T, Moffett A. Human leucocyte antigen (HLA) expression of primary trophoblast cells and placental cell lines, determined using single antigen beads to characterize allotype specificities of anti-HLA antibodies. Immunology 2009; 127(1):26-39.

(17) Allen RL, Raine T, Haude A, Trowsdale J, Wilson MJ. Leukocyte receptor complex-encoded immunomodulatory receptors show differing specificity for alternative HLA-B27 structures. J Immunol 2001; 167(10):5543-5547.

(18) Kollnberger S, Bird L, Sun MY et al. Cell-surface expression and immune receptor recognition of HLA-B27 homodimers. Arthritis Rheum 2002; 46(11):2972-2982.

(19) Carrington M, O'Brien SJ. The influence of HLA genotype on AIDS. Annu Rev Med 2003; 54:535-551.

(20) Huang J, Goedert JJ, Sundberg EJ et al. HLA-B*35-Px-mediated acceleration of HIV-1 infection by increased inhibitory immunoregulatory impulses. J Exp Med 2009; 206(13):2959-2966.

(21) Giles J, Shaw J, Piper C et al. HLA-B27 homodimers and free H chains are stronger ligands for leukocyte Ig-like receptor B2 than classical HLA class I. J Immunol 2012; 188(12):6184-6193.

(22) Mori Y, Tsuji S, Inui M et al. Inhibitory immunoglobulin-like receptors LILRB and PIR-B negatively regulate osteoclast development. J Immunol 2008; 181(7):4742-4751.

(23) Manavalan JS, Rossi PC, Vlad G et al. High expression of ILT3 and ILT4 is a general feature of tolerogenic dendritic cells. Transpl Immunol 2003; 11(3-4):245-258.

(24) Ristich V, Liang S, Zhang W, Wu J, Horuzsko A. Tolerization of dendritic cells by HLA-G. Eur J Immunol 2005; 35(4):1133-1142.

(25) Jones DC, Roghanian A, Brown DP et al. Alternative mRNA splicing creates transcripts encoding soluble proteins from most LILR genes. Eur J Immunol 2009; 39(11):3195-3206.

(26) Kabalak G, Dobberstein SB, Matthias T et al. Association of immunoglobulin-like transcript 6 deficiency with Sjogren's syndrome. Arthritis Rheum 2009; 60(10):2923-2925.

(27) Koch S, Goedde R, Nigmatova V et al. Association of multiple sclerosis with ILT6 deficiency. Genes Immun 2005; 6(5):445-447.

(28) Ordonez D, Sanchez AJ, Martinez-Rodriguez JE et al. Multiple sclerosis associates with LILRA3 deletion in Spanish patients. Genes Immun 2009; 10(6):579-585.

(29) Cao W, Bover L, Cho M et al. Regulation of TLR7/9 responses in plasmacytoid dendritic cells by BST2 and ILT7 receptor interaction. J Exp Med 2009; 206(7):1603-1614.

(30) Cheng H, Mohammed F, Nam G et al. Crystal structure of leukocyte Ig-like receptor LILRB4 (ILT3/LIR-5/CD85k): a myeloid inhibitory receptor involved in immune tolerance. J Biol Chem 2011; 286(20):18013-18025.

(31) Masuda A, Nakamura A, Maeda T, Sakamoto Y, Takai T. Cis binding between inhibitory receptors and MHC class I can regulate mast cell activation. J Exp Med 2007; 204(4):907-920.

(32) Doucey MA, Scarpellino L, Zimmer J et al. Cis association of Ly49A with MHC class I restricts natural killer cell inhibition. Nat Immunol 2004; 5(3):328-336.

(33) Leibson PJ, Pease LR. Having it both ways: MHC recognition in cis and trans. Nat Immunol 2004; 5(3):237-238.

(34) Nakajima H, Samaridis J, Angman L, Colonna M. Human myeloid cells express an activating ILT receptor (ILT1) that associates with Fc receptor gamma-chain. J Immunol 1999; 162(1):5-8.

(35) Colonna M, Nakajima H, Cella M. A family of inhibitory and activating Ig-like receptors that modulate function of lymphoid and myeloid cells. Semin Immunol 2000; 12(2):121-127.

(36) Lee DJ, Sieling PA, Ochoa MT et al. LILRA2 activation inhibits dendritic cell differentiation and antigen presentation to T cells. J Immunol 2007; 179(12):8128-8136.

(37) Cao W, Rosen DB, Ito T et al. Plasmacytoid dendritic cell-specific receptor ILT7-Fc epsilonRI gamma inhibits Toll-like receptor-induced interferon production. J Exp Med 2006; 203(6):1399-1405.

(38) Isakov N. ITIMs and ITAMs. The Yin and Yang of antigen and Fc receptor-linked signaling machinery. Immunol Res 1997; 16(1):85-100.

(39) Colonna M, Navarro F, Bellon T et al. A common inhibitory receptor for major histocompatibility complex class I molecules on human lymphoid and myelomonocytic cells. J Exp Med 1997; 186(11):1809-1818.

(40) Colonna M, Samaridis J, Cella M et al. Human myelomonocytic cells express an inhibitory receptor for classical and nonclassical MHC class I molecules. J Immunol 1998; 160(7):3096-3100.

(41) Sayos J, Martinez-Barriocanal A, Kitzig F, Bellon T, Lopez-Botet M. Recruitment of C-terminal Src kinase by the leukocyte inhibitory receptor CD85j. Biochem Biophys Res Commun 2004; 324(2):640-647.

(42) Cella M, Dohring C, Samaridis J et al. A novel inhibitory receptor (ILT3) expressed on monocytes, macrophages, and dendritic cells involved in antigen processing. J Exp Med 1997; 185(10):1743-1751.

(43) Colonna M, Nakajima H, Navarro F, Lopez-Botet M. A novel family of Ig-like receptors for HLA class I molecules that modulate function of lymphoid and myeloid cells. J Leukoc Biol 1999; 66(3):375-381.

(44) Fanger NA, Cosman D, Peterson L, Braddy SC, Maliszewski CR, Borges L. The MHC class I binding proteins LIR-1 and LIR-2 inhibit Fc receptor-mediated signaling in monocytes. Eur J Immunol 1998; 28(11):3423-3434.

(45) Hayami K, Fukuta D, Nishikawa Y et al. Molecular cloning of a novel murine cell-surface glycoprotein homologous to killer cell inhibitory receptors. J Biol Chem 1997; 272(11):7320-7327.

(46) Kubagawa H, Burrows PD, Cooper MD. A novel pair of immunoglobulin-like receptors expressed by B cells and myeloid cells. Proc Natl Acad Sci U S A 1997; 94(10):5261-5266.

(47) Yamashita Y, Fukuta D, Tsuji A et al. Genomic structures and chromosomal location of p91, a novel murine regulatory receptor family. J Biochem 1998; 123(2):358-368.

(48) Castells MC, Wu X, Arm JP, Austen KF, Katz HR. Cloning of the gp49B gene of the immunoglobulin superfamily and demonstration that one of its two products is an early-expressed mast cell surface protein originally described as gp49. J Biol Chem 1994; 269(11):8393-8401.

(49) Katz HR, Vivier E, Castells MC, McCormick MJ, Chambers JM, Austen KF. Mouse mast cell gp49B1 contains two immunoreceptor tyrosine-based inhibition motifs and suppresses mast cell activation when

coligated with the high-affinity Fc receptor for IgE. Proc Natl Acad Sci U S A 1996; 93(20):10809-10814.

(50) Dennis G, Jr., Stephan RP, Kubagawa H, Cooper MD. Characterization of paired Ig-like receptors in rats. J Immunol 1999; 163(12):6371-6377.

(51) Nikolaidis N, Klein J, Nei M. Origin and evolution of the Ig-like domains present in mammalian leukocyte receptors: insights from chicken, frog, and fish homologues. Immunogenetics 2005; 57(1-2):151-157.

(52) Nikolaidis N, Makalowska I, Chalkia D, Makalowski W, Klein J, Nei M. Origin and evolution of the chicken leukocyte receptor complex. Proc Natl Acad Sci U S A 2005; 102(11):4057-4062.

(53) Viertlboeck BC, Habermann FA, Schmitt R, Groenen MA, Du PL, Gobel TW. The chicken leukocyte receptor complex: a highly diverse multigene family encoding at least six structurally distinct receptor types. J Immunol 2005; 175(1):385-393.

(54) Canavez F, Young NT, Guethlein LA et al. Comparison of chimpanzee and human leukocyte Ig-like receptor genes reveals framework and rapidly evolving genes. J Immunol 2001; 167(10):5786-5794.

(55) Hammond JA, Guethlein LA, bi-Rached L, Moesta AK, Parham P. Evolution and survival of marine carnivores did not require a diversity of killer cell Ig-like receptors or Ly49 NK cell receptors. J Immunol 2009; 182(6):3618-3627.

(56) Hogan L, Bhuju S, Jones DC et al. Characterisation of bovine leukocyte Ig-like receptors. PLoS One 2012; 7(4):e34291.

(57) Lebbink RJ, de RT, Verbrugge A, Bril WS, Meyaard L. The mouse homologue of the leukocyte-associated Ig-like receptor-1 is an inhibitory receptor that recruits Src homology region 2-containing protein tyrosine phosphatase (SHP)-2, but not SHP-1. J Immunol 2004; 172(9):5535-5543.

(58) Kubagawa H, Chen CC, Ho LH et al. Biochemical nature and cellular distribution of the paired immunoglobulin-like receptors, PIR-A and PIR-B. J Exp Med 1999; 189(2):309-318.

(59) Masuda K, Kubagawa H, Ikawa T et al. Prethymic T-cell development defined by the expression of paired immunoglobulin-like receptors. EMBO J 2005; 24(23):4052-4060.

(60) Ujike A, Takeda K, Nakamura A, Ebihara S, Akiyama K, Takai T. Impaired dendritic cell maturation and increased T(H)2 responses in PIR-B(-/-) mice. Nat Immunol 2002; 3(6):542-548.

(61) Kubo T, Uchida Y, Watanabe Y et al. Augmented TLR9-induced Btk activation in PIR-B-deficient B-1 cells provokes excessive autoantibody production and autoimmunity. J Exp Med 2009; 206(9):1971-1982.

(62) Takai T, Li M, Sylvestre D, Clynes R, Ravetch JV. FcR gamma chain deletion results in pleiotrophic effector cell defects. Cell 1994; 76(3):519-529.

(63) Takai T. Paired immunoglobulin-like receptors and their MHC class I recognition. Immunology 2005; 115(4):433-440.

(64) Ono M, Yuasa T, Ra C, Takai T. Stimulatory function of paired immunoglobulin-like receptor-A in mast cell line by associating with subunits common to Fc receptors. J Biol Chem 1999; 274(42):30288-30296.

(65) Maeda A, Kurosaki M, Kurosaki T. Paired immunoglobulin-like receptor (PIR)-A is involved in activating mast cells through its association with Fc receptor gamma chain. J Exp Med 1998; 188(5):991-995.

(66) Syken J, Grandpre T, Kanold PO, Shatz CJ. PirB restricts ocular-dominance plasticity in visual cortex. Science 2006; 313(5794):1795-1800.

(67) Atwal JK, Pinkston-Gosse J, Syken J et al. PirB is a functional receptor for myelin inhibitors of axonal regeneration. Science 2008; 322(5903):967-970.

(68) Nakamura A, Kobayashi E, Takai T. Exacerbated graft-versus-host disease in Pirb-/- mice. Nat Immunol 2004; 5(6):623-629.

(69) Hogarth PM. Fc receptors are major mediators of antibody based inflammation in autoimmunity. Curr Opin Immunol 2002; 14(6):798-802.

(70) Liang S, Baibakov B, Horuzsko A. HLA-G inhibits the functions of murine dendritic cells via the PIR-B immune inhibitory receptor. Eur J Immunol 2002; 32(9):2418-2426.

(71) Yamashita Y, Ono M, Takai T. Inhibitory and stimulatory functions of paired Ig-like receptor (PIR) family in RBL-2H3 cells. J Immunol 1998; 161(8):4042-4047.

(72) Takai T. Roles of Fc receptors in autoimmunity. Nat Rev Immunol 2002; 2(8):580-592.

(73) Ravetch JV, Lanier LL. Immune inhibitory receptors. Science 2000; 290(5489):84-89.

(74) Long EO. Regulation of immune responses through inhibitory receptors. Annu Rev Immunol 1999; 17:875-904.

(75) Maeda A, Kurosaki M, Ono M, Takai T, Kurosaki T. Requirement of SH2-containing protein tyrosine phosphatases SHP-1 and SHP-2 for paired immunoglobulin-like receptor B (PIR-B)-mediated inhibitory signal. J Exp Med 1998; 187(8):1355-1360.

(76) Ho LH, Uehara T, Chen CC, Kubagawa H, Cooper MD. Constitutive tyrosine phosphorylation of the inhibitory paired Ig-like receptor PIR-B. Proc Natl Acad Sci U S A 1999; 96(26):15086-15090.

(77) Endo S, Sakamoto Y, Kobayashi E, Nakamura A, Takai T. Regulation of cytotoxic T lymphocyte triggering by PIR-B on dendritic cells. Proc Natl Acad Sci U S A 2008; 105(38):14515-14520.

(78) Pereira S, Zhang H, Takai T, Lowell CA. The inhibitory receptor PIR-B negatively regulates neutrophil and macrophage integrin signaling. J Immunol 2004; 173(9):5757-5765.

(79) Liu J, Liu Z, Witkowski P et al. Rat CD8+ FOXP3+ T suppressor cells mediate tolerance to allogeneic heart transplants, inducing PIR-B in APC and rendering the graft invulnerable to rejection. Transpl Immunol 2004; 13(4):239-247.

(80) Munitz A, McBride ML, Bernstein JS, Rothenberg ME. A dual activation and inhibition role for the paired immunoglobulin-like receptor B in eosinophils. Blood 2008; 111(12):5694-5703.

(81) Torii I, Oka S, Hotomi M et al. PIR-B-deficient mice are susceptible to Salmonella infection. J Immunol 2008; 181(6):4229-4239.

(82) Maeda A, Scharenberg AM, Tsukada S, Bolen JB, Kinet JP, Kurosaki T. Paired immunoglobulin-like receptor B (PIR-B) inhibits BCR-induced activation of Syk and Btk by SHP-1. Oncogene 1999; 18(14):2291-2297.

(83) Doyle SL, Jefferies CA, Feighery C, O'Neill LA. Signaling by Toll-like receptors 8 and 9 requires Bruton's tyrosine kinase. J Biol Chem 2007; 282(51):36953-36960.

(84) Lee KG, Xu S, Wong ET, Tergaonkar V, Lam KP. Bruton's tyrosine kinase separately regulates NFkappaB p65RelA activation and cytokine interleukin (IL)-10/IL-12 production in TLR9-stimulated B Cells. J Biol Chem 2008; 283(17):11189-11198.

(85) Montecino-Rodriguez E, Dorshkind K. New perspectives in B-1 B cell development and function. Trends Immunol 2006; 27(9):428-433.

(86) Takai T, Nakamura A, Endo S. Role of PIR-B in autoimmune glomerulonephritis. J Biomed Biotechnol 2011; 2011:275302.

(87) Arm JP, Gurish MF, Reynolds DS et al. Molecular cloning of gp49, a cell-surface antigen that is preferentially expressed by mouse mast cell progenitors and is a new member of the immunoglobulin superfamily. J Biol Chem 1991; 266(24):15966-15973.

(88) Castells MC, Klickstein LB, Hassani K et al. gp49B1-alpha(v)beta3 interaction inhibits antigen-induced mast cell activation. Nat Immunol 2001; 2(5):436-442.

(89) Lu-Kuo JM, Joyal DM, Austen KF, Katz HR. gp49B1 inhibits IgE-initiated mast cell activation through both immunoreceptor tyrosine-based inhibitory motifs, recruitment of src homology 2 domain-containing phosphatase-1, and suppression of early and late calcium mobilization. J Biol Chem 1999; 274(9):5791-5796.

(90) Daheshia M, Friend DS, Grusby MJ, Austen KF, Katz HR. Increased severity of local and systemic anaphylactic reactions in gp49B1-deficient mice. J Exp Med 2001; 194(2):227-234.

(91) Feldweg AM, Friend DS, Zhou JS et al. gp49B1 suppresses stem cell factor-induced mast cell activation-secretion and attendant inflammation in vivo. Eur J Immunol 2003; 33(8):2262-2268.

(92) Zhou JS, Friend DS, Feldweg AM et al. Prevention of lipopolysaccharide-induced microangiopathy by gp49B1: evidence for an

important role for gp49B1 expression on neutrophils. J Exp Med 2003; 198(8):1243-1251.

(93) Zhou JS, Friend DS, Lee DM, Li L, Austen KF, Katz HR. gp49B1 deficiency is associated with increases in cytokine and chemokine production and severity of proliferative synovitis induced by anti-type II collagen mAb. Eur J Immunol 2005; 35(5):1530-1538.

(94) Breslow RG, Rao JJ, Xing W, Hong DI, Barrett NA, Katz HR. Inhibition of Th2 adaptive immune responses and pulmonary inflammation by leukocyte Ig-like receptor B4 on dendritic cells. J Immunol 2010; 184(2):1003-1013.

(95) Banchereau J, Briere F, Caux C et al. Immunobiology of dendritic cells. Annu Rev Immunol 2000; 18:767-811.

(96) Liu YJ. Dendritic cell subsets and lineages, and their functions in innate and adaptive immunity. Cell 2001; 106(3):259-262.

(97) Tenca C, Merlo A, Merck E et al. CD85j (leukocyte Ig-like receptor-1/Ig-like transcript 2) inhibits human osteoclast-associated receptor-mediated activation of human dendritic cells. J Immunol 2005; 174(11):6757-6763.

(98) Wagner CS, Walther-Jallow L, Buentke E, Ljunggren HG, Achour A, Chambers BJ. Human cytomegalovirus-derived protein UL18 alters the phenotype and function of monocyte-derived dendritic cells. J Leukoc Biol 2008; 83(1):56-63.

(99) Young NT, Waller EC, Patel R, Roghanian A, Austyn JM, Trowsdale J. The inhibitory receptor LILRB1 modulates the differentiation and regulatory potential of human dendritic cells. Blood 2008; 111(6):3090-3096.

(100) Chang CC, Ciubotariu R, Manavalan JS et al. Tolerization of dendritic cells by T(S) cells: the crucial role of inhibitory receptors ILT3 and ILT4. Nat Immunol 2002; 3(3):237-243.

(101) Cortesini NS, Colovai AI, Manavalan JS et al. Role of regulatory and suppressor T-cells in the induction of ILT3+ ILT4+ tolerogenic endothelial cells in organ allografts. Transpl Immunol 2004; 13(2):73-82.

(102) Suciu-Foca N, Feirt N, Zhang QY et al. Soluble Ig-like transcript 3 inhibits tumor allograft rejection in humanized SCID mice and T cell responses in cancer patients. J Immunol 2007; 178(11):7432-7441.

(103) Vlad G, D'Agati VD, Zhang QY et al. Immunoglobulin-like transcript 3-Fc suppresses T-cell responses to allogeneic human islet transplants in hu-NOD/SCID mice. Diabetes 2008; 57(7):1878-1886.

(104) Beinhauer BG, McBride JM, Graf P et al. Interleukin 10 regulates cell surface and soluble LIR-2 (CD85d) expression on dendritic cells resulting in T cell hyporesponsiveness in vitro. Eur J Immunol 2004; 34(1):74-80.

(105) Suciu-Foca N, Manavalan JS, Scotto L et al. Molecular characterization of allospecific T suppressor and tolerogenic dendritic cells: review. Int Immunopharmacol 2005; 5(1):7-11.

(106) Velten FW, Duperrier K, Bohlender J, Metharom P, Goerdt S. A gene signature of inhibitory MHC receptors identifies a BDCA3(+) subset of IL-10-induced dendritic cells with reduced allostimulatory capacity in vitro. Eur J Immunol 2004; 34(10):2800-2811.

(107) Vlad G, Piazza F, Colovai A et al. Interleukin-10 induces the upregulation of the inhibitory receptor ILT4 in monocytes from HIV positive individuals. Hum Immunol 2003; 64(5):483-489.

(108) Schnabl E, Stockinger H, Majdic O et al. Activated human T lymphocytes express MHC class I heavy chains not associated with beta 2-microglobulin. J Exp Med 1990; 171(5):1431-1442.

(109) Arosa FA, Santos SG, Powis SJ. Open conformers: the hidden face of MHC-I molecules. Trends Immunol 2007; 28(3):115-123.

(110) Pickl WF, Holter W, Stockl J, Majdic O, Knapp W. Expression of beta 2-microglobulin-free HLA class I alpha-chains on activated T cells requires internalization of HLA class I heterodimers. Immunology 1996; 88(1):104-109.

(111) Demaria S, Schwab R, Bushkin Y. The origin and fate of beta 2m-free MHC class I molecules induced on activated T cells. Cell Immunol 1992; 142(1):103-113.

(112) Santos SG, Lynch S, Campbell EC, Antoniou AN, Powis SJ. Induction of HLA-B27 heavy chain homodimer formation after activation in dendritic cells. Arthritis Res Ther 2008; 10(4):R100.

(113) Matko J, Bushkin Y, Wei T, Edidin M. Clustering of class I HLA molecules on the surfaces of activated and transformed human cells. J Immunol 1994; 152(7):3353-3360.

(114) Setini A, Beretta A, De SC et al. Distinctive features of the alpha 1-domain alpha helix of HLA-C heavy chains free of beta 2-microglobulin. Hum Immunol 1996; 46(2):69-81.

(115) Giacomini P, Beretta A, Nicotra MR et al. HLA-C heavy chains free of beta2-microglobulin: distribution in normal tissues and neoplastic lesions of non-lymphoid origin and interferon-gamma responsiveness. Tissue Antigens 1997; 50(6):555-566.

(116) Martayan A, Fiscella M, Setini A et al. Conformation and surface expression of free HLA-CW1 heavy chains in the absence of beta 2-microglobulin. Hum Immunol 1997; 53(1):23-33.

(117) Schaefer MR, Williams M, Kulpa DA, Blakely PK, Yaffee AQ, Collins KL. A novel trafficking signal within the HLA-C cytoplasmic tail allows regulated expression upon differentiation of macrophages. J Immunol 2008; 180(12):7804-7817.

(118) Bodnar A, Bacso Z, Jenei A et al. Class I HLA oligomerization at the surface of B cells is controlled by exogenous beta(2)-microglobulin: implications in activation of cytotoxic T lymphocytes. Int Immunol 2003; 15(3):331-339.

(119) Bodnar A, Jenei A, Bene L, Damjanovich S, Matko J. Modification of membrane cholesterol level affects expression and clustering of class I

HLA molecules at the surface of JY human lymphoblasts. Immunol Lett 1996; 54(2-3):221-226.

(120) Achdout H, Manaster I, Mandelboim O. Influenza virus infection augments NK cell inhibition through reorganization of major histocompatibility complex class I proteins. J Virol 2008; 82(16):8030-8037.

(121) Rouas-Freiss N, Goncalves RM, Menier C, Dausset J, Carosella ED. Direct evidence to support the role of HLA-G in protecting the fetus from maternal uterine natural killer cytolysis. Proc Natl Acad Sci U S A 1997; 94(21):11520-11525.

(122) Carosella ED, Moreau P, LeMaoult J, Rouas-Freiss N. HLA-G: from biology to clinical benefits. Trends Immunol 2008; 29(3):125-132.

(123) Menier C, Rouas-Freiss N, Favier B, LeMaoult J, Moreau P, Carosella ED. Recent advances on the non-classical major histocompatibility complex class I HLA-G molecule. Tissue Antigens 2010; 75(3):201-206.

(124) Hviid TV, Rizzo R, Melchiorri L, Stignani M, Baricordi OR. Polymorphism in the 5' upstream regulatory and 3' untranslated regions of the HLA-G gene in relation to soluble HLA-G and IL-10 expression. Hum Immunol 2006; 67(1-2):53-62.

(125) Gazit E, Slomov Y, Goldberg I, Brenner S, Loewenthal R. HLA-G is associated with pemphigus vulgaris in Jewish patients. Hum Immunol 2004; 65(1):39-46.

(126) Hviid TV. HLA-G in human reproduction: aspects of genetics, function and pregnancy complications. Hum Reprod Update 2006; 12(3):209-232.

(127) Xue S, Yang J, Yao F, Xu L, Fan L. Recurrent spontaneous abortions patients have more -14 bp/+14 bp heterozygotes in the 3'UT region of the HLA-G gene in a Chinese Han population. Tissue Antigens 2007; 69 Suppl 1:153-155.

(128) Glas J, Torok HP, Tonenchi L et al. The 14-bp deletion polymorphism in the HLA-G gene displays significant differences between ulcerative colitis and Crohn's disease and is associated with ileocecal resection in Crohn's disease. Int Immunol 2007; 19(5):621-626.

(129) Carosella ED, Moreau P, Le MJ, Le DM, Dausset J, Rouas-Freiss N. HLA-G molecules: from maternal-fetal tolerance to tissue acceptance. Adv Immunol 2003; 81:199-252.

(130) Shiroishi M, Kuroki K, Ose T et al. Efficient leukocyte Ig-like receptor signaling and crystal structure of disulfide-linked HLA-G dimer. J Biol Chem 2006; 281(15):10439-10447.

(131) Boyson JE, Erskine R, Whitman MC et al. Disulfide bond-mediated dimerization of HLA-G on the cell surface. Proc Natl Acad Sci U S A 2002; 99(25):16180-16185.

(132) Gonen-Gross T, Achdout H, Gazit R et al. Complexes of HLA-G protein on the cell surface are important for leukocyte Ig-like receptor-1 function. J Immunol 2003; 171(3):1343-1351.

(133) Apps R, Gardner L, Sharkey AM, Holmes N, Moffett A. A homodimeric complex of HLA-G on normal trophoblast cells modulates antigen-presenting cells via LILRB1. Eur J Immunol 2007; 37(7):1924-1937.

(134) Rajagopalan S, Long EO. A human histocompatibility leukocyte antigen (HLA)-G-specific receptor expressed on all natural killer cells. J Exp Med 1999; 189(7):1093-1100.

(135) Contini P, Ghio M, Poggi A et al. Soluble HLA-A,-B,-C and -G molecules induce apoptosis in T and NK CD8+ cells and inhibit cytotoxic T cell activity through CD8 ligation. Eur J Immunol 2003; 33(1):125-134.

(136) Cooper MA, Fehniger TA, Caligiuri MA. The biology of human natural killer-cell subsets. Trends Immunol 2001; 22(11):633-640.

(137) Goodridge JP, Witt CS, Christiansen FT, Warren HS. KIR2DL4 (CD158d) genotype influences expression and function in NK cells. J Immunol 2003; 171(4):1768-1774.

(138) Kikuchi-Maki A, Yusa S, Catina TL, Campbell KS. KIR2DL4 is an IL-2-regulated NK cell receptor that exhibits limited expression in humans but triggers strong IFN-gamma production. J Immunol 2003; 171(7):3415-3425.

(139) Fuzzi B, Rizzo R, Criscuoli L et al. HLA-G expression in early embryos is a fundamental prerequisite for the obtainment of pregnancy. Eur J Immunol 2002; 32(2):311-315.

(140) Rizzo R, Melchiorri L, Stignani M, Baricordi OR. HLA-G expression is a fundamental prerequisite to pregnancy. Hum Immunol 2007; 68(4):244-250.

(141) Creput C, Durrbach A, Menier C et al. Human leukocyte antigen-G (HLA-G) expression in biliary epithelial cells is associated with allograft acceptance in liver-kidney transplantation. J Hepatol 2003; 39(4):587-594.

(142) Le RS, Azema C, Krawice-Radanne I et al. Evidence to support the role of HLA-G5 in allograft acceptance through induction of immunosuppressive/ regulatory T cells. J Immunol 2006; 176(5):3266-3276.

(143) Lila N, Carpentier A, Amrein C, Khalil-Daher I, Dausset J, Carosella ED. Implication of HLA-G molecule in heart-graft acceptance. Lancet 2000; 355(9221):2138.

(144) Lila N, Amrein C, Guillemain R, Chevalier P, Fabiani JN, Carpentier A. Soluble human leukocyte antigen-G: a new strategy for monitoring acute and chronic rejections after heart transplantation. J Heart Lung Transplant 2007; 26(4):421-422.

(145) Luque J, Torres MI, Aumente MD et al. sHLA-G levels in the monitoring of immunosuppressive therapy and rejection following heart transplantation. Transpl Immunol 2006; 17(1):70-73.

(146) Naji A, Le RS, Durrbach A et al. CD3+CD4low and CD3+CD8low are induced by HLA-G: novel human peripheral blood suppressor T-cell

subsets involved in transplant acceptance. Blood 2007; 110(12):3936-3948.

(147) Qiu J, Terasaki PI, Miller J, Mizutani K, Cai J, Carosella ED. Soluble HLA-G expression and renal graft acceptance. Am J Transplant 2006; 6(9):2152-2156.

(148) Bukur J, Rebmann V, Grosse-Wilde H et al. Functional role of human leukocyte antigen-G up-regulation in renal cell carcinoma. Cancer Res 2003; 63(14):4107-4111.

(149) Maki G, Hayes GM, Naji A et al. NK resistance of tumor cells from multiple myeloma and chronic lymphocytic leukemia patients: implication of HLA-G. Leukemia 2008; 22(5):998-1006.

(150) Wiendl H, Mitsdoerffer M, Hofmeister V et al. A functional role of HLA-G expression in human gliomas: an alternative strategy of immune escape. J Immunol 2002; 168(9):4772-4780.

(151) Singer G, Rebmann V, Chen YC et al. HLA-G is a potential tumor marker in malignant ascites. Clin Cancer Res 2003; 9(12):4460-4464.

(152) Ibrahim EC, Aractingi S, Allory Y et al. Analysis of HLA antigen expression in benign and malignant melanocytic lesions reveals that upregulation of HLA-G expression correlates with malignant transformation, high inflammatory infiltration and HLA-A1 genotype. Int J Cancer 2004; 108(2):243-250.

(153) Nuckel H, Rebmann V, Durig J, Duhrsen U, Grosse-Wilde H. HLA-G expression is associated with an unfavorable outcome and immunodeficiency in chronic lymphocytic leukemia. Blood 2005; 105(4):1694-1698.

(154) Ye SR, Yang H, Li K, Dong DD, Lin XM, Yie SM. Human leukocyte antigen G expression: as a significant prognostic indicator for patients with colorectal cancer. Mod Pathol 2007; 20(3):375-383.

(155) Morales PJ, Pace JL, Platt JS, Langat DK, Hunt JS. Synthesis of beta(2)-microglobulin-free, disulphide-linked HLA-G5 homodimers in human placental villous cytotrophoblast cells. Immunology 2007; 122(2):179-188.

(156) LeMaoult J, Zafaranloo K, Le DC, Carosella ED. HLA-G up-regulates ILT2, ILT3, ILT4, and KIR2DL4 in antigen presenting cells, NK cells, and T cells. FASEB J 2005; 19(6):662-664.

(157) Gleissner CA, Zastrow A, Klingenberg R et al. IL-10 inhibits endothelium-dependent T cell costimulation by up-regulation of ILT3/4 in human vascular endothelial cells. Eur J Immunol 2007; 37(1):177-192.

(158) Moreau P, drian-Cabestre F, Menier C et al. IL-10 selectively induces HLA-G expression in human trophoblasts and monocytes. Int Immunol 1999; 11(5):803-811.

(159) Huang J, Burke PS, Cung TD et al. Leukocyte immunoglobulin-like receptors maintain unique antigen-presenting properties of circulating

myeloid dendritic cells in HIV-1-infected elite controllers. J Virol 2010; 84(18):9463-9471.

(160) Mamegano K, Kuroki K, Miyashita R et al. Association of LILRA2 (ILT1, LIR7) splice site polymorphism with systemic lupus erythematosus and microscopic polyangiitis. Genes Immun 2008; 9(3):214-223.

(161) Bleharski JR, Li H, Meinken C et al. Use of genetic profiling in leprosy to discriminate clinical forms of the disease. Science 2003; 301(5639):1527-1530.

(162) Huynh OA, Hampartzoumian T, Arm JP et al. Down-regulation of leucocyte immunoglobulin-like receptor expression in the synovium of rheumatoid arthritis patients after treatment with disease-modifying anti-rheumatic drugs. Rheumatology (Oxford) 2007; 46(5):742-751.

(163) Berg L, Riise GC, Cosman D et al. LIR-1 expression on lymphocytes, and cytomegalovirus disease in lung-transplant recipients. Lancet 2003; 361(9363):1099-1101.

(164) Zhang W, Liang S, Wu J, Horuzsko A. Human inhibitory receptor immunoglobulin-like transcript 2 amplifies CD11b+Gr1+ myeloid-derived suppressor cells that promote long-term survival of allografts. Transplantation 2008; 86(8):1125-1134.

(165) Monsivais-Urenda A, Nino-Moreno P, bud-Mendoza C et al. Analysis of expression and function of the inhibitory receptor ILT2 (CD85j/LILRB1/LIR-1) in peripheral blood mononuclear cells from

patients with systemic lupus erythematosus (SLE). J Autoimmun 2007; 29(2-3):97-105.

(166) Wiendl H, Feger U, Mittelbronn M et al. Expression of the immune-tolerogenic major histocompatibility molecule HLA-G in multiple sclerosis: implications for CNS immunity. Brain 2005; 128(Pt 11):2689-2704.

(167) Ince MN, Harnisch B, Xu Z et al. Increased expression of the natural killer cell inhibitory receptor CD85j/ILT2 on antigen-specific effector CD8 T cells and its impact on CD8 T-cell function. Immunology 2004; 112(4):531-542.

(168) O'Connor GM, Holmes A, Mulcahy F, Gardiner CM. Natural Killer cells from long-term non-progressor HIV patients are characterized by altered phenotype and function. Clin Immunol 2007; 124(3):277-283.

(169) Kalmbach Y, Boldt AB, Fendel R, Mordmuller B, Kremsner PG, Kun JF. Increase in annexin V-positive B cells expressing LILRB1/ILT2/CD85j in malaria. Eur Cytokine Netw 2006; 17(3):175-180.

(170) Rouas-Freiss N, Moreau P, Menier C, LeMaoult J, Carosella ED. Expression of tolerogenic HLA-G molecules in cancer prevents antitumor responses. Semin Cancer Biol 2007; 17(6):413-421.

(171) Urosevic M, Kamarashev J, Burg G, Dummer R. Primary cutaneous CD8+ and CD56+ T-cell lymphomas express HLA-G and killer-cell inhibitory ligand, ILT2. Blood 2004; 103(5):1796-1798.

(172) Kuroki K, Tsuchiya N, Shiroishi M et al. Extensive polymorphisms of LILRB1 (ILT2, LIR1) and their association with HLA-DRB1 shared epitope negative rheumatoid arthritis. Hum Mol Genet 2005; 14(16):2469-2480.

(173) Ristich V, Zhang W, Liang S, Horuzsko A. Mechanisms of prolongation of allograft survival by HLA-G/ILT4-modified dendritic cells. Hum Immunol 2007; 68(4):264-271.

(174) Lichterfeld M, Kavanagh DG, Williams KL et al. A viral CTL escape mutation leading to immunoglobulin-like transcript 4-mediated functional inhibition of myelomonocytic cells. J Exp Med 2007; 204(12):2813-2824.

(175) Colovai AI, Tsao L, Wang S et al. Expression of inhibitory receptor ILT3 on neoplastic B cells is associated with lymphoid tissue involvement in chronic lymphocytic leukemia. Cytometry B Clin Cytom 2007; 72(5):354-362.

(176) Sun Y, Liu J, Gao P, Wang Y, Liu C. Expression of Ig-like transcript 4 inhibitory receptor in human non-small cell lung cancer. Chest 2008; 134(4):783-788.

(177) Brown DP, Jones DC, Anderson KJ et al. The inhibitory receptor LILRB4 (ILT3) modulates antigen presenting cell phenotype and, along with LILRB2 (ILT4), is upregulated in response to Salmonella infection. BMC Immunol 2009; 10:56.

(178) Tsuchiya S, Yamabe M, Yamaguchi Y, Kobayashi Y, Konno T, Tada K. Establishment and characterization of a human acute monocytic leukemia cell line (THP-1). Int J Cancer 1980; 26(2):171-176.

(179) Gluzman Y. SV40-transformed simian cells support the replication of early SV40 mutants. Cell 1981; 23(1):175-182.

(180) Pear WS, Nolan GP, Scott ML, Baltimore D. Production of high-titer helper-free retroviruses by transient transfection. Proc Natl Acad Sci U S A 1993; 90(18):8392-8396.

(181) Lozzio BB, Lozzio CB. Properties and usefulness of the original K-562 human myelogenous leukemia cell line. Leuk Res 1979; 3(6):363-370.

(182) Lozzio CB, Lozzio BB. Human chronic myelogenous leukemia cell-line with positive Philadelphia chromosome. Blood 1975; 45(3):321-334.

(183) Kohler PO, Bridson WE. Isolation of hormone-producing clonal lines of human choriocarcinoma. J Clin Endocrinol Metab 1971; 32(5):683-687.

(184) Parham P, Brodsky FM. Partial purification and some properties of BB7.2. A cytotoxic monoclonal antibody with specificity for HLA-A2 and a variant of HLA-A28. Hum Immunol 1981; 3(4):277-299.

(185) Parham P, Barnstable CJ, Bodmer WF. Use of a monoclonal antibody (W6/32) in structural studies of HLA-A,B,C, antigens. J Immunol 1979; 123(1):342-349.

(186) Dendrou CA, Fung E, Esposito L, Todd JA, Wicker LS, Plagnol V. Fluorescence intensity normalisation: correcting for time effects in large-scale flow cytometric analysis. Adv Bioinformatics 2009;476106.

(187) Tsai MF, Lin YJ, Cheng YC et al. PrimerZ: streamlined primer design for promoters, exons and human SNPs. Nucleic Acids Res 2007; 35(Web Server issue):W63-W65.

(188) Livak KJ, Schmittgen TD. Analysis of relative gene expression data using real-time quantitative PCR and the 2(-Delta Delta C(T)) Method. Methods 2001; 25(4):402-408.

(189) Nakajima H, Asai A, Okada A et al. Transcriptional regulation of ILT family receptors. J Immunol 2003; 171(12):6611-6620.

(190) Dendrou CA, Plagnol V, Fung E et al. Cell-specific protein phenotypes for the autoimmune locus IL2RA using a genotype-selectable human bioresource. Nat Genet 2009; 41(9):1011-1015.

(191) Liang S, Baibakov B, Horuzsko A. HLA-G inhibits the functions of murine dendritic cells via the PIR-B immune inhibitory receptor. Eur J Immunol 2002; 32(9):2418-2426.

(192) Zhong M, Weng X, Liang Z et al. Dimerization of soluble HLA-G by IgG-Fc fragment augments ILT2-mediated inhibition of T-cell alloresponse. Transplantation 2009; 87(1):8-15.

(193) Bussmann C, Xia J, Allam JP, Maintz L, Bieber T, Novak N. Early markers for protective mechanisms during rush venom immunotherapy. Allergy 2010; 65(12):1558-1565.

(194) Hirayasu K, Ohashi J, Tanaka H et al. Evidence for natural selection on leukocyte immunoglobulin-like receptors for HLA class I in Northeast Asians. Am J Hum Genet 2008; 82(5):1075-1083.

(195) Tsai MF, Lin YJ, Cheng YC et al. PrimerZ: streamlined primer design for promoters, exons and human SNPs. Nucleic Acids Res 2007; 35(Web Server issue):W63-W65.

(196) Xu X, Zou P, Chen L, Jin G, Zhou H. IL-10 enhances promoter activity of ILT4 gene and up-regulates its expression in THP-1 cells. J Huazhong Univ Sci Technolog Med Sci 2010; 30(5):594-598.

(197) Rouas-Freiss N, Marchal RE, Kirszenbaum M, Dausset J, Carosella ED. The alpha1 domain of HLA-G1 and HLA-G2 inhibits cytotoxicity induced by natural killer cells: is HLA-G the public ligand for natural killer cell inhibitory receptors? Proc Natl Acad Sci U S A 1997; 94(10):5249-5254.

(198) Caumartin J, Favier B, Daouya M et al. Trogocytosis-based generation of suppressive NK cells. EMBO J 2007; 26(5):1423-1433.

(199) Dorling A, Monk NJ, Lechler RI. HLA-G inhibits the transendothelial migration of human NK cells. Eur J Immunol 2000; 30(2):586-593.

(200) van der MA, Lukassen HG, van Lierop MJ et al. Membrane-bound HLA-G activates proliferation and interferon-gamma production by uterine natural killer cells. Mol Hum Reprod 2004; 10(3):189-195.

(201) Rajagopalan S, Fu J, Long EO. Cutting edge: induction of IFN-gamma production but not cytotoxicity by the killer cell Ig-like receptor KIR2DL4 (CD158d) in resting NK cells. J Immunol 2001; 167(4):1877-1881.

(202) Rajagopalan S, Bryceson YT, Kuppusamy SP et al. Activation of NK cells by an endocytosed receptor for soluble HLA-G. PLoS Biol 2006; 4(1):e9.

(203) Fournel S, guerre-Girr M, Huc X et al. Cutting edge: soluble HLA-G1 triggers CD95/CD95 ligand-mediated apoptosis in activated CD8+ cells by interacting with CD8. J Immunol 2000; 164(12):6100-6104.

(204) Lee N, Goodlett DR, Ishitani A, Marquardt H, Geraghty DE. HLA-E surface expression depends on binding of TAP-dependent peptides derived from certain HLA class I signal sequences. J Immunol 1998; 160(10):4951-4960.

(205) Favier B, LeMaoult J, Rouas-Freiss N, Moreau P, Menier C, Carosella ED. Research on HLA-G: an update. Tissue Antigens 2007; 69(3):207-211.

(206) LeMaoult J, Krawice-Radanne I, Dausset J, Carosella ED. HLA-G1-expressing antigen-presenting cells induce immunosuppressive CD4+ T cells. Proc Natl Acad Sci U S A 2004; 101(18):7064-7069.

(207) Riteau B, Menier C, Khalil-Daher I et al. HLA-G inhibits the allogeneic proliferative response. J Reprod Immunol 1999; 43(2):203-211.

(208) Bahri R, Hirsch F, Josse A et al. Soluble HLA-G inhibits cell cycle progression in human alloreactive T lymphocytes. J Immunol 2006; 176(3):1331-1339.

(209) LeMaoult J, Caumartin J, Daouya M et al. Immune regulation by pretenders: cell-to-cell transfers of HLA-G make effector T cells act as regulatory cells. Blood 2007; 109(5):2040-2048.

(210) Riteau B, Rouas-Freiss N, Menier C, Paul P, Dausset J, Carosella ED. HLA-G2, -G3, and -G4 isoforms expressed as nonmature cell surface glycoproteins inhibit NK and antigen-specific CTL cytolysis. J Immunol 2001; 166(8):5018-5026.

(211) Le Gal FA, Riteau B, Sedlik C et al. HLA-G-mediated inhibition of antigen-specific cytotoxic T lymphocytes. Int Immunol 1999; 11(8):1351-1356.

(212) Liang S, Zhang W, Horuzsko A. Human ILT2 receptor associates with murine MHC class I molecules in vivo and impairs T cell function. Eur J Immunol 2006; 36(9):2457-2471.

(213) Kanai T, Fujii T, Kozuma S et al. Soluble HLA-G influences the release of cytokines from allogeneic peripheral blood mononuclear cells in culture. Mol Hum Reprod 2001; 7(2):195-200.

(214) Fons P, Chabot S, Cartwright JE et al. Soluble HLA-G1 inhibits angiogenesis through an apoptotic pathway and by direct binding to CD160 receptor expressed by endothelial cells. Blood 2006; 108(8):2608-2615.

(215) Horuzsko A, Lenfant F, Munn DH, Mellor AL. Maturation of antigen-presenting cells is compromised in HLA-G transgenic mice. Int Immunol 2001; 13(3):385-394.

(216) Favier B, HoWangYin KY, Wu J et al. Tolerogenic function of dimeric forms of HLA-G recombinant proteins: a comparative study in vivo. PLoS One 2011; 6(7):e21011.

(217) Kulkarni O, Mulay S, Darisipudi M et al. HLA-G attenuates renal inflammation in a mouse model of lupus nephritis. Tissue Antigens 2012; 80:84.

(218) Watkins NA, Dafforn TR, Kuijpers M et al. Molecular studies of anti-HLA-A2 using light-chain shuffling: a structural model for HLA antibody binding. Tissue Antigens 2004; 63(4):345-354.

(219) Watkins NA, Brown C, Hurd C, Navarrete C, Ouwehand WH. The isolation and characterisation of human monoclonal HLA-A2 antibodies from an immune V gene phage display library. Tissue Antigens 2000; 55(3):219-228.

(220) Aruffo A. Transient expression of proteins using COS cells. Curr Protoc Neurosci 2001; Chapter 4:Unit.

(221) Allan DS, Colonna M, Lanier LL et al. Tetrameric complexes of human histocompatibility leukocyte antigen (HLA)-G bind to peripheral blood myelomonocytic cells. J Exp Med 1999; 189(7):1149-1156.

(222) Allan DS, Lepin EJ, Braud VM, O'Callaghan CA, McMichael AJ. Tetrameric complexes of HLA-E, HLA-F, and HLA-G. J Immunol Methods 2002; 268(1):43-50.

(223) Morel E, Bellon T. HLA class I molecules regulate IFN-gamma production induced in NK cells by target cells, viral products, or immature dendritic cells through the inhibitory receptor ILT2/CD85j. J Immunol 2008; 181(4):2368-2381.

(224) McIntire RH, Morales PJ, Petroff MG, Colonna M, Hunt JS. Recombinant HLA-G5 and -G6 drive U937 myelomonocytic cell production of TGF-beta1. J Leukoc Biol 2004; 76(6):1220-1228.

(225) Lu HK, Rentero C, Raftery MJ, Borges L, Bryant K, Tedla N. Leukocyte Ig-like receptor B4 (LILRB4) is a potent inhibitor of FcgammaRI-mediated monocyte activation via dephosphorylation of multiple kinases. J Biol Chem 2009; 284(50):34839-34848.

(226) Bainbridge DR, Ellis SA, Sargent IL. HLA-G suppresses proliferation of CD4(+) T-lymphocytes. J Reprod Immunol 2000; 48(1):17-26.

(227) Kapasi K, Albert SE, Yie S, Zavazava N, Librach CL. HLA-G has a concentration-dependent effect on the generation of an allo-CTL response. Immunology 2000; 101(2):191-200.

(228) Le FG, Laupeze B, Fardel O et al. Soluble HLA-G inhibits human dendritic cell-triggered allogeneic T-cell proliferation without altering dendritic differentiation and maturation processes. Hum Immunol 2003; 64(8):752-761.

(229) Liang S, Horuzsko A. Mobilizing dendritic cells for tolerance by engagement of immune inhibitory receptors for HLA-G. Hum Immunol 2003; 64(11):1025-1032.

(230) Zhong M, Weng X, Liang Z et al. Dimerization of soluble HLA-G by IgG-Fc fragment augments ILT2-mediated inhibition of T-cell alloresponse. Transplantation 2009; 87(1):8-15.

(231) Ju XS, Hacker C, Scherer B et al. Immunoglobulin-like transcripts ILT2, ILT3 and ILT7 are expressed by human dendritic cells and down-regulated following activation. Gene 2004; 331:159-164.

(232) Lu HK, Mitchell A, Endoh Y et al. LILRA2 selectively modulates LPS-mediated cytokine production and inhibits phagocytosis by monocytes. PLoS One 2012; 7(3):e33478.

(233) Tilg H, van MC, van den EA et al. Treatment of Crohn's disease with recombinant human interleukin 10 induces the proinflammatory cytokine interferon gamma. Gut 2002; 50(2):191-195.

(234) Tanriver Y, Ratnasothy K, Bucy RP, Lombardi G, Lechler R. Targeting MHC class I monomers to dendritic cells inhibits the indirect pathway of allorecognition and the production of IgG alloantibodies leading to long-term allograft survival. J Immunol 2010; 184(4):1757-1764.

Appendices

Appendix 1: International Union of Pure and Applied Chemistry (IUPAC) code for nucleic acids

Code	Description
A	Adenine
C	Cytosine
G	Guanine
T	Thymine
U	Uracil
R	Purine (A or G)
Y	Pyrimidine (C, T, or U)
M	C or A
K	T, U, or G
W	T, U, or A
S	C or G
B	C, T, U, or G (not A)
D	A, T, U, or G (not C)
H	A, T, U, or C (not G)
V	A, C, or G (not T, not U)
N	Any base (A, C, G, T, or U)